
**INFLUENCE OF NATURAL ORGANIC MATTER ON THE MOBILITY
OF ARSENIC IN AQUATIC SYSTEMS, SOILS AND SEDIMENTS**

Dissertation zur Erlangung des Grades

Doktor der Naturwissenschaften

(Dr. rer. nat.)

an der Fakultät Biologie/Chemie/Geowissenschaften

der Universität Bayreuth

vorgelegt von

Markus Bauer

Geb. am 01.05.1977 in Ingolstadt

Bayreuth, 23. April 2008

Vollständiger Abdruck der von der Fakultät für Chemie/Biologie/Geowissenschaften der Universität Bayreuth genehmigten Dissertation zur Erlangung des Grades eines Doktors der Naturwissenschaften (Dr. rer. nat.).

Prüfungsausschuss:

Prof. Dr. Stefan Peiffer	(Vorsitzender)
PD Dr. Christian Blodau	(1. Gutachter)
Prof. Dr. Egbert Matzner	(2. Gutachter)
Prof. Dr. Hartmut Frank	
PD Dr. Bruno Glaser	

Tag der Einreichung: 20.04.08

Tag des wissenschaftlichen Kolloquiums: 29.10.08

TABLE OF CONTENTS

INFLUENCE OF NATURAL ORGANIC MATTER ON THE MOBILITY OF ARSENIC IN AQUATIC SYSTEMS, SOILS AND SEDIMENTS	I
TABLE OF CONTENTS	I
LIST OF FIGURE	III
LIST OF TABLES	V
SUMMARY	VII
ZUSAMMENFASSUNG	IX
EXTENDED SUMMARY	1
Introduction	1
1. Arsenic health concerns.....	1
2. Arsenic geochemistry and mobility.....	1
3. Natural organic matter.....	4
4. As mobility in environments rich in organic matter.....	7
5. Objectives of the dissertation	8
I. Redox Chemistry of DOM and Electron Transfer Reactions with As	11
1. DOM oxidation and reduction by inorganic compounds (study 1 and 2)	12
2. DOM redox reactivity with As (study 3).....	14
Conclusions	14
II. Aqueous and Surface Complexation Reactions of As and DOM	15
1. Complex and colloid formation in solutions with Fe, DOM and As (study 4 and 5).....	16
2. Influence of DOM on As binding to mineral surfaces (study 6)	18
3. Aqueous and surface complexation reactions and the redox speciation of As.....	18
Conclusions	19
III. Effect of DOM Load on the As Mobilization (study 7)	19
IV. Arsenic Mobility and Retention in Organic Matter Rich Peat Soils	21
1. Arsenic in peat mesocosms subject to drying and rewetting (Study 8).....	22
2. Arsenic in degraded peatland soil (Study 9).....	23
Conclusions	24
Conclusions and Outlook	26
References	29
Contributions to the Different Studies.....	37
APPENDIX	41

Study 1, APPENDIX	45
<i>Electron Transfer Capacities and Reaction Kinetics of Peat Dissolved Organic Matter</i>	
Study 2, APPENDIX	63
<i>Electron Accepting Capacity of Dissolved Organic Matter as determined by Reaction with Metallic Zinc</i>	
Study 3, APPENDIX	85
<i>Oxidation of As(III) and Reduction of As(V) in Dissolved Organic Matter Solutions</i>	
Study 4, APPENDIX	97
<i>Experimental colloid formation in aqueous solutions rich in dissolved organic matter, ferric iron, and As</i>	
Study 5, APPENDIX	119
<i>Evidence for Aquatic Binding of Arsenate by Natural Organic Matter-Suspended Fe(III)</i>	
Study 6, APPENDIX	129
<i>Mobilization of Arsenic by Dissolved Organic Matter from Iron Oxides, Soils and Sediments</i>	
Study 7, APPENDIX	143
<i>Mobilization of Iron and Arsenic from Iron Oxide Coated Sand Columns by Percolation with Dissolved Organic Matter</i>	
Study 8, APPENDIX	159
<i>Arsenic Speciation and Turnover in intact Organic Soil Mesocosms during Experimental Drought and Rewetting</i>	
Study 9, APPENDIX	179
<i>Groundwater Derived Arsenic in High Carbonate Wetland Soils: Sources, Sinks, and Mobility</i>	
Redox reactions and Redox potentials, APPENDIX	193

LIST OF FIGURE

			Page
Figure 1	Extended Summary	E_h-pH diagrams for As	3
Figure 2	Extended Summary	Schematic structure of a DOM molecule	5
Figure 3	Extended Summary	Electron transfer reactions of quinones and DOM	5
Figure 4	Extended Summary	Aqueous and surface complexes of As and DOM	7
Figure 5	Extended Summary	Interactions of As with DOM and Fe	9
Figure 6	Study 1, Fig. 1	Reduction of Fe(III) complexes by DOM	47
Figure 7	Study 1, Fig. 2	Reduction of Fe(III) vs. DOM concentration	48
Figure 8	Study 1, Fig. 3	Reduction of Fe(III) vs. pH	48
Figure 9	Study 1, Fig. 4	Oxidation of H₂S and Zn⁰ by DOM	49
Figure 10	Study 1, Fig. 5	Oxidation of H₂S and Zn⁰ vs. DOM concentration	49
Figure 11	Study 1, Fig. 6	Dependency of ETC and reaction rate constant on E_h⁰	50
Figure 12	Support, Study 1	Aqueous Fe speciation as modelled by Phreeqc	55
Figure 13	Support, Study 1	Aqueous Fe speciation as modelled by Phreeqc	56
Figure 14	Support, Study 1	Variability during modelling	58
Figure 15	Support, Study 1	Formation of Fe(II) in DOM solution	59
Figure 16	Study 2	Zn²⁺, H₂ and H⁺ turnover in DOM solution	71
Figure 17	Study 2	Dependency of Zn release on pH	72
Figure 18	Study 2	Time series of Zn release with different DOM samples	73
Figure 19	Study 2	Zn⁰ oxidation vs. DOM concentration	73
Figure 20	Study 2	Electron accepting capacity vs. DOM concentration	75
Figure 21	Study 2	Reversibility of DOM electron uptake	75
Figure 22	Study 2	Relation of DOM SUVA and FTIR properties to EAC	76
Figure 23	Study 2	Relation of DOM fluorescence properties to EAC	77
Figure 24	Study 3	Time series of As(III) oxidation by DOM	90
Figure 25	Study 3	As(III) oxidation capacity	91
Figure 26	Study 3	Time series of As(V) reduction by DOM	93
Figure 27	Study 3	As(V) reduction capacity	94
Figure 28	Study 4	Colloid formation assays: Standard procedure and variations	101
Figure 29	Study 4	Results of standard colloid filtration experiments	103
Figure 30	Study 4	Time series of formation of Fe-As-DOM aggregates	104
Figure 31	Study 4	Correlation of As, Fe and DOC in aggregates with PPHA	105
Figure 32	Study 4	Dependency of aggregate formation on pH	106
Figure 33	Study 4	Dependency of aggregate formation on DOC concentration	107
Figure 34	Study 4	Dependency of aggregate formation on Fe/C ratio	111
Figure 35	Study 4	Filtration results vs. WINHUMIC model calculations	110

			Page
Figure 36	Support, Study 4	Formation of Fe-As-DOM aggregates with SRDOM	118
Figure 37	Study 5, Fig. 1	Arsenic dialysis experiments without DOM and with SRHPOA	123
Figure 38	Study 5, Fig. 2	Arsenic dialysis experiments with EGFA and SRWW	124
Figure 39	Study 5, Fig. 3	Arsenic mass balance during dialysis experiments	124
Figure 40	Study 5, Fig. 4	DOC and Fe mass balance in dialysis experiments	125
Figure 41	Study 5, Fig. 5	Arsenic complexation dependency on Fe concentration	126
Figure 42	Study 6, Fig. 1	Aqueous As speciation in DOM solution	134
Figure 43	Study 6, Fig. 2	Arsenic sorption on goethite	134
Figure 44	Study 6, Fig. 3	Arsenic desorption from goethite	135
Figure 45	Study 6, Fig. 4	Arsenic desorption by DOM from soil and sediment	137
Figure 46	Study 6, Fig. 5	Time series of As mobilization and speciation	137
Figure 47	Study 7	Breakthrough of chloride and pH in column experiments	148
Figure 48	Study 7	Column effluent concentrations of Fe, As and S	150
Figure 49	Study 7	Dynamics of Fe, S and As within the column	151
Figure 50	Study 7	Column solid phase Fe, S and As content	152
Figure 51	Study 8	Solid phase As and Fe distribution in peat material	164
Figure 52	Study 8	Gas content in the peat cores during drying and rewetting	166
Figure 53	Study 8	Root activity in the peat cores as determined by $d^{13}C$ of CO_2	166
Figure 54	Study 8	Aqueous depth profiles of Fe, S, DOC, and pH	167
Figure 55	Study 8	Temporal dynamics of dissolved As in the peat cores	168
Figure 56	Study 8	Arsenic speciation at the beginning of the drying period	169
Figure 57	Study 8	Temporal dynamics of the As(III) to As(V) ratio	169
Figure 58	Study 8	Temporal dynamics of DMA concentration	170
Figure 59	Study 8	Redox potential values calculated from As, Fe and S couples	170
Figure 60	Study 8	Turnover rates calculated for As and Fe	171
Figure 61	Support, Study 8	Time series of water levels during drying and rewetting	177
Figure 62	Study 9	Aqueous concentration profiles of As, Fe and DOC	183
Figure 63	Study 9	Soil horizon XRD spectra	184
Figure 64	Study 9	Soil content of As, Fe and C in different pools	186
Figure 65	Study 9	Arsenic mobilization by soil organic carbon dispersion	187
Figure 66	Support, Study 9	Setup of the Stella transport model	192
Figure 67	Support, Study 9	Measured and modelled depth profile of As and Cl^-	192

LIST OF TABLES

			Page
Table 1	Study 1, Tab. 1	DOM oxidation and reduction experiments	46
Table 2	Support, Study 1	Properties of DOM samples	52
Table 3	Support, Study 1	List of critical stability constants	54
Table 4	Support, Study 1	Thermodynamic calculations	57
Table 5	Support, Study 1	Literature review of EAC and EDC values	60
Table 6	Study 2	Properties of DOM samples	66
Table 7	Study 3	Experiments of As oxidation and reduction by DOM	88
Table 8	Study 3	Thermodynamic calculations	89
Table 9	Study 4	Complexation and colloid formation experiments	101
Table 10	Study 4	Properties of DOM samples	103
Table 11	Study 4	Fe, DOC and As concentrations in different size fractions	108
Table 12	Study 5, Tab. 1	Properties of DOM samples	121
Table 13	Study 5, Tab. 2	Inorganic constituents of DOM solution	121
Table 14	Study 5, Tab. 3	Results of sequential filtration experiments	126
Table 15	Study 6, Tab. 1	Arsenic sorption and desorption experiments from iron oxide	136
Table 16	Study 6, Tab. 2	Characteristics of soil and sediment samples	138
Table 17	Study 6, Tab. 3	Arsenic content in soil and sediment pools	138
Table 18	Study 7	Column hydraulic characteristics	149
Table 19	Study 7	Mass balances for Fe, S, As and C in column experiments	152
Table 20	Study 8	Solid phase Fe, Al and TRIS content	165
Table 21	Study 8	Correlation of As content with major soil constituents	165
Table 22	Support, Study 8	Solid phase elemental content	178
Table 23	Study 9	Applied extraction procedures	182
Table 24	Study 9	Physical and chemical properties of soil horizons	185
Table 25	Study 9	Solid phase Ca, Fe and As content in soil mineral pools	185
Table 26	Appendix 10	Summary of thermodynamic calculations	194/195

SUMMARY

The element As is today recognized as one of the most dangerous inorganic contaminants and threats for the world's water resources. Arsenic is ubiquitous in the earth crust and humans are especially affected through As polluted drinking water supplies. The occurrence of high As groundwater concentrations is often caused by geogenic processes of As release from the solid phase and accumulation in the water phase. Many contaminated aquifers are also characterized by high concentrations of natural organic matter (NOM). Previous studies showed that NOM presence may affect As mobility, but we are lacking evidence about the reactions pathways and about the importance As-DOM interactions in the environment. We therefore focussed on studying reactions between NOM and As, including redox reactions, complexation, colloid formation and sorption competition in laboratory experiments. Moreover we also studied As behaviour in columns experiments and wetland soils rich in organic matter.

Arsenic mobility strongly depends on its redox state. Dissolved organic matter was previously found to be redox active but its redox properties are only poorly understood. In laboratory experiments we therefore elucidated the electron transfer characteristics of different DOM samples. The results showed the high potential of humic substances to chemically reduce different Fe(III) complexes and oxidize H₂S and metallic Zn. Reactions occurred over short periods of time with reaction rates in the range from 0.03 to 27 h⁻¹. Under otherwise identical conditions rising DOC concentrations caused higher total electron transfer. This supports the assumption that functional groups of DOM, such as quinones, were indeed the redox active moieties involved in the redox reactions. The calculated electron transfer capacities (ETC) ranged from 0.07 to 6.2 mequiv (g C)⁻¹. The wide range of observed reaction rates and ETC values could be related to the different redox potential of the inorganic reactants used. This suggests that DOM molecules contain redox active moieties with different redox potential and that they possibly represent a redox ladder with the capacity to buffer electrons over a wide range of redox conditions. Humic substances also influenced the As redox speciation as dissolved H₃AsO₄ was - either chemically or microbially- reduced to H₃AsO₃ in DOM solution. No oxidation of As(III) to As(V) was found in these experiments. The presence of organic matter thus changes the redox speciation of As as well as that of other environmentally relevant elements like Fe or S. This possibly also contributes to a higher mobility of As due to the presence of reduced As and Fe species.

The formation of complexes on mineral surfaces is one of the most important immobilization processes for As in soils or sediments. DOM strongly interfered with this As sequestration mechanism due to aqueous and surface complexation reactions. Humic substances were found to prevent the precipitation and sedimentation of iron oxide minerals and promote the formation of DOM and Fe containing colloids at aqueous molar Fe/C ratios of up to 0.1. This impeded the co-precipitation and

sedimentation of As with Fe mineral structures and increased the amount of mobile As. Arsenic and Fe content were correlated in the different particle size classes was, suggesting As binding to Fe e.g. in cation bridging complexes or DOM stabilized Fe oxide colloids. DOM sorption on synthetic goethite and natural soil and sediment samples also caused a release of As from these solid phases due to sorption competition for mineral binding sites. Especially the weakly adsorbed fraction of As in the natural samples was affected by this process. Both the formation of aqueous complexes or colloids and the sorption competition in the presence of DOM lead to higher As concentration in the water phase and demonstrate the potential of humic substances to increase As mobility.

In the studied laboratory columns As redox transformation and complexation by DOM could not be identified. Instead As mobilization was dominated by microbial processes in these experiments. At DOM input concentrations between 5 and 100 mg L⁻¹ the release of As occurred mainly due to the reductive dissolution of the Fe oxide sorbent phase during microbial respiration. The occurrence of sulfate reduction and the precipitation of sulfide minerals at the highest DOM concentrations did not represent a substantial immobilization mechanism.

The studied wetland soils represent natural sinks for geogenic As. Fe oxides were the main As sorbents, which is surprising as both soils were temporarily water saturated and likely under reducing conditions. Moreover, the high porewater DOC concentrations and the high organic carbon content in the solid phase apparently did not interfere with As sorption on the iron phases in these soils. Chemical extractions also showed that smaller As fractions were associated with solid phase organic matter pool and with a not identified residual pool, likely sulfide minerals. However, as most As was bound to Fe oxides its fate was strongly affected by changing redox conditions. Fast As immobilization sorption occurred under dry conditions when Fe was oxidized and precipitated, while short-term mobilization of As and Fe in their reduced form was observed upon rewetting. These soils therefore are As sinks as long as oxic conditions are maintained but may turn into As sources when reducing conditions prevail for longer periods of time.

Organic molecules influence the redox state and the complexation of As and are able to shift As partitioning in favour of the solute phase. Our results showed that especially the association of As with aqueous complexes and colloids has a strong potential to reduce As retention and increase As mobility. This has to be considered in future studies of As behaviour in aquifers, surface waters, soils or sediments rich in organic substances. Peatland soils were found to represent sinks for geogenic As, showing that the presence of organic matter not necessarily prevents As immobilization. It also depends on the biogeochemical conditions whether an organic matter rich system will accumulate or release As.

ZUSAMMENFASSUNG

Der toxische, anorganische Schadstoff Arsen wird heute als eine der größten Bedrohungen für die Trinkwasserressourcen der Erde angesehen. Arsen ist in der Erdkruste weit verbreitet und hohe As-Belastungen im Grundwasser sind häufig geogenen Ursprungs. Natürliche Prozesse verursachen die As-Freisetzung aus der Festphase und seine Anreicherung in der Wasserphase. Häufig zeichnen sich As-belastete Aquifere auch durch hohe Gehalte an natürlichem, organischem Material (NOM) aus und es gibt Anhaltspunkte, dass organische Substanzen die Mobilität und Festlegung von As beeinflussen. Reaktion zwischen As und NOM sind nur teilweise untersucht und über ihren Einfluss auf die Mobilität von As in der Umwelt ist wenig bekannt. Für diese Arbeit wurden deshalb einerseits chemische Wechselwirkungen zwischen As und organischem Material, wie Redoxtransformationen, die Bildung von aquatischen Komplexen und Kolloiden sowie die Konkurrenz um Adsorptionsplätze auf Mineralfestphasen, in Laborversuchen untersucht. Andererseits wurde auch das Verhalten von As in natürlichen Moor- und Gleyböden untersucht, die hohe Gehalte an organischem Material aufweisen.

Die Mobilität von As wird stark durch Redoxprozesse beeinflusst. Es ist bekannt, dass gelöstes organisches Material (DOM) über redox-aktive Gruppen verfügt. Da die Redox Eigenschaften organischer Substanzen aber nur unzureichend beschrieben wurden im Rahmen dieser Arbeit der Elektronenaustausch mit verschiedenen anorganischen Reaktanden untersucht. Alle verwendeten Huminstofflösungen waren in der Lage in aquatischen Komplexen vorliegendes Fe(III) zu reduzieren sowie gelöstes H₂S und metallisches Zink zu oxidieren. Die Redoxreaktionen erfolgten schnell und die Reaktionsraten lagen bei 0.03 bis 27 h⁻¹. Eine Anhebung der DOC-Konzentration führte unter sonst gleichen Bedingungen zu einem Anstieg des Elektronentransfers. Dies zeigt, dass redox-aktive, funktionelle Gruppen des organischen Materials, z.B. Chinone, für den Elektronenaustausch verantwortlich sind. Die aus den Experimenten berechnete Elektronentransferkapazität (ETC) der Huminstoffe lag zwischen 0.07 und 6.2 mequiv (g C)⁻¹. Die große Spannweite der ermittelten bestimmten Reaktionsraten und Elektronentransferkapazitäten konnte auf die unterschiedlichen Redoxpotentiale der verwendeten Reaktanden zurückgeführt werden. Dies weist darauf hin, dass Huminstoffmoleküle redox-aktive Gruppen mit unterschiedlicher Reaktivität besitzen und deshalb Redox-Leitern darstellen, die in der Lage sind über einen weiten Redoxpotentialbereich als Elektronenpuffer wirken. DOM beeinflusste auch die Redox-Spezifizierung von As. In Huminstofflösung wurde H₃AsO₄ –entweder chemisch oder mikrobiell- zu H₃AsO₃ reduziert, eine H₃AsO₃-Oxidation wurde jedoch nicht beobachtet. DOM induzierte Elektronentransferreaktionen sind somit sowohl in der Lage die Redoxspezifizierung von As selbst als auch die Spezifizierung von in der Natur wichtigen Elementen wie Fe und S zu verändern. Durch Reduktion von As(V) oder Fe(III) ist dabei von einer Erhöhung der As-Mobilität auszugehen.

Sorption auf Mineraloberflächen ist einer der wichtigsten Immobilisierungsprozesse für As in Böden und Sedimenten. Dieser Festlegungsmechanismus wird durch die Anwesenheit von DOM gestört. In Laborversuchen verringerten Huminstoffen die Ausfällung und Sedimentation von Fe-Oxidpartikeln und förderten die Bildung von kleinen DOC- und Fe-haltigen Komplexen und Kolloiden bei molaren Fe/C-Verhältnissen von < 0.1 . Auch die Entfernung von As aus der Lösung durch Kopräzipitation und Sedimentation mit Fe-Oxiden wurde dadurch vermindert. Die Gehalte von As und Fe in verschiedenen Partikel-Größenfraktionen waren korreliert, was auf die Bindung von As an Fe z.B. in Kationen-Komplexen oder an DOM-stabilisierten Fe-Kolloidoberflächen hinweist. Die Adsorption von organischer Substanz an Mineraloberflächen, wie Goethit oder natürlichen Boden- und Sedimentproben, führte zu Freisetzung von dort gebundenem As durch Konkurrenz um Sorptionplätze und damit ebenfalls erhöhten As-Konzentrationen in der Lösungsphase. Insbesondere die schwach gebundene As-Fraktion war davon betroffen. Sowohl die As-Bindung in DOM-stabilisierten, mobilen Komplexen oder Kolloiden als auch die Sorptionkonkurrenz zwischen As und organischem Material um Sorptionplätze auf Mineraloberflächen fördert somit die As-Mobilität und muss bei der Untersuchung von Umweltsystemen berücksichtigt werden.

In Säulenversuchen war eine direkte Redoxtransformation oder Komplexierung von As durch DOM nicht nachweisbar. Stattdessen war die As-Mobilisierung in erster Linie auf mikrobielle Prozesse zurückzuführen. Bei DOC-Konzentrationen zwischen 5 und 100 mg C L⁻¹ im Säulenperkolat fand die reduktive Auflösung der vorhandenen Fe-Oxide statt und daran gebundenes As wurde freigesetzt. Trotz einsetzender Sulfatreduktion wurde die As-Lösungskonzentration nicht nennenswert durch Bindung an die ausfallenden, sulfidischen Mineralphasen verringert.

Die untersuchten Böden sind natürliche Senken für geogenes As dar. Eisenoxide waren die wichtigsten As-Sorbenten in diesen Systemen, obwohl die Böden zumindest zeitweise wassergesättigte und vermutlich auch reduzierende Bedingungen aufwiesen. Auch die hohen DOM-Konzentrationen im Porenwasser und der hohe Gehalt an organischem Material in der Festphase wirkten der As-Bindung an die Fe-Oxide nicht entgegen. Chemische Extraktionen zeigten, dass nur kleinere As-Fractionen mit der organischen Bodensubstanz und einem nicht identifizierten residualen Bodenbestandteilen, vermutlich sulfidische Minerale, assoziiert war. Schwankende Wasserstände und Veränderungen in den Redoxverhältnisse zu einem schnellen Anstieg bzw. Abfall der Fe- und As-Konzentrationen im Porenwasser. Dies weist auf die rasche Auflösung von labilen Fe-Oxiden mit sorbiertem As unter reduzierenden und die rasche Fe-Oxid-Ausfällung und As-Festlegung unter oxidierenden Bedingungen hin. Langfristig stellen vor allem die Oberbodenhorizonten stabile Senken für geogenes As dar.

Organische Substanz beeinflusst den Redoxzustand und die Komplexierung von As und ist dadurch in der Lage die As-Verteilung zugunsten der Lösungsphase zu verschieben. Unsere Ergebnisse zeigen dass insbesondere die Bindung von As in aquatischen Komplexen und Kolloiden in der Lage ist die As-Festlegung zu verringern und die As-Mobilität zu erhöhen. In zukünftigen

Untersuchungen über das Verhalten von As in Aquiferen, Oberflächengewässern, Böden oder Sedimenten, die reich an organischen Substanzen sind, muss dies berücksichtigt werden. Die untersuchten Moorböden dagegen stellen Senken für geogenes As dar, was zeigt, dass die Präsenz organischer Verbindungen nicht zwangsläufig eine As-Festlegung verhindert. Vielmehr hängt es auch von den geochemischen Randbedingungen ab, ob ein Umweltsystem mit hohem Anteil von natürlichem organischem Material As bindet oder freisetzt.

EXTENDED SUMMARY

Introduction

1. Arsenic health concerns

Water is life. The world's freshwater resources are limited and their quality is under constant pressure. Due to the finding of high arsenic (As) enrichment in groundwater resources of the Bengal basin in South Asia and elsewhere in the world, the toxic element As is today recognized as one of the most dangerous inorganic pollutants and threats for the drinking water supply (Smedley and Kinniburgh, 2002). According to WHO estimations, 30 to 36 million people are exposed to high As concentrations in drinking water alone in Bangladesh and As contaminated aquifers are being reported from an increasing number of countries, including Taiwan, Vietnam, Chile, Argentina and the USA.

Human exposure to As through drinking water, food or air causes a variety of adverse health effects. While acute As poisoning is often fatal, long-term chronic exposure leads to dermal changes, affects organs or the nervous system and causes cancer (Bissen and Frimmel, 2003; Mandal and Suzuki, 2002). The toxic effect of As depends not only on the level of exposure but also on the As speciation and the exposition pathway. The dissolved inorganic As species are generally considered as more toxic than organic forms, and As(III) as more toxic than As(V), which is due to better resorption and higher interference with cellular biochemical processes (Bissen and Frimmel, 2003; Mandal and Suzuki, 2002).

For good reason the WHO guideline value for As in drinking water was provisionally lowered from 50 $\mu\text{g L}^{-1}$ to 10 $\mu\text{g L}^{-1}$ in 1993 (Smedley and Kinniburgh, 2002). The As drinking water limit would be even lower, when standards used for the risk assessment of industrial chemicals were applied, but in practice the compliance to the provisional value of 10 $\mu\text{g L}^{-1}$ is already difficult to achieve. Especially in the most affected developing countries water resource management is complicated. Due to low quality of removal techniques and analytical methods administrations are often unable to ascertain As concentration in drinking water below WHO guideline values. Research about the key factors and processes controlling As concentrations groundwater is therefore all the more important, particularly in the perspective of identifying risk aquifers and anticipating pollution incidents.

2. Arsenic geochemistry and mobility

Arsenic is an ubiquitous element found in the atmosphere, rocks, soils, natural waters and organisms. Arsenic pollution is often caused by anthropogenic activity, including the application of As containing pesticides and mining or smelting operations (Smedley and Kinniburgh, 2002). Exposure of reduced, sulfidic minerals or ores to oxic conditions at the surface leads to mineral dissolution and As release (Stueben et al., 2001). While these As contaminations can be attributed to zones of human

influence and activity, high As concentration in aquifers mostly results from natural, geogenic processes and is less easily located and confined. Two geochemical patterns are characteristic for the majority of As polluted aquifers, though. Firstly, naturally high As concentrations are caused by the dissolution of As binding solid phases under reducing conditions, which is the case in many aquifers of South Asia. Secondly, As desorption occurs from mineral phases due to high pH and high salinity of the groundwater, a mobilization pattern found in arid parts of South America (Smedley and Kinniburgh, 2002). These examples show that the geochemical conditions are important factors controlling the mobility of As. Understanding As speciation and chemical reaction at different pH, redox conditions and solution compositions is therefore crucial for any risk assessment.

2.1 As speciation under different pH and redox conditions

The aqueous speciation is a critical factor influencing the partitioning of As between solid and water phase. In natural waters the inorganic oxyanions of As(V) (H_3AsO_4 , arsenate) and As(III) (H_3AsO_3 , arsenite) are the most important species, as depicted in the stability diagram (Fig. 1). As(III) is considered to be the more mobile As species in the environment (Smedley and Kinniburgh, 2002), which has partly been attributed to charge. Due to a $\text{pK}_1 = 9.2$ inorganic As(III) is uncharged at neutral pH, while As(V) is negatively charged ($\text{pK}_1 = 2.2$; $\text{pK}_2 = 6.8$). Redox transformations between As(III) and As(V) occurs through chemical reactions or microbial processes. As(III) oxidation by oxygen is slow, but increases in the presence of radical species or catalysts (Cherry et al., 1979; Chui and Hering, 2000; Hug and Leupin, 2003; Kim and Nriagu, 2000). The presence of hydrogen sulfide induces the reduction of arsenate to arsenite, but was also shown to cause the formation of aqueous thioarsenic compounds (Rochette et al., 2000; Wilkin et al., 2003). Microorganisms facilitate As redox transformations by oxidizing As(III) for detoxification or by reducing As(V) as terminal electron acceptor during respiration (Oremland and Stolz, 2003). They are furthermore responsible for the production of organic As species, such as monomethylarsonic acid (MMA), dimethylarsinic acid (DMA) and others (Cullen and Reimer, 1989).

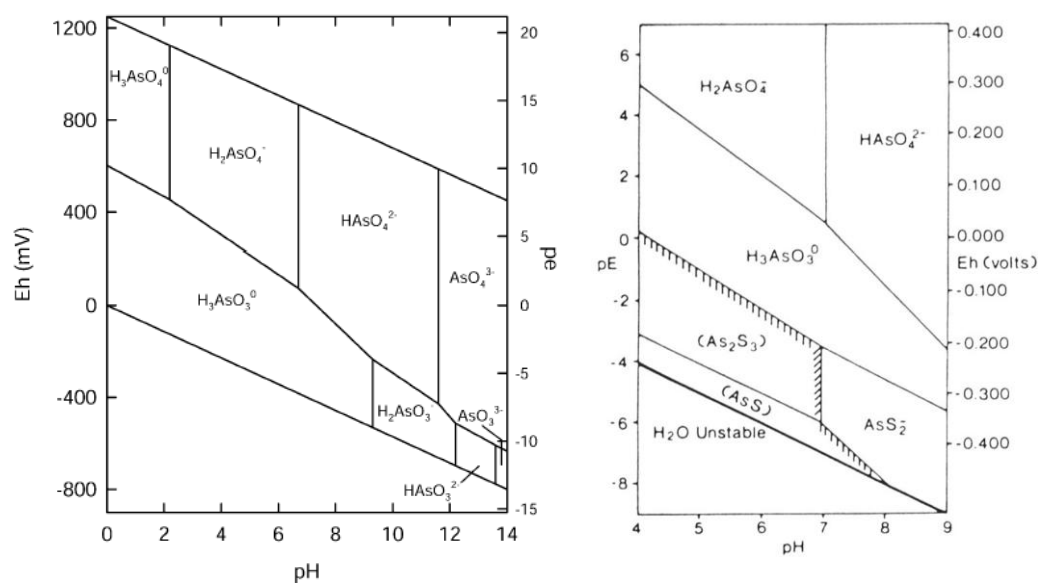
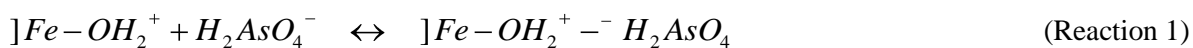


Figure 1 Stability diagram for As species in aqueous systems in the absence and presence of sulfide according to calculation of Smedley and Kinniburgh (2002) and Cherry et al. (1979).

2.2 Interactions of As with solid phases

Because it is a minor component of most environmental systems, As retention and mobilization depends strongly on reactions with solid phases. Arsenic oxyanions are bound to or incorporated in mineral phases by adsorption and (co-)precipitation processes. Fe, Mn, and Al oxides are the most important As sorbents in natural environments under oxic conditions (Dixit and Hering, 2003; Mok and Wai, 1994; Zobrist et al., 2000). This is due to their large surface area and their high pH_{pzc} (pH point of zero charge), causing mineral surfaces to be positively charged at low and neutral pH (Cornell and Schwertmann, 1996; Stumm and Morgan, 1996). Arsenic sorption on Fe oxides occurs in ionic outer and specific inner sphere surface complexes (Reaction 1 and 2) (Sun and Doner, 1998; Waychunas et al., 1993). Arsenic has a high affinity for freshly precipitating Fe oxides, i.e. ferrihydrite, and is incorporated and stabilized within the structure during mineral aging and transformation (Jessen et al., 2005; Pedersen et al., 2006; Roberts et al., 2004). Despite the fact that the capacity of Fe oxides to sorb As oxyanions is little affected by As redox speciation (Dixit and Hering, 2003), there are hints that binding of As(III) on metal oxide surfaces is less stable than binding of As(V), possibly causing an easier release to the water phase (Jain et al., 1999; Waltham and Eick, 2002). Other dissolved anions compete with As for mineral surface sites and interfere with sorption (Grafe et al., 2002; Waltham and Eick, 2002).



Silicates are alternative sorbents for As oxyanions, but due to the negative silicate surface charge at neutral pH the As binding capacity is low compared to metal oxides phases (Goldberg, 2002; Quaghebeur et al., 2005). Arsenic is also bound to calcium carbonates and precipitated as calcium arsenates in carbonate systems, but stability of As in these minerals is low under atmospheric conditions (Magalhães, 2002; Roman-Ross et al., 2006).

Sulfide minerals appear to regulate As levels in anoxic environments. Precipitation and incorporation reactions at the mineral surface were identified as the main binding mechanism of As to FeS and FeS₂ (Bostick and Fendorf, 2003). Arsenic is reduced and bound in inner sphere FeAsS complexes at the mineral surface especially under high pH conditions (Reaction 3). In highly sulfidic solutions also the formation of As sulfide minerals, such as realgar or orpiment, may considerably contribute to As retention (Bostick and Fendorf, 2003; O'Day et al., 2004). Compared to the mechanisms involved in the sorption of As oxyanions, little is yet known about the binding processes of organic As species and thioarsenic compounds.



3. Natural organic matter

In the sediments of South Asia solid phase As is mostly found associated with Fe minerals and hot spots of water contamination were observed in the vicinity of buried peat layers. The presence of natural organic material in these sediments was therefore hypothesized to increase microbial activity and lead to the increase of reductive Fe oxide dissolution with concurrent release of As (Harvey et al., 2002; McArthur et al., 2004; Pedersen et al., 2006). Only recently organic matter rich peat layers were also found to be naturally enriched with As and such possibly represent an As source themselves (Anawar et al., 2003; Meharg et al., 2006).

Peat layers consist of natural organic matter (NOM), which is an inherently complex mixture of polyfunctional organic molecules, derived from the decomposition and recombination of biogenic material from plants, animals and microorganisms (Wang and Mulligan, 2006). The properties of NOM vary widely for different samples and depend on qualities of the original material and the conditions and processes during its transformation. Nonetheless natural organic molecules share common moieties such as polar carboxyl, amino, sulfhydryl, hydroxyl, and phenol groups (Aiken et al., 1985), and also contain nonpolar aliphatic or aromatic structural units. Dissolved organic matter (DOM) is the water soluble fraction of organic molecules and includes molecules of different molecular weight and chemical structure, such as sugars, amino acids and refractory humic substances. While concentrations of dissolved organic matter are normally in the range from 1-20 mg C L⁻¹ in natural fresh waters, they may be lower in most groundwaters and reach peak concentrations of more

than 100 mg C L⁻¹ in or near humic soils, wetlands, or sediments (Aiken et al., 1985). Humic substances often represent a high fraction of dissolved organic matter due to their recalcitrance and have functional moieties with a variety of properties (Fig. 2). This makes them important reactive species in natural waters, which substantially influence the biogeochemistry of metals and trace elements.

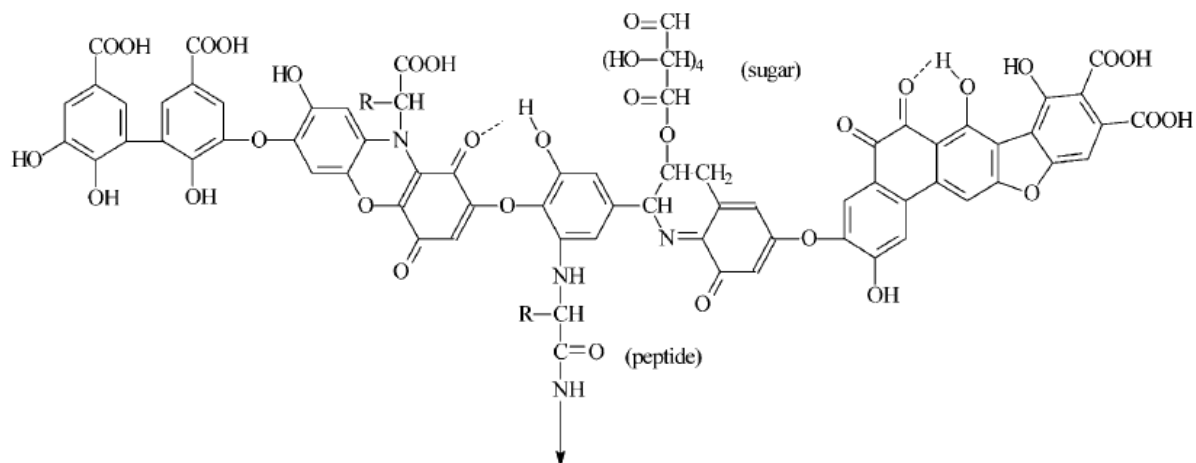


Figure 2 Schematic illustration of a dissolved organic matter molecule (Stevenson, 1994)

3.1 Redox reactions of organic matter

The redox reactions of dissolved organic matter are of high relevance for microbial electron shuttling, pollutant degradation, and metal speciation (Lovley et al., 1996; Redman et al., 2002; Schwarzenbach et al., 1990). They were attributed particularly to quinone type structures, which are ubiquitous in DOM (Cory and McKnight, 2005; Scott et al., 1998) (Fig. 3). Defined model quinones are able to carry out reversible electron accepting and donating reactions with a ratio of two electron per quinone group and at standard redox potentials E_h^0 from $< +0.30$ V to $> +0.69$ V (Helburn and Maccarthy, 1994; Rosso et al., 2004), ranking them in the range of many environmentally relevant redox couples.

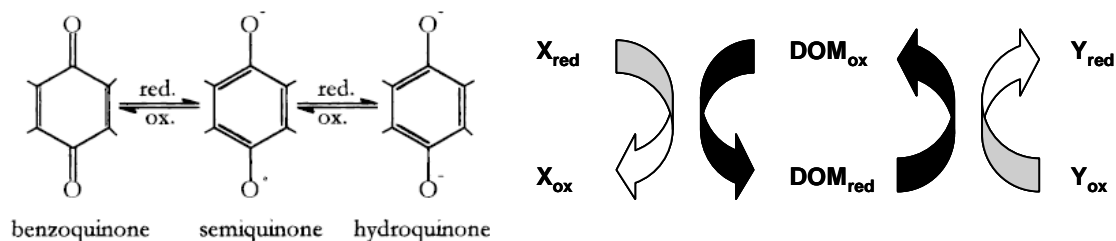


Figure 3 Redox reactions of a quinone structure (left, from Scott et al. 1998); Schematic illustration of the electron transfer reactions of organic substances (right); (Examples: X = H₂S, Zn⁰ or microorganisms; Y = Fe or As)

The determined E_h^0 values for DOM samples are between +0.23 and +0.53 V (Oesterberg and Shirshova, 1997; Palmer et al., 2006). The electron acceptor capacity (EAC) and electron donor capacity (EDC) vary over a wide range from 0.02 mequiv • (g C)⁻¹ to more than 6 mequiv • (g C)⁻¹, depending on DOM and method used (Chen et al., 2003; Kappler and Haderlein, 2003; Klapper et al., 2002; Matthiessen, 1995; Scott et al., 1998; Struyk and Sposito, 2001). The redox activity of natural organic molecules during redox titrations could be reproduced using solutions with different model quinones (Helburn and Maccarthy, 1994; Nurmi and Tratnyek, 2002). Nonetheless, in addition to quinone functionalities, likely other DOM moieties are involved in electron transfer reactions of humic substances, because quinone content alone could not explain the measured amounts of electron transfer (Struyk and Sposito, 2001). DOM was found to change the redox speciation of various inorganic species, like Fe or Cr, and also changes in As speciation were previously observed in the presence of organic matter (Buschmann et al., 2005; Palmer et al., 2006; Redman et al., 2002; Tongesayi and Smart, 2006).

3.2 Organic matter complexation reactions

Carboxylic and phenolic groups of natural organic matter are involved in aqueous and surface complexation reactions (Stumm and Morgan, 1996). The aqueous chelation of cations substantially influences the presence of free metal ions and regulates their availability and mobility in soils and aquatic environments (Christl and Kretzschmar, 2001; Pullin and Cabaniss, 2003; Stumm and Morgan, 1996; Tipping et al., 2002). Organic matter functional groups also sorb in outer sphere and inner sphere complexes on Fe oxides or clay surfaces (Filius et al., 2000; Gu et al., 1994; Kaiser et al., 1996). Finally, aqueous complexation and sorption of organic molecules on mineral surfaces contributes to the formation of colloids by altering mineral surface properties (Liang and Morgan, 1990; Tiller and O'Melia, 1993). Organic matter suspended colloids are important carriers for clay and metal oxide particles in streams and soils (Astrom and Corin, 2000; Pokrovsky et al., 2005).

Aqueous and surface complexation reactions of organic matter strongly affect As speciation and mobility (Fig. 4). Firstly, the sorption of humic anions on mineral phases, such as Fe oxides, results in competition for sorption sites and prevents As sorption or induces As desorption, both leading to a higher As concentration in the water phase (Grafe et al., 2001; Grafe et al., 2002; Redman et al., 2002). Secondly, As can be associated with mobile colloidal particles (Astrom and Corin, 2000; Puls and Powell, 1992; Tadanier et al., 2005) and the organic matter induced mobilization of colloids might such contribute to a higher mobility of As. Finally, binding of As(III) and As(V) oxyanions to humic substances in covalent bonds (Buschmann et al., 2006), ionic associations (Saada et al., 2003) or cationic bridging complexes (Lin et al., 2004; Redman et al., 2002; Thanabalasingam and Pickering, 1986) were shown to change the aqueous phase distribution of As.

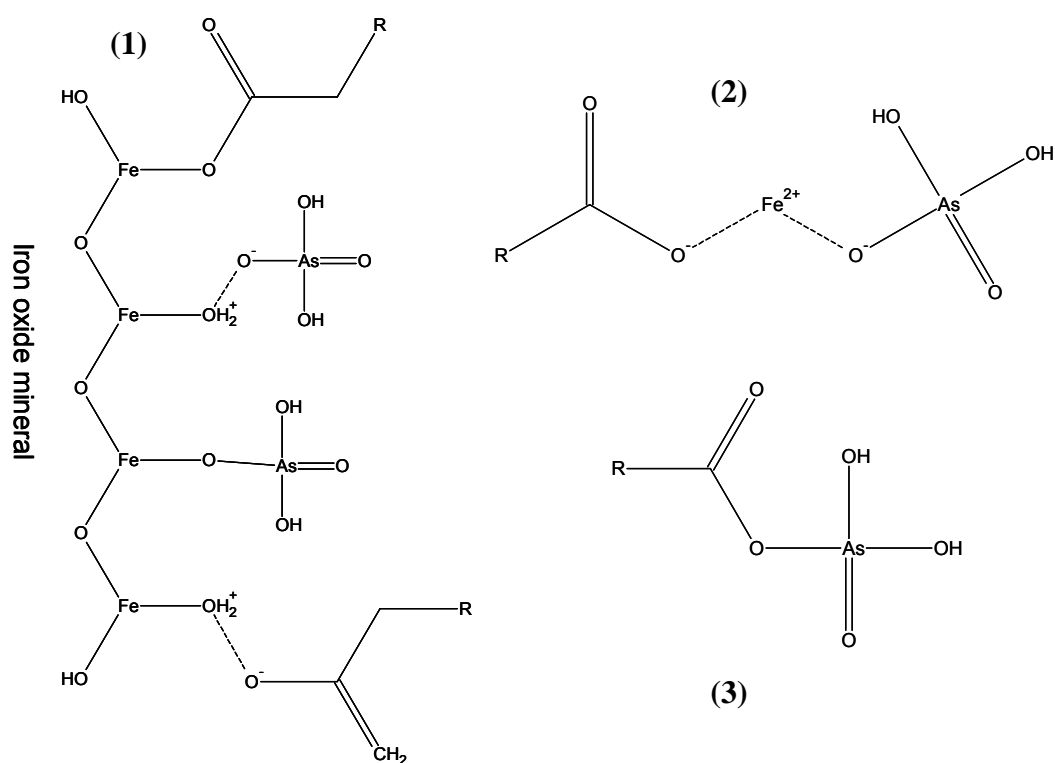


Figure 4 Sorption interactions of As and DOM on mineral oxide phases and proposed aqueous As-DOM complexes. (1) Ionic binding and inner sphere complexation of As and DOM on Fe oxide solid phase or colloidal particles. (2) Aqueous Fe cation bridging complex between As and DOM. (3) Covalent As binding to DOM; R = bulk organic molecule;

4. As mobility in environments rich in organic matter

Humic substances affect the mobility and retention of As through chemical interactions, but in addition the presence of organic matter is crucial for the reductive As release mechanism (Fig. 5). Microorganisms oxidize organic matter to CO_2 , while inorganic substances are reduced as terminal electron acceptors during respiration. The inorganic substrates are normally used according to their energy yield in the order $\text{O}_2 > \text{NO}_3^- > \text{Fe} > \text{SO}_4^{2-}$, leading to the usually observed sequence of redox reactions (Stumm and Morgan, 1996). Arsenic is mobilized partly due to chemical or microbial reduction of As(V) to As(III) (Heimann et al., 2007; Oremland and Stolz, 2003), but first and foremost the reductive dissolution of As containing Fe oxides results in high As concentrations in the water phase (Herbel and Fendorf, 2006; Islam et al., 2004; Kocar et al., 2006; Smedley and Kinniburgh, 2002). Mineral transformation and colloid formation also affect As release (Pedersen et al., 2006; Tadanier et al., 2005). Only under strongly sulfate reducing conditions a re-immobilization of As can be expected during formation of sulfide minerals (Bostick and Fendorf, 2003; Kirk et al., 2004; O'Day et al., 2004).

The availability of degradable organic matter induces microbial processes and cause the reductive release of As in aquifers. Despite high solid phase organic matter contents and high DOM concentrations in the porewater conditions in many organic matter rich wetland and peatland soils

apparently favour As sequestration and were found to lead to As accumulation in the solid phase (Gonzalez et al., 2006; McArthur et al., 2004; Meharg et al., 2006; Pfeifer et al., 2004; Steinmann and Shotyk, 1997). This is why ombrothrophic peats have been used to trace patterns of atmospheric As pollution (Shotyk et al., 1996), but As enrichment was also found in minerotrophic wetland systems rich in organic matter, where As input occurs through the groundwater (Shotyk, 1996; Steinmann and Shotyk, 1997; Szramek et al., 2004).

In mineral soils As dynamics are predominantly controlled by release of As from mineral phases or dissolution of As bearing mineral phases under changing redox conditions. Peatland and wetland soils usually contain a smaller fraction of the mineralic components and are at least partly water saturated. Fe oxides were shown to be among the most important adsorbers for As in these soils, nonetheless (Shotyk, 1996; Steinmann and Shotyk, 1997) Substantial amounts of Fe precipitates were found either in oxic surface layers or at the surfaces of oxygen conducting plant roots (Blute et al., 2004; Jacob and Otte, 2003). Pfeifer et al. (2004) hypothesize, that Fe oxides formed in organic matter rich layers are especially amorphous and have a large surface area available for sorption. The often high concentrations of dissolved organic matter apparently do not impede As sorption to metal oxides in these environments (Grafe et al., 2002). Due to seasonal variations of the water table, peat aging and burial peatland soils can be partly water saturated, resulting in low redox potentials and sulfate reducing conditions. Consequently, As binding to sulfide precipitates may be more important in wetlands than in oxic mineral soils (Bostick and Fendorf, 2003; Gonzalez et al., 2006). Finally, As was also proposed to be associated with the solid phase organic matter in sediments and peatlands (Anawar et al., 2003; Bhattacharya et al., 2001; Gonzalez et al., 2006). Arsenic association with organic matter may proceed through covalent binding or by the formation of metal bridges, as was previously hypothesized for aqueous association of As with DOM (Buschmann et al., 2006; Thanabalasingam and Pickering, 1986).

5. Objectives of the dissertation

Previous studies have shown the potential of natural organic matter to influence the retention and mobilization behaviour of As by altering the aqueous speciation of As and interacting with mineral surfaces. These processes might be of particular importance in naturally organic matter rich environments such as wetland soils, sediments or aquifers. Up to now, however, we are lacking basic information about chemical interactions between DOM and As interfering with the sequestration of As in the solid phase (Fig. 5 A). Moreover, little is also known about As dynamics in natural systems rich in organic matter and the importance of these chemical interactions for As mobility (Fig. 5 B).

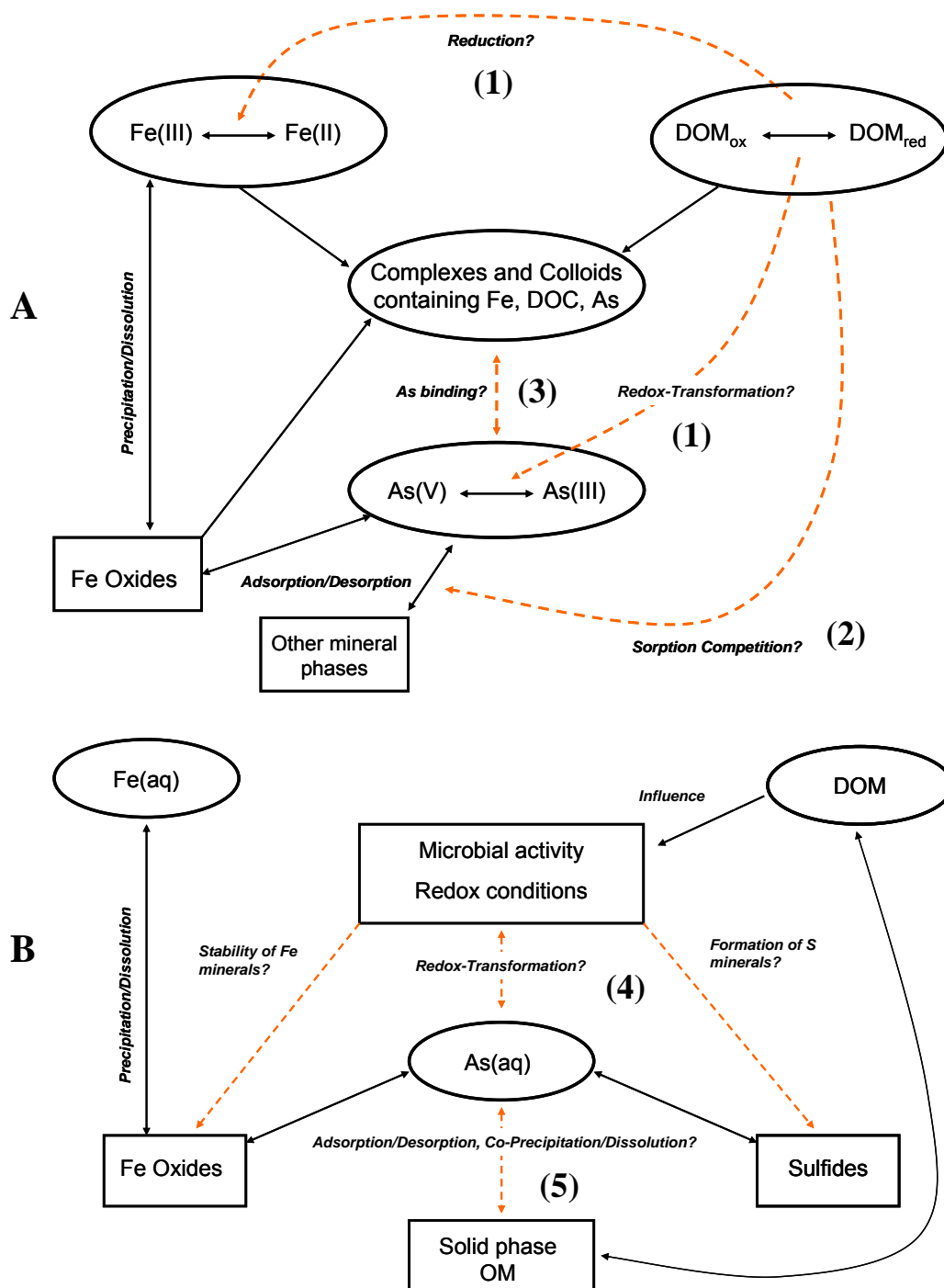


Figure 5 (A) Direct chemical interactions in aqueous systems with Fe, DOM and As; (B) Processes affecting the mobility of As in natural systems. Reactions and processes marked in red are not yet fully understood and were therefore in the focus of this study. This includes: (1) Redox reactions of organic molecules with As and other environmentally relevant elements, like Fe; (2) Effects of sorption competition effects between As and DOM at mineral surfaces; (3) Binding of As in DOM stabilized aqueous complexes or colloid; (4) As sorption on mineral phases under changing redox conditions in organic matter rich systems; (5) Importance of As binding to solid phase organic matter.

It has previously been shown that organic molecules have a substantial content of redox active functionalities. Previous reports of electron transfer capacities, reaction rates and reactivity of DOM with As(V) and As(III) have been inconsistent, suggesting that the reaction mechanisms are not yet fully understood. At the same time especially in environments poor in other electron acceptors and donors or enriched with organic matter, such as peatlands, dystrophic lakes or certain aquifers and soils the redox capacity of DOM may contribute substantially to electron transfer reactions and affect the redox speciation of As and Fe (Fig. 5 A, (1)). The first part of our study, therefore, aimed to acquire consistent data about the electron transfer capacities and the reaction rates of different organic matter samples by performing redox transformation and time series experiments with inorganic reactants of different redox potential, including As(III) and As(V).

Sorption of humic substances on synthetic mineral phases, such as Fe oxides, in surfaces complexes causes As mobilization due to the competition for surface sorption sites. Furthermore mineral phases can be mobilized as colloids. It is unclear, though, whether sorption competition will also lead to the release of As from contaminated soils and sediments (Fig. 5 A, (2)). Also we are lacking knowledge whether DOM stabilized mineral complexes and colloids are able to co-transport As and under which conditions formation of these aggregates in solution is most likely (Fig. 5 A, (3)). In waters with high DOC concentrations these processes have a potential for shifting As partitioning in favour of the mobile water phase. We addressed these research deficiencies by performing batch desorption and colloid formation experiments and by analyzing the distribution of As between aqueous and solid phase and colloidal fractions in the size range between 5 kDa and 0.2 μm . These experiments are discussed in the second part of this work.

In the environment the fate of As is strongly linked to the geochemistry of Fe and under Fe reducing conditions As is co-mobilized from the solid phase Fe oxides. Whether high dissolved organic matter concentrations might induce concurrent sulfate reduction and As immobilization in sulfide minerals is yet unclear (Fig. 5 B, (4)). We tested this hypothesis in column experiments with varying DOC percolate concentrations (Part 3).

In wetland and peatland systems metal oxides, sulfide minerals and the soil organic matter represent potential As binding pools of the solid phase. The relative importance of these solid phase fraction for As sequestration, however, is unknown as well as the stability of the different pools under changing boundary conditions (Fig. 5 B, (4)+(5)). As shown in the fourth part of this work, we studied the solid phase and aqueous phase distribution and dynamics of As in two natural systems containing geogenic As in order to identify the most important As binding phases, elucidate short-term As turnover and long-term As storage in these high organic matter soils.

I. Redox Chemistry of DOM and Electron Transfer Reactions with As

Electron transfer reactions of dissolved organic matter were shown to be involved in microbial activity, pollutant degradation, and metal mobilization (Kappler and Haderlein, 2003; Lovley et al., 1996; Schwarzenbach et al., 1990). This is due to redox active functional units, such as quinones, which are ubiquitous in natural humic substances and act as acceptors or donors for electrons (Helburn and Maccarthy, 1994; Scott et al., 1998). The determined E_h^0 values for bulk DOM samples cover a span from +0.23 to +0.53 V (Oesterberg and Shirshova, 1997; Palmer et al., 2006) and a similar wide range from < 0.30 V to > 0.69 V is also known for defined model quinones (Helburn and Maccarthy, 1994; Rosso et al., 2004). This redox potential of natural organic molecules is therefore in the range of many environmentally relevant redox couples; but depending on redox reaction partner, pH, and DOM sample very different electron acceptor capacities (EAC) and electron donor capacities (EDC) were determined ranging from 0.02 mequiv • (g C)⁻¹ to more than 6 mequiv • (g C)⁻¹ (Chen et al., 2003; Kappler and Haderlein, 2003; Klapper et al., 2002; Matthiessen, 1995; Scott et al., 1998; Struyk and Sposito, 2001).

Humic substances are increasingly recognized as important electron shuttles. But the large differences in determined redox potential values, electron transfer capacities and reaction rates demonstrate that our understanding of organic matter redox properties is still limited by various experimental and conceptual shortcomings. The different experimental protocols, reaction time scales, and organic matter samples used in previous studies prevent a comparison of experimentally determined EDC values. Direct procedures for the measurement of EAC are lacking. Furthermore contrasting results were reported for the redox transformation of As(V) and As(III) by DOM molecules (Buschmann et al., 2005; Palmer et al., 2006; Tongesayi and Smart, 2006). These deficiencies so far precluded the development of a conceptual framework for electron transfer reactions involving natural organic substances.

Our studies addressed research deficiencies concerning the redox reactions and chemical electron transfer of DOM with inorganic reactants. We conducted redox experiments using the same organic matter samples with different inorganic reductants and oxidants to determine the electron transfer capacity and the reaction rate. The inorganic reactants covered a wide range of redox potentials and the assays were run under consistent pH and ionic strength conditions to allow for comparability of the results. We furthermore tested and applied two methods for the direct determination of EAC and attempted to clarify previously encountered contradiction concerning the redox reactivity of aqueous As(III) and As(V) with DOM.

1. DOM oxidation and reduction by inorganic compounds (study 1 and 2)

Details on redox couples and the calculation of redox potentials are provided in Appendix 10. The different organic matter samples used in all studies are described in detail in Appendix 11. All DOM electron transfer experiments were carried out under the exclusion of light, with deoxygenated solutions, and in conditioned headspace vials prepared in an anaerobic glovebox at room temperature. DOM solutions were sterile filtered and incubations were run for 24 to 350 h, depending on the experiment. Samples were taken at different time steps to analyze the concentration of inorganic reaction product in the solution.

For the determination of electron donor capacities PPHA and organic matter rich water from the MerBleue peatland (MBDOM) were oxidized by ferric Fe complexed with different ligands (study 1). $[\text{Fe}(\text{bipyridyl})_3]^{3+}$, $[\text{Fe}(\text{citrate})]^{0}$, $[\text{Fe}(\text{CN})_6]^{3-}$ and $[\text{Fe}(\text{OH})_x]^{(3-x)+}$ were the Fe complexes used to provide reactants with a standard redox potential in the range of -0.3 to +1.1 V under “in assay” conditions. DOC concentrations were varied in the environmentally relevant range from 5-100 mg L⁻¹ and pH values between 4.5 and 8 were tested (Table 1). The experimental electron transfer from DOM to Fe was quantified by spectrophotometric measurement of Fe(III) reduction to Fe(II) and the electron donor capacity (EDC) was calculated by normalization to carbon concentration.

EAC of humic substances was determined indirectly by measuring the EDC to Fe(III) before and after a 4 h electrochemical reduction treatment of the organic molecules. As an alternative to this indirect procedure two methods of direct EAC determination were developed, in which electron transfer from H₂S or Zn(0) to humic substances was quantified by measurement of the oxidized S and Zn reaction products. Details of the sulfur method are described elsewhere (Heitmann and Blodau, 2006). In the Zn experiments DOM solution with DOC concentration of 5-100 mg L⁻¹ was incubated with coarse metallic Zn grains and release of Zn²⁺ into the solution was used to calculate EAC. In addition to organic matter molecules Zn⁰ also reacts with water and forming Zn²⁺ and H₂ in a pH dependent reaction. To estimate the importance of side reactions and elucidate the applicability of the Zn method for the determination of EAC, pH-stat experiments with and without DOM were carried out, in which Zn²⁺ concentration, proton consumption, and H₂ production were monitored.

All organic matter samples used reduced Fe(III) to Fe(II) and were such oxidized (Fig. 6). Ferrous Fe formation increased almost linearly with the DOM concentration, confirming that organic substances were the electron source (Fig. 7). The electron donor capacity of DOM was calculated from Fe(II) production and was between 0.07 to 1.52 mequiv (g C)⁻¹. The reaction rate decreased over time and constant Fe(II) concentrations were reached after 24-160 h. The reaction progress could be adequately modelled using two pools of redox active DOM functionalities, yielding rate constants in the range of 0.03 to 27 h⁻¹. Both EDC and reaction rate constant varied with the aqueous Fe species predominant in solution under experimental pH conditions and determined electron transfer decreased in the order of the Fe complexes $[\text{Fe}(\text{bipyridyl})_3]^{3+} > [\text{Fe}(\text{citrate})]^{0} \sim [\text{Fe}(\text{CN})_6]^{3-} > [\text{Fe}(\text{OH})_x]^{(3-x)+}$.

All DOM samples were also reduced by H₂S or metallic zinc, as the production of thiosulfate respectively Zn²⁺ showed (Fig. 9). Similar to DOM oxidation assays the amount of inorganic reaction product increased with DOC concentration (Fig. 10). The electron accepting capacity of humic substances calculated from S₂O₃²⁻ respectively Zn²⁺ production, amounted to 0.6-6.2 mequiv (g C)⁻¹. Reaction rates decreased over time for the first 50 h and rate constants were between 0.1 and 6.5 h⁻¹.

The DOM reduction by metallic zinc proved to be an applicable and robust method of EAC determination only in short experiments and under careful application due to substantial side reactions. Zn²⁺ release at pH 6.5 in DOM containing assays was substantially higher than in assays lacking DOM during the first 24 h of incubations (Fig. 16). On longer time periods the reaction of Zn with water and possibly also precipitation of Zn hydroxide and reaction of DOM with H₂ occurred (Benz et al., 1998; Stumm and Morgan, 1996) and interfered with the quantification of electron transfer by measurement of dissolved Zn²⁺.

In contrast to previous studies applying reaction time periods between 15 min to 24 h for the determination of electron transfer from DOM to Fe(III) (Chen et al., 2003; Lovley et al., 1996; Matthiessen, 1994; Scott et al., 1998) reactions times ranging from 24 h to 160 h are recommended according to the results of our kinetic experiments. With apparent reaction rates of 0.03 - 27 h⁻¹, however, the electron transfer reactions of organic matter are still sufficiently fast to compete with other redox processes in natural environments such as H₂S facilitated reduction of oxygen or crystalline Fe (Barry et al., 1994; Heitmann and Blodau, 2006).

The range of electron transfer capacities of organic matter reported in literature could be reproduced by varying determination method and inorganic reactant (Chen et al., 2003; Kappler and Haderlein, 2003; Matthiessen, 1994; Scott et al., 1998; Struyk and Sposito, 2001). This suggests that previously observed differences in ETC are likely not due to DOM properties alone but also due to different redox conditions in the experimental assays.

Under “in assay” conditions, the used inorganic reactant had different half reaction redox potential ranging from -0.86 to +1.11 V. The direction and the amount of observed electron transfer was apparently controlled by the E_h of the predominant inorganic redox couple in solution (ETC = 1.016 * E_h - 0.138; R² = 0.87) (Fig. 11). With increasing redox potential from < 0 ([Fe(OH)_x]^{(3-x)+}) to > 1 V ([Fe(bipyridyl)₃]³⁺) the carbon normalized Fe reduction increased (Fig. 11), suggesting that redox active humic moieties of increasing E_h were activated and drawn into electron transfer with increasing solution redox potential (Helburn and Maccarthy, 1994; Matthiessen, 1994). Consistently, the direction of electron transfer was reversed for the DOM reduction assays with H₂S and Zn⁰ and the EAC was higher for Zn (-0.86 V) than for H₂S (-0.19 V). Furthermore the reaction rates appeared to increase with growing E_h. This observation is in agreement with previously found linear free energy relationships between the observed rate constant and the redox potential (Dunnivant et al., 1992).

The high aromatic and humified PPHA sample, as indicated by UV absorbance, fluorescence and FTIR spectroscopy, showed consistently higher electron transfer capacity to ferric iron, sulfide or zinc than less aromatic MBDOM and even lower electron transfer from Zn to DOM was recorded for low aromatic humic substances (SRDOM, BRDOM, EVDOM, Fig. 22 and 23). In accordance with previous studies the potential for electron transfer was linked to aromaticity of the organic matter samples (Scott et al., 1998), suggesting that quinones and polyphenols of different redox potential were the main redox active functionalities also over the wide range of redox potentials applied in our study (Helburn and Maccarthy, 1994).

2. DOM redox reactivity with As (study 3)

Arsenic redox transformation in DOM solutions was tested by incubating As(III) or As(V) with different organic matter samples at pH 6 with DOC concentration from 15 to 75 mg L⁻¹. As(III) was not oxidized by most humic substances on a time scale of 4 to 7 days at pH 6 (Fig. 24 and 25) and this is in accordance with previous findings (Buschmann et al., 2005). Instead, As(V) reduction was observed with most organic matter samples (Fig. 26 and 27). Amount and reaction rate, however, varied strongly and non-systematically for the different assays, DOC concentrations and DOM samples. Inconclusive results were also found when comparing literature data about abiotic DOM induced As(V) reduction (Buschmann et al., 2005; Palmer et al., 2006; Tongesayi and Smart, 2006). We have no evidence for thermodynamic and kinetic effects or experimental artefacts to have caused the observed high variability. On the one hand non-systematic variation of electron transfer and the prevention of As(III) production upon addition of the biocide NaN₃ point to microbial processes as the reason for As(V) reduction in our experiments. On the other hand knowledge about potential reactions of NaN₃ with organic matter is lacking and due to the high measures of precaution taken to sterilize the assays microbial processes also seem unlikely. Such, even though we were unable to identify the mechanisms and determine consistent rates or capacities for the reaction of As(V) with DOM, As(V) reduction occurred in the presence of different organic matter samples.

Conclusions

Our studies showed that DOM is able to chemically reduce ferric iron in different aqueous complexes and oxidize H₂S and metallic Zn. The amount of inorganic reaction product increased with rising DOC concentration, confirming that redox active functional groups of DOM were responsible for the electron transfer reactions. The observed electron transfer capacity and, within limits, also the rate of reaction was affected by the redox potential of the inorganic reactant. According to our results the electron transfer of the studied humic molecules follows a redox ladder that encompasses redox couples ranging from $E_h < -0.48$ V to $> +0.83$ V. DOM redox properties thus provide a functional analogy to DOM acid-base properties, which have been characterized as a continuum of functionalities

with different pK values within the same DOM sample. Due to the low redox potential of the Zn couple and the consequently large electromotive force applied the high EAC determined with the Zn method should be seen as an upper limit that may not be reached in natural systems and possibly caused a irreversible alteration of DOM structure

The results of spectroscopic analysis suggest humified and aromatic rich organic matter to be more capable of electron transfer, supporting previous studies assuming quinones as the most important redox active moieties. Therefore humics from terrestrial origin, such as peatland environments, might be a particularly efficient redox active material and act as electron shuttles, i.e. between microorganisms and inorganic substrates. As peatlands represent environments rich in organic matter but especially poor in other electron acceptors and donors, DOM redox activity may contribute substantially to electron transfer reactions there. Considering the fast kinetics of the electron transfer and the abundance and mobility of DOM, humics may play a role for electron-transfer processes and the buffering of redox potentials also in other environments such aquifers, soils or dystrophic lakes.

In contrast to the other inorganic reactants our experiments indicate that the potential of DOM to chemically reduce or oxidize As is low. In the presence of DOM As(V) was reduced in relatively short periods of time, nonetheless, possibly due to microbially induced reactions. These experiments also show that our understanding of mechanisms and controls on DOM electron transfer reactions is still limited. It remains unclear, whether low reactivity of DOM with As is due to low Gibbs free reaction energy or kinetic and steric effects.

II. Aqueous and Surface Complexation Reactions of As and DOM

In organic matter rich waters the immobilization of As by binding to the solid phase is impeded by the presence of humic substances. Equilibrium concentrations of As(III) and As(V) oxyanions in the aqueous phase are lowered by binding to organic molecules through covalent bonds, ionic interactions or cation bridging complexes (Buschmann et al., 2006; Redman et al., 2002; Saada et al., 2003; Thanabalasingam and Pickering, 1986). Chelation of Fe cations by DOM and sorption of organic molecules on forming Fe oxide surfaces furthermore reduces the formation and sedimentation of Fe oxide mineral phases, which represent an important sorbent for As (Kaiser and Zech, 1997; Pullin and Cabaniss, 2003). Arsenic attached to suspended colloids can be co-transported in aquifers and surface waters (Astrom and Corin, 2000; Puls and Powell, 1992). Also, the competition for mineral sorption sites with DOM anions interferes with the sorption of dissolved As on mineral solid phases, such as Fe and Al oxides or silicates (Grafe et al., 2001; Grafe et al., 2002; Redman et al., 2002; Smith et al., 2002; Waltham and Eick, 2002; Xu et al., 1991).

The presence of organic matter shifts the As sorption equilibrium between mineral phases and liquid phase in favour of the solution and thus increases the mobility of the toxic element. It is unknown, though, whether DOM induced As release also occurs from natural soil or sediment samples, which consist of a mixture of mineral and organic phases. Also we are lacking information about the potential of DOC and Fe containing colloids to bind and co-transport As. Little is known about the conditions, under which these aggregates do form, such as pH, ionic strength and aqueous concentrations of DOC or Fe, about their size range as well as about As binding mechanisms. In order to understand As dynamics in environments rich in organic matter and Fe the knowledge about these processes is strongly required.

This study therefore analyzed on the effect of DOM to increase As presence in the aqueous phase. We examined the experimental formation of aqueous complexes and colloids containing As, Fe and DOM for different initial concentrations, DOM samples and conditions of pH and ionic strength. We aimed to identify the mechanisms contributing to As binding in these colloidal entities. Furthermore As sorption and desorption was investigated with Fe oxides and natural soil or sediment samples from different geochemical origin. In addition to previous studies we also considered possible effects of DOM on the As redox state in these experiments.

1. Complex and colloid formation in solutions with Fe, DOM and As (study 4 and 5)

We carried out aqueous complexation and colloid formation batch experiments with different DOM samples (Table 9). The standard assays were started by mixing aqueous As(V), DOM and Fe(III) at pH 3 (Fig. 28). Raising the pH initiated the formation of aquatic complexes and colloids containing Fe, DOM and As. After incubation for 0.5-144 h, solution aliquots were size fractionated by filtration (0.2 μm , 50 kDa, 5 kDa) and filtrates were analyzed for As, Fe and C concentration. In variation of this standard procedure initial conditions were changed in the range from 0 to 40 mg L^{-1} C, 0 to 200 $\mu\text{mol L}^{-1}$ Fe, and from pH 4 to 8. Alternatively, As association with DOM and Fe containing aggregates was studied in dialysis experiments at pH 6. The partitioning of As between a deionized water phase and organic matter solutions amended with different amounts of Fe(III) was analyzed during incubations of up to 1 month duration by measuring As, Fe and C concentration in the dialysate and dialysis solution.

Preliminary experiments revealed that in the absence of humic substances Fe at a concentration of 80 $\mu\text{mol L}^{-1}$ Fe(III) completely precipitated and sedimented as Fe oxide in aggregates larger than 0.2 μm . All As(V) present in these solutions was adsorbed to this solid phase and also removed by filtration (Dixit and Hering, 2003). In presence of 20 mg L^{-1} DOC, however, substantial amounts of Fe and As were also found in aggregates smaller than 0.2 μm in size (Fig. 29). Organic molecules apparently interfered with the formation and the sedimentation of Fe phases, a phenomenon which has previously been attributed to the aqueous complexation of Fe cations and the formation of DOM stabilized Fe colloid particles (Liang and Morgan, 1990; Pullin and Cabaniss, 2003; Tipping et al.,

2002). Arsenic was still predominantly associated with Fe, as the correlation of As and Fe concentrations suggest, and such the presence of DOM also increased the amount of As in small size classes. The formation of aqueous complexes and colloids took place within the first 24 h of incubation, leading to constant concentrations of Fe, DOC and As in the different size classes (Fig. 30).

The size of forming aggregates varied with the initial ratio of Fe to DOC in the solution (Fig. 34). Fe and DOC containing colloids were smallest at a Fe/DOC ratio < 0.02 (mol mol^{-1}). Aqueous complexation model calculation with the WINHUMIC model (Tipping, 1994) suggested that at these low Fe concentrations DOM was able to bind all Fe cations in aqueous complexes and that way reduced the availability of Fe(III) for mineral precipitation (Fig. 35). Arsenic was mostly in the size class smaller than 5 kDa under these conditions and association of As with aggregates through covalent bonds or cation bridges was apparently low (Buschmann et al., 2006; Redman et al., 2002).

With rising Fe/DOC ratio the amount of Fe in large colloids increased and all Fe was present in structures $> 0.2 \mu\text{m}$ above a molar ratio of Fe/DOC = 0.1 in PPHA solution. According to model results, Fe chelating functionalities of organic matter were saturated at a molar Fe/DOC ratio above 0.02. Excess Fe was therefore subject to Fe oxide precipitation. The sorption of humic substances on the surface of forming Fe mineral phases still substantially interfered with mineral growth and particle sedimentation up to a Fe/DOC ratio of 0.1 (Liang and Morgan, 1990; Pullin and Cabaniss, 2003). The effect of rising Fe/DOC ratio on the As distribution in the different size fractions was similar to that of Fe, indicating that As was predominantly bound to Fe particles despite potential sorption competition effects with organic molecules (Dixit and Hering, 2003; Grafe et al., 2002).

The use of SRDOM limited particle growth more strongly than PPHA (Fig. 30). We attribute this to the initially larger amount of low molecular weight structures compared to PPHA, and the higher availability of Fe chelating carboxyl groups in these low weight fractions (Amirbahman and Olson, 1995). The development of predominantly large DOC, Fe and As containing flocs at a low pH of 4 is explained by charge neutralization and the hydrophobic coagulation of humic substances in the presence of dissolved Fe (Kaiser, 1998; Nierop et al., 2002) (Fig. 32).

Longer reaction time periods of 2 to 4 weeks were required in dialysis experiments, but this was due to equilibration at the dialysis membrane rather than the formation of the aqueous associations containing Fe, DOC and As. In these assays organic matter also served to suspend inherently present or added Fe in the solution by forming non-colloidal DOM-Fe complexes or Fe-DOM colloids (Fig. 37 and 38). In analogy to the batch experiments As was associated with Fe and DOM containing aggregates and As binding to these structures increased with rising Fe concentration of the humic acid solution, i.e. Fe/C ratio (Fig. 41).

2. Influence of DOM on As binding to mineral surfaces (study 6)

Arsenic sorption to mineral surfaces was also analyzed in batch experiments. Synthetic goethite was suspended in As(III) or As(V) solution for 24 h at pH 6. After removal of the supernatant the goethite with sorbed As was resuspended in a solution containing 0 or 25 mg C L⁻¹. In similar assays, As contaminated soil and sediment samples were suspended in solutions with DOC concentration between 0 and 100 mg C L⁻¹. The change in aqueous As concentrations was monitored in intervals for up to 240 h in the assays. The DOM facilitated As release from soil and sediment samples was compared to chemical As extraction from different mineral pools.

The addition of DOM to previously prepared synthetic goethite with sorbed As(V) or As(III) did not result in the formation of As containing colloids > 0.45 µm in size. However, substantial, rapid As release from the solid phase was observed and amounted to 5.3-13.3 µmol (g Goethite)⁻¹ or 10 to 53 % of all goethite bound As (Fig. 44), which was within the range of previously reported data for different Fe oxides (Grafe et al., 2001; Grafe et al., 2002; Redman et al., 2002). Arsenic mobilization increased with DOC concentration and organic matter was concurrently removed from the aqueous phase, suggesting that competition for Fe oxide sorption sites between organic matter and As anions was the main As release mechanism.

DOM solutions also had a strong potential to desorb As from different natural soil and sediment samples (Table 17, Fig. 45). The relative release of 0-2.9 % of total As was substantially lower than from synthetic goethite. In natural samples As was not only sorbed to mineral surfaces but also incorporated in other mineral structures only extractable with strong acids (Keon et al., 2001; Lombi et al., 2000). But similar to experiments with synthetic goethite, As release from soil samples rich in Fe oxides was rapid, increased with DOC concentrations and involved the concomitant sorption of DOM.

3. Aqueous and surface complexation reactions and the redox speciation of As

The As redox speciation was monitored for selected experiments of complexation colloid formation and desorption. Arsenic redox state affected its presence in the aqueous complexes or colloids and the desorption of As from Fe oxide. The fraction of As associated with aqueous aggregates was lower when As(III) was used instead of As(V) under otherwise identical reaction conditions. In accordance with previous observations As(III) was also more easily desorbed from synthetic goethite than As(V) during desorption experiments (Jain et al., 1999; Waltham and Eick, 2002). The presence of DOM, however, did not substantially reduce As(V) to As(III) in both aqueous complexation and desorption assays. Under the experimental conditions As release due to reduction by humic substances was therefore negligible.

Conclusions

Compared to experiments without humic substances the presence of DOM strongly interfered with the precipitation and sedimentation of Fe oxides minerals in DOC and Fe containing solutions and lead to the formation of colloids smaller than $> 0.2 \mu\text{m}$. Organic molecules facilitated the aqueous chelation of Fe^{3+} and prevented mineral growth and sedimentation by binding on Fe oxide surfaces. Consequently the size of the forming colloids decreased with declining Fe concentration and Fe/C ratio. Arsenic content in the colloids strongly related to the presence of Fe, showing that As is predominantly bound to Fe oxide mineral phases.

DOM also had a strong potential to mobilize As from synthetic Fe oxides and natural soil or sediment material by sorption competition between As and organic matter anions for mineral sorption sites. Arsenic was released into the solution as free ion and no mobilization of As containing mineral colloids larger than $0.45\mu\text{m}$ was observed. Organic matter is apparently more efficient in stabilizing small, freshly forming Fe particles in the aqueous phase than in mobilizing large and fully precipitated Fe oxide minerals.

Humic substances are abundant in most natural waters and in rivers and soils a substantial fraction of Fe is transported in chelates or colloidal associations with DOM of 1 kDa to $0.8 \mu\text{m}$ size. According to our results a co-transport of As in these complexes or colloids likely occurs and must be expected in organic matter rich soils, wetlands or groundwater especially under transient redox conditions and with a low Fe/DOC ration in the solute phase. Co-transport leads to a lower As retention and higher As mobility than would be expected for Fe rich systems under oxic conditions. The DOM induced desorption of As must be considered in all systems receiving high organic matter percolate, but only the weakly sorbed fraction of As in natural soils and sediments is affected by the sorption competition with DOM.

III. Effect of DOM Load on the As Mobilization (study 7)

The fate of Fe oxide bound As is important in aquifers and surface waters potentially used as drinking water supply (Smedley and Kinniburgh, 2002), but also in anoxic environments such as near landfills or contaminated sites (Ghosh et al., 2006; Koeber et al., 2005). As shown in the previous chapters, organic matter has a high potential to increase As mobility by chemical reactions especially through aqueous and surface complexation. The relevance of chemical As mobilization mechanisms in microbially active laboratory column experiments has not previously been tested. In these systems normally microbial degradation of organic matter and concurrent reduction of Fe oxides are the dominant As release mechanisms while As is potentially reimmobilized by binding to sulfide minerals under sulfate reducing conditions (Bostick and Fendorf, 2003; Herbel and Fendorf, 2006; Islam et al., 2004; Kirk et al., 2004; Kocar et al., 2006; Koeber et al., 2005; O'Day et al., 2004).

High availability of DOM affects microbial respiration and affects Fe(III) or sulfate reduction and As mobilization. Arsenic release by Fe oxide dissolution under reducing condition could be compensated by binding on forming iron sulfide minerals, but Fe reducing bacteria often outcompete sulfate reducers. Sulfate reduction becomes favourable only when Fe oxides are depleted, thus preventing the simultaneous presence of aqueous Fe(II) and S(-II) and the precipitation of iron sulfide minerals. Alternatively, however, a similar situation may arise when respiration is not limited by the availability of electron donors, i.e. when the availability of degradable organic substrates is high.

It is currently unclear how different DOC loads influence the release and sequestration of As. Our experiments were therefore designed to elucidate the effect of increasing carbon concentration on the rate of anaerobic microbial respiration and the release of Fe and As from a column by mineral dissolution or desorption. Finally we wanted to test whether at high availability of DOC simultaneous reduction of Fe oxides and sulfate occurs and induces As immobilization with sulfide minerals.

To these ends we carried out four column experiments with ferrihydrite coated sand and sorbed As(V), receiving percolate with different dissolved organic matter concentrations. The percolate inflow concentrations were 0, 5, 20 or 100 mg L⁻¹ DOC and 2 mmol L⁻¹ SO₄²⁻ buffered at pH 6.5. Water samples taken in intervals from column outflow and the sampling port along the flowpath were analyzed for Fe²⁺, S²⁻, DOC, CO₂ and As concentrations. At the end of the experiment the column solid phase was chemically extracted and the content of Fe, S and As in different mineral pools were analyzed.

Percolation of the column with dissolved organic matter solution resulted in the export of dissolved As, Fe(II) and S(-II) in the column outflow (Fig. 48). Outflow and sampling port concentrations of these species were higher and increased earlier with rising DOC concentrations in the percolate (Fig. 49). Mass balance calculations furthermore showed that degradation of organic matter and production of CO₂ occurred within the columns. In accordance with our hypothesis an increased supply of degradable organic matter apparently induced higher rates of microbial respiration in the column and lead to a higher release of Fe and As from the solid phase.

Dissolved As concentrations increased almost concurrently with Fe²⁺, suggesting As mobilization mainly due to reductive Fe oxide dissolution (Herbel and Fendorf, 2006; Kocar et al., 2006). After a phase of high As release aqueous concentrations decreased in the columns receiving 20 and 100 mg L⁻¹ DOC. This might indicate re-immobilization or incorporation of mobile As during transformation of ferrihydrite to magnetite (Pedersen et al., 2006), but may also be due to the overall depletion of Fe oxides and solid phase As in parts of the column. Sulfate reduction to sulfide was only observed in the columns receiving 20 and 100 mg L⁻¹ DOC percolates, when Fe oxides were almost depleted and most Fe and As had already been exported. Our hypothesis that raising the DOM load would lead to concurrent reduction of Fe oxides and sulfate and in turn to a partial immobilization of released As with sulfides could not be confirmed (Bostick and Fendorf, 2003; O'Day et al., 2004).

Physicochemical As mobilization by sorption competition or colloid formation between DOM and As was not observed. Arsenic concentrations remained low in the initial phase of all column experiments, in which Fe reduction was still low. Independent of DOM concentration the organic molecules did apparently not substantially release As from the solid phase by redox transformation, desorption or colloid mobilization (Grafe et al., 2002; Tadanier et al., 2005). This might be partly due to reimmobilization of released As on the way through the column, but also shows that the importance of chemical DOM facilitated As mobilization was low compared to the effects of microbial Fe reduction.

Our experiments corroborate earlier studies about the reductive mobilization of As from Fe phases in column experiments. Raising DOM input concentration did not change the sequence of redox processes, but increased the concentrations of DIC, As, Fe²⁺, and S²⁻ in the column porewater and outflow. Arsenic export was coupled to reductive Fe oxide dissolution and Fe oxide transformation processes. Sulfate reduction was observed only when Fe oxides were almost depleted in the column and most Fe and As had already been exported. Our hypothesis that raising the DOM load would lead to concurrent reduction of Fe oxides and sulfate and, in turn, to a partial immobilization of released As with sulfides could not be confirmed. We cannot say to what extent such results can be extrapolated to aquifer materials, but possibly the high reactivity of the freshly precipitated Fe oxides played a role for the predominance of Fe reduction. A physicochemical mobilization of As by DOM due to redox transformation, sorption competition or colloid formation, was not observed. We do not exclude the occurrence of these processes in the studied column experiments, but their importance for overall As mobilization was low compared to the effects of microbial Fe reduction.

IV. Arsenic Mobility and Retention in Organic Matter Rich Peat Soils

Wetland soils cover large areas in valleys and lowlands, where groundwater occurs close to the land surface and represent retention and accumulation zones for trace metals and metalloids including As (Gonzalez et al., 2006; Meharg et al., 2006; Pfeifer et al., 2004; Steinmann and Shotyk, 1997; Szramek et al., 2004). While in most soils and sediments As is mainly bound to mineral phases, such as metal oxides or sulfides, organic matter is a major constituent of peatland soils and potentially an additional As sorbent (Bhattacharya et al., 2001; Gonzalez et al., 2006; Keon-Blute et al., 2004). Dissolved organic molecules, however, might also interfere with As binding on mineral surfaces as a competitor for sorption sites (Grafe et al., 2001; Grafe et al., 2002). Moreover, due to water table fluctuations, e.g. because of seasonal effects, drainage, climate change or peat burial in sediments, many wetland systems are subject to drying and wetting (Gorham, 1991; Meharg et al., 2006). The resulting changes in redox conditions affect the retention and transport of As and may cause As contamination in aquifers or surface waters (Huang and Matzner, 2006; McArthur et al., 2004).

Land use and climate change alter the water regime of wetlands in many areas of the world and in the face of this development information about the geochemistry of As in these environments is strongly required. Little is known, though, about the effect of changing geochemical conditions on the short-term dynamics and the long-term storage of As in organic matter rich soils. Data about the relative importance of different As sorbents in these systems, such as metal oxides, sulfide minerals or solid phase organic matter, is scarce and the effect of changing water tables and fluctuating redox conditions on the strength and stability of As binding in these phases has not yet been studied.

To improve our understanding of As dynamics in organic matter rich systems we carried out laboratory mesocosm experiments and field investigations. In the laboratory study fen soil material was incubated in undisturbed mesocosms, and subjected to a drying and rewetting cycle under controlled boundary conditions. We aimed to identify the important As mobilization and immobilization mechanisms and to elucidate the dynamics of As, Fe and S turnover in the soil in high temporal and spacial resolution. At the field site chemical analyses were conducted out to estimate the As transport and retention longer time scales of years to millenia. The current solid phase distribution of As was used in combination with porewater data and elemental flux calculations to identify current processes of As mobilization and immobilization, and to infer mechanisms and time periods leading to the extraordinary high As contents found in these soils.

1. Arsenic in peat mesocosms subject to drying and rewetting (Study 8)

For the laboratory mesocosm study three peat cores, 70 cm deep, from the minerotrophic Schlöppnerbrunnen II peatland were incubated in a 15°C climate chamber in a dried and rewetted vegetated treatment, a dried and rewetted non-vegetated treatment and a vegetated treatment at constant water level. The mesocosm experiments were run for 10 months and included one cycle of drying and subsequent rewetting. Samples were taken in high spatial and temporal resolution during the experiment and the solute phase was analyzed for reduced and oxidized species of Fe, S and DOC. In weekly intervals the aqueous species As(III) and As(V) were measured. Elemental turnover rates were determined with a mass balance approach. At the end of the experiments dried and ground peat samples were chemically extracted and elemental content was determined for different extraction pools in the soil.

In the peat mesocosms investigated, the As contained in the solid phase decreased with depth and varied between 5 and 25 mg kg⁻¹. Most As was found in acid extracts, which dissolve metal oxides, acid volatile sulfides, and carbonates. A correlation analysis suggested that Fe oxides were the most important sorbents (Dixit and Hering, 2003; Wallmann et al., 1993) (Fig. 51). The residual fraction gained in relative importance in the deeper, mostly anoxic, and strongly reduced peat and may have contained organically bound As and As associated with sulfide minerals (Bostick and Fendorf, 2003; Buschmann et al., 2006; Rochette et al., 2000; Thanabalasingam and Pickering, 1986).

Dissolved As reached high concentrations of 10 to 300 $\mu\text{g L}^{-1}$ under saturated conditions and As(III) was the predominant species at all depth in the peat cores except for the surface layer under highly unsaturated conditions (Fig. 55 and 57). The presence of plants and root activity was important for two reasons. On the one hand Fe oxide coatings are able to precipitate along oxygen transporting roots in the field, increasing the As sorption capacity in the peat core (Jacob and Otte, 2003; Keon-Blute et al., 2004). On the other hand root exudates may have increased As mobilization by sorption competition reactions and as they are easily degradable and enhance microbial respiration.

During drought dissolved As(III) was oxidized to As(V) and total aqueous concentrations dropped. Rewetting resulted in a mobilization pulse of As of 0.018 $\text{mmol m}^{-3} \text{d}^{-1}$ within days and was highly correlated to release of Fe(II) of up to 20 $\text{mmol m}^{-3} \text{d}^{-1}$ (Fig. 60). Thus the dynamics of As during drying and rewetting was coupled to Fe dynamics. Both elements were immobilized following oxidation during the dry period and rapidly released by Fe reduction and associated As mobilization upon rewetting. A similar coupling was previously observed for field studies and laboratory experiments, but was not shown for a peatland with natural As background (La Force et al., 2000; Masscheleyn et al., 1991).

2. Arsenic in degraded peatland soil (Study 9)

At the investigated field site the organic matter rich calcic/mollic gleysols are underlain by dolomitic fluviglacial deposits representing the quarternary aquifer. The two sampling spots about 50 m apart, furthermore referred to as site A and site B, varied especially in the solid phase Fe content, which was 5 times higher on site B than on site A. Soil porewater and groundwater was sampled at both sites from piezometers and suction cups installed at different depths and from a nearby groundwater well. The concentration and speciation of As and Fe was determined in the water samples as well as DOC, CO_2 and the redox sensitive parameters sulfate, nitrate and oxygen. The soil samples were taken at four depths and subjected to X-ray diffractometry and chemical extractions to analyze the mineralogy and As content of various soil mineral pools in different soil horizons.

With up to 3400 mg kg^{-1} in the topsoil the solid phase As content on the degraded peatland field site was very high compared to the studied peat mesosols and other natural sites (Gonzalez et al., 2006; Huang and Matzner, 2006; La Force et al., 2000; Masscheleyn et al., 1991; Steinmann and Shotyck, 1997). Arsenic content decreased strongly with depth to 15 mg kg^{-1} and amorphous and crystalline Fe precipitates were the main sorbents for As in all soil horizons according to results from wet chemical extractions (Fig. 63 and 64). This is not surprising given the high abundance of Fe oxides in the soil and the high affinity of As to sorb on Fe oxides phases (Dixit and Hering, 2003). The association of As with Fe phases also explains the similar depth distribution of both elements and the higher As content of the Fe rich site B compared to site A.

The soil horizons also had a high content of organic carbon and calcite. Arsenic was apparently not associated with the calcite and dolomite phases, but a substantial portion of up to 31 % of As_{tot}

could be mobilized by dispersion of soil organic matter. The importance of this As fraction increased with decreasing Fe content and can be attributed to covalent or ionic binding mechanisms (Buschmann et al., 2006; Ritter et al., 2006; Thanabalasingam and Pickering, 1986). Moreover, the presence of organic matter was hypothesized to cause a more amorphous structure of Fe precipitates leading to a higher availability of surface sorption sites (Pfeifer et al., 2004).

Due to maximum aqueous As concentrations of up to $467 \mu\text{g L}^{-1}$, the groundwater is considered as the primary source of As at the field site. As(III) was the predominant As species in the groundwater, but during the transport towards the surface oxidation, dilution and immobilization of As occurred, causing low aqueous concentrations below $10 \mu\text{g L}^{-1}$ and a dominance of As(V) in the soil porewater (Fig. 61).

According to the results of simple one-dimensional estimates the vertical As transport from the source in the groundwater to the topsoil was slow under the current conditions and to accumulate the amount of Fe and As found in the topsoil horizons today a time period of more than 10.000 years would be required. This suggests that As enrichment started before the beginning of drainage in the peatland soils. Under these likely more reducing conditions As binding to sulfide minerals and solid phase organic matter might have been more important than in the mostly oxic soils found today (Gonzalez et al., 2006; Keon-Blute et al., 2004; Pfeifer et al., 2004). Drainage is likely to have caused the oxidation of the sulfides and organic matter, and released As was efficiently re-adsorbed on the precipitated Fe oxides (Thornburg and Sahai, 2004), which represent the main As sorbent now. The soil mass loss due to the decomposition of the organic peat material under oxic conditions may have intensified the enrichment and accumulation of As, explaining the very high As content found in the topsoil horizon.

Conclusions

Arsenic in peatland mesocosms and degraded peatland soils was predominantly associated with Fe oxide phases, and the aqueous dynamics of As and Fe were essentially coupled for both peatland soils. During dry periods or drainage and in oxic zones As and Fe were immobilized following oxidation, but a rapid mobilization by Fe reduction and associated As release occurred after rewetting of the laboratory mesocosms. In organic matter dominated layers As was partly released by organic matter dispersion and a large residual, probably sulfide bound As fraction was observed in more reduced soil horizons.

In the long-term, both the minerotrophic wetland and the degraded peatland seem to serve as effective sinks for As due to the high abundance of reactive Fe oxides. Aqueous As concentrations declined under oxic conditions. On the degraded peatland site the drawdown of the water table by drainage apparently caused the stabilization and accumulation of As in the oxic topsoil layer due to. Temporarily, however, As can be mobilized at high concentration levels when water saturated and anoxic conditions are established, especially in the uppermost active peat layer, where As was

predominantly sorbed to Fe mineral phases. The mesocosm experiments revealed a quick response of aqueous As concentrations on changes in the boundary conditions.

Conclusions and Outlook

Arsenic is an element highly abundant and ubiquitous in the earth crust. Exposure to As has strongly toxic effects and poses a threat for humans health particularly where drinking water resources are affected. Geochemical processes cause As release from the solid phase and accumulation in the water phase and there is increasing evidence that the presence of natural organic matter strongly affects As mobility.

Our own laboratory studies support the assumption that DOM increases the mobility and lowers the retention of As. In the presence of humic substances aqueous As(V) was - either chemically or microbially- reduced to As(III), which is believed to be less stably bound to metal oxide minerals. Even more clearly organic matter prevented the precipitation and sedimentation of Fe oxide minerals and promoted the formation of DOM and Fe containing colloids and complexes in waters with low to moderate Fe/C ratios up to 0.1. This impeded As co-precipitation and sedimentation, increasing the fraction of mobile As in the ionic or colloidal form. Finally, the addition of DOM solution to As containing synthetic and natural mineral phases also lead to As release into the solute phase by competition between As and DOM anions for mineral sorption sites.

Humic substances thus shifted As partitioning in favour of the aqueous phase in our laboratory batch experiments. The potential of DOM to increase As mobility due to these chemical processes must therefore also be considered in natural systems, such as aquifers, surface waters, and soils or sediments. The DOM induced reduction of As(V) and the competition for mineral sorption sites between DOM and As anions must be expected to increase As mobility in all environments with high DOC concentrations, where metal oxide minerals represent the main As sink. The formation of As containing aqueous complexes and colloids will be of important especially where DOM, Fe and As rich are subject to changing redox conditions, i.e. during water treatment, during groundwater exfiltration into surface waters, or in water discharged from temporarily reducing wetland soils.

Our own findings in the peatland soil studies to some extent contrast the general assumption of an increased As mobility in organic matter rich environments. In accordance to previous observations the two studied peatlands soils represent zones of As retention and natural sinks despite the high organic matter presence in solid and aqueous phase. This is due to the abundance of Fe oxides in these soils. Arsenic was mainly associated with these Fe oxide minerals and consequently the highest As enrichment was found in the most oxic and Fe oxide rich soil layers close to the surface. Neither high DOC concentrations nor the - at least temporarily - high water table interfered with this natural As accumulation process.

The stability of As binding strongly decreased when the redox conditions changed, though. During the laboratory incubation of peatland soil, high water content and more reducing redox conditions lead to an increased As mobilization. Arsenic and Fe were released concurrently from the solid phase in

their reduced redox states in short periods of time due to redox transformation and Fe oxide dissolution. Also in the laboratory column experiments As release was controlled by reductive Fe oxide dissolution, which increased with organic matter load.

Microbially induced reduction processes apparently dominated the As mobilization in both peatland and column systems and our studies did not provide any evidence for a direct chemical As mobilization by DOM. Nonetheless, we can not exclude the occurrence of chemical interactions between As and DOM in the column experiments as the high reaction rates of microbial processes may have concealed the effects of abiotic As release.

Whether organic matter electron transfer reactions contributed to the redox transformation of Fe or As in these natural systems remains unclear. Our experiments, however, support previous finding that organic matter represents a viable electron transfer agent with various inorganic reactants, such as Fe compounds, at considerably fast reaction rates. The electron transfer capacity and reaction rates of organic matter depended on the redox potential and the Gibbs free energy of reaction, and apparently represented a redox ladder, in analogy to the acid base properties of DOM. Thus, DOM moieties might have been involved in electron transfer or shuttling to As or Fe species over a wide range of redox conditions in the soils. Generally, in all environmental systems rich in humic substances the electron transfer capacity of the organic matter must be considered as a temporal or spatial carrier for electrons. This is true for soil, sediments, peats, or in high organic matter groundwaters.

This study is not the first to point out the potential of organic substances to influence the fate of As in the environment, but the information about DOM induced redoxtransformation and the association of As with aqueous complexes and colloids was previously insufficient. Moreover little was known about the relevance of these processes in natural systems. In accordance with previous works our results clearly document DOM-As interactions in laboratory assays and show the potential, especially of complexation and colloid formation reactions, to increase the As fraction in the mobile aqueous phase.

By using natural organic matter samples and solid phase material from different environments and by analyzing peatland soils this work also attempts to elucidate the importance of DOM induced reaction for As mobility in natural systems. Even though different DOM samples induced As release from synthetic mineral phases and natural soil or sediment material, the high organic matter peatland soils represent sinks for geogenic As. It also depends on the biogeochemical conditions whether an organic matter rich soil or sediment will accumulate or release As. The mobility of As in these systems increased when conditions became wetter and more reducing. Changes in the water regime, due to peat drainage, flooding or climatic effects, thus, also directly influence the stability of the As pool in these soils and may lead increased As export. This findings also support previous reports about As release from buried peat layers under reducing conditions being the cause for As contamination of groundwater in parts of South Asia.

To further improve our understanding of As behaviour in natural organic matter rich systems some of the tested laboratory methods should be applied to samples from As and DOM rich environments. This includes the possibility to determine DOM redox state and the procedure to perform size separation and chemical characterization of complexes and colloids. Also, our experiment were mainly carried out with dissolved organic matter fractions, but the by far larger pool of organic matter in soils and sediments is in the solid phase. The properties of solid phase organic matter, whether redox properties or complexation behaviour, are up to now only very poorly understood. While the present functional groups are supposedly similar to dissolved organic molecules, the abundance of polar moieties might be strongly reduced. Whether and how this affects DOM structure and influences the redox or complexation capacities is unknown.

References

- Aiken G. R., McKnight D. M., Wershaw R. L., and MacCarthy P. (1985) *Humic substances in soil, sediment, and water*. Wiley-Interscience.
- Amirbahman A. and Olson T. M. (1995) The Role of Surface Conformations in the Deposition Kinetics of Humic Matter-Coated Colloids in Porous-Media. *Colloids and Surfaces a-Physicochemical and Engineering Aspects* **95**(2-3), 249-259.
- Anawar H. M., Akai J., Komaki K., Terao H., Yoshioka T., Ishizuka T., Safiullah S., and Kato K. (2003) Geochemical occurrence of arsenic in groundwater of Bangladesh: sources and mobilization processes. *J. Geochem. Explor.* **77**(2-3), 109-131.
- Astrom M. and Corin N. (2000) Abundance, sources and speciation of trace elements in humus-rich streams affected by acid sulphate soils. *Aquat. Geochem.* **6**, 367-383.
- Barry R. C., Schnoor J. L., Sulzberger B., Sigg L., and Stumm W. (1994) Iron Oxidation-Kinetics in an Acidic Alpine Lake. *Water Res.* **28**(2), 323-333.
- Benz M., Schink B., and Brune A. (1998) Humic Acid Reduction by *Propionibacterium freudenreichii* and Other Fermenting Bacteria. *Appl. Environ. Microbiol.* **64**(11), 4507-4512.
- Bhattacharya P., Jacks G., Jana J., Sracek O., Gustafsson J. P., and Chatterjee C. (2001) KTH Special Publication, TRITA-AMI-Report 3084.
- Bissen M. and Frimmel F. H. (2003) Arsenic - a review. - Part 1: Occurrence, toxicity, speciation, mobility. *Acta hydrochim. hydrobiol.* **31**(1), 9-18.
- Blute N. K., Brabander D., Hemond H. F., Sutton S., Newville M., and Rivers M. L. (2004) Arsenic sequestration by ferric iron plaque on cattail roots. *Environ. Sci. Technol.* **38**, 6074-6077.
- Bostick B. C. and Fendorf S. (2003) Arsenite sorption on troilite (FeS) and pyrite (FeS₂). *Geochim. Cosmochim. Acta* **67**(5), 909-921.
- Buschmann J., Canonica S., Lindauer U., Hug S. J., and Sigg L. (2005) Photoirradiation of dissolved humic acid induces arsenic(III) oxidation. *Environ. Sci. Technol.* **39**(24), 9541-9546.
- Buschmann J., Kappeler A., Lindauer U., Kistler D., Berg M., and Sigg L. (2006) Arsenite and arsenate binding to dissolved humic acids: Influence of pH, type of humic acid, and aluminum. *Environ. Sci. Technol.* **40**(19), 6015-6020.
- Chen J., Gu B. H., Royer R. A., and Burgos W. D. (2003) The roles of natural organic matter in chemical and microbial reduction of ferric iron. *Sci. Tot. Environ.* **307**(1-3), 167-178.
- Cherry J. A., Shaikh A. U., Tallman D. E., and Nicholson R. V. (1979) Arsenic Species as an Indicator of Redox Conditions in Groundwater. *J. Hydrol.* **43**(1-4), 373-392.
- Christl I. and Kretzschmar R. (2001) Interaction of copper and fulvic acid at the hematite-water interface. *Geochim. Cosmochim. Acta* **65**(20), 3435-3442.
- Chui V. Q. and Hering J. G. (2000) Arsenic adsorption and oxidation at Manganite surfaces: 1. Method for Simultaneous determination of adsorbed and dissolved arsenic species. *Environ. Sci. Technol.* **34**, 2029-2034.

-
- Cornell R. M. and Schwertmann U. (1996) *The iron oxides. Structures, properties, reactions, occurrences and uses*. VCH Verlagsgesellschaft.
- Cory R. M. and McKnight D. M. (2005) Fluorescence Spectroscopy Reveals Ubiquitous Presence of Oxidized and Reduced Quinones in Dissolved Organic Matter. *Environ. Sci. Technol.* **39**(21), 8142-8149.
- Cullen W. R. and Reimer K. J. (1989) Arsenic Speciation in the Environment. *Chemical Reviews* **89**(4), 713-764.
- Dixit S. and Hering J. G. (2003) Comparison of arsenic(V) and arsenic(III) sorption onto iron oxide minerals: Implications for arsenic mobility. *Environ. Sci. Technol.* **37**(18), 4182-4189.
- Dunnivant F. M., Schwarzenbach R. P., and Macalady D. L. (1992) Reduction of Substituted Nitrobenzenes in Aqueous-Solutions Containing Natural Organic-Matter. *Environ. Sci. Technol.* **26**(11), 2133-2141.
- Filius J. D., Lumsdon D. G., Meeussen J. C. L., Hiemstra T., and Van Riemsdijk W. H. (2000) Adsorption of fulvic acid on goethite. *Geochim. Cosmochim. Acta* **64**(1), 51-60.
- Ghosh A., Mukiibi M., Saez A. E., and Ela W. P. (2006) Leaching of arsenic from granular ferric hydroxide residuals under mature landfill conditions. *Environ. Sci. Technol.* **40**(19), 6070-6075.
- Goldberg S. (2002) Competitive adsorption of arsenate and arsenite on oxides and clay minerals. *Soil Sci. Soc. Am. J.* **66**, 413-421.
- Gonzalez Z. I., Krachler M., Cheburkin A. K., and Shotyk W. (2006) Spatial distribution of natural enrichments of arsenic, selenium, and uranium in a minerotrophic peatland, Gola di Lago, Canton Ticino, Switzerland. *Environ. Sci. Technol.* **40**(21), 6568-6574.
- Gorham E. (1991) Northern Peatland - Role in the carbon cycle and probable responses to climate warming. *Ecol. Applicat.* **1**(2), 182-195.
- Grafe M., Eick M. J., and Grossl P. R. (2001) Adsorption of arsenate (V) and arsenite (III) on goethite in the presence and absence of dissolved organic carbon. *Soil Sci. Soc. Am. J.* **65**(6), 1680-1687.
- Grafe M., Eick M. J., Grossl P. R., and Saunders A. M. (2002) Adsorption of arsenate and arsenite on ferrihydrite in the presence and absence of dissolved organic carbon. *J. Environ. Qual.* **31**(4), 1115-1123.
- Gu B. H., Schmitt J., Chen Z. H., Liang L. Y., and McCarthy J. F. (1994) Adsorption and Desorption of Natural Organic-Matter on Iron-Oxide - Mechanisms and Models. *Environ. Sci. Technol.* **28**(1), 38-46.
- Harvey C. F., Swartz C. H., Badruzzaman A. B. M., Keon-Blute N., Yu W., Ali M. A., Jay J., Beckie R., Niedan V., Brabander D., Oates P. M., Ashfaq K. N., Islam S., Hemond H. F., and Ahmed M. F. (2002) Arsenic mobility and groundwater extraction in Bangladesh. *Science* **298**(5598), 1602-1606.
- Heimann A. C., Blodau C., Postma D., Larsen F., Viet P. H., Nhan P. Q., Jessen S., Duc M. T., Hue N. T. M., and Jakobsen R. (2007) Hydrogen Thresholds and Steady-State Concentrations Associated with Microbial Arsenate Respiration. *Environ. Sci. Technol.* **41**(7), 2311-2317.
- Heitmann T. and Blodau C. (2006) Oxidation and incorporation of hydrogen sulfide by dissolved organic matter. *Chem. Geol.* **235**, 12-20.
- Helburn R. S. and Maccarthy P. (1994) Determination of Some Redox Properties of Humic-Acid by Alkaline Ferricyanide Titration. *Analyt. Chim. Acta* **295**(3), 263-272.
- Herbel M. and Fendorf S. (2006) Biogeochemical processes controlling the speciation and transport of arsenic within iron coated sand. *Chem. Geol.* **228**, 16-32.
-

-
- Huang J.-H. and Matzner E. (2006) Dynamics of organic and inorganic arsenic in the solution phase of an acidic fen in Germany. *Geochim. Cosmochim. Acta* **70**(8), 2023-2033.
- Hug S. J. and Leupin O. (2003) Iron-catalyzed oxidation of arsenic(III) by oxygen and by hydrogen peroxide: pH-dependant formation of oxidants in the Fenton reaction. *Environ. Sci. Technol.* **37**, 2734-2742.
- Islam F. S., Gault A. G., Boothman C., Polya D. A., Charnock J. M., Chatterjee D., and Lloyd J. R. (2004) Role of metal-reducing bacteria in arsenic release from Bengal delta sediments. *Nature* **430**(6995), 68-71.
- Jacob D. L. and Otte M. L. (2003) Conflicting processes in the wetland plant rhizosphere: Metal retention or mobilization? *Water Air Soil Pollut.* **3**, 91-104.
- Jain A., Raven K. P., and Loeppert R. H. (1999) Arsenite and arsenate adsorption on ferrihydrite: Surface charge reduction and net OH⁻ release stoichiometry. *Environ. Sci. Technol.* **33**, 1179-1184.
- Jessen S., Larsen F., Koch C. B., and Arvin E. (2005) Sorption and desorption of arsenic to ferrihydrite in a sand filter. *Environ. Sci. Technol.* **39**(20), 8045-8051.
- Kaiser K. (1998) Fractionation of dissolved organic matter affected by polyvalent metal cations. *Organic Geochemistry* **28**(12), 849-854.
- Kaiser K., Guggenberger G., and Zech W. (1996) Sorption of DOM and DOM fractions to forest soils. *Geoderma* **74**(3-4), 281-303.
- Kaiser K. and Zech W. (1997) Competitive sorption of dissolved organic matter fractions to soils and related mineral phases. *Soil Sci. Soc. Am. J.* **61**(1), 64-69.
- Kappler A. and Haderlein S. B. (2003) Natural organic matter as reductant for chlorinated aliphatic pollutants. *Environ. Sci. Technol.* **37**(12), 2714-2719.
- Keon N. E., Swartz C. H., Brabander D. J., Harvey C., and Hemond H. F. (2001) Validation of an arsenic sequential extraction method for evaluating mobility in sediments. *Environ. Sci. Technol.* **35**(13), 2778-2784.
- Keon-Blute N., Brabander D. J., Hemond H. F., Sutton S. R., Newville M. G., and Rivers M. L. (2004) Arsenic sequestration by ferric iron plaque on cattail roots. *Environ. Sci. Technol.* **38**, 6074-6077.
- Kim M.-J. and Nriagu J. (2000) Oxidation of arsenite in groundwater using ozone and oxygen. *Sci. Tot. Environ.* **247**, 71-79.
- Kirk M. F., Holm T. R., Park J., Jin Q. S., Sanford R. A., Fouke B. W., and Bethke C. M. (2004) Bacterial sulfate reduction limits natural arsenic contamination in groundwater. *Geology* **32**(11), 953-956.
- Klapper L., McKnight D. M., Fulton J. R., Blunt-Harris E. L., Nevin K. P., Lovley D. R., and Hatcher P. G. (2002) Fulvic acid oxidation state detection using fluorescence spectroscopy. *Environ. Sci. Technol.* **36**(14), 3170-3175.
- Kocar B., Herbel M., Tufano K., J., and Fendorf S. (2006) Contrasting effects of dissimilatory iron(III) and arsenic (V) reduction on the arsenic retention and transport. *Environ. Sci. Technol.* **40**, 6715-6721.
- Koeber R., Daus B., Ebert M., Mattusch J., Welter E., and Dahmke A. (2005) Compost-Based Permeable Reactive Barriers for the Source Treatment of Arsenic Contaminations in Aquifers: Column Studies and Solid-Phase Investigations. *Environ. Sci. Technol.* **39**(19), 7650-7655.
- La Force M. J., Hansel C. M., and Fendorf S. (2000) Arsenic speciation, seasonal transformations, and co-distribution with iron in a mine waste-influenced palustrine emergent wetland. *Environ. Sci. Technol.* **34**, 3937-3943.
-

-
- Liang L. and Morgan J. J. (1990) Chemical aspects of iron oxide coagulation in water: Laboratory studies and implications for natural systems. *Aquat. Sci.* **51**(1), 32-55.
- Lin H. T., Wang M. C., and Li G. C. (2004) Complexation of arsenate with humic substance in water extract of compost. *Chemosphere* **56**(11), 1105-1112.
- Lombi E., Sletten R. S., and Wenzel W. W. (2000) Sequentially extracted arsenic from different size fractions of contaminated soils. *Water Air Soil Pollut.* **124**(3-4), 319-332.
- Lovley D. R., Coates J. D., BluntHarris E. L., Phillips E. J. P., and Woodward J. C. (1996) Humic substances as electron acceptors for microbial respiration. *Nature* **382**(6590), 445-448.
- Magalhães C. M. F. (2002) Arsenic. An environmental problem limited by solubility. *Pure Appl. Chem.* **74**, 1843-1850.
- Mandal B. K. and Suzuki K. T. (2002) Arsenic round the world: A review. *Talanta* **58**, 201-235.
- Masscheleyn P. H., Delaune R. D., and Patrick W. H. (1991) Effect of Redox Potential and Ph on Arsenic Speciation and Solubility in a Contaminated Soil. *Environ. Sci. Technol.* **25**(8), 1414-1419.
- Matthiessen A. (1994) Evaluating the redox capacity and the redox potential of humic acids by redox titrations. In *Humic substances in the global environment and implications on human health* (ed. N. Senesi and T. M. Miano), pp. 187-192. Elsevier Science.
- Matthiessen A. (1995) Determining the redox capacity of humic substances as a function of pH. *Vom Wasser* **84**, 229-235.
- McArthur J. M., Banerjee D. M., Hudson-Edwards K. A., Mishra R., Purohit R., Ravenscroft P., Cronin A., Howarth R. J., Chatterjee A., Talukder T., Lowry D., Houghton S., and Chadha D. K. (2004) Natural organic matter in sedimentary basins and its relation to arsenic in anoxic groundwater: the example of West Bengal and its worldwide implications. *Appl. Geochem.* **19**, 1255-1293.
- Meharg A. A., Scrimgeour C., Hossain S. A., Fuller K., Cruickshank K., Williams P. N., and Kinniburgh D. G. (2006) Codeposition of organic carbon and arsenic in Bengal Delta aquifers. *Environ. Sci. Technol.* **40**(16), 4928-4935.
- Mok and Wai C. M. (1994) Arseni. In *Arsenic* (ed. J. Nriagu).
- Nierop K., G.J., Jansen B., and Verstraten J. M. (2002) Dissolved organic matter, aluminum and iron interaction: precipitation induced by metal/carbon ratio, pH and competition. *Sci. Tot. Environ.* **300**, 201-211.
- Nurmi J. T. and Tratnyek P. G. (2002) Electrochemical properties of natural organic matter (NOM), fractions of NOM, and model biogeochemical electron shuttles. *Environ. Sci. Technol.* **36**(4), 617-624.
- O'Day P. A., Vlassopoulos D., Root R., and Rivera N. (2004) The influence of sulfur and iron on dissolved arsenic concentrations in the shallow subsurface under changing redox conditions. *Proceedings of the National Academy of Sciences of the United States of America* **101**(38), 13703-13708.
- Oesterberg R. and Shirshova L. (1997) Oscillating, nonequilibrium redox properties of humic acids. *Geochim. Cosmochim. Acta* **61**(21), 4599-4604.
- Oremland R. S. and Stolz J. F. (2003) The ecology of arsenic. *Science* **300**(5621), 939-944.
- Palmer N. E., Freudenthal J. H., and von Wandruszka R. (2006) Reduction of arsenates by humic materials. *Environm. Chem.* **3**(2), 131-136.
- Pedersen H. D., Postma D., and Jakobsen R. (2006) Release of arsenic associated with the reduction and transformation of iron oxides. *Geochim. Cosmochim. Acta* **70**(16), 4116-4129.
-

-
- Pfeifer H. R., Gueye-Girardet A., Reymond D., Schlegel C., Temgoua E., Hesterberg D. L., and Chou J. W. Q. (2004) Dispersion of natural arsenic in the Malcantone watershed, Southern Switzerland: field evidence for repeated sorption-desorption and oxidation-reduction processes. *Geoderma* **122**(2-4), 205-234.
- Pokrovsky O. S., Dupre B., and Schott J. (2005) Fe-Al-organic colloids control of trace elements in peat soil solutions: Results of ultrafiltration and dialysis. *Aquat. Geochem.* **11**(3), 241-278.
- Pullin M. J. and Cabaniss S. E. (2003) The effects of pH, ionic strength, and iron-fulvic acid interactions on the kinetics of nonphotochemical iron transformations. I. Iron(II) oxidation and iron(III) colloid formation. *Geochim. Cosmochim. Acta* **67**(21), 4067-4077.
- Puls R. W. and Powell R. M. (1992) Transport of inorganic colloids through natural aquifer material: Implications for contaminant transport. *Environ. Sci. Technol.* **26**, 614-621.
- Quaghebeur M., Rate A., Rengel Z., and Hinz C. (2005) Desorption kinetics of arsenate from kaolinite as influenced by pH. *J. Environ. Qual.* **34**, 479-486.
- Redman A. D., Macalady D. L., and Ahmann D. (2002) Natural organic matter affects arsenic speciation and sorption onto hematite. *Environ. Sci. Technol.* **36**(13), 2889-2896.
- Ritter K., Aiken G. R., Ranville J., Bauer M., and Macalady D. L. (2006) Evidence for the aquatic binding of arsenate by natural organic matter (NOM)-suspended Fe(III). *Environ. Sci. Technol.* **40**, 5380-5387.
- Roberts L. C., Hug S. J., Ruettimann T., Billah M., Khan A. W., and Rahman M. T. (2004) Arsenic removal with iron(II) and iron(III) waters with high silicate and phosphate concentrations. *Environ. Sci. Technol.* **38**(1), 307-315.
- Rochette E. A., Bostick B. C., Li G., and Fendorf S. E. (2000) Kinetics of Arsenate Reduction by Dissolved Sulfide. *Environ. Sci. Technol.* **34**, 4714-4720.
- Roman-Ross G., Cuello G. J., Turrillas X., Fernandez-Martinez A., and Charlet L. (2006) Arsenite sorption and co-precipitation with calcite. *Chem. Geol.* **233**(3-4), 328-336.
- Rosso K. M., Smith D. M. A., Wang Z. M., Ainsworth C. C., and Fredrickson J. K. (2004) Self-exchange electron transfer kinetics and reduction potentials for anthraquinone disulfonate. *J. Phys. Chem. A* **108**(16), 3292-3303.
- Saada A., Breeze D., Crouzet C., Cornu S., and Baranger P. (2003) Adsorption of arsenic (V) on kaolinite and on kaolinite-humic acid complexes - Role of humic acid nitrogen groups. *Chemosphere* **51**(8), 757-763.
- Schwarzenbach R. P., Stierli R., Lanz K., and Zeyer J. (1990) Quinone and Iron Porphyrin Mediated Reduction of Nitroaromatic Compounds in Homogeneous Aqueous-Solution. *Environ. Sci. Technol.* **24**(10), 1566-1574.
- Scott D. T., McKnight D. M., Blunt-Harris E. L., Kolesar S. E., and Lovley D. R. (1998) Quinone moieties act as electron acceptors in the reduction of humic substances by humics-reducing microorganisms. *Environ. Sci. Technol.* **32**(19), 2984-2989.
- Shotyk W. (1996) Natural and anthropogenic enrichments of As, Cu, Pb, Sb, and Zn in ombrothrophic versus minerotrophic peat bog profiles, Jura mountains, Switzerland. *Water Air Soil Pollut.* **90**, 375-405.
- Shotyk W., Cheburkin A. K., Appleby P. G., Fankhauser A., and Kramers J. D. (1996) Two thousand years of atmospheric arsenic, antimony, and lead deposition recorded in an ombrothrophic peat bog profile, Jura mountains, Switzerland. *Earth. Planet. Sci. Lett.* **145**(1-4), E1-E7.
-

-
- Smedley P. L. and Kinniburgh D. G. (2002) A review of the source, behaviour and distribution of arsenic in natural waters. *Appl. Geochem.* **17**(5), 517-568.
- Smith E., Naidu R., and Alston A. M. (2002) Chemistry of Inorganic Arsenic in Soils: II. Effect of Phosphorus, Sodium, and Calcium on Arsenic Sorption. *J. Environ. Qual.* **31**, 557-563.
- Steinmann P. and Shotyk W. (1997) Geochemistry, mineralogy, and geochemical mass balance on major elements in two peat bog profiles (Jura mountains, Switzerland). *Chem. Geol.* **138**, 25-53.
- Stevenson F. J. (1994) *Humus chemistry-Genesis, Composition, Reactions*. John Wiley and Sons, Inc.
- Struyk Z. and Sposito G. (2001) Redox properties of standard humic acids. *Geoderma* **102**, 329-346.
- Stueben D., Berner Z., Kappes B., and Puchelt H. (2001) Environmental monitoring of heavy metals and arsenic from Ag-Pb-Zn mining. *Environ. Monit. Assess.* **70**, 181-200.
- Stumm W. and Morgan J. J. (1996) *Aquatic chemistry*. Wiley Interscience.
- Sun X. H. and Doner H. E. (1998) Adsorption and oxidation of arsenite on goethite. *Soil Sci.* **163**(4), 278-287.
- Szramek K., Walter L. M., and McCall P. (2004) Arsenic mobility in groundwater/surface water systems in carbonate-rich Pleistocene glacial drift aquifers (Michigan). *Appl. Geochem.* **19**(7), 1137-1155.
- Tadanier C. J., Schreiber M. E., and Roller J. W. (2005) Arsenic mobilization through microbially mediated deflocculation of ferrihydrite. *Environ. Sci. Technol.* **39**(9), 3061-3068.
- Thanabalasingam P. and Pickering W. F. (1986) Arsenic Sorption by Humic Acids. *Environ. Pollut.* **12**(3), 233-246.
- Thornburg K. and Sahai N. (2004) Arsenic Occurrence, Mobility, and Retardation in Sandstone and Dolomite Formations of the Fox River Valley, Eastern Wisconsin. *Environ. Sci. Technol.* **38**, 5087-5094.
- Tiller C. L. and O'Melia C. R. (1993) Natural organic matter and colloidal stability: Models and measurements. *Colloids Surf., A* **73**, 89-102.
- Tipping E. (1994) WHAM - A chemical equilibrium model and computer code for water, sediments, and soils incorporating a discrete/electrostatic model of ion-binding humic substances. *Computer Geosciences* **20**, 973-1023.
- Tipping E., Rey-Castro C., Bryan S. E., and Hamilton-Raylor J. (2002) Al(III) and Fe(III) binding by humic substances in freshwaters, and implications for trace metal speciation. *Geochim. Cosmochim. Acta* **66**(18), 3211-3224.
- Tongesayi T. and Smart R. B. (2006) Arsenic speciation: Reduction of arsenic(v) to arsenic(III) by fulvic acid. *Environm. Chem.* **3**(2), 137-141.
- Wallmann K., Hennies K., Petersen W., and Knauth H. D. (1993) New procedures for determining reactive Fe(III) and Fe(II) minerals and sediments. *Limnol. Oceanogr.* **38**(8), 1803-1812.
- Waltham C. A. and Eick M. J. (2002) Kinetics of arsenic adsorption on goethite in the presence of sorbed silicic acid. *Soil Sci. Soc. Am. J.* **66**(3), 818-825.
- Wang S. L. and Mulligan C. N. (2006) Effect of natural organic matter on arsenic release from soils and sediments into groundwater. *Environ. Geochem. Health* **28**(3), 197-214.
- Waychunas G. A., Rea B. A., Fuller C. C., and Davis J. A. (1993) Surface-Chemistry of Ferrihydrite .1. EXAFS Studies of the Geometry of Coprecipitated and Adsorbed Arsenate. *Geochim. Cosmochim. Acta* **57**(10), 2251-2269.
-

REFERENCES

- Wilkin R. T., Wallschlaeger D., and Ford R. G. (2003) Speciation of arsenic in sulfidic waters. *Geochemical Transactions* **4**(1), 1-7.
- Xu H., Allard B., and Grimvall A. (1991) Effects of Acidification and Natural Organic Materials on the Mobility of Arsenic in the Environment. *Water Air Soil Pollut.* **57-8**, 269-278.
- Zobrist J., Dowdle P. R., Davis J. A., and Oremland R. S. (2000) Mobilization of arsenite by dissimilatory reduction of adsorbed arsenate. *Environ. Sci. Technol.* **34**(22), 4747-4753.

Contributions to the Different Studies

Study 1

Electron transfer capacity and reaction kinetics of peat dissolved organic matter

M. Bauer	75 %	Laboratory work: DOM reaction with Fe species and Zn; Data analysis; Discussion of results; Manuscript preparation
T. Heitmann	10 %	Laboratory work: DOM reactions with H ₂ S; Data analysis;
D. Macalady	5 %	Concept; Discussion of results;
C. Blodau	10 %	Discussion of results; Manuscript preparation

Study 2

Electron accepting capacity of dissolved organic matter as determined by reaction with metallic zinc

M. Bauer	50 %	Concept; Laboratory work: pH stat experiments, DOM reduction, reoxidation and characterization; Data analysis; Discussion of results; Manuscript editing
C. Blodau	35 %	Concept; Data analysis; Discussion of results; Manuscript preparation
S. Regenspurg	10 %	Laboratory work: DOM reduction experiments; Data analysis; Discussion of results
D. Macalady	5 %	Concept; Discussion of results

Study 3

Oxidation of As(III) and reduction of As(V) in dissolved organic matter solutions

M. Bauer	85 %	Concept; Laboratory work; Data analysis; Discussion of results; Text preparation
C. Blodau	15 %	Concept; Discussion of results; Text editing

Study 4

Experimental colloid formation in aqueous solutions rich in dissolved organic matter, ferric iron, and As

M. Bauer	90 %	Concept; Laboratory work; Data analysis; Discussion of results; Manuscript preparation
C. Blodau	10 %	Discussion of results; Manuscript editing

*Study 5***Evidence for the aquatic binding of arsenate by natural organic matter-suspended****Fe(III)**

M. Bauer	10 %	Concept; Laboratory work: Sequential filtration experiments; Discussion of results
K. Ritter	75 %	Concept; Laboratory work: Dialysis experiments; Data analysis; Discussion of the results; Manuscript preparation
G. Aiken	5 %	Concept; Discussion of the results; Manuscript editing
J. Ranville	5 %	Concept; Discussion of the results; Manuscript editing
D. Macalady	5 %	Concept; Discussion of the results; Manuscript editing

*Study 6***Mobilization of arsenic by dissolved organic matter from iron oxides, soils and sediments**

M. Bauer	75 %	Concept; Field sampling and laboratory work; Data analysis; Discussion of results; Manuscript preparation
C. Blodau	25 %	Concept; Discussion of results; Manuscript preparation

*Study 7***Mobilization of iron and arsenic from iron oxide coated sand columns by percolation with dissolved organic matter**

M. Bauer	35 %	Concept; Laboratory work: Preliminary experiments, method development; Data analysis; Discussion of results; Text preparation
M. Raber	50 %	Laboratory work; Data analysis; Discussion of results
C. Blodau	15 %	Concept; Discussion of results; Text editing

Study 8

Arsenic speciation and turnover in intact organic soil mesocosms during experimental drought and rewetting

M. Bauer	10 %	Laboratory methods; Discussion of results
C. Blodau	35 %	Concept; Field work; Discussion of results; Manuscript preparation
B. Fulda	30 %	Laboratory work; Discussion of results
KH. Knorr	25 %	Concept; Field and laboratory work; Isotope measurements; Discussion of results

Study 9

Groundwater derived arsenic in high carbonate wetland soils: Sources, sinks, and mobility

M. Bauer	45 %	Concept; Field and laboratory work: Sampling, chemical analysis, XRD measurements; Data analysis; Discussion of results; Manuscript preparation
B. Fulda	45 %	Field and laboratory work; Data analysis; Discussion of results; Manuscript editing
C. Blodau	10 %	Concept; Field work, discussion of results, manuscript editing

APPENDIX

Study 1

Reproduced with permission from

**Electron Transfer Capacities and Reaction Kinetics of Peat Dissolved
Organic Matter**

Markus Bauer, Tobias Heitmann, Donald L. Macalady, Christian Blodau

Environmental Science & Technology, 2007, 41 (1), pp 139–145

Copyright 2007 American Chemical Society

Electron Transfer Capacities and Reaction Kinetics of Peat Dissolved Organic Matter

MARKUS BAUER,^{*,†} TOBIAS HEITMANN,[†]
DONALD L. MACALADY,[‡] AND
CHRISTIAN BLODAU[†]

*Limnological Research Station and Department of Hydrology,
University of Bayreuth, D-95440 Bayreuth, Germany, and
Department of Chemistry and Geochemistry, Colorado School
of Mines, Golden, Colorado 80401*

Information about electron-transfer reactions of dissolved organic matter (DOM) is lacking. We determined electron acceptor and donor capacities (EAC and EDC) of a peat humic acid and an untreated peat DOM by electrochemical reduction and reduction with metallic Zn and H₂S (EAC), and by oxidation with complexed ferric iron (EDC) at pH 6.5. DOC concentrations (10–100 mg L⁻¹) and pH values (4.5–8) were varied in selected experiments. EAC reached up to 6.2 mequiv·(g C)⁻¹ and EDC reached up to 1.52 mequiv·(g C)⁻¹. EDC decreased with pH and conversion of chelated to colloidal iron, and the electron-transfer capacity (ETC) was controlled by the redox potential E_h of the reactant ($ETC = 1.016 \cdot E_h - 0.138$; $R^2 = 0.87$; $p = 0.05$). The kinetics could be adequately described by pseudo first-order rate laws, one or two DOM pools, and time constants ranging from $2.1 \times 10^{-3} \text{ d}^{-1}$ to $1.9 \times 10^{-2} \text{ d}^{-1}$ for the fast pool. Reactions were completed after 24–160 h depending on the redox couple applied. The results indicate that DOM may act as a redox buffer over electrochemical potentials ranging from -0.9 to +1.0 V.

Introduction

In natural waters, dissolved organic matter (DOM) plays an important role for microbial activity (1), pollutant degradation, and metal mobility due to sorption competition and redox processes (2, 3). Of particular importance are humic substances, which contain redox-active functional units and accumulate in the environment due to their recalcitrance. The redox properties of humic substances have been particularly attributed to quinones (3, 4), which are ubiquitous in DOM (5, 6). Based on studies with model compounds, such as anthraquinone-2,6-disulfonate, juglone, and hydroquinone, a redox transfer of two electrons per quinone unit has been postulated. Standard redox potentials of these substances range from <0.3 to >0.69 V (7, 8).

The transfer of two single electrons was also documented for polyphenolic DOM (9). In addition to quinones, other moieties are likely involved in redox processes, because quinone content alone could not explain the amount of electron transfer (10). DOM redox properties could, for example, be reproduced by redox titration of mixtures of model quinones and phenols (8). Electron acceptor (EAC)

and donor capacities (EDC) varied from 0.02 mequiv·(g C)⁻¹ to more than 6 mequiv·(g C)⁻¹, depending on DOM and method used (5, 10–14), and E_h^0 values ranged from 0.4 to 0.8 V (10, 15), ranking it in the range of many environmentally relevant redox couples.

While our understanding of the redox properties of humic substances has grown, our understanding of redox dynamics in natural waters is impeded by conceptual and experimental shortcomings. It is presently unclear whether the range of reported electron-transfer capacities is the result of DOM properties or variation of experimental procedures. Electrochemical reduction and a diversity of oxidants and reductants have been used as redox partners in chemical reactions and microbial assays, all of which may target specific and different DOM moieties; DOC concentrations ranged from 5 to 2000 mg L⁻¹; and reaction progress was assumed to be completed after 15 min to 24 h. The reversibility of the electron transfer has not been sufficiently addressed and we are missing a theoretical framework that potentially explains the observed range of humic substance redox behavior.

To address these research deficiencies we conducted kinetic experiments with reductants and oxidants for DOM that cover a wide range of redox potentials under consistent conditions of pH and ionic strength. To facilitate comparison to earlier studies, both previously described and new methods to analyze electron transfer were used on a purified peat humic acid of the IHSS and an untreated peat DOM. Our specific objectives were to (1) determine to what extent the electron-transfer capacity and kinetics of humic rich dissolved organic matter depends on the reactants used, and (2) whether electron transfer is related to reactant redox potentials, i.e., the driving force of the reactions.

Materials and Methods

Sample Preparation. Pahokee Peat reference humic acid ("PP-HA"; IHSS) was dissolved at pH ~8, acidified to pH 6 (HCl), filtered (0.45 μm), and diluted to 100 mg C L⁻¹. From an open pit in the Mer Bleue wetland, Canada, DOM solution ("MB-DOM", 71 mg C L⁻¹) was sampled in December, 2004, frozen in small portions, and filtered after thawing (0.45 μm, nylon). Freezing most likely changed the DOM quality, for example due to cell lysis, but it ensured a similar DOM quality for all experiments. The solutions were characterized regarding carbon and metal content and UV-vis, FTIR, and fluorescence absorption (Supporting Information, section 1). Experimental assays were carried out under exclusion of light using reagent grade chemicals and deionized water in an oxygen-free glovebox (95% nitrogen, 5% hydrogen) or in deoxygenated headspace vials (FeCN and H₂S assays). All solutions were purged with nitrogen (>99.99%) for at least 30 min before use. Assays were replicated twice with the exception of reaction of DOM with Zn and H₂S (triplicates) and ferric cyanide (four replicates).

Experiments. To oxidize DOM with varying electromotive force, PP-HA and MB-DOM solutions were incubated with ferric iron complexed by different ligands in batch experiments at buffer concentrations of 30 mM, as described in Table 1. To further vary ferric iron speciation, the pH was altered in the range of 4.5 to 8. Spectrophotometrically determined ferrous iron concentrations were corrected using blanks devoid of ferric iron and DOM. PP-HA and MB solutions were reduced electrochemically or by reaction with H₂S and metallic Zn. The electromotive force applied decreased in the order H₂S < electrochemical reduction < metallic Zn (Table 1). Reduction with metallic Zn represents more strongly reducing conditions than found in most natural

* Corresponding author phone: +49 921 552170; fax: +49 921 552366; e-mail: markus.bauer1@uni-bayreuth.de.

[†] University of Bayreuth.

[‡] Colorado School of Mines.

TABLE 1. Overview of the Experimental Treatments Including the DOM Source, Buffer and pH, the Predominant Redox Couple of the Reactants, and the Reactant E_h at the End of Each Experimental Run; Experimentally Determined Rate Constants $k_{obs}^{(1)}$ for the Rapidly Reacting DOM Pool, Regression Coefficient for the Model Fit, and ETC Values (\pm Standard Deviation) are Also Shown

method	DOM	pH/buffer	predominant redox couple ^a	E_h (V)	$k_{obs}^{(1)}$ (h ⁻¹)	R^2	ETC (mequiv \times (g C) ⁻¹)	SD
Electron Donor Capacity (EDC); Organic Matter Oxidation								
(1)	PP-HA	4.5/acetate	FeBiPy [Fe(bipy) ₃] ³⁺ / [Fe(bipy) ₃] ²⁺	1.11	13.12	0.999	1.52	0.004
(1)	MB-DOM	4.5/acetate			27	0.999	1.4	0.12
(1)	PP-HA	5/acetate			3.54	0.999	1.22	0.004
(1)	PP-HA	5.9 /acetate	FeBiPy [Fe(bipy) ₃] ³⁺ / [Fe(bipy) ₃] ²⁺	1.11 or -0.3	9.28	0.999	0.65	0.006
(1)	MB-DOM	5.9 /acetate			16.2	0.998	0.39	0.11
(1)	PP-HA	6/MES			1.22	0.998	0.52	0.003
(3)	PP-HA	6.5/phosphate/MES	FeCN [Fe(CN) ₆] ³⁻ / [Fe(CN) ₆] ⁴⁻	0.83	0.03	0.999	0.33	0.01
(3)	MB-DOM	6.5 /phosphate/MES			0.05	0.957	1.0	0.01
(2)	PP-HA	5/acetate	FeCi [Fe(citrate)] ⁰ / [Fe(citrate)] ¹⁻	0.77	2.82	0.997	0.11	0.002
(2)	PP-HA	6/MES			2.08	0.800	0.11	0.007
(4)	PP-HA	6/MES	Fe(OH) ₃ Fe(OH) ₃ / Fe ²⁺	-0.3	3.98	0.999	0.23	0.02
(1)	PP-HA	8/carbonate		-0.5	0.96	0.996	0.07	0.002
(2)	PP-HA	8/carbonate		-0.5	2.52	0.997	0.09	0.001
Electron Acceptor Capacity (EAC); Organic Matter Reduction								
(5)	PP-HA	6/carbonate	H ₂ S/S ₂ O ₃ ²⁻	-0.19	0.103	0.995	0.6	0.07
(6)	PP-HA	6.5/phosphate	electrons ^b	-0.48			0.64	0.01
(6)	MB-DOM	6.5/phosphate					0.1	0.01
(7)	PP-HA	6.5/manual	Zn ⁰ /Zn ²⁺	-0.86	6.5	0.996	6.2	1.1
(7)	MB-DOM	6.5/manual					4.5	0.8

^aSpeciation and predominant redox couple are derived in the Supporting Information (section 4). ^b Electrochemical reduction, reoxidation with the FeCN method.

aqueous solutions but was employed to broaden the range of reactant redox potentials.

1. *Oxidation by [Fe(bipyridyl)₃]³⁺ (FeBiPy).* Ferrozine (bipyridyl reagent) and buffer solution (acetate, MES, PIPES, or carbonate) were mixed. FeCl₃ (dropwise) and DOM were added to final concentrations of 10–100 mg L⁻¹ (PP-HA), 10–50 mg L⁻¹ (MB-DOM), 2 mmol L⁻¹ ferrozine, and 0.5 mmol L⁻¹ (FeCl₃), in sealed, deoxygenated headspace vials (10 mL) or in capped plastic cuvettes (3 mL), which delivered identical results. Aliquots were sampled after 0.5–20 h and were analyzed within 15 min. VIS absorption produced by formation of colloidal iron and by addition of ferrozine at pH < 6 (as reported in ref 16) was small and accounted for by blanks.

2. *Oxidation by [Fe(citrate)]⁰ (FeCi).* DOM was added to a final concentration of 50 mg C L⁻¹ to buffer solution containing citrate (10 mM), ferrozine (2 mM), and FeCl₃ (0.5 mM). The solution was prepared and sampled analogously to (1).

3. *Oxidation by [Fe(CN)₆]³⁻ (FeCN).* DOM solution was injected by syringe into deoxygenated ferric cyanide solution contained in 10 mL headspace vials to final concentrations of 0.5 mmol L⁻¹ iron and 25–75 mg L⁻¹ DOM (pH 6.5, phosphate or MES buffer). The solutions were sampled after 24–220 h.

4. *Oxidation by Fe-Hydroxide (colloidal Fe(OH)₃).* Experiments were conducted using PP-HA concentrations of 6.25–50 mg C L⁻¹ in 5 mM MES buffer at pH 6. Dissolved FeCl₃ was added dropwise to a final concentration of 0.1 mmol L⁻¹. Samples were taken after 0.5–72 h.

5. *Reduction by H₂S.* The method has been described in detail by Heitmann and Blodau (17). Briefly, 250 μ mol L⁻¹ of H₂S gas was added to 18 mL of deoxygenated DOM solution

in headspace vials sealed with butyl rubber stoppers (25–100 mg C L⁻¹; pH 6, 50 mM carbonate buffer). After 24 h of incubation, sulfur species (H₂S, S⁰, thiosulfate, sulfite, sulfate) were analyzed. The electron acceptor capacity was calculated from the concentration of thiosulfate, which was the only identifiable inorganic reaction product (17).

6. *Electrochemical Reduction.* DOM was reduced with an electrochemical cell in 30 mM phosphate buffer according to ref 13. Experiments were stopped after 4 h of reaction time when observed currents were low and \pm constant. DOM reoxidation experiments were carried out with the FeCN method.

7. *Reduction by Zn.* Briefly, metallic Zn grains (5 g) were washed in 50 mL of 1 M HCl for 30 min and rinsed twice with deoxygenated deionized water. A volume of 50 mL of N₂-purged DOM solution augmented with KCl (5 mmol L⁻¹) was incubated for 24 h under cautious shaking at pH 6.5 and the release of dissolved Zn was determined. A more detailed description of the method is given in the Supporting Information (section 2).

Analytical Techniques. Iron reduction was measured spectrophotometrically on a Varian Cary 1 E as increase of [Fe(bipyridyl)₃]²⁺ absorption at 562 nm (18) or as decrease of [Fe(CN)₆]³⁻ absorption at 420 nm (14). Thiosulfate was determined in filtered samples (0.2 μ m, nylon) by ion chromatography (Metrohm IC-System, Metrosep Anion Dual 3 column, 0.8 mL min⁻¹ with chemical suppression). For determination of other sulfur species see Supporting Information (section 3). Dissolved Zn concentrations were analyzed on a Perkin-Elmer Optima 3000 ICP AES. Carbon concentrations were measured with a TOC analyzer (Shimadzu TOC-V CPN).

Calculations. Electron donor (EDC) and electron acceptor (EAC) capacities of DOM were calculated from formation of

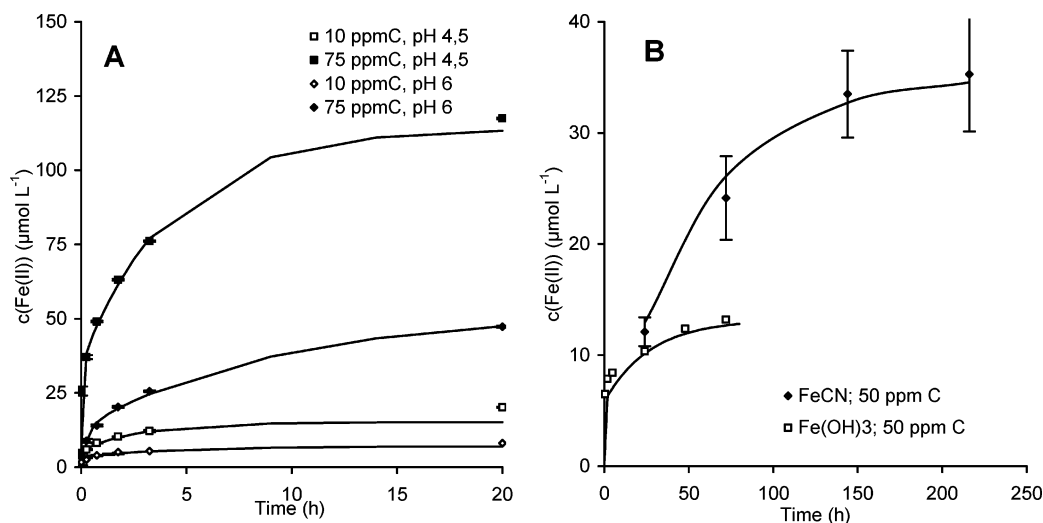


FIGURE 1. Kinetics of PP-HA oxidation by FeBiPy at pH 4.5 and 6 (A), and by FeCN (pH 6.5) and colloidal Fe(OH)₃ (pH 6.0) (B). Mean values ± 1 SD ($n = 2$; $n = 4$ for FeCN).

inorganic reaction products in the assays, and standardized on electron equivalents and mass of carbon ($\text{mequiv} \cdot (\text{g C})^{-1}$). We further define electron-transfer capacity (ETC) as encompassing both EDC (positive values) and EAC (negative values) of DOM. To relate ETC and kinetic constants to redox potential, we calculated in situ half cell potentials of the predominant redox couple from reactant concentrations. Thermodynamic data for ferric iron complexed with bipyridyl (19), cyanide (14, 19), citrate (20), and hydroxide (21), and for Zn(0) to Zn²⁺ and H₂S to S₂O₃²⁻ (22) were used. Iron speciation was calculated using the PHREEQC algorithm version 2.11.0. A detailed description of thermodynamic data and redox potential calculations is provided in the Supporting Information (sections 4 and 5).

In the experiments the inorganic reactants were in surplus. For simplicity we thus assumed a pseudo-first-order rate law with one or two redox-active DOM pools (16) and an apparent time constant k_{obs} . The parameter X represents the concentration of the inorganic product (Fe(II), S₂O₃²⁻, Zn(II)) of the redox reactions.

$$\frac{d[X]}{dt} = -k_{\text{obs}}^{(1)} \times [\text{DOM}]^{(1)} - k_{\text{obs}}^{(2)} \times [\text{DOM}]^{(2)} \quad (1)$$

The time-dependent solution to eq 1 is

$$X(t) = [\text{DOM}]_0^{(1)} (1 - 10^{-k_{\text{obs}}^{(1)} t}) + [\text{DOM}]_0^{(2)} (1 - 10^{-k_{\text{obs}}^{(2)} t}) \quad (2)$$

To examine the variation of DOM pool size by fitting, the total reactive DOM pool was estimated from product formation $[X]$ at the time point of completion for single experiments, and alternatively from the relation between product formation $[X]$ and DOM concentration (mg DOC L^{-1}) for sets of similar assays with different carbon content. Model calculations were carried out using SPSS 10.

Results

EDC. DOM was oxidized by ferric iron in all assays with a decreasing rate over time (Figure 1). Ferrous iron was released to maximum concentrations of 1.4–126 $\mu\text{mol L}^{-1}$, resulting in an EDC ranging from 0.07 to 1.52 $\text{mequiv} \cdot (\text{g C})^{-1}$ (Table 1). The release of ferrous iron markedly differed among experiments and roughly decreased in the sequence FeBiPy (pH 4.5) > FeBiPy (pH 6) > FeCN > FeCi \approx Fe(OH)₃ (Table 1). The time scale of reaction progress also differed. DOM was oxidized within about 20 h by FeBiPy and more slowly, within about 50 and 150 h, by colloidal Fe(OH)₃ and FeCN,

respectively (Figure 1). The concentration of DOC was of little influence on the reaction progress (Figure 1 A). The release of ferrous iron was adequately reproduced using eq 2 and one pool for the reaction with ferric cyanide and two DOM pools for the other reactions, as is further illustrated by Figure 1. The DOM pools were only loosely constrained by final ferrous iron concentrations but similar in experiments with different DOC concentrations, suggesting robust and consistent best model fits. The rapidly reacting pool DOM⁽¹⁾ contributed a fraction of 20–44%, and the more slowly reacting pool DOM⁽²⁾ contributed 56–80% to overall reaction product release (Figure 3s of Supporting Information). Reaction constant $k_{\text{obs}}^{(1)}$ ranged from 0.03 to 27 h⁻¹ (Table 1) and $k_{\text{obs}}^{(2)}$ ranged from 0.03 to 0.25 h⁻¹.

The EDC further increased steadily when the DOC concentration was raised (Figure 2 A and B). This confirms that DOM indeed served as electron source for ferric iron and suggests that the electron transfer occurred in a similar way over a range of DOM concentrations. The EDC of the non-purified MB-DOM was mostly in a range comparable to that of purified PP-HA and varied in a similar manner between assays (Table 1).

The EDC of DOM varied with the iron complex in solution and the pH (Figure 3). Lowering pH from 8 to 4.5 raised EDC using FeBiPy from 0.05 to 1.52 $\text{mequiv} \cdot (\text{g C})^{-1}$. The ligands for ferric iron and proton concentration furthermore interacted in their effect on the electron transfer. As can be seen from Figure 3, the EDC was influenced by pH to a lesser degree in the presence of the more stable FeCi complex. As a result, the EDC was higher using FeBiPy at pH < 6 and lower above this pH. The predominant ligand also visibly altered the formation of colloidal Fe(OH)₃. Raising pH to values >6 induced a visible formation of colloidal Fe(OH)₃ only in the FeBiPy assay. Due to the lower reactivity of DOM with colloidal Fe(OH)₃ (Figure 1 B), the strong effect of pH on the electron transfer in the FeBiPy assay can be attributed to the formation of colloidal Fe(OH)₃.

EAC. DOM oxidized H₂S mainly to thiosulfate, which reached concentrations of up to 8 $\mu\text{mol L}^{-1}$. Concentrations of thiosulfate in blank samples, i.e., without addition of DOM, averaged 2.6 \pm 0.3 $\mu\text{mol L}^{-1}$. Elemental sulfur and sulfite were not detected, and sulfate concentrations remained constant and below 5 μM (17). Incubation of metallic Zn with DOM released Zn²⁺ to concentrations of up to 250 $\mu\text{mol L}^{-1}$. These values correspond to an EAC range from 0.6 to 6.2 $\text{mequiv} \cdot (\text{g C})^{-1}$, and overall the EAC decreased in the order metallic Zn > electrochemical reduction \approx H₂S (Table 1).

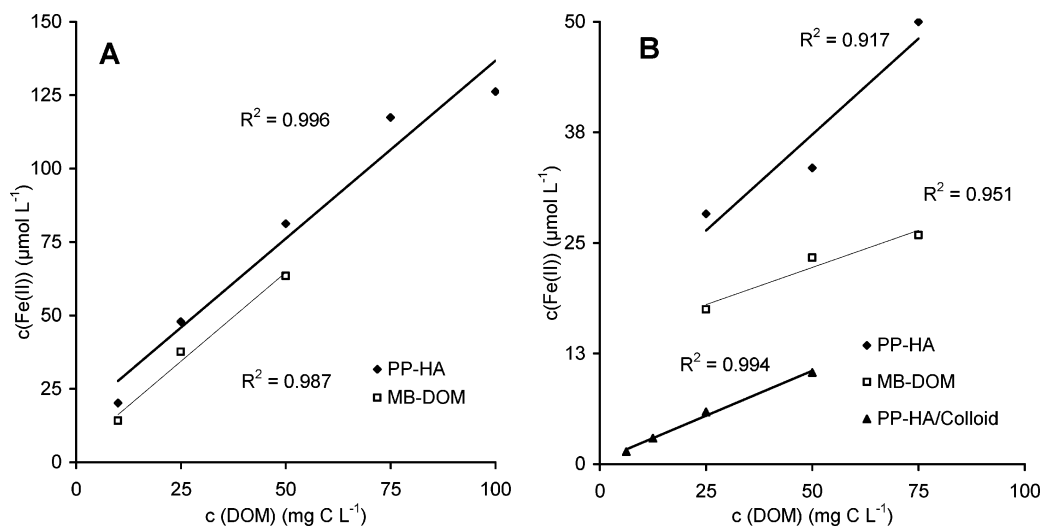


FIGURE 2. Relationships between experimental end-point concentration of ferrous iron and DOC concentration in EDC assays using FeBiPy (A), FeCN and colloidal Fe(OH)₃ (B). Mean values (SD within data point; $n = 2$; $n = 4$ for FeCN). FeBiPy: $[\text{Fe}^{2+}] = 0.9 \times [\text{DOC, PP-HA}] + 4.1$; $[\text{Fe}^{2+}] = 1.2 \times [\text{DOC, MB-DOM}] + 4.1$; FeCN: $[\text{Fe}^{2+}] = 0.4 \times [\text{DOC, PP-HA}] + 15.5$; $[\text{Fe}^{2+}] = 0.2 \times [\text{DOC, MB-DOM}] + 13.8$; colloidal Fe(OH)₃: $[\text{Fe}^{2+}] = 0.2 \times [\text{DOC, PP-HA}] + 0.4$.

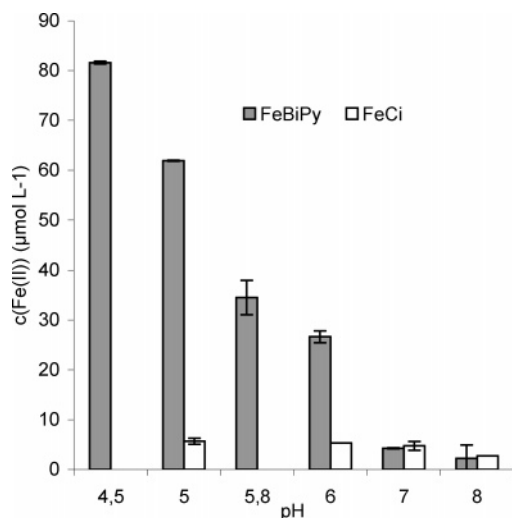


FIGURE 3. Effect of experimental pH on Fe(III) reduction by DOM, as indicated by release of Fe²⁺. Iron was either complexed by ferrozine (FeBiPy) or by citrate (FeCi). Mean values ± 1 SD ($n = 2$).

DOM was reduced electrochemically within about 4 h, as indicated by a decreasing electrode current, and by reaction with metallic Zn and H₂S within about 20–50 h. The release of thiosulfate was adequately reproduced by eq 2 with one DOM pool. With Zn⁰ the rapid pool DOM⁽¹⁾ contributed 8.4% and the slowly reacting pool DOM⁽²⁾ contributed 91.6% to overall reaction product release. Reaction constant $k_{obs}^{(1)}$ ranged from 0.10 h⁻¹ to 6.5 h⁻¹ (Table 1). Similarly to EDC, EAC was tightly correlated to DOC concentrations (Figure 5) but carbon normalized EAC decreased with DOC concentration when DOM was reduced by H₂S (Figure 5).

Effect of Electromotive Force on ETC and Kinetics. The direction of the electron transfer was controlled by reactant E_h . A positive E_h resulted in net release of electrons from DOM and negative E_h resulted in net uptake (Table 1). Electron-transfer capacities were further linearly related to the calculated E_h in solution (Figure 6). The increase of ETC was calculated to be ~100 mequiv·(g C)⁻¹ per 100 mV for PP-HA using the relation $\text{ETC} = 1.016 \times E_h - 0.138$ ($R^2 = 0.87$; $p = 0.05$), and was less steep for MB-DOM ($\text{ETC} = 0.596 \times E_h + 0.202$; $R^2 = 0.72$; $p = 0.05$). The reaction with metallic

Zn represents an exception, as the EAC was larger than expected from the above relationship (Figure 6). From these equations, an average E_h of DOM was estimated from the x -axis intercept ($y = 0$) for the applied “in assay” conditions. It is 0.136 V for PP-HA and -0.336 V for MB-DOM.

The reactant E_h apparently also influenced reaction kinetics. Using PP-HA, rate constants of the rapidly reacting DOM⁽¹⁾ pool increased with growing absolute values of E_h (Figure 6; $k_{obs}^{(1)} = 7.91 \times E_h + 0.404$; $R^2 = 0.81$). A weaker correlation occurred between E_h and $k_{obs}^{(2)}$ ($R^2 = 0.48$). As the number of data pairs for MB-DOM was limited, no regression model was tested.

Discussion

Controls on ETC. Electron-transfer capacities have been determined using reaction time periods of 0.25 h for reaction with FeCi (1, 5, 12), 100 min with FeCl₃, and 24 h with FeCN (11, 14, 16, 23). Our results suggest that these time periods do not suffice to complete the electron transfer, and that reaction periods ranging from 24 to 160 h are recommended, depending on the assay used (Figures 1 and 4). Electrochemical reduction stands out in this respect as the reaction was completed within about 4 h. Electron-transfer capacities have further ranged from 0.02 to >6 mequiv·(g C)⁻¹ in previous studies that were based on various methods and experimental protocols (5, 10–14). The methodological comparison demonstrates that the reported ETCs can be reproduced by variation of methods and reactants (Table 1). In comparison, the ETC difference between non-purified MB-DOM and PP-HA is small. It may, therefore, be that different ETC values that have been determined for DOM of the same source were caused by differences in experimental approach and conditions.

The electron transfer between reactants and DOM consistently increased with DOC concentration (Figures 2 and 5) and proceeded kinetically in a similar manner at different DOC concentrations (Figure 1). DOC concentration in the environmentally relevant range had thus little influence on carbon normalized ETC and the kinetics of the reactions. An exception was the reaction with H₂S, in which carbon normalized EAC slightly decreased at higher DOC concentrations, possibly due to incorporation of H₂S into the DOM (17).

It has been pointed out previously that redox properties of DOM change with increasing pH due to deprotonation

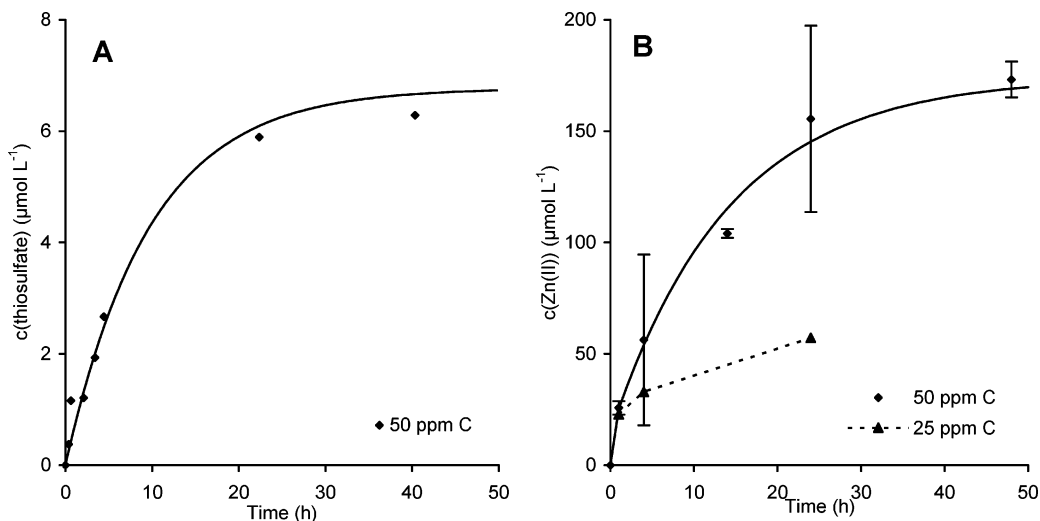


FIGURE 4. Kinetics of PP-HA reduction by hydrogen sulfide (pH 6.0) (A) and metallic Zn (pH 6.5) (B). Mean values \pm 1 SD ($n = 3$).

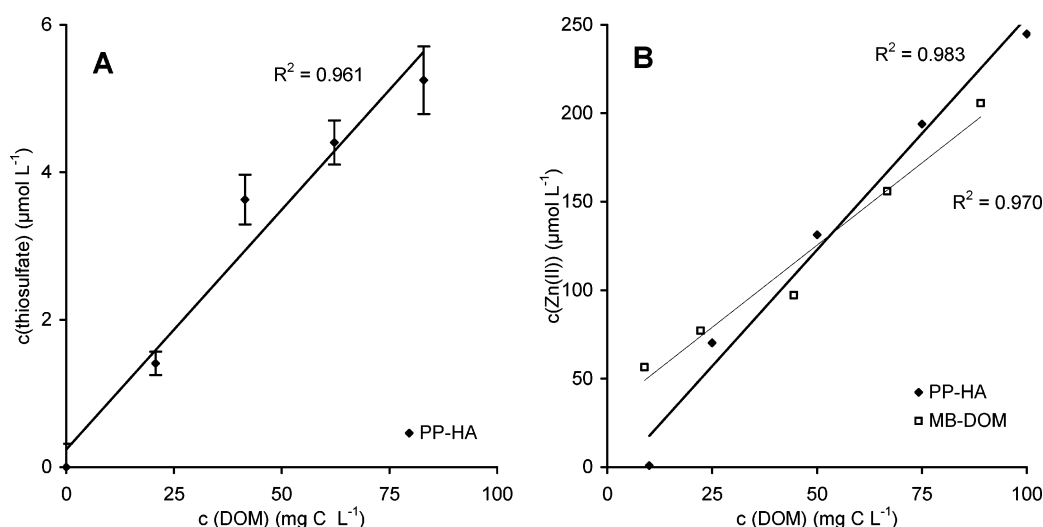


FIGURE 5. Relationships between experimental end-point concentration of reaction product and DOC concentration in EAC assays. Mean values \pm 1 SD ($n = 3$). H₂S (A): $[\text{S}_2\text{O}_3^{2-}] = 0.07 \times [\text{DOC, PP-Ha}] + 0.24$; Zn (B): $[\text{Zn}^{2+}] = 2.6 \times [\text{DOC, PP-Ha}] - 8.6$; $[\text{Zn}^{2+}] = 1.9 \times [\text{DOC, MB-DOM}] + 32.5$.

and molecular relaxation of DOM, leading to lower functional group redox potentials and an increased amount of redox active groups available for reaction (8, 14). A higher EDC with increasing pH should thus be expected. In the reaction with FeBiPy— and to a lesser extent in the reaction with FeCi— such an effect was masked by a formation of colloidal Fe(OH)₃. Iron speciation further strongly controlled the ETC and partially also the kinetics of the reaction with DOM. As the assays may be viewed as analogues to chemical conditions in natural environments, where ferric iron becomes available as a reactant to DOM, we assume that pH increase will similarly lower, rather than raise, electron-transfer rates and capacities of DOM by changing iron speciation.

The direction, quantity, and rate of the electron transfer were related to the redox potential of the predominant redox couple in solution (Figure 6). From reaction with redox active elements, E_h^0 values of 0.3–0.8 V, or $E_h(W)$ values (E_h^0 at pH 7) of 0–0.5 V, have been determined for natural organic compounds (3, 10, 15, 24). Under “in assay” conditions, net electron transfer was observed from DOM to Fe(OH)₃ ($E_h(W)$ 0 V) and the total quantity of electrons transferred to iron increased with rising $E_h(W)$ (up to >1 V). This suggests that redox active moieties of increasing E_h were drawn into the electron transfer up to a fairly high $E_h(W)$ and confirms that the activation of DOM functional groups depends on the

redox potential in solution (8). Consistent with these results, the direction of net electron transfer of DOM reversed at pH 6 between the couples of Fe(OH)₃/Fe²⁺ ($E_h = 0.06$ V) and H₂S/S₂O₃²⁻ ($E_h = -0.09$ V), and the EAC further strongly increased when metallic Zn was employed as reductant instead of H₂S or electrochemical reduction (Table 1, Figure 6). The EAC values obtained by the strong reductant Zn may be seen as an upper limit for DOM and may not be reached in natural environments. The electron transfer from Zn to DOM could further only be partially reversed by reaction with FeBiPy (M. Bauer, unpublished data), suggesting irreversible changes in DOM structure.

The variability of ETC values with reactant E_h is in principle not surprising regarding the structural variability of natural DOM (25) and the E_h^0 range of <0.3 V to >0.69 V reported for quinone moieties alone (7–9). As not only quinones, but also other polyphenolic moieties and complexed ferric iron may be involved in DOM redox reactions (10), the E_h of redox active functional groups may also exceed this range. In this study, contents of iron and other metals were very small and obviously not related to the observed EAC, so that ETC has to be attributed to organic moieties.

Raising pH strongly decreased EDC in FeBiPy assays, as has been previously reported (11, 16), and less so in FeCi assays. This pH dependency of EDC is not in conflict with

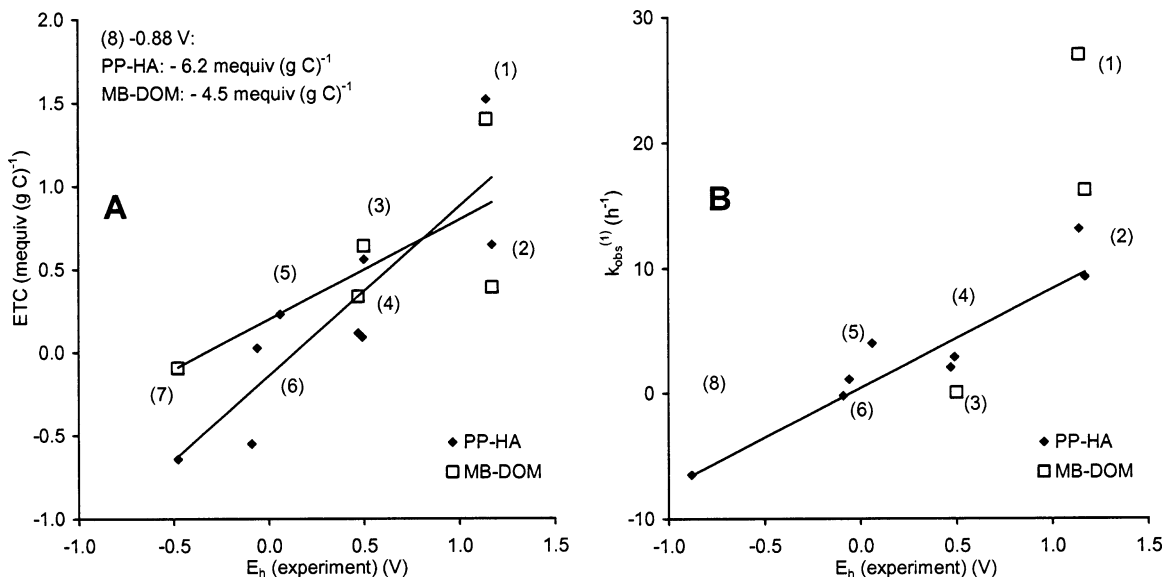


FIGURE 6. Change in ETC (A), and rate constant $k_{obs}^{(1)}$ (B) with reactant redox potential E_h , which was calculated for experimental conditions and chemical composition of the solution. Positive γ -values indicate DOM serving as electron donor (EDC), and negative γ -values indicate DOM serving as electron acceptor (EAC). Redox reactants were (1) FeBiPy, pH 4.5; (2) FeBiPy, pH 6; (3) FeCN; (4) FeCi; (5) colloidal Fe(OH)₃; (6) H₂S; (7) electrons; and (8) metallic Zn.

a thermodynamic control, as the pH changed iron speciation (Figure 1, Figure 3, Table 1). FeBiPy and FeCi complexes were stable up to pH 6–6.5 (Figure 1s of Supporting Information). Below this value the electron transfer to Fe(III) is thus higher with FeBiPy as the predominant complex (E_h of 1.14 V) compared to FeCi (0.47 V). Above pH 6–6.5, both complexes are quantitatively replaced by aqueous or colloidal Fe(OH)₃ with an even lower redox potential (below –0.3 V). Hence, the redox potential may have indirectly controlled the net electron transfer of DOM to ferric iron. The interpretation is somewhat speculative regarding the formation of colloidal Fe(OH)₃, which may differ in reaction rate and EDC, independently of thermodynamic properties.

Kinetics. The electron-transfer could be adequately reproduced based on pseudo-first-order kinetics and one or two reactive DOM pools, although this assumption is simplistic in view of the range of putative redox couples within DOM, and our own and earlier results (8, 9). From the observation that the kinetic constant $k_{obs}^{(1)}$ of PP-HA was controlled by the in situ E_h of the reactants (Figure 6), we further conclude that the reactivity of redox active moieties increased with a growing ΔE_h . Previously, linear free energy relationships (LFERs) between k_{obs} and E_h have been established for the reduction of defined monosubstituted nitrobenzenes by DOM in the presence of H₂S (26). Albeit our database was too small to investigate a LFER, our results do not disagree with such a relationship and show that $k_{obs}^{(1)}$ was a function of E_h for a diverse group of oxidants and reductants. From the magnitude of the apparent $k_{obs}^{(1)}$ of 0.03–27 h⁻¹ we further conclude that chemical electron transfer is sufficiently fast to function as an alternative to known microbially mediated electron shuttling (1). Reduction of ferric iron was, for example, fairly rapid in comparison to dissolved ferric iron production in lake water and sediments and associated k values of 10⁻⁵ to 10⁻² h⁻¹ at pH 4.8–5.8 (27), suggesting that DOM may effectively scavenge produced ferric iron in such environments. Oxidation of H₂S was also faster than electron transfer from H₂S to molecular oxygen and H₂S to crystalline Fe(oxy)hydroxides, and somewhat slower than transfer to poorly crystalline forms of Fe(III) (17). Hence, DOM is able to chemically scavenge oxidants and reductants at considerable rates, to compete with other relevant redox

processes, and likely also to chemically shuttle electrons from H₂S to ferric iron species and oxygen at redox interfaces in DOM rich aquatic systems. Electron shuttling has for example been postulated to occur at the oxycline of a permanently stratified lake, based on changes in the redox rate of DOM (28).

In conclusion, natural DOM may act as a redox buffer over a wide range of redox potentials, and the capacity and reactivity of this redox buffer should be controlled by the electrochemical gradient to the reactant. The redox properties of DOM thus provide a functional analogy to the range of acid–base properties that has been reported for DOM. According to our results, PP-HA and MB-DOM represent a redox ladder that encompasses redox couples ranging from $E_h < -0.48$ V to $> +0.83$ V. Considering the fast kinetics of the electron transfer and the abundance and mobility of DOM in environments such as peatlands, organic-rich aquifers, and dystrophic lakes, the contribution of DOM to electron-transfer processes and the buffering of redox potentials in these environments might be substantial.

Acknowledgments

We thank A. Kappler (ZAG, Tübingen) for access to an electrochemical cell and S. Hammer and K. Soellner for technical support. The study was funded by Deutsche Forschungsgemeinschaft (DFG) grant BL 563 2-1 to C.B.M.B. was in part supported by fellowship from the German Academic Exchange Service (DAAD).

Supporting Information Available

Characterization of humic substances; procedures during reduction of DOM with Zn and H₂S; iron speciation and stability of complexes; calculation of the in situ redox potentials; quality of kinetic modeling results; summary of electron-transfer capacities and rate constants for DOM redox reactions in literature. This material is available free of charge via the Internet at <http://pubs.acs.org>.

Literature Cited

- (1) Lovley, D. R.; Blunt-Harris, E. L.; Phillips, E. J. P.; Woodward, J. C. Humic substances as electron acceptors for microbial respiration. *Nature* **1996**, *382*, 445–448.

- (2) Redman, A. D.; Macalady, D. L.; Ahmann, D. Natural organic matter affects arsenic speciation and sorption onto hematite. *Environ. Sci. Technol.* **2002**, *36*, 2889–2896.
- (3) Schwarzenbach, R. P.; Stierli, R.; Lanz, K.; Zeyer, J. Quinone and iron porphyrin mediated reduction of nitroaromatic compounds in homogeneous aqueous solution. *Environ. Sci. Technol.* **1990**, *24*, 1566–1574.
- (4) Tratnyek, P. L.; Macalady, D. L. Abiotic reduction of nitro aromatic pesticides in anaerobic laboratory systems. *J. Agric. Food Chem.* **1989**, *37*, 248–257.
- (5) Scott, D. T.; McKnight, D. M.; Blunt-Harris, E. L.; Kolesar, S. E.; Lovley, D. R. Quinone moieties act as electron acceptors in the reduction of humic substances by humics-reducing microorganisms. *Environ. Sci. Technol.* **1998**, *32*, 2984–2989.
- (6) Cory, R. M.; McKnight, D. M. Fluorescence Spectroscopy Reveals Ubiquitous Presence of Oxidized and Reduced Quinones in Dissolved Organic Matter. *Environ. Sci. Technol.* **2005**, *39*, 8142–8149.
- (7) Rosso, K. M.; Smith, D. M. A.; Wang, Z.; Ainsworth, C. C.; Fredrickson, J. K. Self-Exchange Electron-Transfer Kinetics and Reduction Potentials for Anthraquinone Disulfonate. *J. Phys. Chem. A* **2004**, *108*, 3292–3303.
- (8) Helburn, R. S.; MacCarthy, P. Determination of some redox properties of humic acid by alkaline ferricyanide titration. *Anal. Chim. Acta* **1994**, *295*, 263–272.
- (9) Nurmi, J. T.; Tratnyek, P. G. Electrochemical Properties of Natural Organic Matter (NOM), Fractions of NOM, and Model Biogeochemical Electron Shuttles. *Environ. Sci. Technol.* **2002**, *36*, 617–624.
- (10) Struyk, Z.; Sposito, G. Redox properties of standard humic acids. *Geoderma* **2001**, *102*, 329–346.
- (11) Chen, J.; Gu, B.; Royer, R. A.; Burgos, W. D. The roles of natural organic matter in chemical and microbial reduction of ferric iron. *Sci. Total Environ.* **2003**, *307*, 167–178.
- (12) Klapper, L.; McKnight, D. M.; Blunt-Harris, E. L.; Nevin, K. P.; Lovley, D. R.; Hatcher, P. G. Fulvic acid oxidation state detection using fluorescence spectroscopy. *Environ. Sci. Technol.* **2002**, *36*, 3170–3175.
- (13) Kappler, A.; Haderlein, S. Natural Organic Matter as Reductant for Chlorinated Aliphatic Pollutants. *Environ. Sci. Technol.* **2003**, *37*, 2714–2719.
- (14) Matthiessen, A. Determining the redox capacity of humic substances as a function of pH. *Vom. Wasser* **1995**, *84*, 229–235.
- (15) Skogerboe, R. K.; Wilson, S. A. Reduction of Ionic Species by Fulvic Acid. *Anal. Chem.* **1981**, *53*, 228–232.
- (16) Pullin, M. J.; Cabaniss, S. E. The effects of pH, ionic strength, and iron-fulvic acid interactions on the kinetics of non-photochemical iron transformations. II. The kinetics of thermal reduction. *Geochim. Cosmochim. Acta* **2003**, *67*, 4079–4089.
- (17) Heitmann, T.; Blodau, C. Oxidation and incorporation of hydrogen sulfide by dissolved organic matter. *Chem. Geol.* **2006**, *235*, 12–20.
- (18) Stookey, L. Ferrozine - a new spectrophotometric reagent for iron. *Anal. Chem.* **1970**, *42*, 779–781.
- (19) Bard, A. J.; Parsons, R.; Jordan, J. *Standard Potentials in Aqueous Solutions*; International Union of Pure and Applied Chemistry: New York, 1985.
- (20) Straub, K. L.; Benz, M.; Schink, B. Iron metabolism in anoxic environments at near neutral pH. *FEMS Microbiol. Ecol.* **2001**, *34*, 181–186.
- (21) Majzlan, J.; Navrotsky, A.; Schwertmann, U. Thermodynamics of iron oxides: Part III. Enthalpies of formation and stability of ferrihydrite (Fe(OH)₃), schwertmannite (FeO(OH)_{3/4}(SO₄)_{1/8}), and -Fe₂O₃. *Geochim. Cosmochim. Acta* **2004**, *68*, 1049–1059.
- (22) Stumm, W.; Morgan, J. J. *Aquatic Chemistry*; Wiley Interscience: New York, 1996.
- (23) Benz, M.; Schink, B.; Brune, A. Humic Acid Reduction by *Propionibacterium freudenreichii* and Other Fermenting Bacteria. *Appl. Environ. Microbiol.* **1998**, *64*, 4507–4512.
- (24) Oesterberg, R.; Shirshova, L. Oscillating, nonequilibrium redox properties of humic acids. *Geochim. Cosmochim. Acta* **1997**, *61*, 4599–4604.
- (25) Aiken, G. R.; McKnight, D. M.; Wershaw, R. L.; MacCarthy, P. *Humic Substances in Soil, Sediment, and Water*; Wiley-Interscience: New York, 1985.
- (26) Dunnivant, F. M.; Schwarzenbach, R. P.; Macalady, D. L. Reduction of substituted nitrobenzenes in aqueous solutions containing natural organic matter. *Environ. Sci. Technol.* **1992**, *26*, 2133–2141.
- (27) Barry, R. C.; Schnoor, J. L.; Sulzberger, B.; Sigg, L.; Stumm, W. Iron oxidation kinetics in an acidic alpine lake. *Water Res.* **1993**, *28*, 323–333.
- (28) Fulton, J.; McKnight, D.; Foreman, C.; Cory, R.; Stedmon, C.; Blunt, E. Changes in fulvic acid redox state through the oxycline of a permanently ice-covered Antarctic lake. *Aquat. Sci. Research Across Boundaries* **2004**, *66*, 27–46.

Received for review June 2, 2006. Revised manuscript received September 21, 2006. Accepted September 27, 2006.

ES061323J

Supporting Information

1 Characterization of humic substances

Humic substances were characterized by spectroscopy on a Varian Cary 1 E using quartz cuvettes (UV/VIS range, 250 – 700 nm), a Bruker Vector 22 FTIR using KBr pellets (IR range 4000 - 500 cm^{-1}) and a SFM 25 fluorescence spectrometer (BIO-TEK Instruments). Synchronous scans were recorded in 1 cm cuvettes (1) at excitation wavelength range 300–550 nm, a scan speed of 100 nm min^{-1} and $\Delta\lambda$ of 18 nm. Elemental composition of DOM was measured on a Perkin Elmer Optima 3000 ICP AES.

Both PP-HA and MB-DOM were derived from peatland environments and characterized by the high specific UV absorbance ($\text{SUVA}_{254\text{nm}}$) and low E_2/E_3 and E_4/E_6 ratios typical for polyphenolic, condensed humic substances. FTIR peak ratios (normalized on intensity at 1150 cm^{-1}) suggested an abundance of carboxylic and aromatic groups. PP-HA was more condensed and humified based on the high 470 nm/360 nm ratio in the fluorescence measurement. Both DOM had low total metal content, with iron values of only 0.3 $\mu\text{mol g}^{-1}$ in PP-HA and 0.9 $\mu\text{mol g}^{-1}$ in MB-DOM.

Table 2 Total elemental (ash) contents, spectroscopic characteristics (absorbance intensity of characteristic peaks of UV-VIS; FTIR and synchronous fluorescence ratios) of DOM used.

DOM Parameter	PP-HA	MB-DOM
[DOC] (mg L^{-1})	50	71
$\Sigma [A]^*$ ($\mu\text{mol g}^{-1}$)	3.0	13.1
[Fe] ($\mu\text{mol g}^{-1}$)	0.3	0.9
E_4/E_6 **	6.2	14.6
E_2/E_3 **	2.8	3.9
$\text{SUVA}_{254 \text{ nm}}$ ($\text{L} \cdot \text{mg C}^{-1}$)	0.060	0.051
IR 1725/1150 (cm^{-1})	2.1	1.1
IR 1620/1150 (cm^{-1})	2.8	1.2
IR 1270/1150 (cm^{-1})	1.1	0.56
F 400/360 (nm)	1.69	1.63
F 470/360 (nm)	2.55	1.11
F 470/400 (nm)	0.67	0.68

* ash (Na, K, Ca, Mg, Fe, Mn, Si); ** Ratio of UV/VIS absorption: 465 and 665 nm; 254 and 365 nm

2 DOM reduction by metallic Zn

Release of dissolved Zn was determined by mixing and cautiously shaking 50 ml of N_2 -purged DOM sample solution and 5 g of acid washed and twofold rinsed coarse Zn grains (Riedel-de-Haen, coarse powder, $\varnothing > 0,1 \text{ mm}$) under exclusion of oxygen. Preliminary tests showed that fine Zn powder ($\varnothing < 0.45\mu\text{m}$) could not be used due to excessive Zn release in blank samples. The Zn was washed in 50 ml of 1 M HCl for 30 min. Chemicals were reagent grade, and deionized water (el. conductivity <

0,06 μS) was used. Assays were carried out in an anoxic glovebox (95 % nitrogen, 5 % hydrogen). To prevent photoreactions (e.g. (2)), all vessels used for reactions and reagent storage were wrapped in aluminium foil. Blank experiments were conducted analogously to kinetic and batch assays in the absence of humic acid. All experiments were carried out in triplicates. Experimental ionic strength was 5 mM (KCl) and pH was adjusted to 6.5. To determine the reaction progress over time, aliquots were taken in regular intervals. In these experiments pH was regularly readjusted (< 12 h) using 0.01 M NaOH or HCl. To determine the dependency of Zn release on DOM concentrations, Zn was processed with DOM solutions diluted to 75, 50, 25 and 10 % of the original solution concentration. The procedure is more thoroughly described in (3).

3 Supplemental analyses of sulfur species

Total sulfide was determined by the methylene blue method (4). The ZnOAc buffer (0.1 mol L^{-1}) used was deoxygenated with nitrogen ($>99.999\%$ N_2) and overlaid by argon. Sulfite was stabilized in a preliminary experiment with $20 \mu\text{M}$ formaldehyde and measured as hydroxymethanesulfonate (5). Elemental sulfur was determined by HPLC (C18-column, 0.4 ml min^{-1} flowrate with methanol as eluent, UV detector at 265 nm). Samples were diluted 1:5 with methanol, extracted for 1 h and filtered over a disposable syringe filter ($0.2 \mu\text{m}$ nylon). Matrix effects and reproducibility were tested using an aqueous solution of S^0 -spiked humic acid (IHSS 1R103H) and a methanolic laboratory standard.

4 Conditional stability constants and calculation of iron speciation

The distribution of iron species at pH 4 – 9 in the presence or absence of complexing anions was modelled using PhreeqC algorithm version 2.11.0 (6). Reaction stoichiometry and stability constants for the various iron complexes with bipyridyl and citrate were derived from literature ((7), (8), (9)). Stability constants for the other species were adopted from the databases Llnl resp. Minteq included in PhreeqC (Table 2). For DOM (50 mg C L^{-1}) a complexation capacity of $0.5 \text{ mmol Fe g}^{-1}$ with $\log K = 10.4$ was assumed (10). Both values are in the upper range of reported data and therefore result in a maximum estimation of 0.025 mM iron binding groups in the DOM. Cation complexation of MES and PIPES buffer is known to be low (11,12) and were therefore neglected. All the displayed stability constants were used for the PhreeqC model calculations with the following initial species concentrations:

- FeBiPy experiments: 0.5 mM FeCl_3 or FeCl_2 ; 2 mM Bipyridyl ; 20 mM buffer (Acetate, Phosphate or Carbonate); $0.025 \text{ mM iron binding groups of DOM}$;
- FeCi experiments: 0.5 mM FeCl_3 or FeCl_2 ; 2 mM Bipyridyl ; $10 \text{ mM Citrate (C}_6\text{O}_7\text{H}_8)$; 20 mM buffer (Acetate, Phosphate or Carbonate); $0.025 \text{ mM iron binding groups of DOM}$;
- FeCN experiments: $0.5 \text{ mM } [\text{Fe}(\text{CN})_6]^{3-}$; 20 mM buffer (Phosphate); $0.025 \text{ mM iron binding groups of DOM}$;

Table 3 Conditional stability constants of Fe(II) and Fe(III) complexes for the reaction stoichiometry: $x \cdot \text{Metal} + y \cdot \text{Ligand} = \text{M}_x\text{L}_y$ -Complex

Chelator	Stoichiometry	Fe(II)		Fe(III)	
		Log K	Ref.	Log K	Ref.
Bipyridyl	ML/M.L	4.65	(7)	4.2	(8)
	ML2/M.L ₂	7.9	(7)	5	(8)
	ML3/M.L ₃	17.2	(7)	17.06	(8)
	M2L4/M ₂ .L ₄			16.29	(7)
Citrate	ML/M.L	4.4	(7)	11.85	(9)
	MHL/M.HL	2.65	(7)	11.44	(9)
	MHL2/M.L ₂ H	1.73	(7)		
	MOHL/M.LOH			9.4	(9)
	MOH2L/M.LOH ₂			1.9	(9)
	ML2/M.L ₂			15.3	(9)
	MHL2/M.L ₂ H			19.12	(9)
	MOHL2/M.L ₂ OH			10.46	(9)
CN-	ML6/M.L ₆	45.6	Minteq	52.6	Minteq
	MHL6/M.L ₆ H	49.9	Minteq		
	MH2L6/M.L ₆ H ₂	52.4	Minteq		
	M2L2/M ₂ .L ₂			56.9	Minteq
OH-	ML/M.L	-9.5	Minteq	-2.19	Minteq
	ML2/M.L ₂	-20.5	Minteq	-5.67	Minteq
	ML3/M.L ₃	-31	Minteq	-13	Minteq
	ML4/M.L ₄			-21.6	Minteq
	ML3/M.L ₃ (s) (Ferrihydrite)			4.8	Minteq
Acetate	ML/M.L	1.4	Minteq	3.2	Minteq
	ML2/M.L ₂		Minteq	6.5	Minteq
	ML3/M.L ₃		Minteq	8.3	Minteq
CO ₃ ²⁻	ML/M.L (s) (Siderite)	10.55	Minteq		
PO ₄ ³⁻	MHL/M.HL	3.6	Llnl	8.3	Llnl
	MH2L/M.LH ₂	2.7	Llnl	3.47	Llnl
	ML/M.L (s) (Strengite)			26.4	Minteq
DOM	ML/M.L	7.5	(10)	10.4	(10)

In solutions containing ferrozine (FeBiPy treatment) or both citrate and ferrozine (FeCi treatment), the preferential Fe(II) species was the bipyridyl complex. The most stable Fe(III) species at lower pH were complexes with ferrozine (FeBiPy treatment; Fig. 1s A and C) or citrate (FeCi treatment; Fig. 1s B and D). Aqueous iron hydroxides in equilibrium with iron precipitates quantitatively gained in importance above pH 6 (Fig. 1s). Free iron concentrations were below 10⁻⁵ mM (pH 4) and further decreased with increasing pH (< 10⁻¹² mM at pH 7). In cyanide containing solutions (FeCN treatment) both ferric and ferrous iron were quantitatively present as cyanide

complex over a wide pH range (no figure shown). Complexation by DOM and precipitation of iron phosphate or carbonate were of minor relevance.

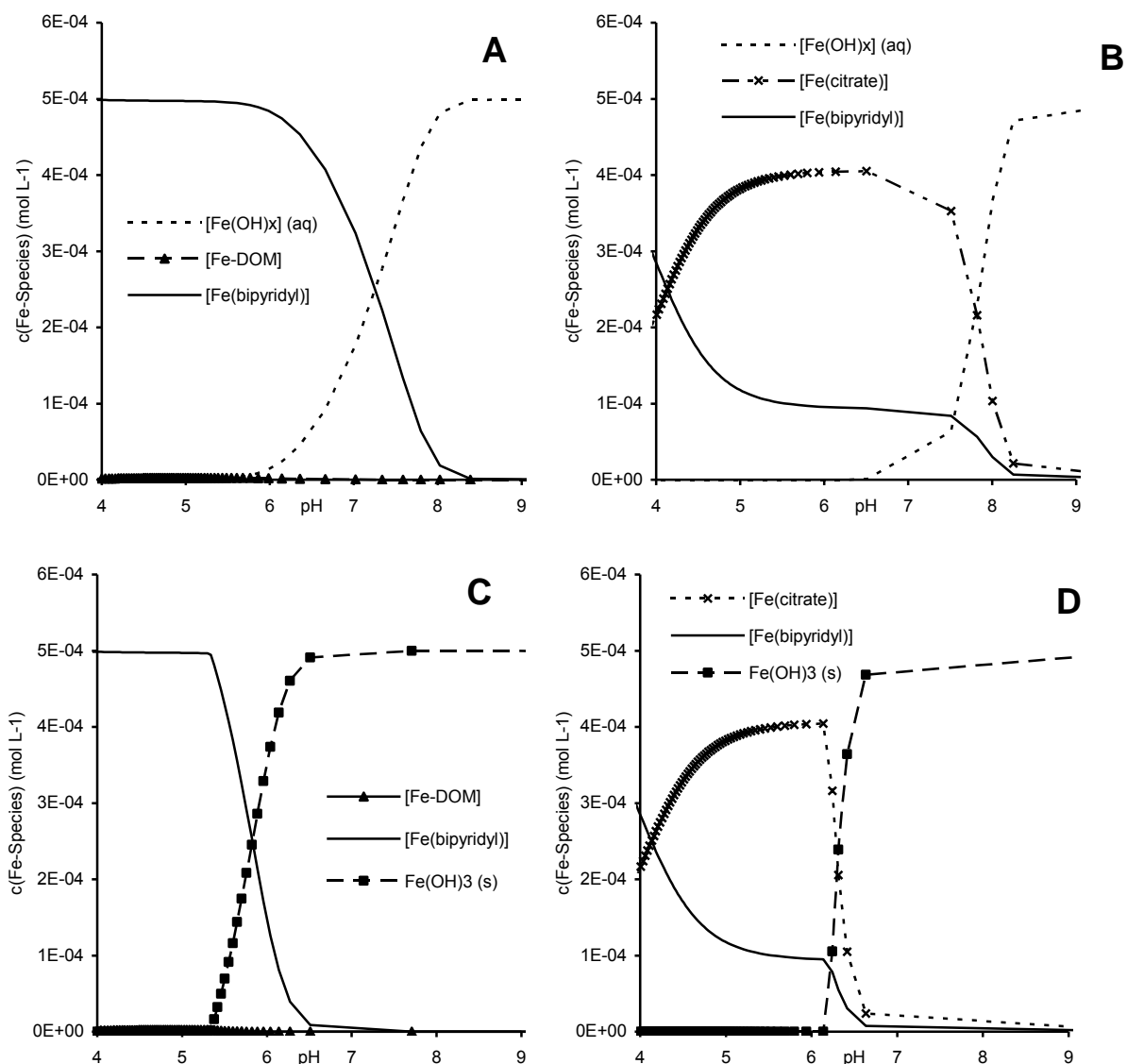


Figure 12 Modelled distribution of various Fe(III) species. Panels A and C: Solutions with DOM and bipyridyl and without citrate; Figures B and D: DOM with bipyridyl and citrate; Figures A and B: No precipitation; Figures C and D: With precipitation of Fe(OH)_3 (s); $[\text{Fe(bipyridyl)}] = [\text{Febipy}]^{3+} + [\text{Fe(bipy)}_2]^{3+} + [\text{Fe(bipy)}_3]^{3+}$; $[\text{Fe(citrate)}] = [\text{FeCit}]^0 + [\text{FeCitH}]^+ + [\text{FeCitOH}]^- + [\text{FeCit(OH)}_2]^{2-} + [\text{Fe(Cit)}_2]^{3-} + [\text{Fe(Cit)}_2\text{H}]^{2-} + [\text{Fe(Cit)}_2\text{OH}]^4$; Fe(OH)_x (aq) = $\text{Fe(OH)}^{2+} + \text{Fe(OH)}_2^- + \text{Fe(OH)}_3$ (aq) + Fe(OH)_4^- ;

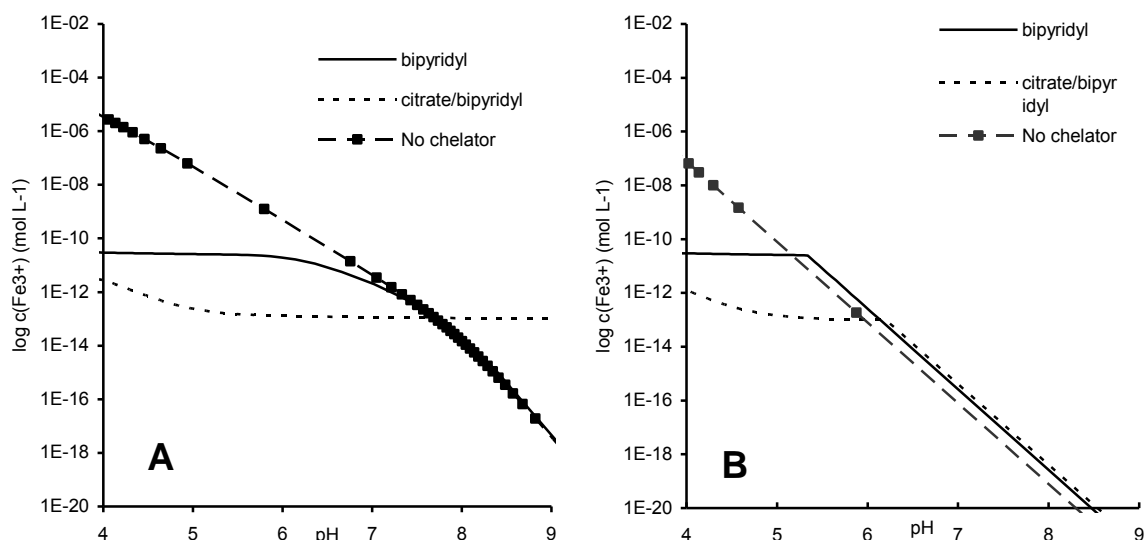
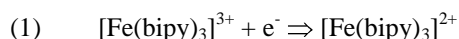


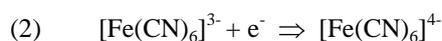
Figure 13 Modelled concentration of free Fe(III) in solutions containing a variety of complexing agents for pH 4 - 9; Panel A: No precipitation; panel B: With precipitation of Fe(OH)₃ (s).

5 Estimation of *in situ* redox potentials

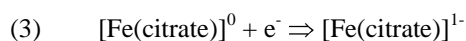
In situ redox potentials of assays were calculated using equations 1 – 6 for the quantitatively predominant redox couple reacting with DOM. Redox potential values were either taken from literature ([Fe(bipy)₃]³⁺/[Fe(bipy)₃]²⁺ (13); [Fe(CN)₆]³⁻/[Fe(CN)₆]⁴⁻ (14,15); [Fe(citrate)]⁰/[Fe(citrate)]¹⁻ (16)) or calculated from Gibbs free energy (Fe(OH)₃/Fe²⁺ (17); Zn⁰/Zn²⁺ and H₂S/S₂O₃²⁻ (15)). Redox potential values for the iron complexes were only available for the reaction stoichiometry 1:3 with bipyridyl, 1:1 with citrate and 1:6 with cyanide. E_h⁰ values were adjusted for *in situ* pH conditions and furthermore corrected for the ratio of reactant species found in the experiments at initial and final conditions.



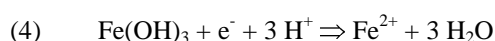
$$E_{h,Fe} = E_h^0 + 0.059 \cdot \lg \frac{a([\text{Fe}(\text{bipy})_3]^{3+})}{a([\text{Fe}(\text{bipy})_3]^{2+})} \quad E_h^0 = +1.11 \text{ V}$$



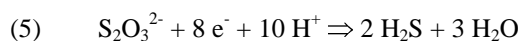
$$E_{h,Fe} = E_h^0 + 0.059 \cdot \lg \frac{a([\text{Fe}(\text{CN})_6]^{3-})}{a([\text{Fe}(\text{CN})_6]^{4-})} \quad E_h^0 = +0.36 \text{ V}$$



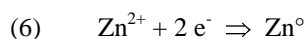
$$E_{h,Fe} = E_h^0 + 0.059 \cdot \lg \frac{a([\text{Fe}(\text{citrate})]^0)}{a([\text{Fe}(\text{citrate})]^{1-})} \quad E_h^0 = +0.372 \text{ V}$$



$$E_{h,Fe} = E_h^0 - 0.177 \cdot \text{pH} + 0.059 \cdot \lg \frac{1}{a(\text{Fe}^{2+})} \quad E_h^0 = +0.84 \text{ V}$$



$$E_{h,Fe} = E_h^0 - 0.073 \cdot pH + \frac{0.059}{8} \cdot \lg \frac{a(S_2O_3^{2-})}{a(H_2S)^2} \quad E_h^0 = +0.34 \text{ V}$$



$$E_{h,Zn} = E_h^0 + \frac{0.059}{2} \cdot \lg a(Zn^{2+}) \quad E_h^0 = -0.76 \text{ V}$$

Table 4 Standard redox potentials E_h^0 for used half reactions and potential values taking into account the in situ pH and initial, respectively final, reactant concentrations.

Redox Couple	E_h^0 V	pH (in situ)	E_h (in situ pH) V	E_h (initial) V	E_h (final) V
$[Fe(bipy)_3]^{3+}/[Fe(bipy)_3]^{2+}$	1.11	5	1.11	1.49	1.15
$[Fe(bipy)_3]^{3+}/[Fe(bipy)_3]^{2+}$	1.11	6	1.11	1.49	1.17
$[Fe(bipy)_3]^{3+}/[Fe(bipy)_3]^{2+}$	1.11	7	1.11	1.49	1.23
$[Fe(bipy)_3]^{3+}/[Fe(bipy)_3]^{2+}$	1.11	8	1.11	1.49	1.25
$[Fe(citrate)]^0/[Fe(citrate)]^{1-}$	0.372	5	0.372	0.77	0.49
$[Fe(citrate)]^0/[Fe(citrate)]^{1-}$	0.372	6	0.372	0.77	0.49
$[Fe(citrate)]^0/[Fe(citrate)]^{1-}$	0.372	7	0.372	0.77	0.49
$[Fe(citrate)]^0/[Fe(citrate)]^{1-}$	0.372	8	0.372	0.77	0.51
$[Fe(CN)_6]^{3-}/[Fe(CN)_6]^{4-}$	0.36	6	0.43	0.83	0.50
$Fe(OH)_3/Fe^{2+}$	0.84	5	-0.042	0.56	0.22
$Fe(OH)_3/Fe^{2+}$	0.84	6	-0.219	0.38	0.06
$Fe(OH)_3/Fe^{2+}$	0.84	7	-0.396	0.20	-0.06
$Fe(OH)_3/Fe^{2+}$	0.84	8	-0.573	0.03	-0.21
$S_2O_3^{2-}/H_2S$	0.34	6	-0.1	-0.13	-0.09
Zn^{2+}/Zn^0	-0.76	6.5	-0.76	-1.06	-0.88

6 Redox kinetics: Quality of kinetic modelling results and additional kinetic experiments

To evaluate the quality of the kinetic modelling, we collated model results for the FeBiPy and colloidal $Fe(OH)_3$ experiments, which were conducted at more than 2 DOM concentration levels. Pool sizes and rate constants were determined for each DOM concentration. Average pool size in % of the total reactive pool and rate constant are depicted in Figure 3, including minimum and maximum values as error bars. The results suggest that fitted pool sizes were robust with respect to different experimental conditions. With the exception of experiments with colloidal iron, fast rate constants were in a narrow range from 0.2 to 0.5 min^{-1} . The fraction of reactive pool sizes was different for the two DOMs analyzed but was fairly constant for the various assays.

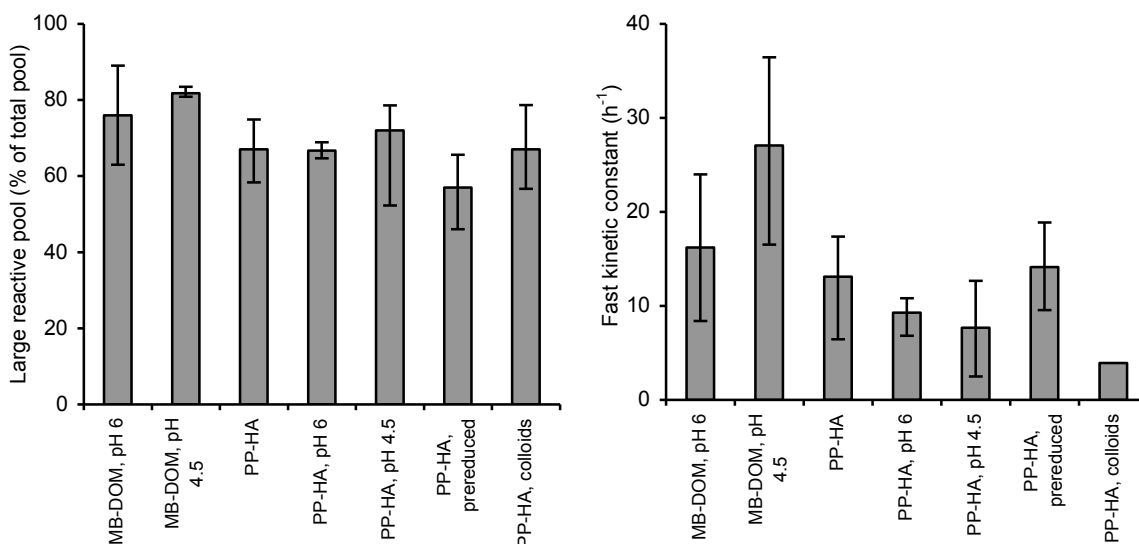


Figure 14 Average relative size of large reactive pool DOM⁽²⁾ (left) and fast rate constant $k_{(obs)}^{(1)}$ (right) calculated from kinetic model fits. Error bars indicate minimum and maximum and, therefore, the range of values found.

More kinetic experiments were performed than are depicted in the main part of the manuscript. This additional data is presented in here, and show the similar course of reaction progress for the various iron methods.

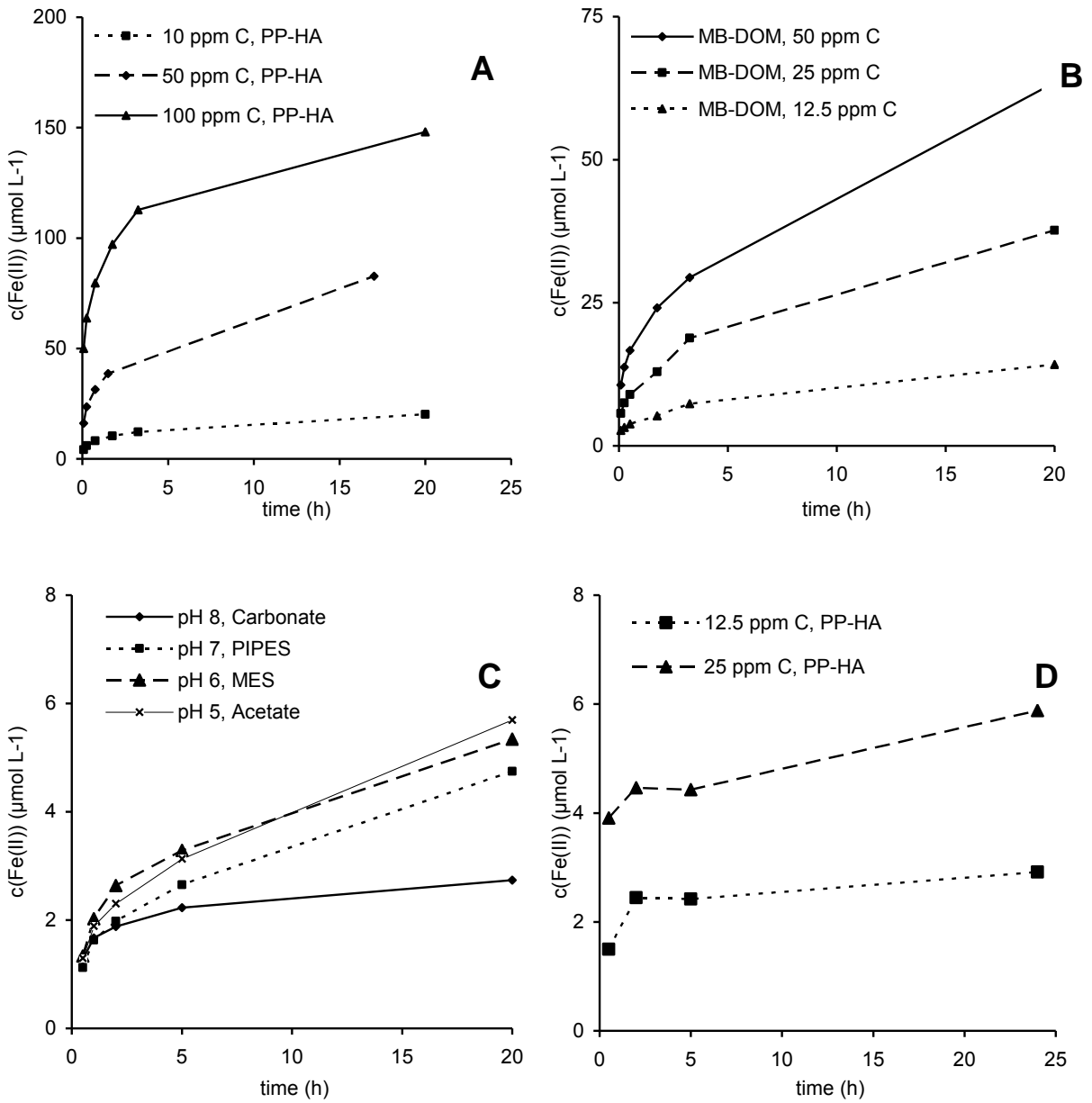


Figure 15 Production of Fe(II) over time by DOM; **A** FeBiPy method at pH 4.5 with PP-HA; **B** FeBiPy method at pH 4.5 with MB-DOM; **C** FeCi method different pH with PP-HA (50 ppm C); colloidal Fe(OH)₃ method at pH 6 with PP-HA;

7 Literature values for capacity and rate constant of electron transfer reactions

Table 5 Literature values of experimentally determined electron transfer capacities and rate constants for humic acids (HA) or fulvic acids (FA) with a variety of inorganic reactant.

DOM type	pH	Predominant redox couple	E _h (in situ pH) (V)	k _(obs) ⁽¹⁾ (h ⁻¹)	ETC (mequiv • (g C) ⁻¹)	Author
HA	3	Fe ³⁺ /Fe ²⁺	0.31	2	1.4	(18)
HA	7		-0.39		0.7	(18)
FA	6	Fe(OH) ₃ /Fe ²⁺	-0.22	1.1	0.25	(19)
FA	8		-0.57	0.21	0.08	(19)
HA	3				0.4	(18)
HA	7				0.125	(18)
HA	6.				0.34	(20)
	8	Fe(citrate) ⁰ / [Fe(citrate)] ¹⁻	0.372			
HA	6.				0.35-0.7	(21)
	8					
HA	6.				0.68	(22)
	8					
Syn. HA	6- 7				3.5-8	(14)
HA	6- 7	[Fe(CN) ₆] ³⁻ / [Fe(CN) ₆] ⁴⁺	0.43		0.3-0.7	(23)
HA	6- 7				2.5	(24)
HA	5	I ₂ /2 I ⁻	0.621		3.3	(25)
HA	7	I ₂ /2 I ⁻	0.621		1.5	(25)
HA	3	CrO ₄ ²⁻ /Cr ³⁺	1.1	0.05	0.4-1.8	(26)

Literature Cited

- (1) Miano, T. M.; Senesi, N. Synchronous excitation fluorescence spectroscopy applied to soil humic substances chemistry. *Sci. Tot. Environ.* **1992**, *1992*, 41-51.
- (2) Fukushima, M.; Tatsumi, K. Light acceleration of iron(III) reduction by humic acid in the aqueous solution. *Colloids Surf., A* **1999**, *155*, 149-258.
- (3) Blodau, C.; Bauer, M.; Regenspurg, S.; Macalady, D. L. Electron accepting capacity of dissolved organic matter as determined by reaction with elemental zinc. *Chem. Geol.* **2007**, *submitted*.
- (4) Cline, J. D. Spectrofluorometric determination of hydrogen sulfide in natural waters. *Limnol. Oceanogr.* **1969**, *14*, 454-458.
- (5) Lindgren, M.; Cedergren, A.; Lindberg, J. Conditions for sulfite stabilization and determination by ion chromatography. *Analyt. Chim. Acta* **1982**, *141*, 279-286.
- (6) Parkhurst, D. L.; Appelo, C. A. J. *User's guide to PHREEQC - A computer program for speciation, batch-reaction, one dimensional transport, and inverse geochemical calculations*; US department of the interior, 1999.
- (7) Martell, A. E.; Smith, R. M. *Critical stability constants* New York, 1975.
- (8) Cheng, K. L.; Ueno, K.; Imamura, T. *CRC Handbook of organic analytical reagents*; CRC Press, Inc.: Boca Raton, 1985.

- (9) Königsberger, L.-C.; Königsberger, E.; May, P. M.; Hefter, G. T. Complexation of iron(III) and iron(II) by citrate. Implications for iron speciation in blood plasma. *Journal of inorganic biochemistry* **2000**, *78*, 175-184.
- (10) Rose, A. L.; Waite, D. T. Kinetics of iron complexation by dissolved natural organic matter in coastal waters. *Marine chemistry* **2003**, *84*, 85-103.
- (11) Mash, H. E.; Chin, Y.-P.; Sigg, L.; Hari, R.; Xue, H. Complexation of Copper by Zwitterionic Aminosulfonic (Good) Buffer. *Analyt. Chem.* **2003**, *75*, 671-677.
- (12) Yu, Q.; Kandedgedara, A.; Xu, Y.; Rorabacher, D. B. Avoiding Interferences from Good's Buffers: A Contiguous Series of Noncomplexing Tertiary Amine Buffers Covering the Entire Range of pH 3–11. *Analytical Biochemistry* **1997**, *253*, 50-56.
- (13) Bard, A. J.; Parsons, R.; Jordan, J. *Standard potentials in aqueous solutions*; International Union of pure and applied chemistry: New York, 1985.
- (14) Matthiessen, A. Determining the redox capacity of humic substances as a function of pH. *Vom Wasser* **1995**, *84*, 229-235.
- (15) Stumm, W.; Morgan, J. J. *Aquatic chemistry*; Wiley Interscience, 1996.
- (16) Straub, K. L.; Benz, M.; Schink, B. Iron metabolism in anoxic environments at near neutral pH. *FEMS Microbiol. Ecol.* **2001**, *34*, 181-186.
- (17) Majzlan, J.; Navrotsky, A.; Schwertmann, U. Thermodynamics of iron oxides: Part III. Enthalpies of formation and stability of ferrihydrite (Fe(OH)₃), schwertmannite (FeO(OH)_{3/4}(SO₄)_{1/8}), and -Fe₂O₃. *Geochim. Cosmochim. Acta* **2004**, *68*, 1049-1059.
- (18) Chen, J.; Gu, B. H.; Royer, R. A.; Burgos, W. D. The roles of natural organic matter in chemical and microbial reduction of ferric iron. *Sci. Tot. Environ.* **2003**, *307*, 167-178.
- (19) Pullin, M. J.; Cabaniss, S. E. The effects of pH, ionic strength, and iron-fulvic acid interactions on the kinetics of nonphotochemical iron transformations. II. The kinetics of thermal reduction. *Geochim. Cosmochim. Acta* **2003**, *67*, 4079-4089.
- (20) Lovley, D. R.; Coates, J. D.; Blunt-Harris, E. L.; Phillips, E. J. P.; Woodward, J. C. Humic substances as electron acceptors for microbial respiration. *Nature* **1996**, *382*, 445-448.
- (21) Scott, D. T.; McKnight, D. M.; Blunt-Harris, E. L.; Kolesar, S. E.; Lovley, D. R. Quinone moieties act as electron acceptors in the reduction of humic substances by humics-reducing microorganisms. *Environ. Sci. Technol.* **1998**, *32*, 2984-2989.
- (22) Klapper, L.; McKnight, D. M.; Fulton, J. R.; Blunt-Harris, E. L.; Nevin, K. P.; Lovley, D. R.; Hatcher, P. G. Fulvic acid oxidation state detection using fluorescence spectroscopy. *Environ. Sci. Technol.* **2002**, *36*, 3170-3175.
- (23) Benz, M.; Schink, B.; Brune, A. Humic Acid Reduction by *Propionibacterium freudenreichii* and Other Fermenting Bacteria. *Appl. Environ. Microbiol.* **1998**, *64*, 4507-4512.
- (24) Kappler, A.; Haderlein, S. B. Natural organic matter as reductant for chlorinated aliphatic pollutants. *Environ. Sci. Technol.* **2003**, *37*, 2714-2719.
- (25) Struyk, Z.; Sposito, G. Redox properties of standard humic acids. *Geoderma* **2001**, *102*, 329-346.
- (26) Gu, B.; Chen, J. Enhanced microbial reduction of Cr(VI) and U(VI) by different natural organic matter fractions. *Geochim. Cosmochim. Acta* **2003**, *67*, 3575-3582.

Study 2

Submitted to *Chemical Geology*

Electron accepting capacity of dissolved organic matter as determined by reaction with metallic zinc

Christian Blodau¹, Markus Bauer¹, Simona Regenspurg^{1,2}, Donald Macalady²

¹Limnological Research Station and Department of Hydrology, University of Bayreuth, D-95440 Bayreuth, Germany

²Department of Chemistry & Geochemistry, Colorado School of Mines Golden, Colorado 80401, USA

Abstract

Information about the chemical electron accepting capacity (EAC) of dissolved organic matter (DOM) is scarce owing to a lack of applicable methods. We quantified the electron transfer from metallic Zn to natural DOM in batch experiments at DOC concentrations of 10 – 100 mg L⁻¹ and related it to spectroscopic information obtained from UV-, synchronous fluorescence, and FTIR-spectroscopy. The electron donating capacity of DOM and pre-reduced DOM was investigated using Fe(CN)₆³⁻ as electron acceptor. Presence of DOM resulted in release of dissolved Zn, consumption of protons, and slower release of hydrogen compared to reaction of metallic Zn with water at pH 6.5. Comparison with reaction stoichiometry confirmed that DOM accepted electrons from metallic Zn. The release of dissolved Zn was dependent on pH, DOC concentration, ionic strength, and organic matter properties. The reaction appeared to be completed within about 24 hours and was characterized by pseudo first order kinetics with rate constants of 0.5 to 0.8 h⁻¹. EAC per mass unit of carbon ranged from 0.22 mmol g⁻¹ C to 12.6 mmol g⁻¹ C. Depending on the DOM, 11 – 65 % of the electrons transferred from metallic Zn to DOM could be subsequently donated to Fe(CN)₆³⁻. EAC decreased with DOC concentration, and increased with aromaticity, carboxyl, and phenolic content of the DOM. The results indicate that an operationally defined EAC of natural DOM can be quantified by reaction with metallic Zn and that DOM properties control the electron transfer. Shortcomings of the method are the coagulation and precipitation of DOM during the experiment and the production of hydrogen and dissolved Zn by reaction of metallic Zn with water, which may influence the determined EAC.

Introduction

Dissolved organic matter (DOM) influences microbial activity (Lovley et al., 1996), pollutant degradation, and metal mobility in the subsurface due its involvement in complexation, sorption, and redox processes (Redman et al., 2002; Schwarzenbach et al., 1990). Humic substances are of importance with respect to redox processes because they contain redox-active units, such as polyphenolic quinones (Schwarzenbach et al., 1990), which are ubiquitous structures in DOM (Cory and McKnight, 2005; Scott et al., 1998). A redox transfer of two electrons per quinone unit has been postulated based on studies with model compounds (Scott et al., 1998). Other moieties are likely also involved in redox reactions, because quinone content did not suffice to explain electron transfer (Struyk and Sposito, 2001). This concept is supported by redox titrations showing similar results for humic substances and mixtures of quinones and other phenols (Helburn and Maccarthy, 1994). The capacity of DOM to transfer electrons by this mechanism is especially important in environments poor in other electron acceptors and donors, such as peatlands and dystrophic lakes. In these environments, electron transfer of DOM may drive a relevant fraction of chemical and microbially mediated elemental transformations, for example by oxidation of hydrogen sulfide and organic intermediates of organic matter decomposition, and by reduction of ferric iron (Fulton et al., 2004; Heitmann and Blodau, 2006; Heitmann et al., 2007).

From reaction with redox active elements, such as mercury, vanadium, iron, and iodine, standard E_h values of 0.4 to 0.8 V have been determined for DOM of varying acid-base properties and origin (Skogerboe and Wilson, 1981; Struyk and Sposito, 2001). A range of redox potentials was also indicated by application of cyclic voltametry of DOM dissolved in the organic solvent dimethyl sulfoxide (Nurmi and Tratnyek, 2002). Also relevant for electron transfer from DOM to redox partners are complexed ferric iron contents and conformational changes of the DOM structure, which depend on pH and dissolved organic carbon (DOC) concentration (Chen et al., 2003a; Coates et al., 2000; Struyk and Sposito, 2001). Electron transfer capacities (ETC) of DOM samples have been shown to vary from 0.02 mmol_c g⁻¹ C to more than 6 mmol_c g⁻¹ C, depending on the particular redox couple, experimental assay and DOM used (Chen et al., 2003a; Kappler and Haderlein, 2003; Klapper et al., 2002; Matthiessen, 1995; Scott et al., 1998; Struyk and Sposito, 2001).

Quinones and DOM serve as organic electron acceptors for a variety of microorganisms, such as *Geobacter* and *Shewenella* species (Cervantes et al., 2000; Coates et al., 2000; Coates et al., 2002; Straub et al., 2004). This capability has been utilized to quantify an electron accepting capacity of DOM (EAC), combining microbial reduction and quantification of electron transfer by chemical re-oxidation with complexed ferric iron (Scott et al., 1998). To date, however, we are lacking robust chemical methods to determine EAC directly. An exception in this respect is the determination of an EAC by reduction of DOM with H₂S and the subsequent analysis of reaction products (Heitmann and Blodau, 2006). The applicability of this method, however, is limited by the complexity of possible reactions between sulfur and DOM, and by presence of ferrous iron and other scavengers for sulfide.

To alleviate the lack of methods to quantify EAC, we tested an approach using granular metallic Zn as reductant and applied it to several DOM samples in batch experiments varying in origin and structural characteristics. The reaction taking place can be written as reaction (1) with -Q standing for quinone, -QH₂ for reduced hydroquinone groups and Zn(0) for metallic Zn:



As metallic Zn is thermodynamically instable in aqueous solution, also reaction (2) with water has to be considered:



Molecular hydrogen is a reductant itself and may react with DOM according to reaction (3):



Our specific objectives were (I) to characterize the occurrence and kinetics of reaction (1) across a range of DOC concentrations, (II) to relate EAC to structural properties of DOM, and (III) to determine the ‘reversibility’ of the electron transfer. Reversibility in this context means that electrons accepted by DOM can be subsequently donated to an oxidant. This process allows a DOM moiety to repeatedly undergo oxidation-reduction cycles and to effectively shuttle electrons between reduced and oxidized compounds that do not react, or that are spatially separated. A full reversibility of the electron transfer of DOM cannot be assumed a priori. A one electron transfer oxidation of phenols, for example, can involve a subsequent polymerization of phenoxy radicals, which may inhibit further redox reactions (Helburn and Maccarthy, 1994).

In our investigation, batch experiments were carried out comparing the release of dissolved Zn in a DOM solution (‘treatment’) to release of Zn in an experiment without DOM (‘control’ or ‘blank’). The difference in dissolved Zn release was then used to infer the reaction of DOM with metallic Zn, i.e. reaction (1) and to calculate the electron accepting capacity of DOM. In a selected number of experiments, also hydrogen partial pressures and proton balances were determined in pH-stat. experiments. The difference in proton consumption between ‘treatment’ and ‘control’ was used to independently verify the stoichiometry of reaction (1) and (2). The difference in hydrogen release between ‘treatment’ and ‘control’ was further calculated to assess a possible contribution of reaction (3) to the overall reduction of DOM. Finally, we also recorded DOM concentrations in the experiments, as DOM may precipitate and adsorb on metallic Zn surfaces.

Materials and methods

Dissolved organic matter

DOM was sampled in Canada and the United States (Mer Bleue, Ontario; Suwannee River, Georgia; Black River, upper Michigan; Everglades, Florida; Table 1). All solutions were directly taken

from open water in opaque canisters, stored in the dark at 4°C and filtered (0.45 µm, nylon) before use. Additionally, Pahokee peat (PP-HA) reference humic acid standard, obtained from IHSS, was dissolved at pH ~ 8, acidified to pH 6 (HCl), filtered (0.45 µm), and diluted to 100 mg C L⁻¹. Assays were prepared by dilution.

DOM was characterized by UV-VIS spectrometry between 250 – 600 nm in diluted form of 10 mg L⁻¹ on a Varian Cary 1E spectrophotometer using quartz cuvettes. An ‘aromaticity’ index (SUVA_{254 nm}) in units of L (mg C • cm)⁻¹ was calculated by standardizing UV absorption at 254 nm to DOC concentration (Chin et al., 1994; Kalbitz et al., 1999). Fourier-transformed infrared (FTIR) spectra were determined on freeze-dried samples on a Bruker Vector 22 instrument using KBr pellets (200 mg KBr + 1 mg sample, 32 scans from 4000 to 500 cm⁻¹ at 1 cm⁻¹, automatic background correction). Spectra were baseline corrected. Relative changes in peak intensity ratios, as proposed by Niemeyer et al. (1992), were used to identify structural differences among DOM. Synchronous scan fluorescence spectra were recorded on a SFM 25 spectrometer (BIO-TEK Instruments) in the excitation wavelength range 300–550 nm with a scan speed of 100 nm min⁻¹, Δλ of 18 nm (Miano and Senesi, 1992), and 1 cm cuvettes. Samples were diluted to 10 mg C L⁻¹ for these analyses.

Table 6 Total elemental (ash) contents, spectroscopic characteristics (absorbance intensity of characteristic peaks of UV-VIS; FTIR and synchronous fluorescence ratios) of DOM used, and results of EAC and EDC measurements (mmol_c g⁻¹ C; mean of n = 3 – 5) at pH 6.5. ‘EDC_{Zn}’ represents the electron transfer of DOM, pre-reduced with metallic Zn (mmol_c g⁻¹ C), to FeCN. (n.d. = not determined)

DOM Parameter	Pahokee Peat	Mer Bleue	Suwannee River	Black River	Everglades
[DOC] (mg L ⁻¹)	50	44.5	41.2	31.5	60
Σ [Ash] [*] (mmol L ⁻¹)	1.7	0.5	0.7	0.5	7.1
[Fe] (µmol g ⁻¹)	0.3	0.9	0.5	0.2	0.0
E 465/665 ^{**}	6.2	14.6	17.8	7.9	23.2
SUVA _{254nm} (L (mg C • cm) ⁻¹)	0.060	0.051	0.045	0.045	0.036
IR 1725/1150 (cm ⁻¹)	1.83	2.01	1.10	0.34	0.68
IR 1620/1150 (cm ⁻¹)	1.72	2.68	1.25	1.23	2.40
IR 1270/1150 (cm ⁻¹)	1.34	1.19	0.75	0.27	0.13
F 400/360 (nm)	1.69	1.63	1.35	1.34	0.84
F 470/360 (nm)	2.55	1.11	0.78	0.62	0.32
F 470/400 (nm)	0.66	0.68	0.58	0.46	0.38
EAC _{Zn}	4.57	3.32	2.86	2.77	0.22
EDC	0.70	n.d.	0.076	0.28	0.36
EDC _{Zn}	0.50	n.d.	1.78	1.80	0.30

^{*} ash (Na, K, Ca, Mg, Fe, Mn, Si) ^{**} Ratio of UV/VIS absorption at 465 to 665 nm (E 465/665)

Identification of reactions between metallic Zn, water and DOM

To identify the occurrence and relative importance of reactions (1-3) and the removal of DOM from solution we conducted a series of pH-stat. experiments on a autotitrator (716 DMS Titrino. Metrohm). In the first type of experiment ('blank?'), only deionized water was added to the metallic Zn; in a second type, the deionized water was replaced with a DOM solution. In the experiments, which were carried out each in four replicates, headspace concentrations of H₂, dissolved concentrations of dissolved Zn and DOC, and proton consumption were recorded.

To this end, 5 grams of Zn were washed with HCl (1M) for 30 minutes and subsequently rinsed twice with degassed (1 h) deionized water and filled into butyl-rubber stoppered, air tight flasks as described by Heitmann and Blodau(2006). The flasks were equipped with sealed pH-electrodes (WTW Sentix 21/Schott Blue Line 22 pH), a canula for adding titration solution, and a magnetic stirrer. The titration solutions (0.1 M HCl and NaOH) were degassed before use as well. A volume of 50 mL of degassed blank or DOM solution, respectively, was then added under an argon stream to the reaction flask with the electrode mounted, leaving a headspace of 163.5 ± 3.5 mL. Immediately thereafter, the autotitrator was started to correct deviation from the starting pH of 6.5. The first samples were taken immediately and then 1, 3, 8, and 24 hours thereafter. Three replicate gas samples of 0.5 mL were withdrawn for the quantification of H₂, two replicates of 0.5 mL water for dissolved Zn, and one sample of 1 mL volume for DOC analysis. The solutions added to the metallic Zn contained none or 50 mg C L⁻¹ Pahokee Peat DOM and 10 mM NaCl to keep ionic strength constant. In another series of experiments, the stirring rate of the magnetic stirrer was changed from 500 rpm, which was the standard in all other experiments, to 250 rpm, and 1000 rpm. These experiments were carried out in duplicates.

Reduction of DOM

Five grams of acid-washed (50 mL of 1 M HCl for 30 min) and twice rinsed coarse metallic Zn grains (Riedel-de-Haen granular Zn, $\varnothing > 0,1$ mm) were added to 50 ml of N₂-purged DOM sample solution and cautiously shaken under exclusion of oxygen. Preliminary tests showed that fine Zn powder ($\varnothing < 0.45\mu\text{m}$) could not be used due to excessive Zn release in blank samples. The ionic strength was 5 mM (KCl) and the pH was repeatedly adjusted to 6.5 with dilute HCl or NaOH. For the experiments, DOM solutions were vacuum degassed and purged with nitrogen for at least 30 min. Assays were carried out in an oxygen-free glove box, containing an atmosphere of 95 % nitrogen and 5 % hydrogen. All flasks used for reactions and reagent storage were wrapped in aluminum foil to prevent photoreactions (Fukushima and Tatsumi, 1999). Blank experiments were conducted analogously to batch assays in the absence of humic acid. The following experiments were carried out with three or four replicates:

- (1) To test the limits of applicability of the method across a pH range, the release of dissolved Zn by reaction with deionized water was determined after 24 h at different pH values (2.0, 2.8, 4.0, 6.0, and 6.8), adjusted with HCl (0.1 M).
- (2) In a separate experiment, the reaction progress over time was determined by taking aliquots at regular intervals. In these experiments pH was regularly readjusted to 6.5 at intervals < 12 h using 0.01 M NaOH or HCl. After the experiment, additional samples were taken for DOC measurements.
- (3) To determine the dependency of dissolved Zn release on DOC concentrations, metallic Zn was incubated with DOM solutions diluted to 75, 50, 25, and 10 % of the original concentrations.

Reoxidation of DOM

To test the reversibility of electron acceptance by DOM, the DOM that had been reduced with metallic Zn was re-oxidized with potassium ferricyanide ($[\text{Fe}(\text{CN})_6]^{3-}$) ('FeCN') as oxidant according to (Matthiessen, 1995). The use of this oxidizing agent has long standing history, especially with respect to the oxidation of phenols (Haynes et al., 1959) and the detection of polyphenolic compounds such as tannins (Hagerman and Buttler (1989) and Graham (1992)). Four millilitres of untreated or Zn-reduced DOM solution were mixed with 1 ml FeCN solution in centrifuge tubes inside the glove box to final concentrations of 0.25 mM Fe, 5 mM MES buffer, and a pH of 6.5. Transformation of the coloured ferric iron complex to the ferrous iron complex, which remains colourless under the chosen chemical conditions, was determined photometrically at 420 nm. Mean values were determined as

$$\Delta \text{Absorption} = \overline{M}(\text{Abs}_{\text{Fe}(\text{CN})_6}) + \overline{M}(\text{Abs}_{\text{DOM}}) - \overline{M}(\text{Abs}_{\text{Fe}(\text{CN})_6 + \text{DOM}})$$

Analytical methods

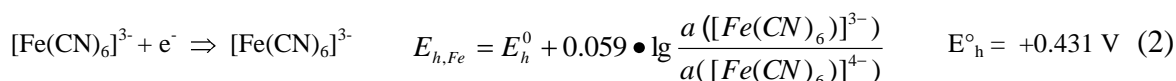
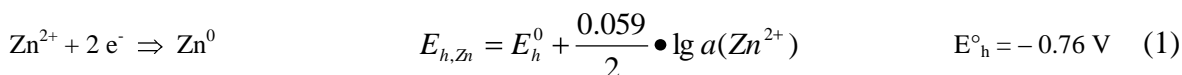
Iron was measured photometrically in capped plastic cuvettes at 420 nm (FeCN; (Matthiessen, 1995)). DOC concentration was determined after filtration (0.45 μm , nylon) on a Shimadzu 5050 TOC analyzer, and elemental composition of DOM and dissolved Zn concentrations by ICP AES (Perkin Elmer Optima 3000) and flame AAS (Varian SpectrAA-20), respectively. Hydrogen (H_2) was quantified with a mercury bed oxidation analyzer (Trace Analytical TA3000r); samples were taken directly from the headspace of the reaction flasks. Dissolved H_2 concentrations were recalculated by Henry's law ($K_{\text{H}, \text{H}_2} = 7.8 * 10^{-4} \text{ mol L}^{-1} \text{ atm}^{-1}$, at 22 $^\circ\text{C}$, from Sander (1999)) and volumes of headspace and liquid phase. Reagent grade chemicals and deionized water with an electric conductivity < 0.06 μS were used in all experiments.

Calculations

Electron acceptor (EAC_{Zn}) and electron donor (EDC) capacities of DOM were calculated from formation of dissolved Zn and ferrous Fe, respectively, and standardized on electron equivalents (charge, subscript c) and mass units of carbon ($\text{mmol}_c \text{ g}^{-1} \text{ C}$). Complexation of dissolved Zn by DOM

was modelled using the WINHUMIC equilibrium model, which is based on humic ion binding Model V, and considers aqueous speciation of Zn (Tipping, 1994; Tipping and Hurley, 1992). The model calculates the binding of metals by DOM functional groups in monodendate and bidendate complexes. The concentration of carboxyl and phenol functional groups contained in DOM was taken from IHSS data and calculated from own titration experiments (Bauer and Blodau, 2008).

Standard potentials (E_h°) for the oxidation of Zn to Zn^{2+} and reduction of ferric iron complexed by cyanide were taken from (Matthiessen, 1995; Stumm and Morgan, 1996). An experimental ‘*in situ*’ potential of the redox couples was calculated from standard potentials according to stoichiometries and equations (1) and (2), and the chemical composition of the solution at the endpoint of the reaction. We did not consider complexation by DOM, which may have accounted for 20 to 30% of total dissolved Zn at the endpoint of the reaction (see results). Iron and Zn speciation in solution was calculated using the PhreeqC algorithm, version 2.11.0, and Minteq database.



Zinc was in surplus in the experiments. For estimating kinetic constants we assumed a pseudo-first order kinetics with two redox-active DOM pools (Pullin and Cabaniss, 2003) and apparent (observed) time constants k_{obs} (eq. 3). For simplicity, the total redox active pool is labelled DOM-Q(uinone) in equation (3).

$$-\frac{d[Zn_{aq}]}{dt} = \frac{d[DOM-Q]}{dt} = -k_{obs}^{(1)} \bullet [DOM-Q]^{(1)} - k_{obs}^{(2)} \bullet [DOM-Q]^{(2)} \quad (3)$$

The time dependent solution to equation (3) is:

$$[Zn_{aq}](t) = [DOM-Q]_0^{(1)} \bullet (1 - 10^{-k_{obs}^1 \bullet t}) + [DOM-Q]_0^{(2)} \bullet (1 - 10^{-k_{obs}^2 \bullet t}) \quad (4)$$

The total reactive DOM pool was estimated from formation of dissolved Zn after completion of the reaction. The DOM pools are thus only constrained by dissolved Zn release. Calculations were carried out using the statistics package SPSS, release 13.01.

Results

Identification of reactions between metallic Zn, water and DOM

In the pH-stat experiments, at pH 6.5, metallic Zn reacted with water under release of hydrogen and dissolved Zn (Fig. 1). The stoichiometry of the release essentially followed reaction (2) with average stoichiometric factors of 0.96 – 0.99 for $\text{H}_2/\text{Zn}(\text{aq})$ and -2.11 – -2.17 for $\text{H}^+/\text{Zn}(\text{aq})$, based on the last two sampling times. Before, less H_2 was liberated into the headspace than expected, possibly due to incomplete equilibration between water and gas phase. Replacement of deionized water by the Pahokee Peat DOM solution resulted in increased dissolved Zn release, increased proton consumption, and decreased dissolved hydrogen release (Fig. 1). The additional Zn release was completed after about 8 hours in this experiment and afterwards, concentrations declined on average by 9 %.

After 24 hours, the mean additional Zn release of 146 to 166 $\mu\text{mol L}^{-1}$ in the DOM treatment was in rough agreement with a mean additional proton consumption of 352 $\mu\text{mol L}^{-1}$ and the stoichiometry of the reaction of DOM-Q with metallic Zn (1). Before, however, fewer protons were consumed than expected based on this stoichiometry. The slower release of hydrogen in the DOM compared to the blank experiments (Figure 1) suggests that hydrogen produced from reaction of metallic Zn with water was incorporated into DOM, possibly by reduction of DOM-Q to DOM-QH₂, or that the release of H_2 was restricted by the addition of DOM. Calculations with the WINHUMIC model indicated that 40 – 60 $\mu\text{mol Zn}(\text{aq})$ could be potentially complexed by the Pahokee Peat DOM, given the DOM concentrations employed.

Measured DOM concentrations decreased with time on average from 18 mg L^{-1} to 4 mg L^{-1} when results from experiments were lumped together (Supporting Information, Figure 1S). After 24 hours, a brownish layer was present on the Zn grains and the previously dissolved organic matter thus probably partly adsorbed on the solid surfaces, partly it may have hydrophobically coagulated due to the presence of dissolved Zn. Hence, the organic matter was fairly homogeneously distributed in the flasks only for the first hours of the experiments. A variation of stirring speed in another series of experiments did not produce conclusive information; the results are presented in the supporting information (Fig. 2s).

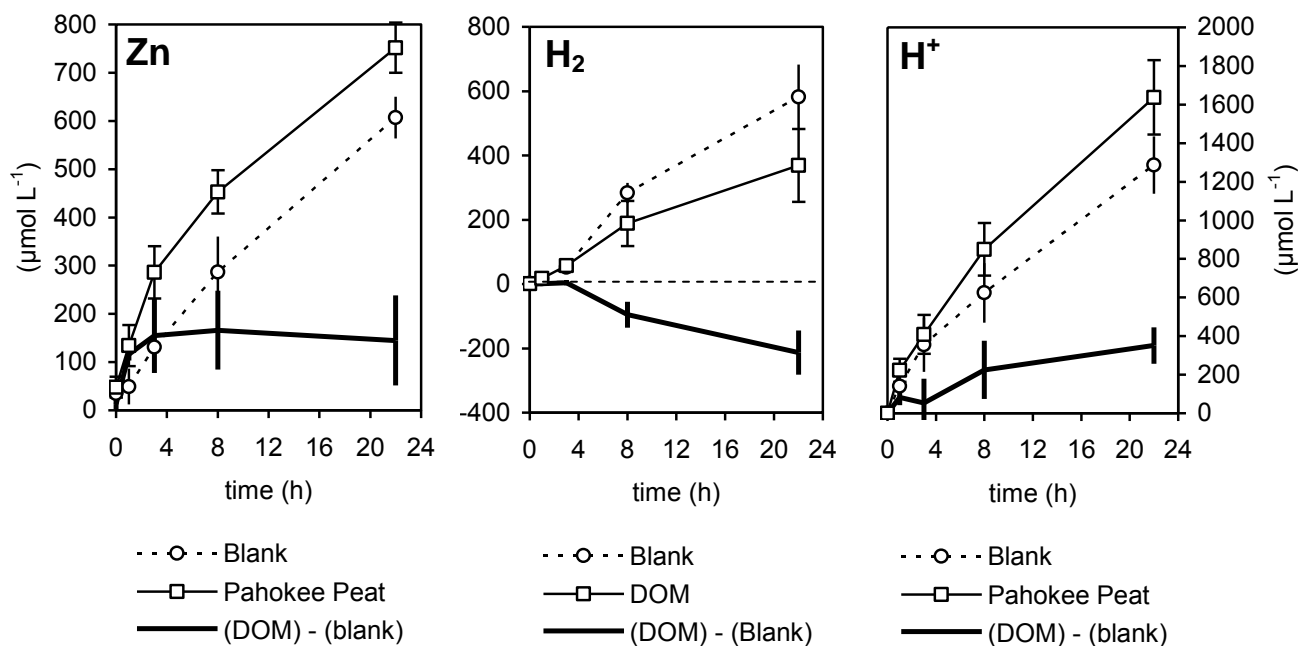


Figure 16 Release of dissolved Zn and dissolved H₂, and consumption of protons in pH-stat. experiments. ‘Blank’ represents assays in which metallic Zn reacted with water only, and ‘DOM’ represents assays in which Pahokee Peat DOM was used. (n = 4, ± s.e.)

Zinc release by reaction with water versus pH

Between pH 4.0 and 6.8, Zn(aq) concentrations ranged from 21 to 26 μmol L⁻¹ after 24 hours in blank experiments in the absence of DOM, and increased up to 4700 μmol L⁻¹ when the batch was acidified to pH 2 (Fig. 2 A). Zinc release by reaction with water does thus restrict the applicability of the method to a pH equal or higher than 4. Even at near neutral pH this reaction occurs, which increases the error in EAC with decreasing DOC concentration or EAC per unit mass of carbon.

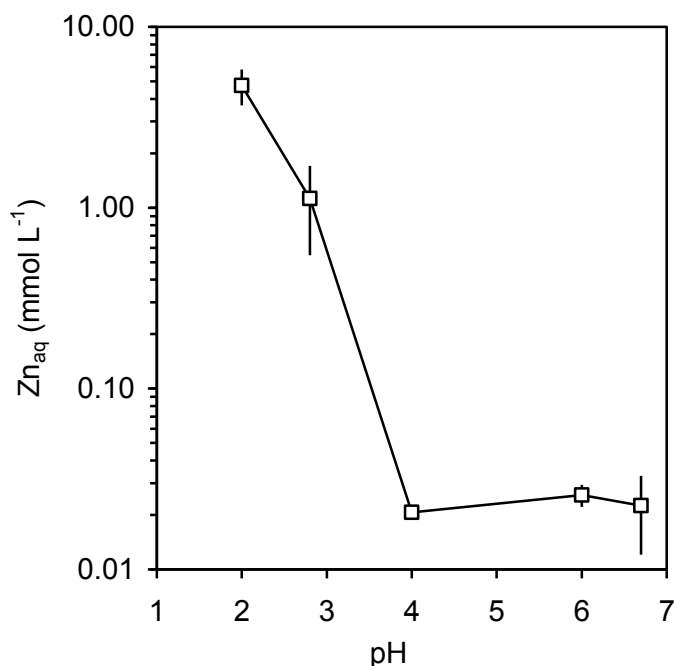


Figure 17 Dissolved Zn (Zn_{aq}) release in deionized water in dependency of pH and measured after 24 hours. (\pm s.d., $n = 3$)

Kinetics of Zn release

DOM was initially rapidly reduced by contact with metallic Zn, which reached dissolved concentrations of 112 to 172 $\mu\text{mol L}^{-1}$ in excess of concentrations in blank samples after 24 to 48 h (Fig. 3). The total release of $Zn(aq)$ was thus very similar as observed in the more strictly controlled pH-stat. experiments but it occurred more slowly (compare Fig. 1 and 3). In these experiments also less DOC, i.e. 17 – 26 %, was eliminated from solution, in comparison to the pH-stat. experiments (Supporting Information, Table 1s).

The release of $Zn(aq)$ roughly followed a log-linear relationship, suggesting a pseudo-first order reaction with respect to redox-active groups in DOM ($R^2 = 0.93 - 0.95$). However, the fitted function overestimated concentrations from 4 to 24 hours, and underestimated them before and after. A better fit could be obtained using equation (4), assuming presence of two DOM pools of differing reactivity. Reaction rate constants were 6.5 h^{-1} and 0.07 h^{-1} (Pahokee Peat). With respect to Suwannee River DOM the fit could not be improved using two DOM pools. The rate constant obtained was 0.48 h^{-1} . Dissolved Zn release decreased in the order Pahokee Peat > Black River > Suwannee River > Everglades, but reaction progress was similar in all samples (not shown). This suggests that DOM samples contained different quantities of functional groups of similar reactivity. Zinc release increased steadily with DOC concentration (Fig. 4) at low and high ionic strength, albeit not strictly linearly at

lower DOC concentrations (also compare Fig. 5). The dissolved Zn release by application of Pahokee Peat and Mer Bleue DOM was characterized by a similar dependency on DOC concentration, whereas Suwannee River DOM relatively released more dissolved Zn at higher DOC concentrations (Fig. 4).

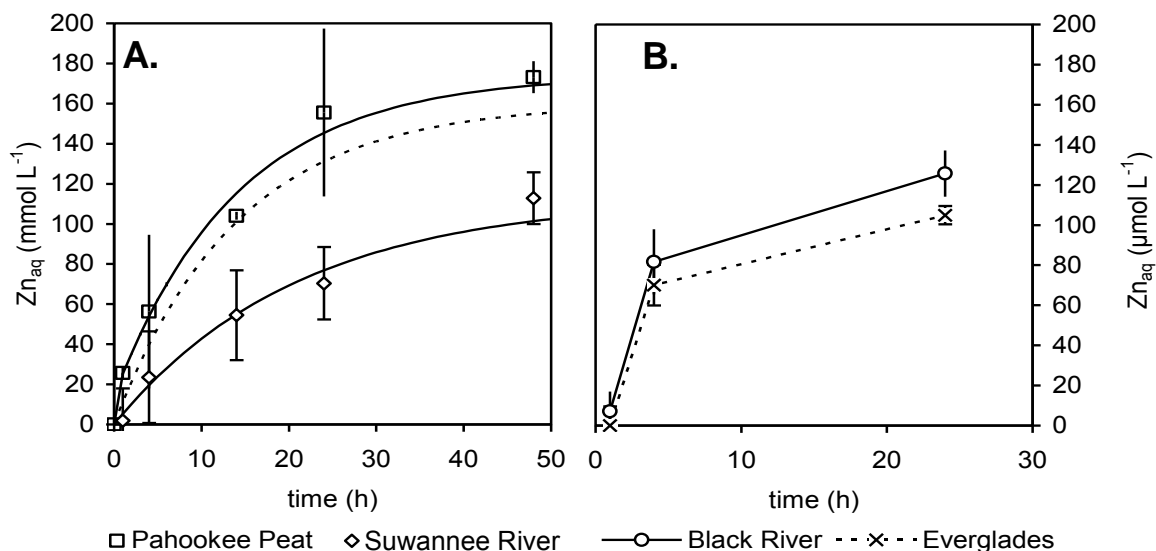


Figure 18 Reaction progress of dissolved Zn (Zn_{aq}) release with different DOM. In panel A., release was fitted to a first order expression with one DOM pool (Suwannee River) and two DOM pools (Pahokee Peat) The dotted line represent the calculated contribution of the slow DOM pool to Zn_{aq} release for the Pahokee Peat sample. Panel B. shows Zn_{aq} release with blanks not considered, owing to an analytical problem with some of the blank measurements in this assay. (\pm s.d., n = 3 – 4)

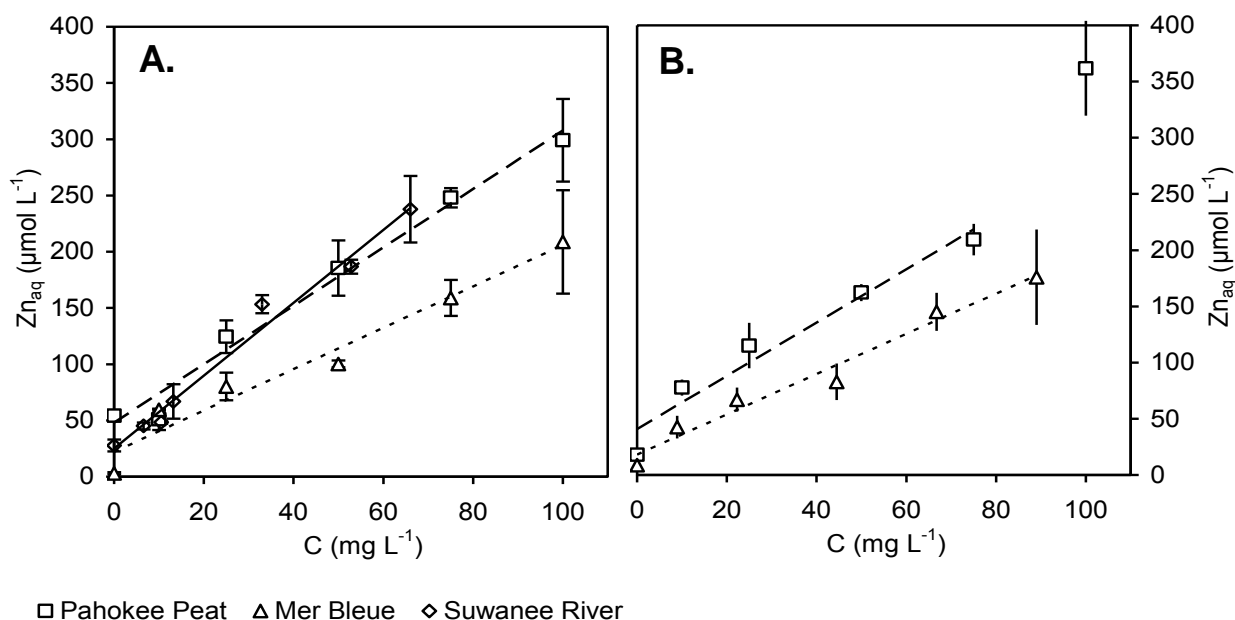


Figure 19 Dependency of dissolved Zn (Zn_{aq}) release on DOM concentration in deionized water and NaCl solution (10 mmol L⁻¹). (\pm s.d., n = 3)

Determination of EAC

The EAC of undiluted samples (Suwannee and Black Rivers, Everglades) and samples diluted to 50 mg L⁻¹ (Pahokee Peat) and 45 mg L⁻¹ (Mer Bleue) ranged from 0.22 to 4.6 mmol_c g⁻¹ C (Table 1). EAC increased in the order Everglades < Black River ~ Suwannee River < Mer Bleue < Pahokee Peat (Table 1). EAC was dependent on DOC concentration. Standardized on unit mass of carbon, EAC increased when DOC concentrations were lowered to less than 40 mg L⁻¹ and reached 11.9 mmol_c g⁻¹ C (Pahokee Peat) and 12.6 mmol_c g⁻¹ C (Mer Bleue, Fig. 5). EAC decreased with DOC concentration roughly following a power function (Fig. 5). Increasing ionic strength decreased EAC consistently in Mer Bleue samples by 19 – 40 %, and increased them by –1 – 29 % in Pahokee peat solutions. Ionic strength thus had an influence on EAC quantification with metallic Zn but not in a predictable direction. The calculated *in-situ* redox potential (E_h) of Zn(0)/Zn²⁺ was –0.88 V when the reaction was completed.

EDC and 'reversibility' of electron transfer

The EDC of untreated DOM ranged from 0.08 to 0.70 mmol_c g⁻¹ C using FeCN as oxidant and increased in the order Suwannee River ~ Black River < Everglades < Pahokee Peat (Fig. 6). The *in-situ* redox potential (E_h) was +0.50 V. DOM pre-treated with metallic Zn reduced much larger quantities of FeCN than untreated DOM, but reduction with metallic Zn was not fully reversible with values of 11 % (Pahokee Peat), 62 and 65 % (Suwannee and Black River). The Everglades sample donated more electrons to FeCN than it had received from metallic Zn. As the EAC of this DOM solution was very small (Fig. 6), the accuracy of the EAC value was probably limited and may have caused this phenomenon.

Spectroscopic DOM properties vs. EAC

The different DOM distinctly differed in their UV, IR, and fluorescence spectroscopic properties (Fig. 7; Fig. 8, Table 1). Pahokee Peat and Mer Bleue in particular were characterized by high SUVA_{254nm} of 0.06 and 0.051 L (mg C)⁻¹ (cm)⁻¹, strong IR-absorption at characteristic wave number of 1725 cm⁻¹ (C=O stretch of COOH) and 1620 cm⁻¹ (aromatic C=C stretch/asymmetric –COO⁻ stretch), an absorption peak/shoulder at 1270 cm⁻¹ (C–OH stretch of phenolic –OH), and weak absorption in the range of 1050 – 1200 cm⁻¹ (mostly aliphatic –OH typical for carbohydrates (Niemayer et al., 1992)). A similar spectrum was also recorded with respect to Suwannee River DOM but absorption in the range of 1050 – 1200 cm⁻¹ was more prominent. The terrestrial DOM was further characterized by a maximum of fluorescence intensity at high wave lengths of 400 to 470 nm. This pattern has been linked to a high degree of polycondensation and larger relative quantities of conjugated aromatic π-electron systems (Chen et al., 2003b), owing to their electron-withdrawing qualities (Pullin and Cabaniss, 1995).

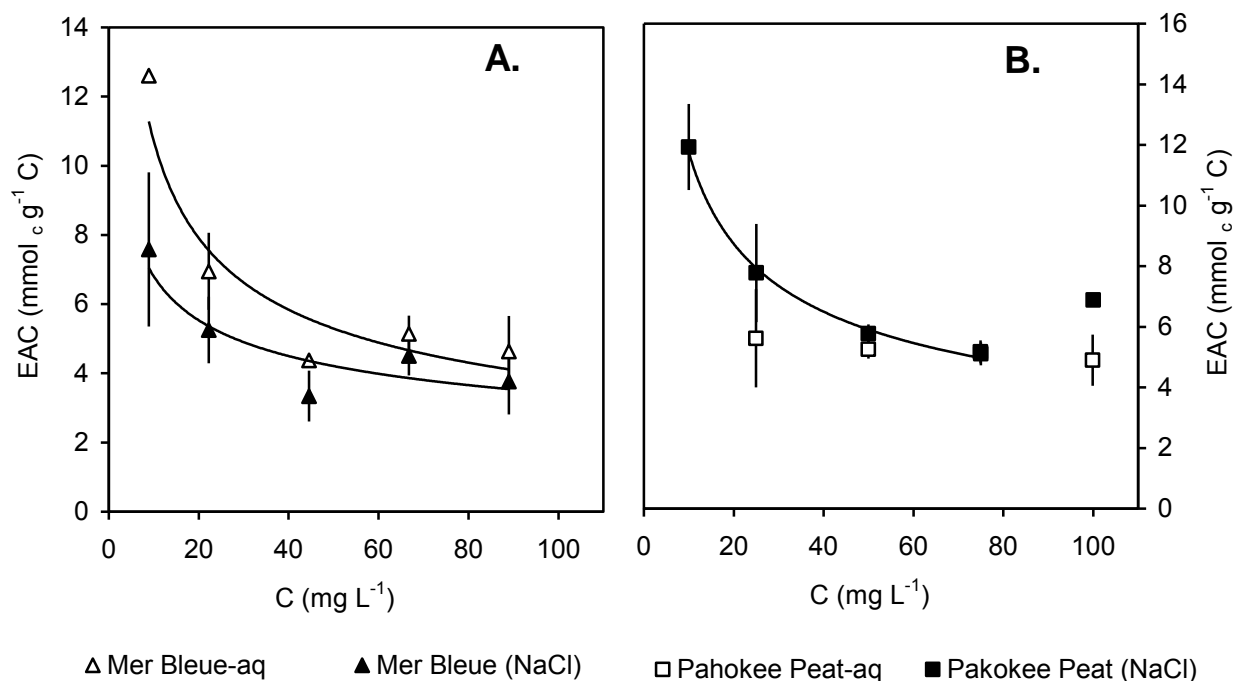


Figure 20 Dependency of EAC per unit mass of carbon on DOM concentration in deionized water and NaCl solution (10 mmol L⁻¹). A best fit could be obtained using exponential functions (MB = Mer Bleue; PP = Pahokee Peat; units in mg L⁻¹ DOC and mmol_e g⁻¹ C EAC). (± s.d., n = 3)

$$\begin{aligned} \text{EAC}_{\text{aq}} (\text{MB}) &= 29.4 [\text{DOC}]^{-0.43}, & R^2 &= 0.87 \\ \text{EAC}_{\text{NaCl}} (\text{MB}) &= 13.5 [\text{DOC}]^{-0.29}, & R^2 &= 0.75 \\ \text{EAC}_{\text{NaCl}} (\text{PP}) &= 31.4 [\text{DOC}]^{-0.43}, & R^2 &= 0.99 \end{aligned}$$

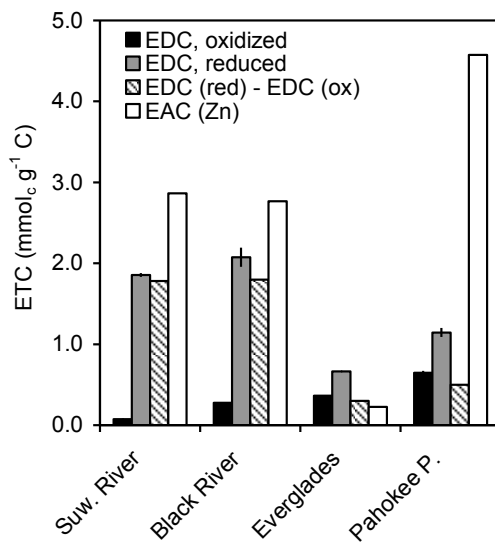


Figure 21 Electron accepting capacity (EAC) of DOM using metallic Zn and electron donor capacity (EDC) of the DOM using [Fe(CN)₆]³⁻ as oxidant. EDC was determined for untreated DOM, labelled 'EDC (ox)', and Zn-prereduced DOM, labelled 'EDC (red)'. Full reversibility of the electron transfer is given when EAC equals the difference between EDC (ox) and EDC (red).

The other DOM samples (Black River River and Everglades) were characterized by lower absorption around 1725 cm⁻¹ and 1270 cm⁻¹, and relatively strong absorption in the 1620 cm⁻¹ IR range (Fig. 7). The Everglades DOM was furthermore characterized by strong absorption bands around 1450 cm⁻¹, likely related to carbonate precipitates. A relatively larger contribution of less humified, low molecular weight compounds is typical for a maximum in fluorescence peak intensity at low wave lengths of about 350 nm (Fig. 8) (Chen et al., 2003b). Standardized on IR absorption at 1150 cm⁻¹, the relative contribution of carboxylic moieties decreased in the order Mer Bleue > Pahokee Peat > Suwannee River > Everglades > Black River and of phenolic moieties in the order Pahokee Peat > Mer Bleue > Suwannee River > Black River > Everglades (Table 1).

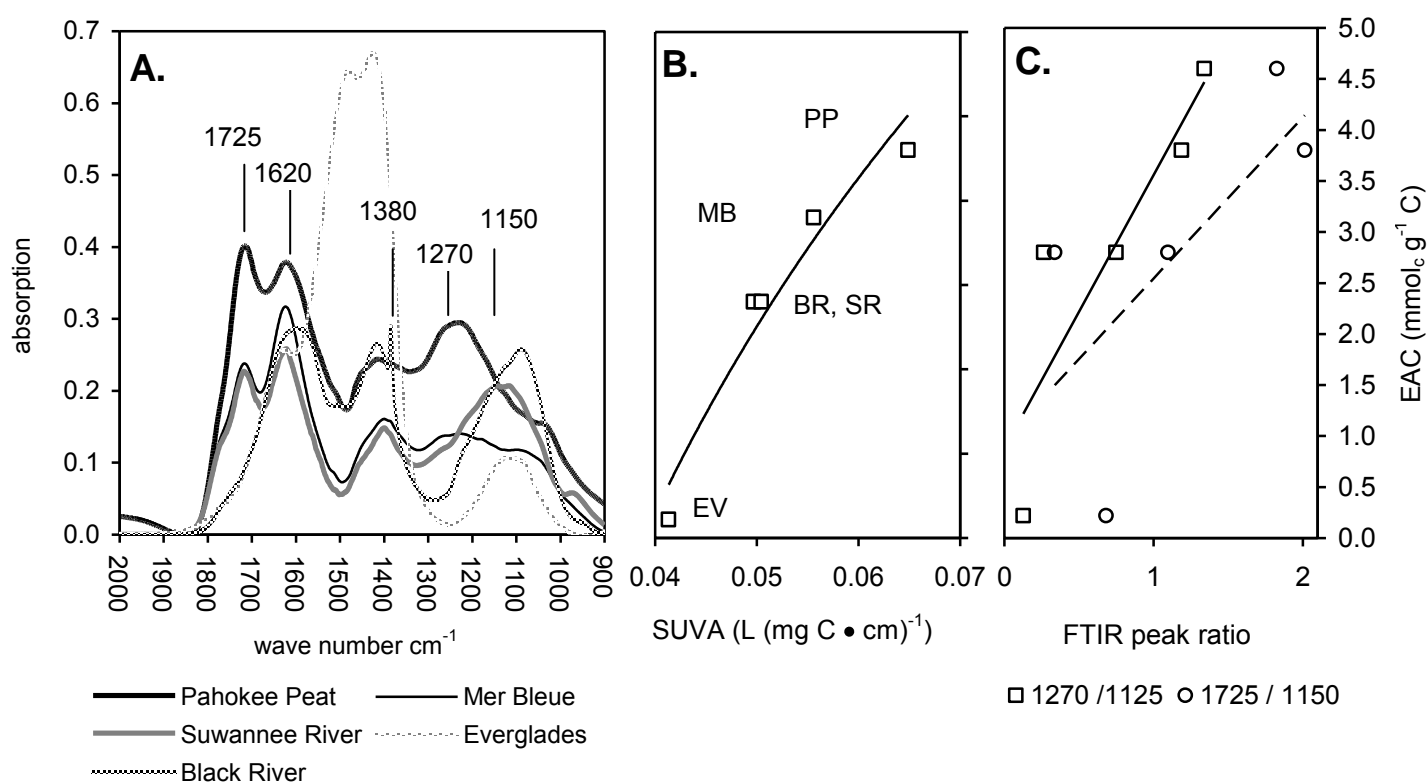


Figure 22 FTIR spectra of DOM used (A.), correlation of EACZn against SUVA_{254nm} (B.), and correlation of EACZn with FTIR absorption intensity in the range of 1725 cm⁻¹ (C=O stretch in COOH), 1620 cm⁻¹ (aromatic C=C stretch) and 1270 cm⁻¹ (C–OH stretch of phenolic C), standardized to the range of 1150 cm⁻¹ (C–OH stretch of aliphatic OH) (Niemayer et al., 1992). For the calculation of ratios a maximum of absorption within ± 25 cm⁻¹ of reported absorption maxima was used. Regression equations are as follows:

$$\begin{aligned} \text{EACZn} &= 8.8 \ln [\text{SUVA}] + 29 & R^2 &= 0.95 \\ \text{EACZn} &= 2.7 [\text{E} (1270/1150)] + 0.88 & R^2 &= 0.77 \\ \text{EACZn} &= 1.6 [\text{E} (1725/1150)] + 0.96 & R^2 &= 0.47 \end{aligned}$$

EAC was related to ‘aromaticity’ as determined by SUVA_{254nm}, the relative contribution of phenolic and to a lesser degree carboxylic moieties, as obtained by FTIR spectroscopy (Fig. 7 B. and C.), and the relative contents of aromatic, polycondensed moieties, as determined by characteristic fluorescence intensity ratios (Fig. 8 B.). No relationship existed with respect to normalized IR

absorption at 1620 cm^{-1} since the Everglades DOM spectrum absorbed strongly in this range but had only a very small EAC. High relative contents of carboxylic and phenolic groups, and likely also aromatic structures overall seemed to promote electron uptake by DOM. A best fit with respect to $\text{SUVA}_{254\text{nm}}$ and fluorescence data could be obtained using logarithmic relationships between the spectroscopic properties and EAC (Fig. 7, 8).

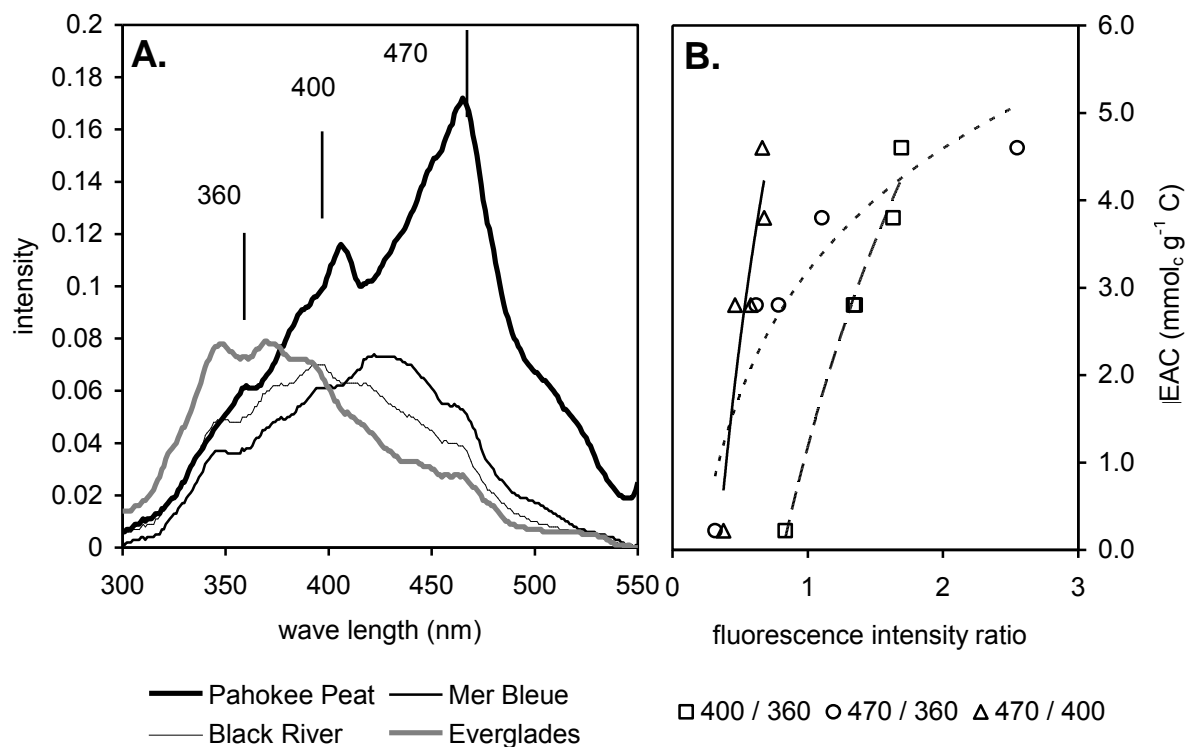


Figure 23 Synchronous fluorescence spectra of DOM used (A.) and correlation of EACZn with fluorescence ratios characteristic (B.) of the degree of ‘polycondensation’ (470 nm / 360 nm and 470 nm / 400nm), and phenolic- and quinone-type moieties (400 nm / 360nm) (Chen et al., 2003a). Regression equations are as follows:

$$\begin{aligned} \text{EACZn} &= 5.8 [\text{E} (400/360)] + 1.2 & \text{R}^2 &= 0.98 \\ \text{EACZn} &= 2.0 \ln [\text{E} (470/360)] + 3.2 & \text{R}^2 &= 0.90 \\ \text{EACZn} &= 6.1 \ln [\text{E} (470/400)] + 6.58 & \text{R}^2 &= 0.85 \end{aligned}$$

Discussion

Reaction of metallic Zn with DOM

In the pH-stat. blank experiments, the evolution of dissolved Zn and hydrogen, and the consumption of protons were in agreement with the described reaction (2) of metallic Zn with water (Stumm and Morgan, 1996). Exchange of water by Pahokee Peat DOM increased dissolved Zn release and proton consumption, which is in agreement with a reduction of DOM by metallic Zn according to reaction (1), and furthermore reduced hydrogen production. The fate of the produced hydrogen in the experiments with DOM cannot be clarified conclusively. A reduction of DOM by hydrogen, for example according to reaction (3), has been documented in presence of palladium (Pd) as catalyst and also been used to quantify an electron accepting capacity indirectly (Benz et al., 1998; Kappler et al.,

2004). We are not aware that metallic Zn surfaces could have a similar catalytic function as Pd but cannot exclude this possibility.

More likely than such an effect, however, seems a developing passivation of metallic Zn surfaces by precipitation of DOM, which may have reduced the propensity of the metallic Zn to react with water. Such an effect is argued for by the small difference between treatment and control with respect to hydrogen release in the beginning and the increasing lag of hydrogen release with increasing DOC loss in the DOM treatments (Fig. 1). If correctly interpreted, the difference of hydrogen release between control and DOM treatment in Figure 1 does not reflect a reduction of DOM by hydrogen, which would have to be added to the electron accepting capacity of the DOM, as quantified from the release of dissolved Zn. A potential passivation of metallic zinc poses a similar problem, however, because the EAC is calculated by subtraction of zinc release in blank assays from DOM assays. An overestimation of the dissolved Zn release in the DOM assay thus leads to an underestimate of the true EAC of the DOM.

The loss of DOM from solution possibly also influenced the release of dissolved Zn and the dissolved Zn concentration, and consequently the calculation of the EAC. In the pH-stat. experiments with Pahokee Peat DOM (Fig. 1), the additional release of dissolved Zn in DOM treatments was completed after only 8 hours and thereafter a decline in concentrations of 9 % occurred on average, which may have been caused by the co-precipitation of Zn complexed with DOM. Using the WINHUMIC software, we estimated that 40 to 60 $\mu\text{mol L}^{-1}$ Zn, or about 20 – 30 %, were potentially complexed by DOM in our experiments. Given the average decrease in DOC concentration of 6 mg L^{-1} , or 30 % of the initial DOC concentration in the period between 8 h and 24 h, a co-precipitation of Zn with DOM in the recorded order of magnitude seems plausible. In the kinetic experiments with the same DOM (Fig. 3) reaction progress occurred more slowly and asymptotically reached a concentration maximum only after 24 to 48 hours, which also raises the question if the stronger DOM precipitation in the pH-stat. experiments reduced the capacity of the DOM to react with metallic Zn. This was apparently not the case, though, as the total dissolved Zn release was similar (compare Figs. 1 and 3).

Regardless of the obvious methodological difficulties encountered in this heterogeneous chemical system the pH-stat. experiments suggested that humic DOM was reduced by metallic Zn and that the additional dissolved Zn release compared to blank samples cannot be solely attributed to a catalytic effect of DOM on the reaction of metallic Zn with water, as no additional H_2 was concurrently released. This conclusion is substantiated by the fact that the total dissolved Zn released increased linearly with the DOC concentration used (Figure 4). An increase in electron accepting capacity in the solution resulted in the predicted increase in oxidation of metallic Zn. The study thus demonstrates that an EAC of DOM can be quantified by reaction with metallic Zn in a DOC concentration range of 10 – 100 mg L^{-1} , which is a range typical for carbon rich aquifers, soils, sediments, and dystrophic lakes. It must be emphasized, however, that this capacity is operationally defined for the specific

experimental conditions chosen and that changes in the redox state of a particular DOM, as well as comparisons between different sources of DOM, can only be quantified when the experimental conditions are kept constant and no strong differences in DOM precipitation occur between experimental runs.

Apart from DOM precipitation, DOC concentration itself was a factor influencing the EAC_{Zn} of DOM, particularly at DOC concentration below 40 mg L^{-1} , and ionic strength also alter EAC_{Zn} in a direction that could not be predicted *a priori*. Both effects are not easily explained based on the data obtained, and are likely related to conformational changes of the DOM that were not analyzed. Higher DOC concentration, for example, may lead to coagulation of DOM molecules (Buffle and Leppard, 1995) reduce the accessibility of reactive structures (Coates et al., 2000) and thus lower EAC per mass unit of carbon (Fig. 5). The reaction of DOM with metallic Zn represents a heterogeneous reaction that will require contact of DOM with a Zn surface that is probably partly charged due to the release of Zn^{2+} and local formation of Zn hydroxide. It was shown previously that increasing DOM concentrations may reduce surface tension and increase hydrophobicity of humic acids (Coates et al., 2000). It can be speculated that the propensity of DOM to undergo a reaction with metallic Zn surfaces was lowered by such changes. Regardless of the exact cause of such effects these observations also emphasize that EAC_{Zn} cannot be considered an intrinsic quality of the DOM and that experimental conditions need to be standardized if comparability between samples is sought.

Electron accepting and donating capacities

EAC values of $2.8 \text{ mmol}_c \text{ g}^{-1} \text{ C}$ to $4.6 \text{ mmol}_c \text{ g}^{-1} \text{ C}$, as determined for four of the five DOM solutions used, are in the upper range of electron transfer capacities determined. Reported ETC values for various isolated humic acids have ranged from 0.01 to 21 (median: 0.9) $\text{mmol}_c \text{ g}^{-1} \text{ C}$ (Chen et al., 2003a; Kappler et al., 2004; Lovley et al., 1996; Struyk and Sposito, 2001). This range reflects differences in pH, redox potential of oxidants and reductants, and structural properties of DOM (Bauer and Blodau, 2006; Chen et al., 2003a). Heitmann and Blodau (2006) reported an EAC of $0.6 \text{ mmol}_c \text{ g}^{-1} \text{ C}$ by reducing Pahokee Peat humic acid with H_2S . An EDC of $0.41 \text{ mmol}_c \text{ g}^{-1} \text{ C}$ was determined at pH 6.9 using $FeCl_3$ as oxidant (Scott et al., 1998), and of $4.1 \text{ mmol}_c \text{ g}^{-1} \text{ C}$ at pH 5.0 using iodine as oxidant (Struyk and Sposito, 2001). Comparatively small EDC values of 0.001 to $0.7 \text{ mmol}_c \text{ g}^{-1} \text{ C}$ were determined also in the study by Struyk and Sposito (2001).

The reasons for such differences in ETC have not been systematically investigated, but are probably to some extent related to the redox potentials of the oxidants and reductants employed (Bauer and Blodau, 2006). For the experimental conditions used (pH 6.5, composition of the solution after 24 h) we obtained *in situ* E_h values of -0.88 V (Zn/Zn^{2+} , eq. 1) and $+0.50 \text{ V}$ ($FeCN$, eq. 2). Previously, E_h° values of 0.4 to 0.8 V have been determined for DOM of varying acid-base properties and origin (Skogerboe and Wilson, 1981; Struyk and Sposito, 2001). Standard redox potentials of quinone model compounds range from $< 0.3 \text{ V}$ to $> 0.69 \text{ V}$ (Helburn and Maccarthy, 1994; Rosso et al., 2004).

Considering the relative differences in redox potentials between DOM and reactants, the differences in magnitudes of EAC and EDC determined in this study are not surprising. The electromotive force applied by reduction with metallic Zn was much larger than by oxidation with ferric iron. It is thus likely that a wider range of redox active moieties were involved in the electron transfer. However, differences in electromotive force do not explain the incomplete reversibility of the electron transfer, as moieties reduced at low potentials should transfer electrons to ferric iron. The structure of the DOM may, therefore, have been irreversibly altered by the reduction with metallic Zn. Such a process is, for example, known from one electron transfer oxidation of phenols, involving subsequent polymerization of phenoxy radicals (Helburn and MacCarthy, 1994).

From a practical point of view, it further has to be considered that metallic Zn is also an extraordinary strong reductant compared to relevant electron donors in the aqueous environment, such as H₂ and H₂S. Reduction of DOM with metallic Zn may thus be seen as an upper limit of EAC present in aqueous environmental samples and may not be reached *in situ*. This conclusion is further emphasized because electron transfer from metallic Zn to DOM was only partly reversible using complexed ferric iron as oxidant (Fig. 6).

Electron accepting capacity versus DOM characteristic

The comparison between spectroscopic properties and EAC suggested that the electron transfer from metallic Zn to DOM was related to particular structural moieties in the DOM (Fig. 7). The relationships obtained should not be viewed as general and reliable, though. The number of samples was small and the analytical parameters are semiquantitative, albeit metrically scaled (Kalbitz et al., 1999; Niemayer et al., 1992). The intensity of IR absorption was found not to correlate with DOM concentration in FTIR measurements. Therefore, we standardized absorption intensity of bands characteristic for structural moieties related to ETC on absorption intensity bands unrelated to ETC (Fig. 7). Such a procedure has previously been shown to provide fairly consistent information about structural characteristics across a range of organic matter concentrations (Niemayer et al., 1992).

It has been shown that ETC is related to quinone content by means of electron spin resonance spectroscopy and to contents of aromatic structures by ¹³C NMR spectroscopy (Scott et al., 1998). Furthermore it has been conjectured that other moieties, such as polyphenols, are also redox-active units within humic substances because mixtures of model compounds provided very similar redox titration results compared to humic acids (Helburn and MacCarthy, 1994). This conclusion was supported comparing ETC to quinone contents, because contents did not suffice to explain electron transfer (Struyk and Sposito, 2001). The authors furthermore suggested that contents of complexed iron were partly responsible for the observed electron transfer and may constitute an important electron shuttle.

In this study, contents of iron were very small and iron content appeared not to be related to the determined EAC, as the comparison between EAC values and iron contents in Table 1 illustrates. EAC

increased with phenolic and to a lesser degree also carboxylic content within the DOM, when standardized to an IR absorption band window unrelated to electron transfer (Fig. 7). The results from FTIR spectroscopy were further supported by synchronous fluorescence spectroscopy. The EAC increased with shifting synchronous fluorescence intensity to wave lengths > 350 nm. This patterns has been linked to relative contents of phenols and ketones (wave lengths of 380 - 430 nm) and to polycondensed conjugated aromatic structures in DOM (wave lengths of about 450 - 480 nm; (Chen et al., 2002; Chen et al., 2003b; Kalbitz et al., 1999). The consistency of reaction progress of electron transfer over time among the DOM solutions (Fig. 3) further suggested that the reactivities of the structures responsible for electron transfer were similar among different DOM samples, and that apparently primarily the contents of these structures varied among the DOM solutions. The relative importance of functional moieties responsible for the electron transfer cannot be conclusively evaluated from the results obtained. Still, the analysis confirms that the strongly aromatic, phenolic, and carboxylated humic substances of terrestrial origin carry a particularly high potential to accept electrons.

Conclusions

The study demonstrates that the reaction of DOM with metallic Zn can be used to quantify an operationally defined electron accepting capacity of DOM at $\text{pH} > 4$ and DOM concentrations of 10 – 100 mg L^{-1} . The electron transfer was dependent on DOC concentration, was mostly completed within 48 h, and could be reproduced using a pseudo first order kinetics with one or two DOM pools. The electron transfer was furthermore at least partly reversible using dissolved ferric iron cyanide as oxidant. Since DOM concentration and ionic strength affected EAC, the obtained EAC has to be viewed as operationally defined for particular conditions. Shortcomings of the method are in particular the precipitation of DOM on the metallic Zn surfaces, and the production of hydrogen by the reaction of Zn with water, which is also a potential reductant for DOM. Both processes would cause an experimental underestimate of the true potential of the DOM to accept electrons from metallic zinc. It needs to be considered further that the obtained DOM likely represents an upper estimate in aqueous natural environments owing to the large electromotive force applied. The correlation to spectroscopic properties suggested that the strongly humified and carboxylated humic substances of terrestrial origin carry a particularly high EAC.

Acknowledgements

We thank K. Kalbitz for providing access and help with a fluorescence spectrometer at the Department of Soil Ecology, University of Bayreuth. The technical assistance of Jan Schwieker, S. Hammer and K. Soellner was much appreciated. The study was funded by DFG grant BL 563 2/1 to

C. Blodau. M. Bauer was in part supported by a fellowship from DAAD and S. Regensburg by a postdoctoral fellowship (DFG RE 1679 1/1).

References

- Bauer M. and Blodau C. (2006) Mobilization of arsenic by dissolved organic matter from iron oxides, soils and sediments. *Sci. Tot. Environ.* **354**, 179-190.
- Bauer M. and Blodau C. (2008) Experimental colloid formation in aqueous solutions rich in dissolved organic matter, ferric iron, and As. *Geochim. Cosmochim. Acta* **submitted**.
- Benz M., Schink B., and Brune A. (1998) Humic Acid Reduction by *Propionibacterium freudenreichii* and other Fermenting Bacteria. *Appl. Environ. Microbiol.* **64**(11), 4507-4512.
- Buffle J. and Leppard G. G. (1995) Characterization of Aquatic Colloids and Macromolecules .1. Structure and Behavior of Colloidal Material. *Environ. Sci. Technol.* **29**(9), 2169-2175.
- Cervantes F. J., Van der Velde S., Lettinga G., and Field J. A. (2000) Competition between methanogenesis and quinone respiration for ecologically important substrates in anaerobic consortia. *FEMS Microbiol. Ecol.* **34**, 161-171.
- Chen J., Gu B. H., LeBoeuf E. J., Pan H. J., and Dai S. (2002) Spectroscopic characterization of the structural and functional properties of natural organic matter fractions. *Chemosphere* **48**(1), 59-68.
- Chen J., Gu B. H., Royer R. A., and Burgos W. D. (2003a) The roles of natural organic matter in chemical and microbial reduction of ferric iron. *Sci. Tot. Environ.* **307**(1-3), 167-178.
- Chen J., LeBoeuf E. J., Dai S., and Gu B. H. (2003b) Fluorescence spectroscopic studies of natural organic matter fractions. *Chemosphere* **50**(5), 639-647.
- Chin Y.-P., Aiken G. R., and O'Loughlin E. (1994) Molecular weight, polydispersity and spectroscopic properties of aquatic humic substances. *Environ. Sci. Technol.* **28**(1853-1858).
- Coates J. D., Chakraborty R., O'Connor S. M., Schmidt C., and Thieme J. (2000) The geochemical effects of microbial humic substances reduction. *Acta hydrochim. hydrobiol.* **28**(7), 420-427.
- Coates J. D., Cole K. A., Chakraborty R., O'Connor S. M., and Achenbach L. A. (2002) Diversity and ubiquity of bacteria capable of utilizing humic substances as electron donors for anaerobic respiration. *Appl. Environ. Microbiol.* **68**(5), 2445-2452.
- Cory R. M. and McKnight D. M. (2005) Fluorescence Spectroscopy Reveals Ubiquitous Presence of Oxidized and Reduced Quinones in Dissolved Organic Matter. *Environ. Sci. Technol.* **39**(21), 8142-8149.
- Fukushima M. and Tatsumi K. (1999) Light acceleration of iron(III) reduction by humic acid in the aqueous solution. *Colloids Surf., A* **155**, 149-258.
- Fulton J. R., McKnight D. M., Foreman C. M., Cory R. M., Stedmon C., and Blunt E. (2004) Changes in fulvic acid redox state through the oxycline of a permanently ice-covered Antarctic lake. *Aquat. Sci.* **66**(1), 27-46.
- Graham H. D. (1992) Stabilization of the Prussian Blue color in the determination of polyphenols. *J. Agric. Food Chem.* **40**, 801-805.
- Hagerman A. E. and Butler L. G. (1989) Choosing appropriate methods and standards for assaying tannin. *J. Chem. Ecol.* **15**, 1795-1810.
- Haynes C. G., Turner A. H., and Waters W. A. (1959) The oxidation of monohydric phenols by alkaline ferricyanide. *J. Americ. Chem. Soc.* **81**, 2323-2331.

- Heitmann T. and Blodau C. (2006) Oxidation and incorporation of hydrogen sulfide by dissolved organic matter. *Chem. Geol.* **235**, 12-20.
- Heitmann T., Goldhammer T., Beer J., and Blodau C. (2007) Electron transfer of dissolved organic matter and its potential significance for anaerobic respiration in a northern bog. *Global Change Biol.* **13**(8), 1771-1785.
- Helburn R. S. and Maccarthy P. (1994) Determination of Some Redox Properties of Humic-Acid by Alkaline Ferricyanide Titration. *Analyt. Chim. Acta* **295**(3), 263-272.
- Kalbitz K., Geyer W., and Geyer S. (1999) Spectroscopic properties of dissolved humic substances-a reflection of land use history in a fen. *Biogeochemistry* **47**, 219-238.
- Kappler A., Benz M., Schink B., and Brune A. (2004) Electron shuttling via humic acids in microbial iron(III) reduction in a freshwater sediment. *FEMS Microbiol. Ecol.* **47**, 85-92.
- Kappler A. and Haderlein S. B. (2003) Natural organic matter as reductant for chlorinated aliphatic pollutants. *Environ. Sci. Technol.* **37**(12), 2714-2719.
- Klapper L., McKnight D. M., Fulton J. R., Blunt-Harris E. L., Nevin K. P., Lovley D. R., and Hatcher P. G. (2002) Fulvic acid oxidation state detection using fluorescence spectroscopy. *Environ. Sci. Technol.* **36**(14), 3170-3175.
- Lovley D. R., Coates J. D., Blunt-Harris E. L., Phillips E. J. P., and Woodward J. C. (1996) Humic substances as electron acceptors for microbial respiration. *Nature* **382**(6590), 445-448.
- Matthiessen A. (1995) Determining the redox capacity of humic substances as a function of pH. *Vom Wasser* **84**, 229-235.
- Miano T. M. and Senesi N. (1992) Synchronous excitation fluorescence spectroscopy applied to soil humic substances chemistry. *Sci. Tot. Environ.* **1992**(117/118), 41-51.
- Niemayer J., Chen Y., and Bollag J. M. (1992) Characterization of humic acids, composts, and peat by diffuse reflectance fourier-transformed infrared spectroscopy. *Soil Sci. Soc. Am. J.* **56**, 135-140.
- Nurmi J. T. and Tratnyek P. G. (2002) Electrochemical properties of natural organic matter (NOM), fractions of NOM, and model biogeochemical electron shuttles. *Environ. Sci. Technol.* **36**(4), 617-624.
- Pullin M. J. and Cabaniss S. E. (1995) Rank analysis of the pH-dependent synchronous fluorescence spectra of six standard humic substances. *Environ. Sci. Technol.* **29**, 1460-1467.
- Pullin M. J. and Cabaniss S. E. (2003) The effects of pH, ionic strength, and iron-fulvic acid interactions on the kinetics of nonphotochemical iron transformations. I. Iron(II) oxidation and iron(III) colloid formation. *Geochim. Cosmochim. Acta* **67**(21), 4067-4077.
- Redman A. D., Macalady D. L., and Ahmann D. (2002) Natural organic matter affects arsenic speciation and sorption onto hematite. *Environ. Sci. Technol.* **36**(13), 2889-2896.
- Rosso K. M., Smith D. M. A., Wang Z. M., Ainsworth C. C., and Fredrickson J. K. (2004) Self-exchange electron transfer kinetics and reduction potentials for anthraquinone disulfonate. *J. Phys. Chem. A* **108**(16), 3292-3303.
- Sander R. (1999) Compilation of Henry's Law constants for inorganic and organic species of potential importance in environmental chemistry (Version 3). <http://www.mpch-mainz.mpg.de/~sander/res/henry.html>.

- Schwarzenbach R. P., Stierli R., Lanz K., and Zeyer J. (1990) Quinone and Iron Porphyrin Mediated Reduction of Nitroaromatic Compounds in Homogeneous Aqueous-Solution. *Environ. Sci. Technol.* **24**(10), 1566-1574.
- Scott D. T., McKnight D. M., Blunt-Harris E. L., Kolesar S. E., and Lovley D. R. (1998) Quinone moieties act as electron acceptors in the reduction of humic substances by humics-reducing microorganisms. *Environ. Sci. Technol.* **32**(19), 2984-2989.
- Skogerboe R. K. and Wilson S. A. (1981) Reduction of Ionic Species by Fulvic-Acid. *Analyt. Chem.* **53**(2), 228-232.
- Straub K. L., Kappler A., and Schink B. (2004) Enrichment and isolation of iron(III) and humic acid reducing bacteria. *Methods Enzym.* **397**, 58-77.
- Struyk Z. and Sposito G. (2001) Redox properties of standard humic acids. *Geoderma* **102**, 329-346.
- Stumm W. and Morgan J. J. (1996) *Aquatic chemistry*. Wiley Interscience.
- Tipping E. (1994) WHAM - A chemical equilibrium model and computer code for water, sediments, and soils incorporating a discrete/electrostatic model of ion-binding humic substances. *Computer Geosciences* **20**, 973-1023.
- Tipping E. and Hurley M. A. (1992) A unifying model of cation binding by humic substances. *Geochim. Cosmochim. Acta* **56**, 3627-3641.

Study 3

submitted to *Water Research*

Oxidation of As(III) and reduction of As(V) in dissolved organic matter solutions

Markus Bauer¹, Christian Blodau¹

¹Limnological Research Station and Department of Hydrology, University of Bayreuth, D-95440 Bayreuth, Germany

Abstract

The redox state of arsenic significantly affects the mobility and transport behaviour of this toxic element. In this study we tested influence of different dissolved organic matter (DOM) samples on the abiotic As(V) reduction and As(III) oxidation at circumneutral pH. Experimental assays were carefully sterilized and kept under anoxic conditions. As(III) oxidation could not be observed under these conditions on time scales of 4-7 d. As(V) reduction to As(III) instead occurred in assays with different DOM samples and DOC concentrations. Amount and rate of As(III) production, however, varied strongly for different experiments and could not be ascribed to systematic variations in experimental protocols. Microbial processes are a potential cause for this high variability in As(V) reduction, but also chemical reactions may have contributed. In summary, a direct chemical effect of organic matter on the redox speciation of As could not be proven. The observed effects were mostly slow and possibly microbially induced. This leads us to the conclusion that direct effects of humic substances on As speciation may be negligible compared to microbial processes in natural systems.

Introduction

The mobility of the toxic element As is strongly related to redox processes. The oxidative weathering of As containing sulfide minerals or the reductive dissolution of metal oxides are just two examples for mechanisms of As mobilization involving redox reactions (Mandal and Suzuki, 2002; Smedley and Kinniburgh, 2002). Arsenic release under reducing conditions from iron oxides endangers the groundwater resources of millions of people in Southeast Asia, and has been linked to the presence of degradable organic matter in sediments and water phase (McArthur et al., 2004; Meharg et al., 2006).

Microbial activity and degradation of organic matter causes Fe(III) reduction, leading to the dissolution of the As containing iron oxide phases and the release of As into the water phase (Herbel and Fendorf, 2006; Kocar et al., 2006). Additionally, microorganisms may also use As(V) as an electron acceptor and mediate the transformation to the more toxic and mobile As(III) species (Oremland and Stolz, 2003). Reoxidation of aqueous As(III) can take place microbially (Cullen and Reimer, 1989). Abiotic As(III) oxidation, however, is known to be slow with oxygen and higher reaction rates require the presence of radical species, irradiation or catalysts (Chui and Hering, 2000; Hug and Leupin, 2003).

It has previously been shown that humic substances are capable of electron transfer reactions with metals or organic pollutants (Kappler and Haderlein, 2003; Schwarzenbach et al., 1990). Quinones and similar structural entities were made responsible for these reactions (Scott et al., 1998). The redox potential of organic matter redox active functionalities and the electron transfer capacities were found to vary over a wide range (Bauer et al., 2006). Dissolved organic matter is often found in high concentrations in aquifers affected by reductive dissolution of Fe oxides and As release (Harvey et al., 2002; McArthur et al., 2004) and might therefore be a possible reaction partner in redox transformations of aqueous or solid phase As. Yet, it is unknown whether abiotic reactions with organic matter molecules could have the potential to affect the mobility of As mobilization in these environments.

Irradiation substantially increased the oxidation of As(III) in humic acid solution by inducing the formation of organic radicals, but no As(V) reduction occurred (Buschmann et al., 2005). Laboratory experiments in darkness, however, had strongly contrasting results. Redman et al. (2002) found high As(III) oxidation in whole water DOM solutions under oxic conditions after 48 h. Tongesayi and Smart (2006) also found As(III) transformation in Suwannee River fulvic acid solution after 50 to 250 h, but Buschmann et al. (2005) observed As(III) oxidation in Suwannee River humic acid solution only after weeks of incubation and in the presence of phosphate buffer. As(V) reduction in the same humic acid solution was found only after an initial lag phase of 19 h and attributed to microbial reactions, as the reaction could be prevented by application of the biocide NaN_3 (Buschmann et al., 2005). In contrast other studies reported abiotic As(V) reduction in time scales of 200 min to 200 h by

different organic matter samples (Palmer et al., 2006; Redman et al., 2002; Tongesayi and Smart, 2006).

The contradictory results of these previous studies do not provide a consistent pattern concerning the conditions and time scales for As redox transformation by aqueous organic matter. Comparison of these studies is furthermore impeded by the fact that various organic matter samples and experimental protocols were used. Additionally different methods As speciation measurements were applied, including HPLC-ICP-MS to detect both As(V) and As(III), but also ion chromatography and voltametry, which allow only the quantification of one As species. Our aim was therefore to elucidate (1) rate and capacity of abiotic As(III) and As(V) redox transformation in (2) a simple experimental setup with (3) different organic matter samples.

Materials and methods

All reaction vials and storage bottles were preconditioned with 1 % HNO₃, rinsed twice with deionized water, and sterilized by autoclaving (121°C, wet heat), annealing (250°C, glassware) or rinsing with isopropanol (plastic). Sterile pipette tips, canules and syringes were used for solution transfer and sampling. Stock solutions were prepared with MilliQ water from Na₂HAsO₄, NaAsO₂ (Fluka) and NaCl (Merck) salts and purified Pahokee Peat humic acid (PPHA) powder. The whole water DOM samples from Suwannee River (Georgia/USA; SRDOM), Black River (Upper Michigan/USA; BRDOM), the Mer Bleue peatland (Quebec/Canada; MBDOM), the Everglades (Florida/USA; EVDOM), and Monitoring Well 6 in the Tennessee Park wetland (Colorado/USA, MWDOM) were used after sterile-filtered (0.2 µm Nylon, Roth). All solutions were purged with nitrogen (99.99 %) for at least 30 min and transferred into an anaerobic glovebox with N₂/H₂ atmosphere (95 % N₂, 5 % H₂).

The experiments were started by mixing different volumes of stock and DOM solution in 20 ml glass headspace vials to reach final concentrations shown in Table 1 for the experiments 1-6. Ionic strength was 5-10 mmol L⁻¹ NaCl and pH was adjusted manually to the values shown. The headspace vials were then wrapped in aluminum foil and sealed with teflon lined butyl rubber stoppers. Hydrogen was removed by a threefold evacuation and purging of the vial with nitrogen. NaN₃ in a final concentrations of 1 mol L⁻¹ was added to experiment 4 after this step. The assays were incubated in duplicates, respectively triplicates for experiment 3, in a climate chamber at 20°C on a horizontal shaker. Blank experiments lacking organic matter solution were executed in duplicates for all protocols.

Sampling was carried out by syringe after different periods of time (Table 1). Total As concentrations were quantified on a Graphite Furnace AAS (Analytik Jena, Zeenith 60). The arsenic speciation was measured by HPLC-ICP-MS (PRP X100 column, Hamilton; Agilent 7500ce). The separation method of (Francesconi et al., 2002) allows for the quantification of arsenite, arsenate,

dimethylarsinic acid (DMA) and monomethylarsonic acid (MMA). Dissolved organic carbon (DOC) was measured as non-purgable organic carbon (NPOC) on a Shimadzu TOC analyzer (TOC V CPN).

Table 7 Reaction conditions in the different experimental assays

	Humic substance	C(DOM)	As species	c(As)	pH	Time	Sterilization
		mg L ⁻¹		μg L ⁻¹		h	
1	PPHA	20	As(III), As(V)	45	7	0-120	Annealing and Isopropanole rinsing
2	PPHA	25	As(V)	60	7	0-200	
3	PPHA	25	As(V)	60	7	0-350	
4	PPHA + NaN ₃	25	As(III), As(V)	60	7	0-350	
5	PPHA	25, 50, 75	As(III), As(V)	60	6.5	48	Autoclaving
6	PPHA	50	As(III), As(V)	75	4, 6, 8	120	
	SRDOM	56					
	BRDOM	15					
	MBDOM	62					
	EVDOM	39					
MWDOM	45						

The direction of electron transfer in redox reactions depends on the energy yield during reaction of two redox partners (Eq. 1). Positive net values for the electro motive force (EMF) indicate energy yield and therefore a thermodynamically favourable process. Half cell redox potentials E_h were calculated from E_h^0 values for in assay pH conditions for the reactions of $H_2AsO_4^-/H_3AsO_3$, $HAsO_4^{2-}/H_3AsO_3$, different organic matter model compounds and bulk organic matter. The concentration ratio of oxidized versus reduced species, as shown in the Nernst equation (Eq. 2), was not considered. E_h^0 values were determined from standard energy of formation values (Eq. 3).

$$EMF = E_{h,Reduction} - E_{h,Oxidation} \quad \text{Eq. 1}$$

$$E_h = E_h^0 + \frac{R * T}{n * F} * \ln \left(\frac{\prod_i \{Ox\}^m}{\prod_j \{Red\}^n} \right) \quad \text{Eq. 2}$$

$$E_h^0 = \frac{-\Delta G^0}{n * F} \quad \text{Eq. 3}$$

Results and Discussion

Thermodynamic considerations

Half reaction E_h (pH 6.5) values for different As species and different quinone organic compounds were estimated for pH 6.5 (Table 2). While As redox pairs have an E_h value of +70 mV to +90 mV, redox potentials of quinoid type organic molecules vary over a wider range from -130 mV to +320

mV, depending on the quinone molecular structure. For positive EMF, calculated according to Eq. 3 with the E_h (pH 6.5) values shown in Table 2 for the reaction of As with model quinones, the reduction of As(V) proceeds under energy yield, while for negative EMF As(III) oxidation is the thermodynamically favourable process. The EMF values for the different model quinones vary between -250 mV for reaction As I with hydroquinone and +220 mV for reaction As II with AQDS. For juglone and lawsone, which are known to occur in the environment, low positive EMF values of 30 mV to +120 mV suggest that As(V) reduction should take place. The direction of electron flow therefore is controlled by the type of quinone involved in the reaction.

Table 8 Reduction half reactions of As, model quinones and bulk humic substance, the respective standard redox potential E_h^0 and the redox potential E_h calculated for the reaction at pH 6.5

	Reaction	E_h^0	E_h (pH 6.5)	Source
		mV	mV	
As I	$H_2AsO_4^- + 2 e^- + 3 H^+ = H_3AsO_3 + H_2O$	+ 640	+ 70	(Stumm and Morgan, 1996)
As II	$HAsO_4^{2-} + 2 e^- + 4 H^+ = H_3AsO_3 + H_2O$	+ 860	+ 90	(Stumm and Morgan, 1996)
Hydroquinone	$Q + 2 e^- + 2 H^+ = H_2Q$	+ 699	+320	(Helburn and Maccarthy, 1994)
Juglone	$Jug + 2 e^- + 2 H^+ = H_2Jug$	+ 430	+40	(Schwarzenbach et al., 1990)
Lawsone	$Law + 2 e^- + 2 H^+ = H_2Law$	+ 350	-30	(Schwarzenbach et al., 1990)
AQDS	$AQDS + 2 e^- + 2 H^+ = AH_2QDS$	+ 250	-130	(Rosso et al., 2004)
Humics	$DOM_{(ox)} + 2e^- + 2H^+ = DOM_{(red)}$	+228 to +528	-180 to +250	(Oesterberg and Shirshova, 1997) (Palmer et al., 2006)

Dissolved bulk organic matter redox properties are hard to measure and depend on the molecular structure of the DOM sample. Redox activity of heterogeneous humic molecules may in fact not only be limited to different quinone structures and have been suggested to cover a wide range of redox active moieties with different redox potentials and possibly include DOM bound metal (Bauer et al., 2006; Redman et al., 2002). Differences in determined bulk E_h values of humics are, therefore, not surprising and the uncertainty and variability concerning the redox potential of humic substance functionalities prevents to derive conclusions regarding the direction of electron transfer reactions between DOM and As(V) or As(III). Moreover the low EMF values calculated for reaction of As with juglone or lawsone also suggest that small changes in experimental conditions, i.e. pH or species concentrations might result in large differences in direction, rate and or capacity of electron flux.

As(III)-Oxidation

Oxidation of As(III) by humic substances was low in the dark using different DOM samples, carbon concentrations, and pH values between 4 and 8 for up to 120 h (Figure 1). As(III) was substantially oxidized to As(V) only in the EVDOM solution (Figure 2). This is consistent with previous findings of negligible dark As(III) oxidation by Suwannee River humic acid over 26 d (Buschmann et al., 2005). Other studies, however, showed substantial formation of As(V) in oxygen containing DOM solutions. Tongesayi and Smart (2006) reported a oxidation of 20 % of initially present As(III) in purified Suwannee River fulvic acid solution, and Redman et al. (2002) found substantial As(III) oxidation in MWDOM and SRDOM solutions also used in our study. The latter suggested that Fe or Mn contained in their whole water organic matter solutions might be involved in electron transfer reactions. Given the negligible As(V) production in our study, however, a trace contamination with oxygen is a more likely explanation for the observed As(III) oxidation in their experiments. The high As(III) oxidation in the EVDOM sample, which had a high natural ionic strength, possibly indicates that electron exchange between As(III) and redox active organic matter functionalities is limited by electrostatic or steric effects at the DOM surface. Compression of the electric double layer at high ionic strength might ease direct molecular interactions and therefore increase reactivity of humics with As(III).

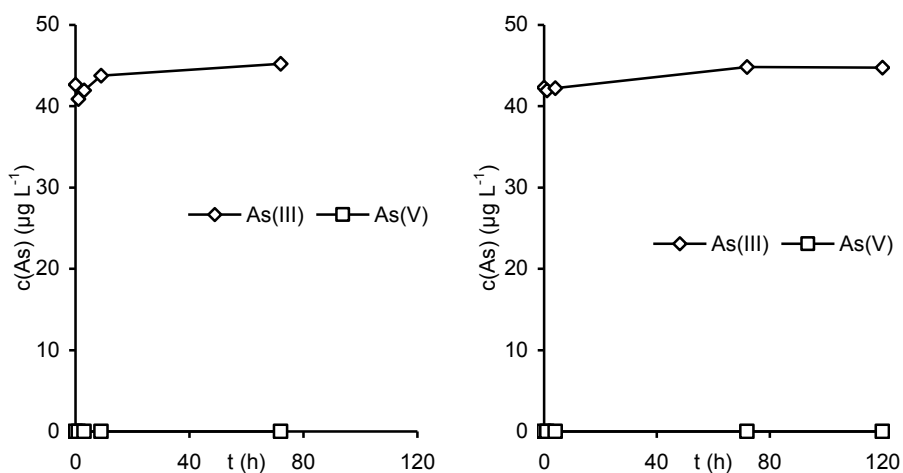


Figure 24 Concentrations of As(III) and As(V) as determined by HPLC-ICP-MS in MilliQ water (left) and PPHA solution (right) in experiment 1. Error bars depict the standard deviation between assays, which was low in all samples.

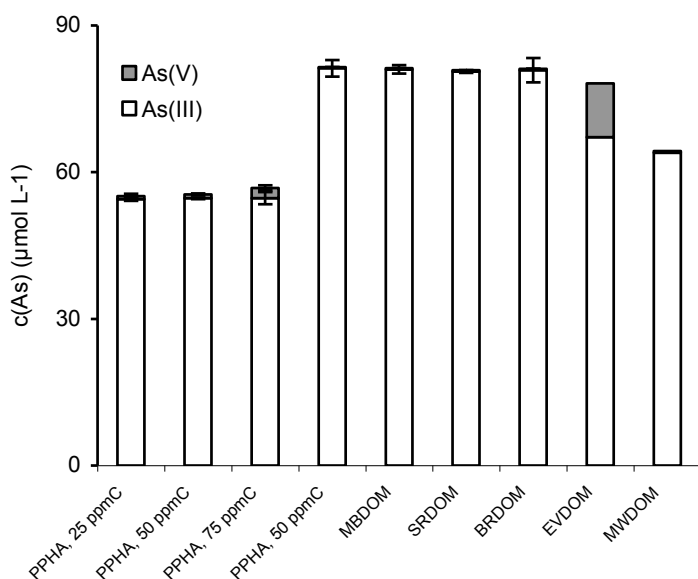


Figure 25 Concentration of As(III) and As(V) as determined by HPLC-ICP-MS after 24 h in different DOM solutions of experiments 4 and 5. Error bars depict the standard deviation between assays.

As(V)-Reduktion

In contrast to the low fraction of As(III) being oxidized in DOM solution, As(V) was reduced in most experiments with humic substances at neutral pH. However, the time scales and the fraction of As(V) reduced varied strongly, not only between different DOM samples, but also between different assays with similar experimental protocols (Table 1).

Three different time series experiments with PPHA and the corresponding respective blank experiments lacking DOM illustrate this clearly (Figure 3). Little As(III) was produced after 120 h in experiment 1. More As was reduced in experiments 2 and 3, in which 20-60 % of initial As(V) had disappeared already after 24 h and more than 75 % were in As(III) form at the end of the experiments. In the blank experiments 1 and 2, As speciation was mostly unchanged for up to 200 h, but in experiment 3 As was reduced to a similar extent as in PPHA containing assays. As_{tot} concentrations determined by graphite furnace AAS were within 10 % of initial values at all time steps and the sum of As(III) and As(V) accounted for more than 90 % of As_{tot} , increasing our confidence in the quality of our speciation measurements.

When the added quantity of PPHA was altered, the fraction of As(V) being reduced after 48 h varied from 20 to 90 %. A relationship to the initial DOC concentration was not apparent (Figure 4). As(III) production varied in a similar range with different DOM samples and deviations between the transformation at pH 4, 6 and 8 were low (data not shown). In EVDOM solution, no As(V) was reduced, and in MWDOM solution As recovery was diminished, supposedly due to the high natural iron concentration. Between 0.02 and 0.1 mequiv (g C)⁻¹ electrons were transferred from DOM to As(V) in our experiments.

The reduction of As(V) in solutions containing humic substance was observed also in other studies. Within periods of 48 h to 200 h, the electron transfer to As ranged from 0.03 to ~0.6 mequiv (g C)⁻¹ (Redman et al., 2002; Tongesayi and Smart, 2006), which is similar to the values found in our experiments. The experiments of Palmer et al. (2006), in contrast, found much higher As(V) reduction rates which led to a completion of the reaction after only 2 h. The calculated electron transfer capacities amounted to 14-42 mequiv (g C)⁻¹ and were partly higher than the maximum capacities of ~20 mequiv (g C)⁻¹ estimated for hydroquinone assuming an uptake of two electrons for every 6 carbon atoms. We thus believe that consumption of aqueous As(V) on that scale must have been partly caused by other processes, such as complexation reactions, or by measurement artefacts in these experiments with very high DOC concentrations.

With the exception of EVDOM solution, in all of our DOM samples, and also in the experiments of (Tongesayi and Smart, 2006) with Suwannee River fulvic acid, As(V) reduction occurred. Reaction rates and capacities, however, varied strongly in our assays and were independent of DOC concentrations. In contrast, only 1 out of 6 DOM samples was capable to reduce As in the study by Redman et al. (2002). This raises the question whether redox active humic functionalities indeed facilitate a chemical electron transfer to As.

The reduction of As(V) in experiments with Suwannee River humic acid was reported to be caused by microbial processes (Buschmann et al., 2005). As(V) reduction by microbes is a thermodynamically favourable dissimilatory process when electron donors such as acetate or hydrogen are available and oxygen and nitrate are absent (Heimann et al., 2007), and also serves as an important detoxification mechanism in heterotrophic bacteria (Oremland and Stolz, 2003). The occurrence of microbial processes is supported by the observation that the reactivity increased only after an initial lag phase of 19 h (Buschmann et al., 2005). Also in our experiments and the assays of Tongesayi and Smart (2006), As(V) was reduced at an increasing rate over time. This is an unlikely kinetics for chemical reactions, as the driving force of the reaction and the concentrations of the reactants are at maximum initially. Additionally, the application of the biocide NaN₃ completely prevented formation of As(III) for long periods of time in our own and other experiments. Differences in microbial activity seem a reasonable explanation for the high variability in the extent of As(V) reduction observed in experiments lacking an inhibitor of microbial respiration.

The data available in the literature to date is insufficient to make the case for a microbially mediated As transformation in such, supposedly sterile, batch experiments conclusively. The precautions taken, i.e. a filtration to 0.2 µm, commonly known as 'sterile-filtration', the sterilization of laboratory hardware, and the use of purified and refractory humic material should impede the development of a microbial community in the short periods of time used in the experiments. NaN₃ does not oxidize As(III) in aqueous solution, as preliminary test indicated, but an effect of the electron rich N₃⁻ molecule on the electron transfer reactions of DOM and As cannot be excluded. Our thermodynamic calculations furthermore showed that energy yield and direction of electron flow in

systems with As and DOM is difficult to predict and may vary for little changes in experimental conditions or protocols. This might have contributed to the high variability and inconsistency of the data obtained.

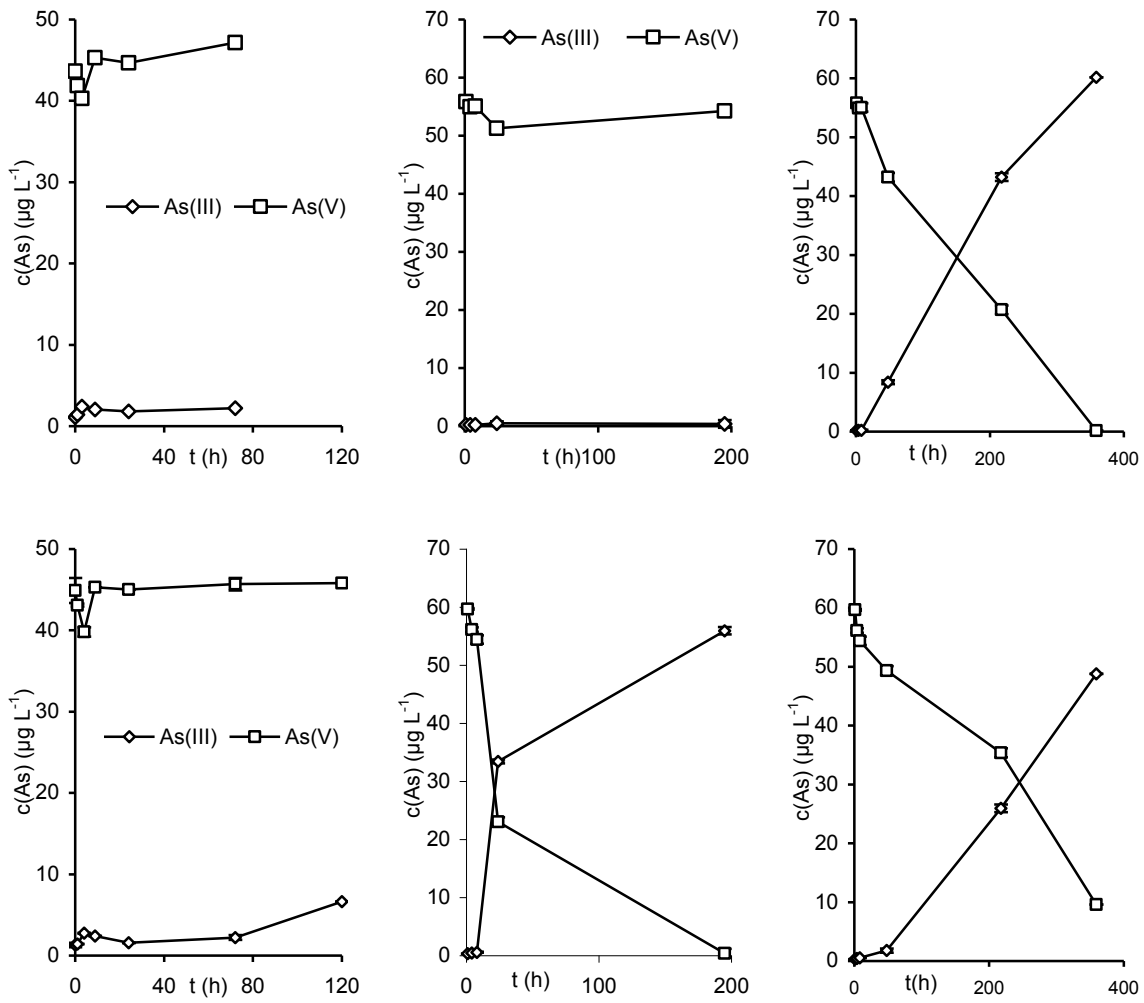


Figure 26 Concentration of As(III) and As(V) determined by HPLC-ICP-MS over time in MilliQ water (top) and PPHA solution (bottom) in experiment 1 to 3. Error bars depict the standard deviation between assays, which was low in all samples.

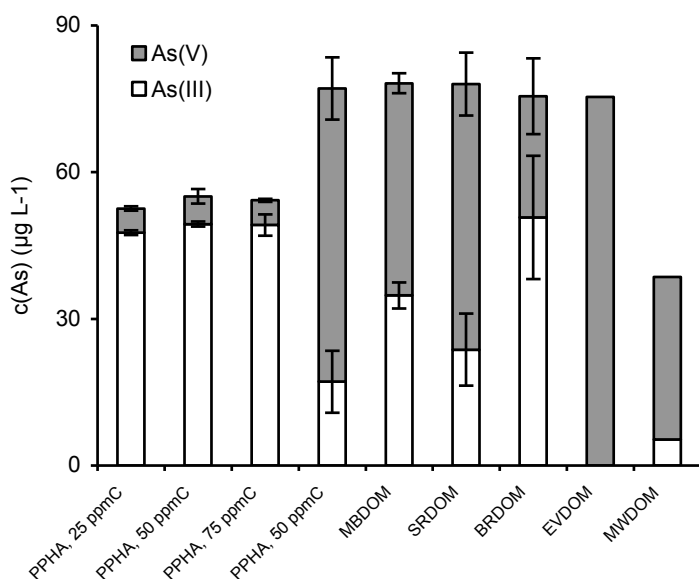


Figure 27 Concentration of As(III) and As(V) determined by HPLC-ICP-MS after 24 h in different DOM solutions of experiment 4 and 5. Error bars depict the standard deviation between assays.

Conclusions

This study suggests that DOM does not chemically oxidize As(III) in darkness at circumneutral pH. Whether this finding is caused by a thermodynamic limitation or a kinetic slowness of the process could not be resolved by our data set. Regardless, the potential of DOM to chemically oxidize As(III), for example in reduced aquifers, is likely low. In contrast, As(V) was reduced in almost all DOM solutions, albeit with different rates and quantities. Initially, As(III) production was slow in most cases and increased over time. If we take the high variability in reduction rates in consideration this suggests that –unknown- microbial processes were the cause for As(V) reduction. In summary a chemical effect of DOM on the redox speciation of As could not be proven. The observed effects were mostly slow and possibly microbially induced. This leads us to the conclusion that direct effects of humic substances on As speciation may be negligible compared to microbial processes in natural systems, which often operate at high rates.

Acknowledgments

We thank Gunther Ilgen from the Bayreuth Center for Ecology and Environmental Research (BAYCEER) for help during As speciation measurements and Donald Macalady from the Colorado School of Mines for providing various natural dissolved organic matter solutions. Finally we want to thank the German Research foundation (DFG) for their support through grant BL563/7-2 to Christian Blodau.

References

- Bauer M., Heitmann T., Macalady D. L., and Blodau C. (2006) Electron transfer capacities and reaction kinetics of peat dissolved organic matter. *Environ. Sci. Technol.* **41**(1), 139-145.
- Buschmann J., Canonica S., Lindauer U., Hug S. J., and Sigg L. (2005) Photoirradiation of dissolved humic acid induces arsenic(III) oxidation. *Environ. Sci. Technol.* **39**(24), 9541-9546.
- Chui V. Q. and Hering J. G. (2000) Arsenic adsorption and oxidation at Manganite surfaces: 1. Method for Simultaneous determination of adsorbed and dissolved arsenic species. *Environ. Sci. Technol.* **34**, 2029-2034.
- Cullen W. R. and Reimer K. J. (1989) Arsenic Speciation in the Environment. *Chemical Reviews* **89**(4), 713-764.
- Francesconi K., Visoottiviseth P., Sridokchan W., and Goessler W. (2002) Arsenic species in an arsenic hyperaccumulating fern, *Pityrogramma calomelanos*: a potential phytoremediator of arsenic-contaminated soils. *Sci. Tot. Environ.* **284**(1-3), 27-35.
- Harvey C. F., Swartz C. H., Badruzzaman A. B. M., Keon-Blute N., Yu W., Ali M. A., Jay J., Beckie R., Niedan V., Brabander D., Oates P. M., Ashfaque K. N., Islam S., Hemond H. F., and Ahmed M. F. (2002) Arsenic mobility and groundwater extraction in Bangladesh. *Science* **298**(5598), 1602-1606.
- Heimann A. C., Blodau C., Postma D., Larsen F., Viet P. H., Nhan P. Q., Jessen S., Duc M. T., Hue N. T. M., and Jakobsen R. (2007) Hydrogen Thresholds and Steady-State Concentrations Associated with Microbial Arsenate Respiration. *Environ. Sci. Technol.* **41**(7), 2311-2317.
- Helburn R. S. and Maccarthy P. (1994) Determination of Some Redox Properties of Humic-Acid by Alkaline Ferricyanide Titration. *Analyt. Chim. Acta* **295**(3), 263-272.
- Herbel M. and Fendorf S. (2006) Biogeochemical processes controlling the speciation and transport of arsenic within iron coated sand. *Chem. Geol.* **228**, 16-32.
- Hug S. J. and Leupin O. (2003) Iron-catalyzed oxidation of arsenic(III) by oxygen and by hydrogen peroxide: pH-dependant formation of oxidants in the Fenton reaction. *Environ. Sci. Technol.* **37**, 2734-2742.
- Kappler A. and Haderlein S. B. (2003) Natural organic matter as reductant for chlorinated aliphatic pollutants. *Environ. Sci. Technol.* **37**(12), 2714-2719.
- Kocar B., Herbel M., Tufano K., J., and Fendorf S. (2006) Contrasting effects of dissimilatory iron(III) and arsenic (V) reduction on the arsenic retention and transport. *Environ. Sci. Technol.* **40**, 6715-6721.
- Mandal B. K. and Suzuki K. T. (2002) Arsenic round the world: A review. *Talanta* **58**, 201-235.
- McArthur J. M., Banerjee D. M., Hudson-Edwards K. A., Mishra R., Purohit R., Ravenscroft P., Cronin A., Howarth R. J., Chatterjee A., Talukder T., Lowry D., Houghton S., and Chadha D. K. (2004) Natural organic matter in sedimentary basins and its relation to arsenic in anoxic groundwater: the example of West Bengal and its worldwide implications. *Appl. Geochem.* **19**, 1255-1293.
- Meharg A. A., Scrimgeour C., Hossain S. A., Fuller K., Cruickshank K., Williams P. N., and Kinniburgh D. G. (2006) Codeposition of organic carbon and arsenic in Bengal Delta aquifers. *Environ. Sci. Technol.* **40**(16), 4928-4935.
- Oesterberg R. and Shirshova L. (1997) Oscillating, nonequilibrium redox properties of humic acids. *Geochim. Cosmochim. Acta* **61**(21), 4599-4604.
- Oremland R. S. and Stolz J. F. (2003) The ecology of arsenic. *Science* **300**(5621), 939-944.
- Palmer N. E., Freudenthal J. H., and von Wandruszka R. (2006) Reduction of arsenates by humic materials. *Environm. Chem.* **3**(2), 131-136.

- Redman A. D., Macalady D. L., and Ahmann D. (2002) Natural organic matter affects arsenic speciation and sorption onto hematite. *Environ. Sci. Technol.* **36**(13), 2889-2896.
- Rosso K. M., Smith D. M. A., Wang Z. M., Ainsworth C. C., and Fredrickson J. K. (2004) Self-exchange electron transfer kinetics and reduction potentials for anthraquinone disulfonate. *J. Phys. Chem. A* **108**(16), 3292-3303.
- Schwarzenbach R. P., Stierli R., Lanz K., and Zeyer J. (1990) Quinone and Iron Porphyrin Mediated Reduction of Nitroaromatic Compounds in Homogeneous Aqueous-Solution. *Environ. Sci. Technol.* **24**(10), 1566-1574.
- Scott D. T., McKnight D. M., Blunt-Harris E. L., Kolesar S. E., and Lovley D. R. (1998) Quinone moieties act as electron acceptors in the reduction of humic substances by humics-reducing microorganisms. *Environ. Sci. Technol.* **32**(19), 2984-2989.
- Smedley P. L. and Kinniburgh D. G. (2002) A review of the source, behaviour and distribution of arsenic in natural waters. *Appl. Geochem.* **17**(5), 517-568.
- Stumm W. and Morgan J. J. (1996) *Aquatic chemistry*. Wiley Interscience.
- Tongesayi T. and Smart R. B. (2006) Arsenic speciation: Reduction of arsenic(v) to arsenic(III) by fulvic acid. *Environm. Chem.* **3**(2), 137-141.

Study 4

Reproduced in parts with permission from

Experimental colloid formation in aqueous solutions rich in dissolved organic matter, ferric iron, and As

Markus Bauer¹, Christian Blodau¹

Geochimica et Cosmochimica Acta, 2008, in press

Copyright 2008 Elsevier B.V.

¹Limnological Research Station and Department of Hydrology, University of Bayreuth, D-95440 Bayreuth, Germany

Abstract

Due to the widespread contamination of groundwater resources with arsenic (As), controls on As mobility have to be identified. In this study we focused on colloid formation in solutions rich in ferric iron, natural dissolved organic matter (DOM) and As(V). Laboratory filtration experiments were used to quantify the elemental concentrations in different size fractions. A steady-state particle size distribution with stable elemental concentration in the different particle size classes was attained within 24 hours. The presence of humic substances partly inhibited the formation of large Fe oxide particles when initially adjusted molar Fe/C ratios in solution were < 0.1 . DOM thus stabilized Fe in complexed and colloidal form. Dissolved As concentrations and the quantity of As bound to particles smaller than $0.2 \mu\text{m}$ increased in the presence of DOM as well. Dissolved As concentrations increased due to the competition between As and organic molecules for sorption sites on Fe phases and the amount of As bound to small particles was raised because Fe oxide colloids with sorbed As fell into smaller size fractions. At intermediate Fe/C ratios of $0.02 - 0.1$, a strong correlation between As and Fe concentration occurred in all size fractions ($R^2=0.989$). At Fe/C ratios < 0.02 , As was mainly present in the free ionic form. The size of As containing colloidal particles also depended strongly on the initial size of the humic substance, which was larger for purified humic acids than for natural river or soil porewater samples. Arsenic in the size fraction larger than $0.2 \mu\text{m}$ additionally decreased in the order of $\text{pH } 4 \gg 6 > 8$. The presence of As in the ionic form and in small colloids affects the retention and transport behavior of the toxic element. Under organic matter rich solution co-precipitation and immobilization of As will be of lesser importance than expected in iron rich waters and this has to be considered in aquifers, wetland draining rivers, and water treatment facilities.

Introduction

Due to the contamination of groundwater resources in many regions worldwide, the identification of As mobilizing processes has become an important scientific challenge. Arsenic mobilization at solid-solute interfaces was often linked to zones of low redox potential and high aqueous Fe and organic matter concentrations (McArthur et al., 2004). Adsorption, desorption, precipitation, and dissolution processes in these environments are fairly well understood. The presence of Fe and organic matter is an important factor controlling the exchange processes of As between aqueous and solid phase, as a number of field observations and experimental results suggested. Under oxic conditions As has a strong affinity for Fe oxides (Dixit and Hering, 2003) and sulfate reducing conditions promote the formation of As containing Fe sulfides (O'Day et al., 2004). Humic substances can change the redox speciation of free As (Buschmann et al., 2005; Redman et al., 2002), and compete with DOM for sorption sites on mineral phases (Bauer and Blodau, 2006; Grafe et al., 2002).

Much less is known about the fate of dissolved As in the aqueous phase in the presence of high dissolved Fe and organic matter concentrations. Humic substances were shown to bind As by covalent mechanisms (Buschmann et al., 2006). Moreover, high concentrations of Fe, Mn and Al, which are chelated by functional groups of DOM (Christl and Kretzschmar, 2001; Pullin and Cabaniss, 2003; Tipping, 1994), have been suggested to increase As binding by organic matter through ternary bridging complexes (Lin et al., 2004; Redman et al., 2002). Arsenic was also found in DOM-Fe particles, which formed by Fe precipitation (Ritter et al., 2006) or by mobilization of particles from the solid phase (Davis et al., 2001; Tadanier et al., 2005).

The resulting colloids are entities with a supramolecular structure and a size range 1 nm - 1 μ m, and are small enough as not to quickly sediment without further aggregation (Buffle et al., 1998). Colloids often represent mineral particles or precipitates that are mobilized and stabilized by organic matter (Kretzschmar et al., 1999). An important factor regarding the stability of colloids is the surface charge. High negative or positive surface charges imply large repulsing forces between particles, low attachment efficiency and therefore a high colloid stability (Liang and Morgan, 1990; Mikutta et al., 2006). Solution properties, like pH and ion concentration, influence surface charge. Of particular importance is furthermore DOM, such as humic substances, which can neutralize and reverse the positive charge of Fe oxide surfaces and may induce a mobilization of particles (Amirbahman and Olson, 1995; Liang and Morgan, 1990; Tiller and O'Melia, 1993).

The formation of As bearing complexes and colloids changes the mobility of the element compared to the free ionic form. The resulting mobility may not always be lowered, though. Even large colloidal structures or spheroids were shown to travel up to some kilometers in aquifers (Harvey et al., 1995; Kaplan et al., 1995), and also the transport velocity of colloids was found to be higher than of water due to size exclusion effects (Kretzschmar and Sticher, 1997). Mobile Fe colloids stabilized by association with DOM are furthermore common in soils (Pokrovsky et al., 2005), aquifers (Schmitt et al., 2003), and surface waters (Pokrovsky and Schott, 2002). Co-transport has

thus been recognized as an efficient mechanism of trace metal and organic chemical mobility (Kretzschmar et al., 1999), but little attention has yet been paid to co-transport of As. Among the few reports available, As was found in rivers of Finland draining contaminated peatland sites, and was bound to colloids rich in DOM and Fe (Astrom and Corin, 2000). Organic matter rich soils or sediments with a high Fe content may therefore be preferred environments for the formation of mobile and As containing particles or complexes, especially under transient geochemical conditions (McArthur et al., 2004; Meharg et al., 2006).

The interactions of DOM with aqueous Fe and Fe oxides have been studied thoroughly, but the effect of these interactions on As dynamics has not yet been sufficiently examined. We are lacking information about the effects of geochemical conditions on the formation of colloids in solutions rich in Fe, DOM, and As, data about the size range of forming aggregates, and about the influence of DOM properties on the aggregation process. In our laboratory experiments we induced the formation of As containing complexes or colloids in Fe and DOM rich solutions. The setup was designed to elucidate, whether and in what way factors such as DOM properties, pH, ionic strength, Fe and dissolved organic carbon (DOC) concentration change the distribution of As between dissolved and colloidal phase. An ultrafiltration method was used to separate size fractions and to determine the elemental composition and speciation in the solutions passing the filter. We examined a variety of DOM samples and the effects of pH, ionic strength and initial dissolved Fe/C ratios. The occurrence of complexation reactions and colloid formation were considered for the interpretation of the experimental results. Our aim was to identify (I) the effect of DOM on the amount of As present in certain molecular weight and size classes, (II) the rate of colloid formation and (III) the key factors controlling the distribution of As, Fe and DOM among molecular weight and size classes. We furthermore aimed at identifying the mechanism controlling the fate of As in this chemical system, i.e. sorption competition between DOM and As, and stabilization of colloids by interactions of Fe and DOM.

Materials and Methods

Dissolved Organic Matter Samples

Stock solutions of Pahokee Peat humic acid (PPHA), Suwannee River humic acid (SRHA) and Suwannee River fulvic acid (SRFA) were prepared with MilliQ water at pH 8-9 from the purified samples acquired from the International Humic Substances Society (IHSS). We also used whole water DOM samples from Suwannee river (Georgia/USA; SRDOM), Black river (Upper Michigan/USA; BRDOM), the Mer Bleue peatland (Quebec/Canada; MBDOM), the Everglades (Florida/USA; EVDOM), and from Monitoring Well 6 in the Tennessee Park wetland (Colorado/USA, MWDOM). MBDOM was frozen at -29°C and all other DOM samples were stored in PE bottles in darkness at 4 °C. Before use each solution was filtered (0.45 µm; Nylon, Roth).

Specific UV absorption at 254 nm ($SUVA_{254nm}$), calculated from measurements on a Varian Cary 1E spectrophotometer in quartz cuvettes, and Fourier-transformed infrared (FTIR) spectra, determined with freeze-dried samples on a Bruker Vector 22 instrument, were used to estimate aromaticity and relative carboxyl content of DOM samples (Kalbitz et al., 1999). Acid-base titrations were conducted from pH 3.5 to 10 in 50 mmol L⁻¹ NaCl solution. A volume of 50 ml of each DOM solution was adjusted to pH 3 (1 M HCl s.p.) in a 100 ml glass reaction vessel sealed with a septum, and purged with N₂ for 30 min to remove dissolved inorganic carbon. An autotitrator (716 DMS Titrino, Metrohm) equipped with a Mettler Toledo pH electrode was employed to measure solution pH and to control addition of titration solution (0.05 M NaOH). Titrations were performed continually in increments of 6 µl NaOH every 30 s. The total proton donor capacity of DOM was calculated by difference from water blank experiments and divided on the basis of pH between carboxylic (pH 3.5-8) and phenolic (pH 8-10) groups (Ritchie and Perdue, 2003). DOM solution chemistry was characterized by ion chromatography (Metrosep Anion Dual 3 column, 0.8 mL min⁻¹, with chemical suppression) and ICP-OES (Varian Vista-Pro).

Experimental Setup

A flow diagram with the setup of the standard experiments is provided in Figure 1. Stock solutions of 10 mmol L⁻¹ FeCl₃ (Merck), 6 mg L⁻¹ As(V) (Fluka), 1 mol L⁻¹ NaCl (Merck), 10 mmol L⁻¹ HCl (from 32 % HCl stock, Merck), and 10 and 100 mmol L⁻¹ NaOH (from pellets, Merck) were prepared. To start the experiment As, NaCl, and DOM solution were mixed and adjusted to pH 3 with HCl in preconditioned 50 ml PE centrifuge tubes (VWR) wrapped in aluminum foil. Fe solution was added under constant stirring to reach a final solution volume of 40 ml with concentrations of 60 µg L⁻¹ As(V), 80 µmol L⁻¹ Fe(III), 20 mg L⁻¹ DOC and 5 mmol L⁻¹ NaCl. After immediate adjustment to pH 6 with NaOH the centrifuge tubes were capped and mounted on a horizontal shaker (100 rpm) at 20°C. The pH was controlled after 0.5 and 2 h and readjusted when required. After 24 h of incubation, aliquots were fractionated by size using frontal (0.2 µm; Nylon syringe filters; Roth) and centrifugal filtration (50 kDa and 5 kDa; regenerated cellulose; Millipore; 15 ml; 5000 rpm, 35 min). All filters were rinsed with 10 mmol L⁻¹ NaOH followed twice by Millipore water prior to the experiments. This standard protocol was carried out in duplicates with the different DOM samples. Blank experiments at pH 6 contained As(V) but were either lacking Fe or DOM or both (Figure 1). Time series experiments with the organic matter samples PPHA and SRDOM were also carried out under standard conditions. The sensitivity of the experimental system regarding different initial reaction conditions was tested by varying the parameters pH, ionic strength, DOC concentrations and Fe concentrations in separate experiments (Table 1, Figure 1).

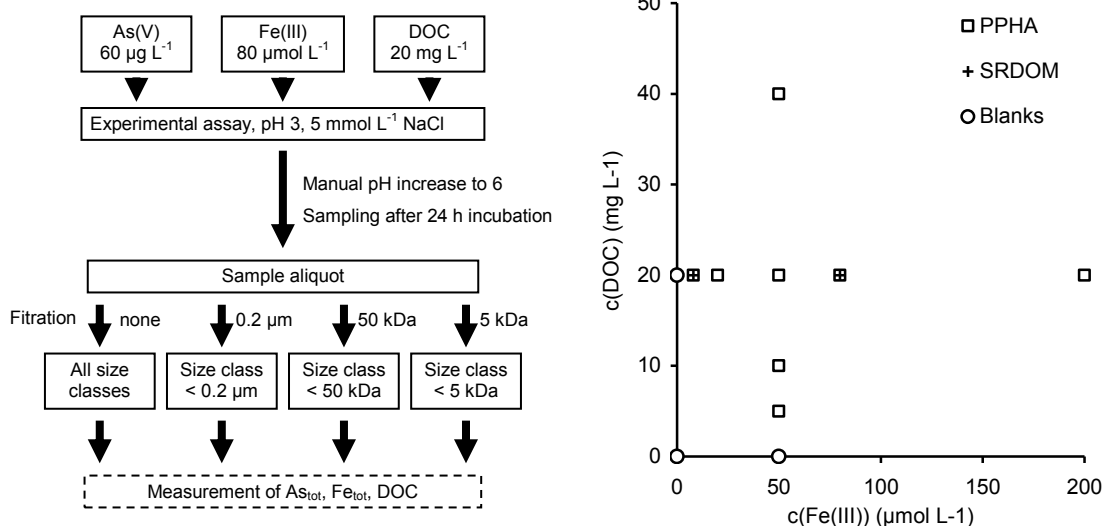


Figure 28 Flow diagram for the standard experiment with PPHA and SRDOM (left). Experimental variations of the standard Fe and C conditions including the blanks are depicted in the Fe vs. DOC diagram (right). Additional variations include pH, ionic strength and DOM sample and are summarized in table 1.

Table 9 Summary of experimental assays; $c(\text{As}) = 60 \mu\text{g L}^{-1}$

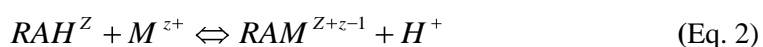
Experiment type	DOM type	$c(\text{DOC})$ mg L^{-1}	$c(\text{Fe})$ $\mu\text{mol L}^{-1}$	Variation
Time series	PPHA, SRDOM	20	80	$t = 2, 24, 72, 144 \text{ h}$
pH	PPHA, SRDOM	20	80	$\text{pH} = 4, 6, 8$
Ionic strength	PPHA	20	80	$I = 0.5, 5, 50 \text{ mmol L}^{-1}$
Fe/C ratio	PPHA	20	0, 8, 20, 80, 200	$\text{Fe/C} = 0.005\text{-}0.12$
Fe/C ratio	PPHA	0, 5, 10, 20, 40	50	$\text{Fe/C} = 0.02\text{-}0.019$
Fe/C ratio	SRDOM	0, 5, 20	0, 8, 80	$\text{Fe/C} = 0.005\text{-}0.019$
Natural OM	various	9 - 22 (by DOM)	80	DOM type

Analytical Techniques and Calculations

Filtrate solutions were analyzed for As, Fe(II), Fe(tot), and DOM concentrations. Fe(II) was analyzed spectrophotometrically on a Varian Cary 1 E using absorption of $[\text{Fe}(\text{bipyridyl})_3]^{2+}$ at 562 nm. Fe(III) was determined by difference between total Fe after reduction with ascorbate and measurement of Fe(II) (Tamura et al., 1974). Total As concentrations were quantified on a Graphite Furnace AAS (Analytik Jena, Zeenith 60). DOC was measured as non-purgable organic carbon (NPOC) on a Shimadzu TOC analyzer (TOC V CPN).

Statistical correlations were determined with the SPSS software (Version 10.0; Pearson correlation coefficients; significance level of 0.05; 2-tailed). Chemical equilibrium calculations were carried out using $c(\text{H}_3\text{AsO}_4) = 60 \mu\text{g L}^{-1}$, $c(\text{Fe}^{3+}) = 80 \mu\text{mol L}^{-1}$, $c(\text{Cl}^-) = 5.24 \text{ mmol L}^{-1}$ and $c(\text{Na}^+) = 5$

mmol L⁻¹ as input data. Saturation indices for ferrihydrite (Log K_{sp} = 4.89) and goethite (Log K_{sp} = 0.50) were determined by the Phreeq C computer code (Parkhurst and Appelo, 1999). Complexation of dissolved ferric iron by DOM was modeled using the WINHUMIC equilibrium model, which is based on humic ion binding Model V, and considers aqueous speciation and precipitation of Fe (Tipping, 1994; Tipping and Hurley, 1992). The model calculates the binding of metals by DOM functional groups in monodendate and bidendate complexes (Eq. 1+2). The concentration of carboxyl and phenol functional groups contained in DOM was taken from IHSS data and calculated from our own titration experiments. Model calculations were run for varying pH, ionic strength, Fe/C ratio, and in- and excluding Fe precipitation.



RA: DOM compound with carboxylic or phenolic group; M: metal, Z and z: humic and metal charge.

Results

DOM Chemistry

DOM chemistry is only briefly discussed here and a summary of DOM characteristics is presented in Table 2 and Figure 2. Anion and cation concentrations were low in the DOM samples except for EVDOM, which was characterized by high salinity, and MWDOM, which contained high concentrations of Fe and sulfate. PPHA had the highest SUVA_{254nm} values. The aromaticity index decreased in the order PPHA > MBDOM > BRDOM > SRDOM > EVDOM. The FTIR ratio for carboxyl to aromatic content (1725 nm/1620 nm) indicated that the IHSS samples PPHA, SRHA and SRFA were relatively enriched in carboxyl groups compared to the BRDOM, EVDOM and MWDOM samples. The high carboxylic content of these samples was in agreement with their large capacity to donate protons in titration experiments. A similar carboxylic and phenolic group content was reported by IHSS (Ritchie and Perdue, 2003) and confirmed our confidence in the quality of our titration experiments. The non-purified DOM in whole water samples had a distinctly lower content of proton donating groups. The DOM samples were characterized by very different molecular size distributions (Figure 2) While PPHA derived molecules had a size maximum in the 50 kDa - 0.2 μm range, the highest abundance of SRDOM molecules was in the size fraction smaller than 5 kDa.

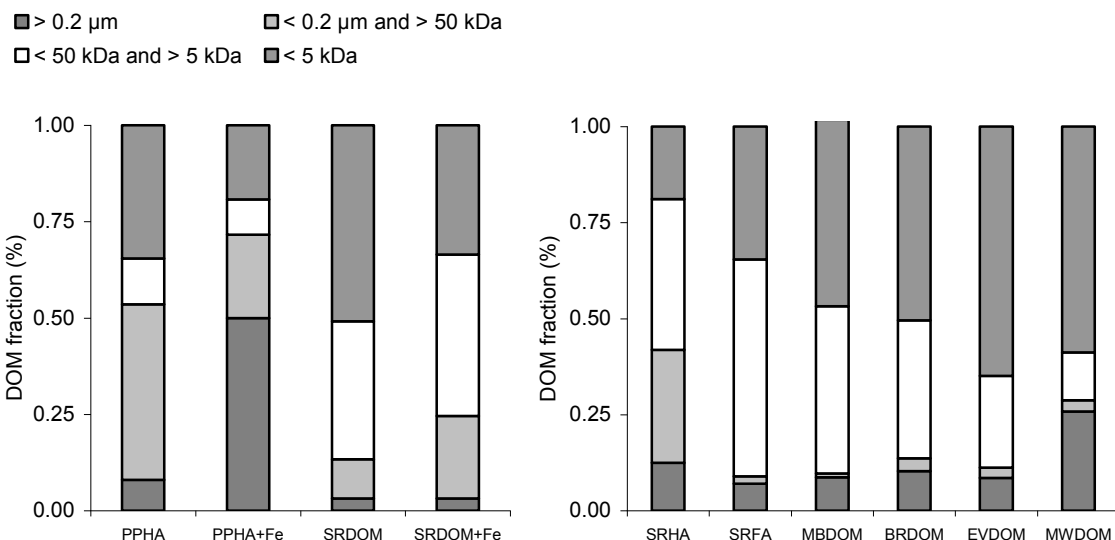


Figure 29 Carbon amounts in the different size classes for PPHA and SRDOM before and after 24 h incubation with $80 \mu\text{mol L}^{-1}$ Fe(III) at pH 6 (left) and for the other DOM samples without Fe addition (right).

Table 10 Chemical characterization of DOM samples

DOM	Carboxylic groups meq (g C) ⁻¹	Phenolic groups L/(m*mg)	SUVA 254 nm	FTIR ratio	Na mmol L ⁻¹	Ca µmol L ⁻¹	Fe µmol L ⁻¹	Al µg L ⁻¹	Cl ⁻ µg L ⁻¹	SO ₄ ²⁻ µg L ⁻¹
				$\frac{1725\text{nm}}{1620\text{nm}}$						
PPHA	8.1 / 8.9*	1.3 / 2.0*	0.06	1.06	0.1	0	0	0	0.1	0
SRFA	13.4 / 11.2*	1.8 / 2.8*		1.68	0.1	0	0	0	0.1	0
SRHA	8.7 / 9.1*	1.4 / 3.7*		1.16	0.1	0	0	0	0.1	0
MBDOM	5.4	1.8	0.05	0.75	0.7	0.1	40	27	11.4	1.7
SRDOM	6.4	2.1	0.04	0.88	0.5	0.35	18	63	5.9	7.1
BRDOM	2.3	0.7	0.05	0.28	0.1	0.31	6	0	1.8	3.0
EVDOM	4.6	1.8	0.04	0.28	8.8	3.1	0	6	154	12.9
MWDOM	7.2	5.3	0.06	0.20	0.6	1.3	740	27	1.8	109

*Values provided by the IHSS

Colloid and Particle Formation Experiments

The blank experiments at pH 6 contained As(V) but were either lacking Fe or DOM or both (Figure 1). In blank experiments over 24 h without Fe and DOM, As was almost unaffected by filtration and $93 \pm 2\%$ of total As were found in size fraction smaller than 5 kDa. In the presence of PPHA the portion of As in the size fraction > 5 kDa increased but still $84 \pm 2\%$ of total As passed the 5 kDa filter membrane. In contrast, in blank experiments with iron and without DOM, 100 % of Fe and As were in the size fraction larger than $0.2 \mu\text{m}$ after 24 h of reaction time.

The additional presence of DOM in the standard experiments lead to higher concentration of Fe and As in small size fractions, i.e. limited aggregate growth. This was the case in the PPHA solution

in which $27 \mu\text{mol L}^{-1}$ Fe (34 %) and $26 \mu\text{g L}^{-1}$ As (47 %) were contained in aggregates $<0.2 \mu\text{m}$ (Figure 3). As and Fe concentrations also increased in the smaller size fraction in the DOM containing assays compared to those lacking DOM. As the aggregates were stable in the solution and did not settle, they can be operationally characterized as colloids of different size.

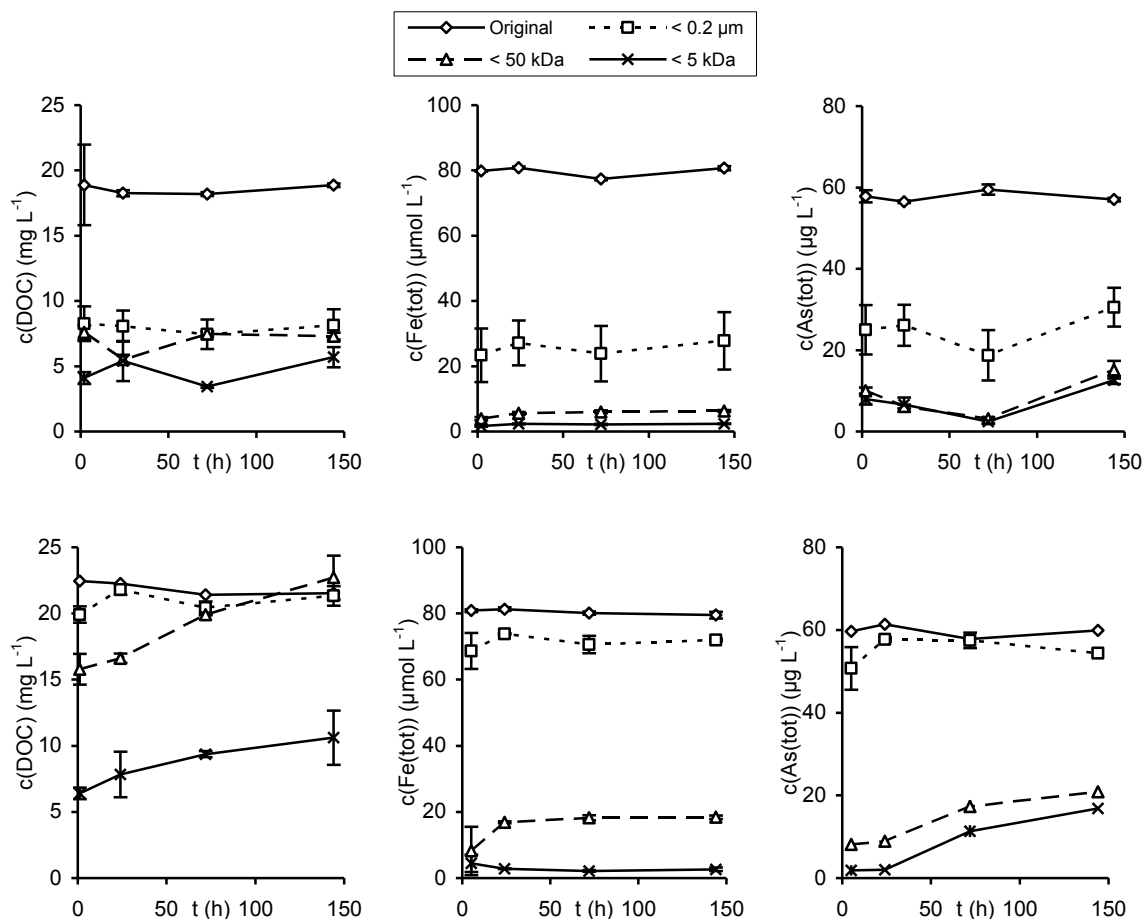


Figure 30 Kinetics of colloid formation with PPHA (top) and SRDOM (bottom) solution. The data points represent the concentration of DOC, Fe and As (left to right) found in the original solution (diamonds) and in the solution after size fractionation with a $0.2 \mu\text{m}$ (squares), 50 kDa (triangles) and 5 kDa (cross) filter. Initial conditions: 5 mmol L^{-1} NaCl, $60 \mu\text{g L}^{-1}$ As, $80 \mu\text{mol L}^{-1}$ Fe(III), $\sim 20 \text{ mg L}^{-1}$ C, pH 6.

Organic molecules were integral parts of the forming colloids, and the nature of the used DOM was of some importance for colloid formation. The size of the DOM containing particles increased substantially in the presence of Fe compared to reference assays without Fe (Figure 2). While the percentage of DOC in the size fraction $>0.2 \mu\text{m}$ increased from 8 to 50 % in PPHA solution, SRDOM molecules were much less affected. Also in the SRDOM solution the amount of Fe and As contained in the small size classes $<0.2 \mu\text{m}$ was higher and amounted to $71 \mu\text{mol L}^{-1}$ Fe (88.0 %) and $57 \mu\text{g L}^{-1}$ As (93.2 %).

The formation of aggregates was fast in PPHA and SRDOM solutions and lead to constant concentrations of DOC, Fe and As in the unfiltered and the $0.2 \mu\text{m}$ filtered solution after 24 h reaction time (Figure 3). DOC and As concentrations in the size fractions smaller 50 and 5 kDa increased over

longer reaction time periods of up to 144 h. The concentration of Fe was correlated with the concentration of As ($R^2=0.989$) and DOC ($R^2=0.739$) in very same size class of the PPHA and SRDOM experiments (Figure 4). Thus the experimental assay induced the formation of colloids containing Fe, DOM and As. The size of these aggregates varied with the type of DOM sample used, but in any case the size of As containing aggregates was smaller than in the reference assays with iron only.

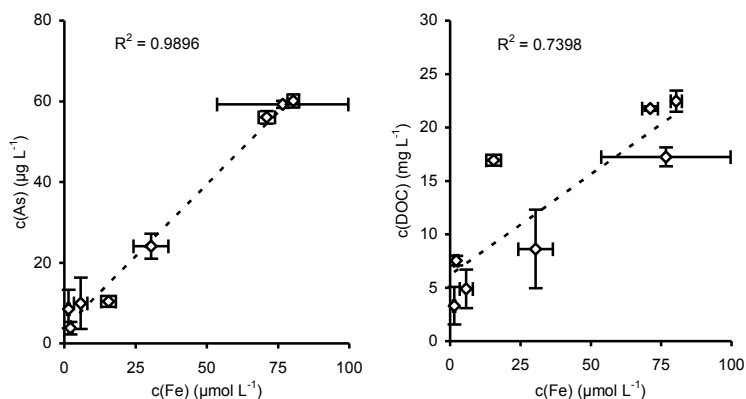


Figure 31 Correlation of Fe and As (left) respectively Fe and C (right) concentration in the size classes of PPHA and SRDOM

Influence of pH, Ionic Strength and Fe/C Ratio on Colloid Formation

The pH had a considerable influence on the colloid formation. In contrast to experiments conducted at pH 6, incubation of Fe, As and PPHA at pH 4 resulted in the immediate formation of clearly visible, fluffy, brown aggregates $> 0.2 \mu\text{m}$, containing 80-90% of all Fe, DOM and As after 24 h of reaction time (Figure 5). The remainder of the elements was contained in the size fraction smaller than 5 kDa. In contrast, no flocs were visible at pH 6 and 8, and Fe, As and DOC concentrations were elevated in particles and molecules smaller than $0.2 \mu\text{m}$. The effect of ionic strength on the size distribution of DOM, Fe, and As was small. An ionic strength increase from 0.5 to 50 mmol L⁻¹ NaCl did not alter Fe concentration in any size fraction. Concentrations of As and DOM increased by 16 - 20 % in aggregates smaller than 50 and 5 kDa.

Changing the initial concentration of DOC relative to ferric iron had a substantial effect on the formation of aggregates in experiments with PPHA. Increasing the DOC concentration from 5 to 40 mg L⁻¹ at a constant Fe concentration of 50 µmol L⁻¹ raised the amount of Fe contained colloids $< 0.2 \mu\text{m}$ from 4 to 92 % and the Fe concentration increased also in the $< 50 \text{ kDa}$ and $< 5 \text{ kDa}$ fractions (Figure 6). Likewise As association with particles in the small size classes increased with DOM concentrations.

Plotting Fe, As and DOC filtration results against the molar Fe/C ratio the amount of colloids larger than $0.2 \mu\text{m}$ increased sharply above Fe/C = 0.02 (Figure 7). At lower Fe/C ratios substantial amounts of Fe and DOC were present in particles between 5 kDa and $0.2 \mu\text{m}$ in size, but As was predominantly in the size class smaller than 5 kDa ($> 80 \%$). When Fe/C ratios were between 0.02 and

0.1 the quantity of colloids $> 0.2 \mu\text{m}$ continually increased, affecting the concentration of all three components. Above $\text{Fe}/\text{C} = 0.1$ all Fe and As was present in aggregates larger than $0.2 \mu\text{m}$.

The dependence of colloid formation on pH and Fe/C ratios was similar when the SRDOM solution was used. However, as could be seen already for the time series experiment, the particles forming were generally smaller than in the PPHA solution. The amount of Fe and As in compounds $< 0.2 \mu\text{m}$ was considerably higher using SRDOM (Figure A1 of the appendix). Even at a Fe/C ratio of 0.15 some Fe and As was present in particles smaller than $0.2 \mu\text{m}$, which was not the case using PPHA.

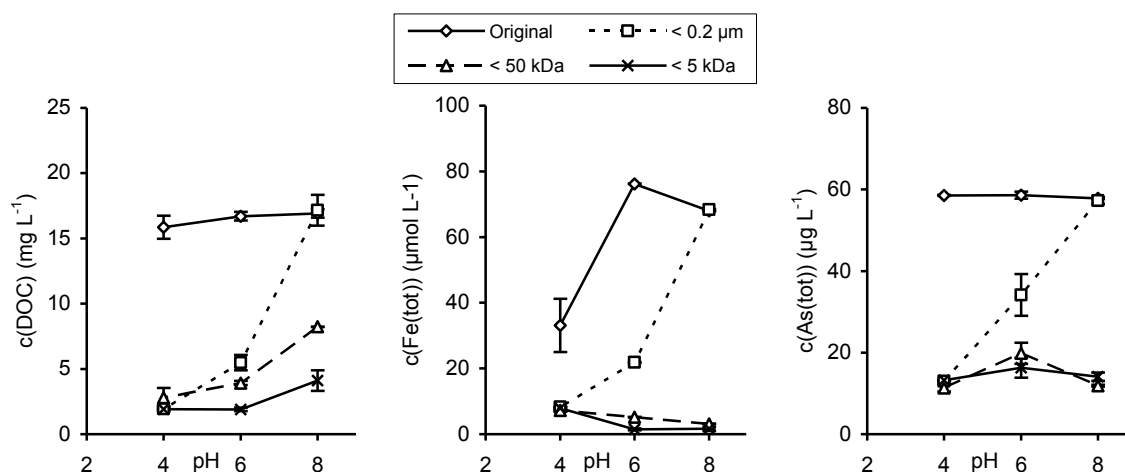


Figure 32 The pH dependence of colloid formation with PPHA solution. The data points represent the concentration of DOC, Fe and As (left to right) found in the original solution (diamonds) and in the solution after size fractionation with a $0.2 \mu\text{m}$ (squares), 50 kDa (triangles) and 5 kDa (cross) filter. Initial conditions: $5 \text{ mmol L}^{-1} \text{ NaCl}$, $60 \mu\text{g L}^{-1} \text{ As}$, $80 \mu\text{mol L}^{-1} \text{ Fe(III)}$, $\sim 20 \text{ mg L}^{-1} \text{ C}$.

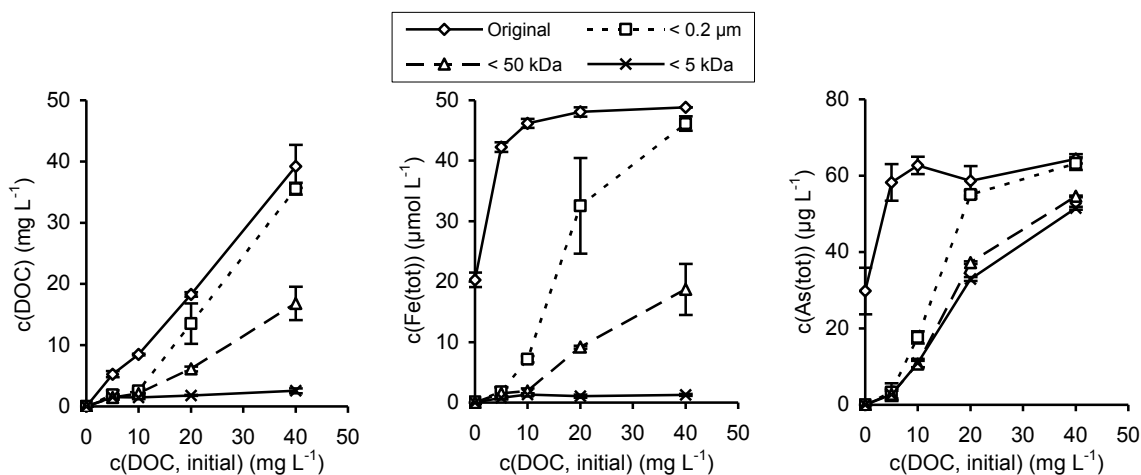


Figure 33 Colloid formation at different concentration of PPHA. The data points represent the concentration of DOC, Fe and As (left to right) found in the original solution (diamonds) and in the solution after size fractionation with a 0.2 μm (squares), 50 kDa (triangles) and 5 kDa (cross) filter. Initial conditions: 5 mmol L⁻¹ NaCl, 60 μg L⁻¹ As, 80 μmol L⁻¹ Fe(III), 0-40mg L⁻¹ C, pH 6.

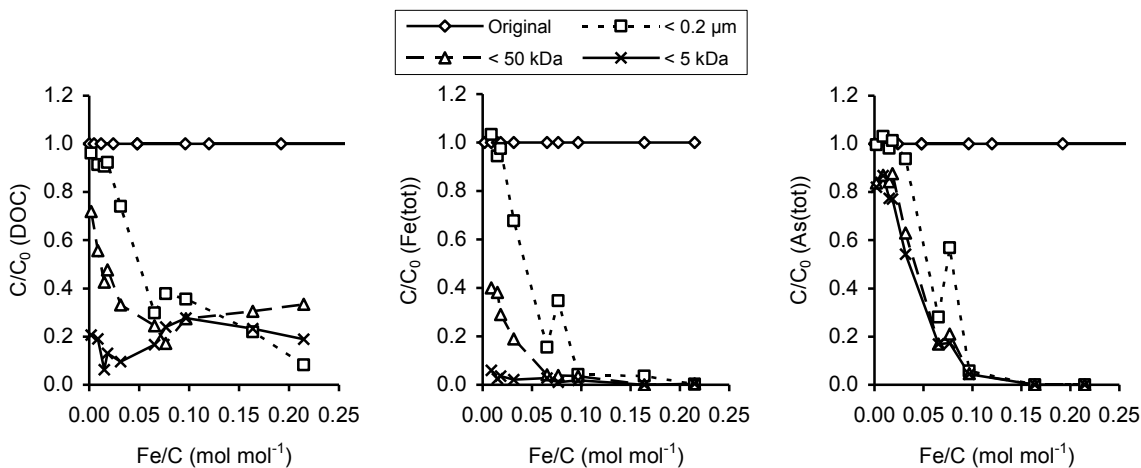


Figure 34 Colloid formation at different molar Fe/C ratios in PPHA solution. The data points represent the concentration of DOC, Fe and As (left to right) found in the original solution (diamonds) and in the solution after size fractionation with a 0.2 μm (squares), 50 kDa (triangles) and 5 kDa (cross) filter. Initial conditions: 5 mmol L⁻¹ NaCl, 60 μg L⁻¹ As, 0-200 μmol L⁻¹ Fe(III), 0-40mg L⁻¹ C, pH 6.

Influence of DOM Chemistry on Colloid Formation and Model Calculations

The quantity of Fe contained in aggregates larger than 0.2 μm increased in the order SRDOM (12 %) < SRFA (21 %) < SRHA (34 %) < PPHA (60 %) ~ MBDOM (62 %), and of As in the order SRDOM (7 %) < SRHA (18 %) < SRFA (47 %) < PPHA (59 %) ~ MBDOM (62 %) (Table 3). In solutions of BRDOM, EVDOM and MWDOM at least 90 % of As and Fe were found in aggregates of that size fraction.

A statistical analysis was carried out including the experimental results shown in Table 3. The amounts of As and Fe in each individual size class, in % of the original concentration, were positively correlated ($R^2 > 0.9$), but no correlation was found for As and Fe with DOC. A positive correlation was

also found between the initial Fe/C ratio and the Fe contained in the particle size class larger than $> 0.2 \mu\text{m}$ ($R^2=0.70$). Weak negative correlations occurred between the percentage of Fe and As in colloids $>0.2 \mu\text{m}$ and the carboxyl content and the 1725nm/1620nm FTIR peak ratio of DOM (R^2 between -0.58 and -0.79).

Table 11 Concentrations of C, Fe and As in the size fractions of different DOM samples in the experimental assays under standard conditions

DOM sample	Original sample	$< 0.2 \mu\text{m}$	$< 50 \text{ kDa}$	$< 5\text{kDa}$
	DOC (mg L^{-1}) / Fe ($\mu\text{mol L}^{-1}$) / As ($\mu\text{g L}^{-1}$)			
PPHA	17.2 / 76.6 / 59.3	8.6 / 30.4 / 24.1	4.9 / 5.7 / 9.9	3.3 / 1.4 / 8.5
SRHA	19.4 / 74.8 / 66.4	14.5 / 49.3 / 54.3	12.8 / 14.6 / 24.1	7.5 / 3.3 / 21.4
SRFA	21.9 / 68.2 / 60.6	20.2 / 53.9 / 32.1	17.0 / 17.4 / 16.9	8.7 / 3.8 / 10.3
SRDOM	22.5 / 80.3 / 60.1	21.8 / 71.1 / 56.0	16.9 / 15.5 / 10.4	7.5 / 2.2 / 3.8
MBDOM	16.1 / 74.6 / 62.6	14.9 / 28.3 / 23.8	10.7 / 10.19 / 7.8	3.8 / 2.7 / 6.2
BRDOM	9.2 / 77.1 / 64.5	7.3 / 4.1 / 0.4	6.8 / 3.1 / 0	4.4 / 0.6 / 0
EVDOM	19.2 / Nd / 67.8	17.7 / Nd / 15.9	14.9 / Nd / 4.5	10.9 / Nd / 4.5
MWDOM	12.2 / 196.5 / 58.6	8.8 / 17.7 / 4.4	6.9 / 2.2 / 0	5.4 / 1.3 / 0

According to thermodynamic equilibrium calculations, $\text{Fe}(\text{OH})_2^-$ predominated in solution among aqueous Fe species at pH 6 and the solution was supersaturated with respect to ferrihydrite. The maximum of Fe complexation by PPHA, SRHA and SRFA at pH 6 amounted to $46 \text{ mmol Fe (mol C)}^{-1}$ in WINHUMIC calculations, not considering iron precipitation. Including the process of iron oxide formation into the model, the modeled Fe complexation in equilibrium decreased to 17-20 $\text{mmol Fe (mol C)}^{-1}$, corresponding to 28 - 33 % of the total Fe present in the experiment. These calculations were based the standard experimental conditions of 5 mmol L^{-1} NaCl, $80 \mu\text{mol L}^{-1}$ Fe(III), a DOC concentration of 20 mg L^{-1} and a DOM carboxylic group content of 100-130 mmol (mol C)^{-1} with an average pK_a of 3.5-4.5, as suggested by IHSS data (Ritchie and Perdue, 2003).

Discussion

Impact of DOM on Colloid Formation

The presence of DOM strongly increased the amount of dissolved As and of As contained in small and more mobile colloids in our batch experiments. Furthermore, the size of As containing iron oxide aggregates decreased when compared to a solution containing only Fe and As, which is also an important finding. Ferric iron oxides are one of the most important natural As scavengers (Dixit and Hering, 2003) and easily form at a near neutral pH, which we also used in our experiments. A straight forward explanation for the increased presence of As in the water phase is a competition between

DOM and As for sorption sites. A strong affinity of DOM for Fe oxides has been documented. Sorption capacities of 0.7-1 mol kg⁻¹ DOC have been reported, based on experiments with ferrihydrite at pH 6, and the competition for sorption sites mobilized As (Grafe et al., 2002). However, a competition between DOM and As for sorption sites on Fe oxide colloids alone is not adequate for explaining our experimental results. First, As containing particles remained in an intermediate size range of 0.2 μm to 5 kDa in the presence of DOM; As was not predominantly in the free ionic form. Second, Fe was also found in smaller size classes in presence of DOM. This implies that the DOM altered the type of associations that developed, and thus the surface area available for As adsorption. And third, the presence of Fe lead to a bigger portion of As contained in larger particle sizes, when compared to solutions containing only DOM and As. This result implies that Fe oxides were still involved in the As binding reactions, even in presence of DOM. The binding of As in dissolved metal-DOM bridging complexes or metal-DOM associations of intermediate particle size may explain such observations (Lin et al., 2004; Redman et al., 2002; Ritter et al., 2006; Thanabalasingam and Pickering, 1986).

Before evaluating the relative importance of complexation reactions and colloid formation with regard to As behavior, it is necessary to inspect the interactions between DOM and Fe more closely. The presence of DOM decreased the retention of Fe and increased the retention of DOM during filtration. This suggests that DOM induced the formation of small, DOM and Fe bearing associations, likely due to the aqueous complexation of Fe(III) by humic carboxyl or phenol groups. As we were unable to quantify the amount of complexed Fe directly, the WINHUMIC model was used for this purpose. We estimated a maximum Fe complexation capacity of to 46 mmol Fe (mol C)⁻¹. Metal complexation by fulvic and humic acids in equilibrium titrations has been reported at similar levels, i.e. 72 mmol Cu (mol C)⁻¹ (Christl and Kretzschmar, 2001).

In natural DOM solutions often less Fe is found in aqueous complexes and values of 0.1 to 30 mmol complexed Fe (mol C)⁻¹ have been reported by Tipping et al. (2002). In addition to Fe aquatic chelation, however, organic molecules have also been shown to prevent mineral growth and sedimentation by covering mineral surfaces and changing surface charge (Liang and Morgan, 1990; Peiffer et al., 1999; Pullin and Cabaniss, 2003). In rivers and soils the substantial aqueous transport of Fe occurs in colloidal associations with DOM of 1 kDa to 0.8 μm size (Pokrovsky et al., 2005; Pokrovsky and Schott, 2002), supporting that DOM stabilized Fe oxide particles are a relevant and important fraction of iron also in natural waters.

The complexation of Fe by DOM dropped to 17-20 mmol (mol C)⁻¹ or 28-33 % of Fe present in the WINHUMIC calculations for standard conditions when a precipitation of Fe oxides to thermodynamic equilibrium was allowed. This leaves about 70 % of the total Fe available for the formation of DOM stabilized Fe oxide particles under the specific conditions in our batch experiments. Several observations suggest that surface adsorption of DOM on Fe oxides played a role in inhibiting the formation of larger Fe oxide particles in our experiments (Figure 2, 3 and 7): (I) Fe addition increased

the portion of the DOC in larger size classes. (II) The solutions were supersaturated with respect to ferrihydrite at pH 6, but no observable sedimentation of Fe oxides occurred. (III) The particle size changed with the Fe/C ratio of the experiment.

The relative importance of Fe complexed by DOM to Fe in colloids stabilized by DOM depended on the Fe/C in the solution. (Ritter et al., 2006) found a positive and nearly linear correlation between Fe removal by filtration and the initial Fe/C ratio, showing that the potential of organic molecules to suspend Fe decreased with an increasing Fe/C ratio. Our results suggest that this relationship is not always linear. Retention of Fe during filtration in our experiments rose strongly only between Fe/C = 0.02 and 0.1 in presence of PPHA. The reasons for this non-linearity in the growth of iron oxide colloids in presence of DOM can be understood by applying the WINHUMIC model. In the calculations, the fraction available for Fe colloid formation increased when Fe concentrations exceeded the DOM complexation capacity (Figure 8). The DOM complexing groups were saturated with Fe above Fe/C = 0.018 according to the model, and this value corresponds well to the experimentally determined increase of Fe retention during filtration above Fe/C = 0.02. With lower Fe/C ratios, Fe can be considered as mainly complexed and chelated by organic matter in solution, whereas at higher ratios the colloidal Fe particles accounted for a growing fraction of the initially added Fe. Both experimental observations and model calculations agree that at Fe/C ratios > 0.1 Fe is predominantly precipitated and present in the large colloidal fraction > 0.2 μm (Figure 7 and 8).

In accordance with findings of (Pullin and Cabaniss, 2003), the ionic strength had a negligible impact on colloid formation in our experimental systems. This suggests that specific surface reactions, such as As and DOM surface complexation on Fe oxide, were more important than electrostatic interactions (Gu et al., 1994; Sun and Doner, 1998; Tiller and O'Melia, 1993). Reduction of ferric Fe by DOM was observed previously (Bauer et al., 2006), but did not influence Fe concentration in different size fractions in these experiments. Less than 5 % of the total Fe was present in form of Fe(II) after 24 h at pH 6. In addition, any potential effect on the mobility of Fe was small, as Fe(II) was also associated with the formed colloids. In summary, we believe that during our standard experiments and at pH 6, a maximum of 20-30% of the initially added Fe remained complexed in solution, <10 % was reduced by DOM, and the remaining amount was present in form of particles.

These conclusions are only valid for pH 6 and 8, at which small DOM-Fe colloids prevailed. In contrast, reducing the pH to 4 induced the development of large Fe and DOM containing flocs. At this pH, metal binding was likely strongly reduced due to protonation and steric inaccessibility of carboxylic groups (Christl and Kretzschmar, 2001) and excess metal concentrations caused the complete neutralization of negative DOM charge and induced the hydrophobic coagulation of DOM-metal flocs (Kaiser, 1998). The flocs larger than 0.2 μm formed in our experiments at a Fe/C ratio of 0.05 contained more than 90 % of Fe and C. Nierop et al. (2002) found only 50 % of iron and carbon in large coagulates at the same Fe/C ratio, but this might be due to different DOM properties and the lower size selectivity of their separation method.

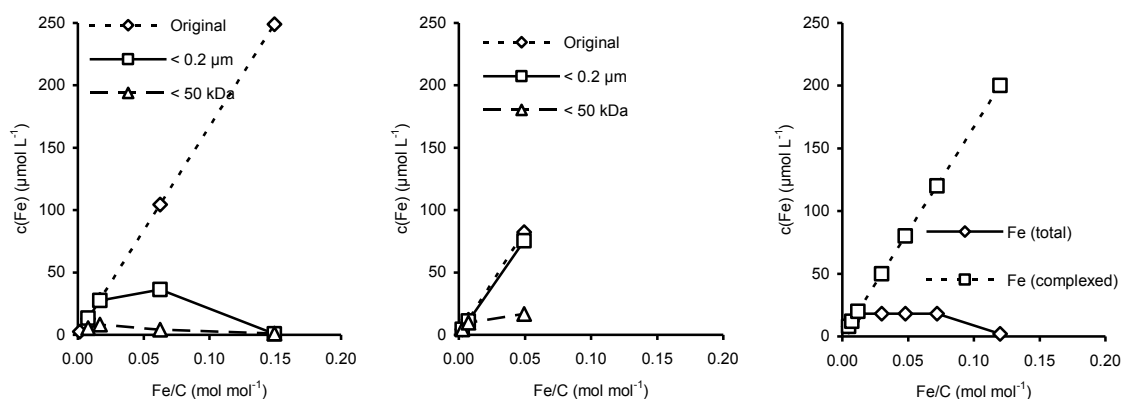


Figure 35 Fe/C ratio effect on Fe concentrations in different size classes of PPHA (left) and SRDOM (middle) experiments and on Fe complexation as calculated with the WINHUMIC model (right).

Impact on the Binding of As by Colloids

As shown in the previous chapter, the size of Fe containing colloids varied with Fe/C ratio of the experiment. For $Fe/C < 0.02$ most Fe was found in small aggregates supposedly chelated with organic molecules. Larger Fe colloids became more important with increasing Fe/C ratio and large mineral particles prevailed at $Fe/C > 0.1$. Arsenic binding in complexes or colloids was strongly related to these variations in colloid formation. Arsenic binding is thus also discussed with respect to experimental Fe/C ratio when the nature of As interactions with Fe and DOM is interpreted.

When Fe concentrations and Fe/C ratios were large, i.e. > 0.1 in experiments with PPHA, Fe and As were completely removed by 0.2 μm filtration even though 20-30 % DOC remained in solution. This pattern implies that large amorphous Fe oxides rapidly formed and that organic molecules were unable to limit the growth of these Fe colloids. Arsenic was retained when filtered due to the well known and efficient binding in surface complexes on the iron oxide particles (Dixit and Hering, 2003). Concurrently 70-80 % of the present DOM were also retained, presumably because of sorption on the iron particles surfaces (Gu et al., 1994; Kaiser and Zech, 1997). This did apparently not result in considerable competition for sorption sites between As and DOM anions (Grafe et al., 2002).

When Fe/C ratios were small, i.e. < 0.02 in experiments with PPHA, Fe chelation in solution was the predominant form of Fe binding according to calculations with the WINHUMIC model. This prediction was supported by our filtration results as Fe was mainly present in the small molecular size fractions (Figure 8). In this small Fe/C range, most As was in the size class smaller than 5 kDa and, therefore, either contained in small aggregates or present in the free ionic form. In our experiments the amount of As in particles larger than 5 kDa was unaffected by changes in Fe/C ratio for $Fe/C < 0.02$, suggesting the presence of As in the free ionic form rather than in aqueous DOM-Fe bridging complexes or colloids. This interpretation is in agreement with the fact that high concentration of negatively charged DOM likely neutralized the positive charge of ionic Fe or Fe oxide particles, thus

preventing interactions As(V). Alternatively low amounts of As might also have been associated with organic molecules as proposed by Buschmann et al. (2006).

Most of our experiments were carried out with intermediate Fe/C ratios of 0.02 to 0.1. The Fe concentration in the large particles size fractions increased almost linearly in this range with rising Fe/C ratio, and the same pattern was found for As concentrations. Iron and As concentrations were correlated ($R^2=0.989$) in the different size fractions of the PPHA and SRDOM time series experiments (Fe/C = 0.048). Intermediate Fe/C ratios, between 0.02 and 0.1 in experiments with PPHA, represent the transition zone between the low Fe/C range, where As is predominantly in the free ionic form, and the high Fe/C, where As is efficiently adsorbed to large iron oxide mineral particles.

A linear correlation of As and Fe concentrations was previously observed for dialysis experiments with dissolved organic matter solution (Ritter et al., 2006). The authors stressed that the iron concentration of a DOM solution was critical to its ability to bind As(V). Other studies documented that As binding to DOM increases with the concentration of metals, especially Fe, Al and Mn, in solution (Lin et al., 2004; Redman et al., 2002).

In contrast to experiments with PPHA solution, the use of SRDOM lead to a larger amount of As in colloids smaller than 0.2 μm , and even for a Fe/C ratio as high as 0.15 As was still present in aggregates smaller than 0.2 μm . The higher presence of Fe and As in particles of small size classes compared to PPHA was observed for all Fe/C ratio > 0.02 , and suggests that SRDOM limited particle growth more strongly. We attribute this to differences in the molecular properties of both DOM samples. SRDOM initially had a larger portion of structures with a low molecular weight than PPHA and the small fulvic molecules have a higher density of carboxyl group and lower acidity constants (Amirbahman and Olson, 1995). Consequently, a more efficient Fe binding in aqueous chelates or colloids is likely due to the greater charge of DOM. Furthermore, the formed aggregates were smaller because of the lower initial molecular weight of SRDOM.

The initial molecular size of the carbon structures was the only DOM property, which could be linked to the size of the forming aggregates. No dependence on the DOM carboxyl group density or aromaticity parameters (SUVA, FTIR ratio) was found. SRDOM contained more small molecules in the fulvic acid size range and was more representative for organic matter from surface waters, while the high amounts of larger humic molecules like in PPHA may naturally only be found in peatland waters. Therefore we expect smaller colloids to form in surface waters at similar solution composition, reducing colloid sedimentation and increasing As mobility.

The reaction progress of complex formation and development of colloidal aggregates was fast and occurred mainly within the first 24 h. Similar reaction time scales were previously documented with respect to iron oxide precipitation, the formation of colloids in the presence of organic matter, and As binding reactions to iron phases in the presence and absence of organic matter (Dixit and Hering, 2003; Grafe et al., 2002; Pullin and Cabaniss, 2003). The formation of As containing aggregates must

therefore be considered for most natural water bodies, in which residence times of DOC, Fe and As containing waters are generally longer than 24 h.

Our experiments simulated a natural environment with high aqueous Fe, DOC and As concentrations with redox conditions changing from reduced to oxidized, causing the precipitation of ferric iron minerals at circumneutral pH. Examples for this scenario are found where reduced As contaminated groundwater is subjected to oxic conditions, i.e. during water treatment or during groundwater exfiltration into surface waters or wetlands (Bauer et al., 2008; Smedley and Kinniburgh, 2002; Szramek et al., 2004). Peat or wetland soils were previously found to accumulate considerable amounts of As (Gonzalez et al., 2006; Pfeifer et al., 2004; Steinmann and Shoty, 1997), which was released to the porewater under reducing conditions and may discharged together with mobilized Fe and DOC (Astrom and Corin, 2000; Blodau et al., 2007; Huang and Matzner, 2006). The presence of As in colloidal form thus must be considered when the mobility of As is studied in these environments. Only at low pH, the forming As containing flocs were large and sedimented quickly. A negligible transport of As with colloids may thus be expected in acidified soils or naturally acidic peatlands.

Laboratory and field studies documented a formation of colloids involving iron and containing arsenate or phosphate, which are structural analogons (Astrom and Corin, 2000; Gschwend and Reynolds, 1987; Tadanier et al., 2005). Occurrence of these aggregates may strongly affect As mobility as colloidal transport can take place over considerable distances (Kaplan et al., 1995) and size exclusion effects may lead to a faster movement of colloids compared to free ions (Kretzschmar and Sticher, 1997; Puls and Powell, 1992). Furthermore particle bound As makes predictions about retention or transport in soils, aquifers, rivers or treatment plants more complicated. Arsenic contained in colloids will not be removed from the solution by adsorption to positively charged adsorption sites. Instead the mobility of the element will be controlled by chemical conditions inducing coagulation and settling of colloids, such as changes in pH or increasing solution salt concentrations (Liang and Morgan, 1990). Arsenic bearing colloids also have to be considered during sampling and analysis of natural waters to avoid erroneous concentration estimates.

Conclusions

The presence of organic matter in our experimental system substantially influenced the size of As containing iron oxide aggregates. Arsenic was completely sorbed and sedimented with iron oxide precipitates at neutral pH only in the absence of DOM. In presence of DOM, a precipitation and sedimentation of iron oxides and associated As was impeded by the formation of aqueous Fe chelates and inhibition of Fe colloid growth. Arsenic remained partly in solution, was partly complexed in aqueous state and partly contained in small colloids. The relative importance of the different pools of As varied strongly with the Fe/C ratio of the solution. A smaller initial Fe/C ratio promoted a transfer

of As into the small molecular size fractions. The size of forming aggregates also depended on pH and the initial size of DOM molecules.

The occurrence of As containing colloids in DOM and Fe rich solutions likely has important implications for the mobility of As in aquatic systems, particularly near anoxic-oxic boundaries. The mobility of As in the ionic and colloidal form will be promoted in runoff when DOM and Fe are concurrently present and conditions change from anoxic to oxic. Under such conditions, co-precipitation and immobilization of As will be of lesser importance than expected in iron rich waters. The geochemical and hydrological setting necessary for the outlined processes supporting As mobility are for example given in wetlands, surface waters draining wetlands, and aquifers with transient redox conditions (Astrom and Corin, 2000; Smedley and Kinniburgh, 2002; Szramek et al., 2004). In agreement with this idea the MWDOM groundwater, for instance, has been shown to contain large amounts of Fe colloids stabilized by DOM (Peiffer et al., 1999). The role and extent of dissolved organic matter facilitated As transport in natural environments should be addressed by future research on the basis of this study.

Acknowledgements

The authors thank Donald Macalady for providing different dissolved organic matter samples and helpful discussions especially in the initial stage of the experiments. Thanks also go to Martina Rohr, Jutta Eckert and Lina Fürst for technical support. The study was funded by German Research Foundation (DFG) grant BL 563/2-2 to C. Blodau.

References

- Amirbahman A. and Olson T. M. (1995) The Role of Surface Conformations in the Deposition Kinetics of Humic Matter-Coated Colloids in Porous-Media. *Colloids Surf., A* **95**(2-3), 249-259.
- Astrom M. and Corin N. (2000) Abundance, sources and speciation of trace elements in humus-rich streams affected by acid sulphate soils. *Aquat. Geochem.* **6**, 367-383.
- Bauer M. and Blodau C. (2006) Mobilization of arsenic by dissolved organic matter from iron oxides, soils and sediments. *Sci. Tot. Environ.* **354**, 179-190.
- Bauer M., Fulda B., and Blodau C. (2008) Groundwater derived arsenic in high carbonate wetland soils: Sources, sinks and mobility. *Sci. Tot. Environ.* **submitted**.
- Bauer M., Heitmann T., Macalady D. L., and Blodau C. (2006) Electron transfer capacities and reaction kinetics of peat dissolved organic matter. *Environ. Sci. Technol.*
- Blodau C., Fulda B., Bauer M., and Knorr K.-H. (2007) Arsenic speciation and turnover in intact organic soils during experimental drought and rewetting. *Geochim. Cosmochim. Acta* **submitted**.
- Buffle J., Wilkinson K. J., Stoll S., Filella M., and Zhang J. W. (1998) A generalized description of aquatic colloidal interactions: The three-colloidal component approach. *Environ. Sci. Technol.* **32**(19), 2887-2899.
- Buschmann J., Canonica S., Lindauer U., Hug S. J., and Sigg L. (2005) Photoirradiation of dissolved humic acid induces arsenic(III) oxidation. *Environ. Sci. Technol.* **39**(24), 9541-9546.
- Buschmann J., Kappeler A., Lindauer U., Kistler D., Berg M., and Sigg L. (2006) Arsenite and arsenate binding to dissolved humic acids: Influence of pH, type of humic acid, and aluminum. *Environ. Sci. Technol.* **40**(19), 6015-6020.
- Christl I. and Kretzschmar R. (2001) Interaction of copper and fulvic acid at the hematite-water interface. *Geochim. Cosmochim. Acta* **65**(20), 3435-3442.
- Davis C. C., Knocke W. R., and Edwards M. (2001) Implications of aqueous silica sorption to iron hydroxide: Mobilization of iron colloids and interference with sorption of arsenate and humic substances. *Environ. Sci. Technol.* **35**(15), 3158-3162.
- Dixit S. and Hering J. G. (2003) Comparison of arsenic(V) and arsenic(III) sorption onto iron oxide minerals: Implications for arsenic mobility. *Environ. Sci. Technol.* **37**(18), 4182-4189.
- Gonzalez Z. I., Krachler M., Cheburkin A. K., and Shotyk W. (2006) Spatial distribution of natural enrichments of arsenic, selenium, and uranium in a minerotrophic peatland, Gola di Lago, Canton Ticino, Switzerland. *Environ. Sci. Technol.* **40**(21), 6568-6574.
- Grafe M., Eick M. J., Grossl P. R., and Saunders A. M. (2002) Adsorption of arsenate and arsenite on ferrihydrite in the presence and absence of dissolved organic carbon. *J. Environ. Qual.* **31**(4), 1115-1123.
- Gschwend P. M. and Reynolds M. D. (1987) Monodisperse ferrous phosphate colloids in an anoxic groundwater plume. *J. Cont. Hydrol.* **1**(3), 309-327.
- Gu B. H., Schmitt J., Chen Z. H., Liang L. Y., and McCarthy J. F. (1994) Adsorption and Desorption of Natural Organic-Matter on Iron-Oxide - Mechanisms and Models. *Environ. Sci. Technol.* **28**(1), 38-46.
- Harvey R. W., Kinner N. E., Bunn A., MacDonald D., and Metge D. (1995) Transport behavior of groundwater protozoa and protozoan-sized microspheres in sandy aquifer sediments. *Appl. Environ. Microbiol.* **61**(1), 209-217.

- Huang J.-H. and Matzner E. (2006) Dynamics of organic and inorganic arsenic in the solution phase of an acidic fen in Germany. *Geochim. Cosmochim. Acta* **70**(8), 2023-2033.
- Kaiser K. (1998) Fractionation of dissolved organic matter affected by polyvalent metal cations. *Organic Geochemistry* **28**(12), 849-854.
- Kaiser K. and Zech W. (1997) Competitive sorption of dissolved organic matter fractions to soils and related mineral phases. *Soil Sci. Soc. Am. J.* **61**(1), 64-69.
- Kalbitz K., Geyer W., and Geyer S. (1999) Spectroscopic properties of dissolved humic substances—a reflection of land use history in a fen. *Biogeochemistry* **47**, 219-238.
- Kaplan D. I., Bertsch P. M., and Adriano D. C. (1995) Facilitated transport of contaminant metals through an acidified aquifer. *Ground Water* **33**, 708-717.
- Kretzschmar R., Borkovec M., Grolimund D., and Elimelech M. (1999) Mobile subsurface colloids and their role in contaminant transport. In *Advances in Agronomy, Vol 66*, Vol. 66, pp. 121-193.
- Kretzschmar R. and Sticher H. (1997) Transport of humic-coated iron oxide in a sandy soil: Influence of Ca²⁺ and Trace metals. *Environ. Sci. Technol.* **31**, 3497-3504.
- Liang L. and Morgan J. J. (1990) Chemical aspects of iron oxide coagulation in water: Laboratory studies and implications for natural systems. *Aquat. Sci.* **51**(1), 32-55.
- Lin H. T., Wang M. C., and Li G. C. (2004) Complexation of arsenate with humic substance in water extract of compost. *Chemosphere* **56**(11), 1105-1112.
- McArthur J. M., Banerjee D. M., Hudson-Edwards K. A., Mishra R., Purohit R., Ravenscroft P., Cronin A., Howarth R. J., Chatterjee A., Talukder T., Lowry D., Houghton S., and Chadha D. K. (2004) Natural organic matter in sedimentary basins and its relation to arsenic in anoxic groundwater: the example of West Bengal and its worldwide implications. *Appl. Geochem.* **19**, 1255-1293.
- Meharg A. A., Scrimgeour C., Hossain S. A., Fuller K., Cruickshank K., Williams P. N., and Kinniburgh D. G. (2006) Codeposition of organic carbon and arsenic in Bengal Delta aquifers. *Environ. Sci. Technol.* **40**(16), 4928-4935.
- Mikutta C., Lang F., and Kaupenjohann M. (2006) Citrate impairs the micropore diffusion of phosphate into pure and C-coated goethite. *Geochim. Cosmochim. Acta* **70**(3), 595-607.
- Nierop K., G.J., Jansen B., and Verstraten J. M. (2002) Dissolved organic matter, aluminum and iron interaction: precipitation induced by metal/carbon ratio, pH and competition. *Sci. Tot. Environ.* **300**, 201-211.
- O'Day P. A., Vlassopoulos D., Root R., and Rivera N. (2004) The influence of sulfur and iron on dissolved arsenic concentrations in the shallow subsurface under changing redox conditions. *Proceedings of the National Academy of Sciences of the United States of America* **101**(38), 13703-13708.
- Parkhurst D. L. and Appelo C. A. J. (1999) User's guide to PHREEQC - A computer program for speciation, batch-reaction, one dimensional transport, and inverse geochemical calculations. In *Water-resources investigations report 99-4259*. US department of the interior.
- Peiffer S., Walton-Day K., and Macalady D. L. (1999) The interaction of natural organic matter with iron in a wetland (Tennessee Park, Colorado) receiving acid mine drainage. *Aquat. Geochem.* **5**(2), 207-223.
- Pfeifer H. R., Gueye-Girardet A., Reymond D., Schlegel C., Temgoua E., Hesterberg D. L., and Chou J. W. Q. (2004) Dispersion of natural arsenic in the Malcantone watershed, Southern Switzerland: field evidence for repeated sorption-desorption and oxidation-reduction processes. *Geoderma* **122**(2-4), 205-234.

- Pokrovsky O. S., Dupre B., and Schott J. (2005) Fe-Al-organic colloids control of trace elements in peat soil solutions: Results of ultrafiltration and dialysis. *Aquat. Geochem.* **11**(3), 241-278.
- Pokrovsky O. S. and Schott J. (2002) Iron colloids/organic matter associated transport of major and trace elements in small boreal rivers and their estuaries (NW Russia). *Chem. Geol.* **190**, 141-179.
- Pullin M. J. and Cabaniss S. E. (2003) The effects of pH, ionic strength, and iron-fulvic acid interactions on the kinetics of nonphotochemical iron transformations. I. Iron(II) oxidation and iron(III) colloid formation. *Geochim. Cosmochim. Acta* **67**(21), 4067-4077.
- Puls R. W. and Powell R. M. (1992) Transport of inorganic colloids through natural aquifer material: Implications for contaminant transport. *Environ. Sci. Technol.* **26**, 614-621.
- Redman A. D., Macalady D. L., and Ahmann D. (2002) Natural organic matter affects arsenic speciation and sorption onto hematite. *Environ. Sci. Technol.* **36**(13), 2889-2896.
- Ritchie J. D. and Perdue E. M. (2003) Proton-binding study of standard and reference fulvic acids, humic acids, and natural organic matter. *Geochim. Cosmochim. Acta* **67**(1), 85-96.
- Ritter K., Aiken G. R., Ranville J., Bauer M., and Macalady D. L. (2006) Evidence for the aquatic binding of arsenate by natural organic matter (NOM)-suspended Fe(III). *Environ. Sci. Technol.* **40**, 5380-5387.
- Schmitt D., Saravia F., Frimmel F. H., and Schuessler W. (2003) NOM-facilitated transport of metal ions in aquifers: importance of complex-dissociation kinetic and colloid formation. *Water Res.* **37**, 3541-3550.
- Smedley P. L. and Kinniburgh D. G. (2002) A review of the source, behaviour and distribution of arsenic in natural waters. *Appl. Geochem.* **17**(5), 517-568.
- Steinmann P. and Shotykh W. (1997) Geochemistry, mineralogy, and geochemical mass balance on major elements in two peat bog profiles (Jura mountains, Switzerland). *Chem. Geol.* **138**, 25-53.
- Sun X. H. and Doner H. E. (1998) Adsorption and oxidation of arsenite on goethite. *Soil Sci.* **163**(4), 278-287.
- Szramek K., Walter L. M., and McCall P. (2004) Arsenic mobility in groundwater/surface water systems in carbonate-rich Pleistocene glacial drift aquifers (Michigan). *Appl. Geochem.* **19**(7), 1137-1155.
- Tadanier C. J., Schreiber M. E., and Roller J. W. (2005) Arsenic mobilization through microbially mediated deflocculation of ferrihydrite. *Environ. Sci. Technol.* **39**(9), 3061-3068.
- Tamura H., Goto K., Yotsuyan.T, and Nagayama M. (1974) Spectrophotometric Determination of Iron(II) with 1,10-Phenanthroline in Presence of Large Amounts of Iron(III). *Talanta* **21**(4), 314-318.
- Thanabalasingam P. and Pickering W. F. (1986) Arsenic Sorption by Humic Acids. *Environ. Pollut.* **12**(3), 233-246.
- Tiller C. L. and O'Melia C. R. (1993) Natural organic matter and colloidal stability: Models and measurements. *Colloids Surf., A* **73**, 89-102.
- Tipping E. (1994) WHAM - A chemical equilibrium model and computer code for water, sediments, and soils incorporating a discrete/electrostatic model of ion-binding humic substances. *Computer Geosciences* **20**, 973-1023.
- Tipping E. and Hurley M. A. (1992) A unifying model of cation binding by humic substances. *Geochim. Cosmochim. Acta* **56**, 3627-3641.
- Tipping E., Rey-Castro C., Bryan S. E., and Hamilton-Raylor J. (2002) Al(III) and Fe(III) binding by humic substances in freshwaters, and implications for trace metal speciation. *Geochim. Cosmochim. Acta* **66**(18), 3211-3224.

Supporting Information

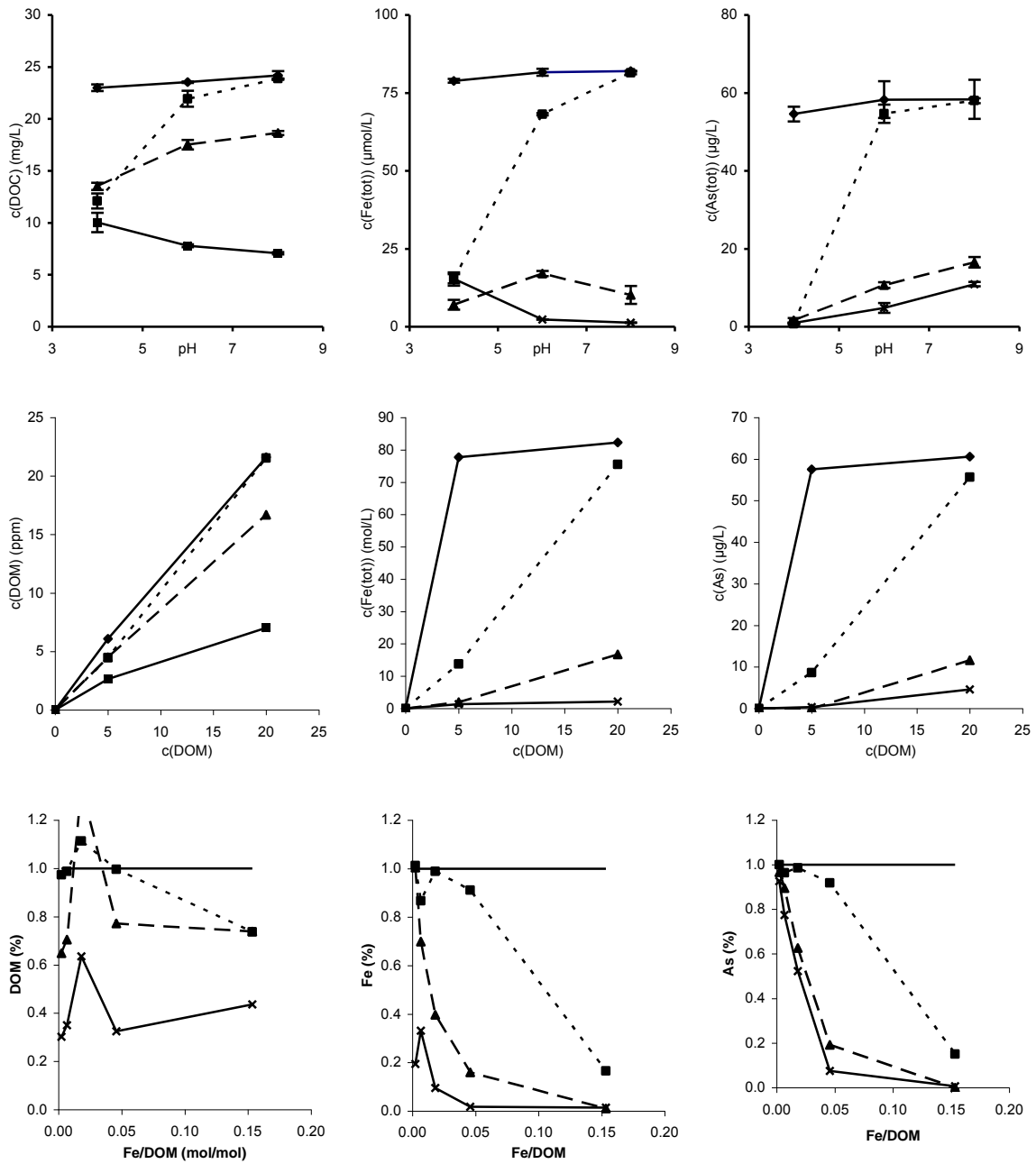


Figure 36 Dependence of compound formation on pH, (top), C concentration (middle) and Fe/C ratio(bottom) in SRDOM solution.

Study 5

Reproduced with permission from

**Evidence for the Aquatic binding of Arsenate by Natural Organic Matter-
Suspended Fe(III)**

Kaylene Ritter, George R. Aiken, James F. Ranville, Markus Bauer and Donald L. Macalady

Environmental Science & Technology, 2006, 40, pp 5380–5387

Copyright 2006 American Chemical Society

Evidence for the Aquatic Binding of Arsenate by Natural Organic Matter—Suspended Fe(III)

KAYLENE RITTER,[†] GEORGE, R. AIKEN,[‡] JAMES F. RANVILLE,[†] MARKUS BAUER,^{†,§} AND DONALD L. MACALADY^{*,†}

Department of Chemistry and Geochemistry, Colorado School of Mines, Golden, Colorado, and U.S. Geological Survey, Water Resources Discipline, Boulder, Colorado

Dialysis experiments with arsenate and three different NOM samples amended with Fe(III) showed evidence confirming the formation of aquatic arsenate–Fe(III)–NOM associations. A linear relationship was observed between the amount of complexed arsenate and the Fe(III) content of the NOM. The dialysis results were consistent with complex formation through ferric iron cations acting as bridges between the negatively charged arsenate and NOM functional groups and/or a more colloidal association, in which the arsenate is bound by suspended Fe(III)–NOM colloids. Sequential filtration experiments confirmed that a significant proportion of the iron present at all Fe/C ratios used in the dialysis experiments was colloidal in nature. These colloids may include larger NOM species that are coagulated by the presence of chelated Fe(III) and/or NOM-stabilized ferric (oxy)hydroxide colloids, and thus, the solution-phase arsenate–Fe(III)–NOM associations are at least partially colloidal in nature.

Introduction

Arsenic is a toxic substance and a carcinogen threatening the drinking water of millions within the United States and around the world (1–3). Hence, understanding the factors influencing its aqueous concentration and mobility is an issue of current concern. An important control on arsenic mobility in natural systems is adsorption to iron and other metal (oxy)hydroxides (4–8). Natural organic matter (NOM) is ubiquitous to aquatic systems, including those affected by arsenic. Arising from the decomposition of biomass, it is a complex material possessing carboxylic, amino, nitroso, sulfhydryl, hydroxyl, and phenolic moieties (9–11). It has recently been shown that natural organic matter can influence arsenic adsorption to iron oxides (12, 13). It was found that NOM competes with arsenic for adsorption to iron oxide surfaces (12, 13) and possibly forms aquatic associations with arsenic (12). The net result of both of these processes, the latter of which being the focus of this study, is higher concentrations and greater mobility of arsenic in aquatic systems.

Arsenic has two oxidation states relevant to natural environments and is typically present as either arsenite or

arsenate, depending upon redox conditions. Arsenite, with pK_a 's of 9.2, 12.1, and 13.4, exists as a neutral species in most natural systems. Arsenate has pK_a 's of 2.2, 6.9, and 11.5 and thus takes the form of $H_2AsO_4^-$ and/or $HAsO_4^{2-}$ in waters of circum-neutral pH (14). The suggestion that arsenate and NOM form aquatic complexes is hence somewhat surprising, as NOM functional groups are also predominantly negatively charged at circum-neutral pH (9 and refs therein). However, it has been suggested that natural organic matter may associate with anions in solution through bridging mechanisms. The solubilities of transition metal cations such as Fe(III) increase significantly due to complexation with NOM functional groups, such as carboxyls (15–17). Thanabalasingam and Pickering (18) proposed that these cations could then link negatively charged NOM functional groups and inorganic anions in tertiary complexes. Warwick et al. (19) provide some evidence for aquatic binding of arsenic by organic matter through ultrafiltration experiments. Lin et al. (20) report to have identified arsenate–cation–NOM complexes through dialysis experiments. Though interesting, their results cannot be exclusively attributed to the formation of As–organic matter associations, as the observed arsenic behavior could also be explained by inorganic associations involving dissolved cations present in their system.

Iron and NOM are also known to form colloidal associations, in which the NOM is coagulated by chelating iron cations and/or NOM molecules bind and suspend iron (oxyhydr)oxide colloids in solution (21–27). NOM–Fe colloids have been reported to be 50–100 nm in diameter (21) and hence are considered to be within the dissolved phase, as defined by filtration at 0.45 μ m. The iron in these suspended colloids could then provide binding sites for oxyanions such as arsenate. The result for arsenate would then be stable, colloidal As–Fe–NOM associations that may involve As bridging with chelated Fe(III) cations and/or (oxy)hydroxide surface complexation. It has been suggested that such NOM-suspended iron colloidal associations occur with phosphate (28), and hence they might also occur with arsenate.

There are many implications of the formation of aquatic associations between arsenate and Fe-bearing NOM. Aside from resulting in greater arsenic concentrations and mobility than would be otherwise predicted in oxide-sorption controlled systems, such associations may influence the bioavailability of arsenic (29). Further, there are possible deleterious implications for arsenic treatment processes that are based on the removal of arsenic through adsorption/coprecipitation with iron (and/or aluminum) oxides. We hypothesized that arsenate does form aquatic associations with NOM, occurring via one or both of the discussed mechanisms involving ferric iron. Accordingly, the purpose of this work was to investigate the formation of aquatic associations between arsenate and NOM, and the role of NOM-suspended Fe(III) in such complexes, through dialysis experiments.

Experimental Section

NOM Samples. Three different natural organic matter samples were employed: a Suwannee River (SR-WW) whole water, the hydrophobic acid fraction of a Suwannee River water sample (SR-HPOA), and the fulvic acid fraction of a water sample collected in the Everglades (EG-FA). The SR-WW NOM sample, originating from the outlet of the Okefenokee Swamp in Georgia, was collected in April 2002 and was stored in the dark at 4 °C until use. The SR-HPOA and EG-FA water samples were collected and the fractions isolated in 1995 and 1997, respectively. HPOA consists of

* Corresponding author. Phone: (303)273-3610. Fax: (303)273-3629. E-mail: dmacalad@mines.edu.

[†] Colorado School of Mines.

[‡] U.S. Geological Survey.

[§] Permanent address: Limnological Research Station and Department of Hydrology, University of Bayreuth, D-95444 Bayreuth, Germany.

TABLE 1. Characteristics of the Natural Organic Matter Solutions

NOM	molecular weight (Da)	specific UV absorption (L cm ⁻¹ (mg C) ⁻¹)	Fe (μg/L)
SR-HPOA	810	0.044	280
SR-WW	710	0.038	500
EG-FA	700	0.040	(bdl)

TABLE 2. Other Inorganic Constituents of the Natural Organic Matter Samples Present in the Original NOM Solutions (and in the Dialysis Bags after Equilibration)^{a,b,c}

NOM	Al	Ca	Cu	Mg	Mn	S	Zn
SR-HPOA	bdl (bdl)	31.0 (9.32)	24.2 (bdl)	74.8 (2.47)	bdl (bdl)	61.9 (bdl)	5.37 (bdl)
SR-WW	72.3 (37.3)	94.2 (4.68)	bdl (bdl)	73.8 (bdl)	bdl (bdl)	248 (bdl)	5.77 (bdl)
EG-FA	bdl (bdl)	75.8 (23.7)	bdl (bdl)	42.8 (bdl)	bdl (bdl)	135 (bdl)	2.80 (bdl)

^a All values are in μg/L. ^b bdl = below detection limit. ^c Detection limits in μg/L: Al = 29.6; Ca = 3.40; Cu = 4.70; Mg = 1.57; Mn = 0.759; S = 46.1; Zn = 2.62.

90–95% fulvic acid and 5–10% humic acid, and the HPOA and FA fractions were prepared according to the method described by Aiken et al. (30). The whole water sample, SR-WW, was not subject to any fractionation or treatment, other than filtering at 0.45 μm immediately prior to use. The NOMs were characterized according to their molecular weight, specific UV absorption (SUVA) at 254 nm, acidity, and metals content (Tables 1 and 2).

NOM Characterization. SUVA values of the three NOMs were determined by dividing their UV absorbance at 254 nm, measured with a Hatch DR/4000U spectrophotometer, by the dissolved organic carbon (DOC) concentration (31). Molecular weights of the NOMs used in this study were obtained by size exclusion chromatography, using a Superdex peptide column (Amersham Pharmacia Biotech), which separates compounds within the approximate MW range of 7–0.1 kDa, coupled to a UV detector set to 254 nm (Dionex), according to the method described by Jackson et al. (32).

Reagents. Arsenate stock solutions were made from reagent grade sodium arsenate and adjusted to pH 6 using 0.1 M HNO₃. Fe(III) stock solutions for the dialysis experiments were made with reagent grade Fe(NO₃)₃·9H₂O and acidified to pH 2 with 1 M HNO₃. High-purity (18 MΩ) deionized water was used throughout.

Analyses. Arsenic analyses were performed with a Perkin-Elmer Analyst 800 graphite furnace atomic absorption (GF-AAS) spectrometer, with a detection limit of 4 μg/L As (0.05 μM As). Dissolved organic carbon was determined using a Sievers total organic carbon analyzer, model 800, with a detection limit of 80 μg/L (6.67 μM) organic carbon. Total iron and other metals content of the NOM solutions were measured employing a Perkin-Elmer Optima 4300DV ion-coupled plasma atomic emission spectrometer (ICP-AES), with a total iron detection limit of 4 μg/L (0.07 μM). The detection limits of other relevant metals are given in the text. All samples were stored at 4 °C in the dark and were analyzed for As, DOC, and metals within 1 week of sampling.

Dialysis Experiments. Comparable to dialysis studies by Van Loon et al. (33) for characterizing radionuclide–NOM complexes, the aquatic binding of arsenate by Fe-bearing NOM was identified through arsenate concentration differences across a dialysis membrane. Ideally, the membrane is chosen such that its pore size allows the passage of arsenate anions but not of the larger NOM or As(V)–Fe(III)–NOM complexes. Hence, in experiments in which dialysis bags are

filled with iron-amended NOM solutions and surrounded by an electrolyte solution spiked with arsenate, after a period of equilibration, the formation of As(V)–Fe(III)–NOM associations is indicated by higher total arsenic concentrations inside (arsenate anions + As(V)–Fe(III)–NOM complexes) than outside (arsenate anions only) the dialysis bags.

Arsenate–Fe(III)–NOM Experiments. The dialysis experiments were conducted with Spectra-Por CE (cellulose ester) 1000 molecular weight cutoff (MWCO) dialysis membranes. This pore size was chosen based on arsenate kinetics experiments (described below) because it allowed As equilibration within a reasonable time period, while minimizing NOM bleed through the membrane. All experiments were undertaken at pH 6, 10 mM NaNO₃. Acid-cleaned, autoclaved 125 mL borosilicate glass jars with Teflon-lined caps were filled with 95 mL of the 10 mM NaNO₃, pH 6 solution. Dialysis bags to be placed in the jars were filled with 5 mL of the appropriate NOM solution and were sealed by tying knots.

The NOM-filled dialysis bags were prerinsed in pH 6, 10 mM NaNO₃ solutions for 1 week. In recognition of the large membrane pore size relative to the MWs of the NOMs (Table 1), the purpose of the prerinse was to flush out smaller NOM molecules, thereby avoiding excessive leaching during the course of the experiments. The rinsing solutions were sampled for DOC for mass balance purposes. For consistency, the dialysis bags containing control solutions (no NOM) were also prerinsed.

After completion of the 1 week prerinse, the dialysis bags were placed in the jars. The electrolyte solution in the jars was then spiked with the arsenate stock, resulting in a concentration outside the bags of 90 μg/L (1.2 μM) arsenate in the case of initial SR-HPOA experiments or 720 μg/L (9.6 μM) arsenate for all subsequent experiments. After a 2 week equilibration period, aliquots were taken from the solutions in the jars and in the dialysis bags. These were analyzed for total arsenic, DOC, total iron, and metal content. The 2 week equilibration period was determined based on the kinetics experiments described below.

Preparation of NOM and Fe(III)-Amended NOM Solutions. The SR-HPOA and EG-FA solutions were made by dissolving 10 mg of the freeze-dried material into 100 mL of water, resulting in a concentration of 100 mg NOM/L (or ~50 mg C/L; 4.2 mM C) and were filtered at 0.45 μm. The SR-WW sample (60 mg C/L; 5 mM C) was also filtered at 0.45 μm. All three NOMs were adjusted to pH 6 with 0.1 M HNO₃ and/or 0.1 M NaOH. Note that while iron was below detection in the EG-FA NOM, both the SR-HPOA and the SR-WW had inherent iron contents (Table 1), and all iron concentrations reported henceforth refer to total iron (inherent + added). To make the Fe(III)-amended NOM solutions, the NOM solutions were spiked with the Fe(III) stock solution. In the case of the initial SR-HPOA studies conducted with 90 μg/L (1.2 μM) arsenate, the SR-HPOA was spiked to make 1 mg/L (0.02 mM) Fe(III). The solution was allowed to equilibrate for 24 h, filtered again at 0.45 μm, and the pH readjusted to 6. The second filtration step removed some of the added Fe(III). A portion of the Fe(III) was also leached during the 1 week prerinse period (presumably iron that was associated with bled NOM), resulting in final Fe(III) concentrations measured in the dialysis bags upon completion of the experiment of 0.6 mg/L (0.01 mM) Fe(III). Following the same procedure, the Fe(III)-amended EG-FA and SR-WW NOM solutions used in the experiments with 720 μg/L (9.6 μM) arsenate were spiked to make 5 mg/L (0.09 mM) Fe(III). Filtering removed approximately 1 mg/L (0.020 mM) Fe(III) from the amended EG-FA and 0.5 mg/L (0.009 mM) Fe(III) from the amended SR-WW solution. The final solutions in the dialysis compartments were approximately 2 mg/L (0.04 mM) Fe(III).

Experiments were also undertaken with solutions of SR-HPOA and 720 $\mu\text{g/L}$ arsenate with incremental amounts of Fe(III), in which the final concentrations measured in the dialysis bags were 0.3 mg/L (0.005 mM), 2.4 mg/L (0.04 mM), 6.1 mg/L (0.1 mM), and 11.6 mg/L (0.21 mM) Fe. Ferric iron control experiments (no NOM) were conducted with solutions of Fe(III) prepared following the same procedure (pH 6, 10 mM NaNO_3 , 0.45 μm filtered), with and without spiking with arsenate. Other control experiments included the pH 6, 10 mM NaNO_3 electrolyte solution in the jar and bag, not spiked with arsenate, 10 mM NaNO_3 in the jar and bag and spiked with arsenate, and NOM in the bag, 10 mM NaNO_3 in the jar, not spiked with arsenate. No attempt was made to keep solutions from laboratory light.

It is noted that NOM, Fe, and As(V) are both abiotically and bacterially mediated redox active (13, 34 and refs therein). Hence, even though the solutions were initially oxygenated and exposed to the atmosphere during the experiments, it is possible that a small fraction of the iron and arsenic initially added as ferric iron and arsenate may have been reduced to arsenite and ferrous iron. However, this does not detract from the validity of the experimental method nor the evidence they provide for the aquatic interactions under study; it simply means that a fraction of the arsenic and/or iron involved in the aquatic interactions may have been present in reduced form.

Arsenate Kinetics Dialysis Experiments. The purpose of the kinetics experiments, conducted with 500, 1000, 2000, and 3500 MWCO Spectra-Por CE membranes, was to select an appropriate MWCO membrane for use in the NOM–arsenate and NOM–arsenate–Fe(III) experiments and establish the time required to reach arsenic equilibrium across the dialysis membrane. A similar procedure was followed as described above, except the dialysis bags were filled with the electrolyte solution (10 mM NaNO_3 , pH 6) rather than NOM, and sampling occurred on an hourly, daily, and weekly basis, up to a total period of 1 month.

With the exception of the arsenic kinetics and preliminary SR-HPOA experiments, which were conducted in duplicate, all experiments were conducted in triplicate, with error bars depicting 1 standard deviation from the mean. The error bars for the kinetics experiments represent the range of the data, and individual replicate data are shown for the initial SR-HPOA experiments, with the error bars showing 1 standard deviation of triplicate instrument analyses.

Fe(III)-Amended NOM Sequential Filtration Experiments. To ascertain the nature of the ferric iron amended to the NOM solutions (colloidal vs noncolloidal chelated cations), sequential filtration experiments were conducted with the SR-WW NOM at two different dilutions: 10 mg C/L (0.08 mM C) and 40 mg C/L (3.3 mM C). The SR-WW NOM was diluted from its original concentration of 60 mg C/L (5 mM C). The samples were spiked with the stock solution to make 5.5 mg/L (0.1 mM) Fe and 0.28 mg/L (0.005 mM) Fe. The pH was adjusted to 6 with NaOH. The samples were allowed to equilibrate for 5 h. Aliquots were then taken and filtered at 0.45 μm and then at 0.1 μm . Prior to filtering, and after each filtering step, samples were taken for analysis of total iron.

Results and Discussion

Arsenate Kinetics Dialysis Experiments. It was found that an equilibration time of 2 weeks was required to reach $[\text{arsenate}]_{\text{bag}} = [\text{arsenate}]_{\text{jar}}$ for the Spectra-Por CE 1000 MWCO dialysis membrane (Figure 1A), and this membrane pore size was chosen for use in the arsenate–NOM experiments. Equilibrium was not reached with the 500 MWCO membrane after 1 month, and hence it was not suitable for the intended experiments. The 2000 and 3500 MW membranes reached equilibrium in a slightly shorter time than

the 1000 MWCO membrane. However, there was concern that these pore sizes would permit excessive passage of the NOM. The 2 week equilibration time required for the 1000 MWCO membrane and lack of equilibrium after 1 month with the 500 MWCO membrane, despite the small size of the arsenate oxyanion relative to the membrane pore dimensions, can be attributed to electrostatic effects. The rate of diffusion of across Spectra-Por CE membranes decreases with increasing negative charge on the species, presumably due to repulsion between the diffusing anion and negatively charged membrane surface groups (35).

Arsenate–NOM Aquatic Associations: Initial SR-HPOA Experiments. The results of the initial dialysis experiments conducted with SR-HPOA, 90 $\mu\text{g/L}$ (1.2 mM) arsenate, and 0.6 mg/L (0.01 mM) Fe(III) are summarized in Figure 1B. Arsenic equilibrium in the control experiments (no NOM) was reached in 2 weeks, as predicted by the kinetics experiments. In contrast, the concentration of arsenate in the dialysis bags containing SR-HPOA was approximately 6% greater than the concentration in the surrounding jar solution. Experiments in which the equilibration time was extended up to 4 weeks (data available upon request) showed no further mobilization of arsenate into the dialysis bags, indicating that, as with the arsenic-only experiments, the 2 week period was adequate to reach arsenic equilibrium in the presence of the NOM. There is also partitioning of the As(V) into the dialysis bags when the SR-HPOA was amended with Fe(III) for a total concentration of 0.6 mg/L (0.01 mM) Fe(III). Noting that the SR-HPOA has an inherent iron content of 280 $\mu\text{g/L}$ (5.1 μM) Fe (Table 1), and a final concentration measured in the dialysis bags of 80 $\mu\text{g/L}$ (1.5 μM) Fe, the results of these experiments were consistent with the aquatic binding of arsenate by NOM with ferric iron acting as an intermediary.

Formation of Arsenate–Fe(III)–NOM Aquatic Associations with EG-FA and SR-WW. Experiments were conducted with SR-WW and EG-FA to determine if the aquatic binding of arsenic would occur with a broader range of organic matter samples and to further evaluate the role of Fe(III). A higher arsenate concentration of 720 $\mu\text{g/L}$ (9.6 μM) arsenate was used, in anticipation of greater arsenate partitioning due to the higher levels of Fe(III) employed in these studies. It was found that elevated concentrations of arsenate in the dialysis bags relative to that of the surrounding solutions also occurred in the experiments conducted with SR-WW and EG-FA (Figure 2A). However, analysis of the bag and jar concentrations for EG-FA and SR-WW via a Student *t*-test revealed that, at the 95% confidence level, only the SR-WW bag and jar arsenate concentrations were statistically different, while the EG-FA data were not. The results were consistent with the importance of iron in the aquatic binding of arsenate by NOM, as the SR-WW had an inherent iron concentration of 500 $\mu\text{g/L}$ (9.1 μM) Fe and a final concentration in the dialysis bags of 100 $\mu\text{g/L}$ (1.8 μM) Fe, while Fe was below detection in the EG-FA sample (Table 1). Amending the NOMs with approximately 2 mg/L (0.04 mM) Fe(III) resulted in significantly more arsenate in the dialysis bags for both NOM samples, confirming the role of the transition metal in arsenate–NOM interactions (Figure 2B).

Arsenate mass balances were 100% ($\pm 8\%$) for the experiments with all three NOMs (Figure 3), with data shown for the iron-amended SR-WW and EG-FA experiments (~ 2 mg/Fe(III)), as well as for the SR-HPOA experiment with 2.5 mg/L (0.05 mM) Fe(III) that is discussed below. The DOC mass balances were 100% ($\pm 10\%$) and show that the 1 week pre-rinse successfully flushed out a significant portion of the smaller NOM molecules, which amounted to roughly 35–50% of the total initial DOC. A further 12–20% of the initial DOC concentration passed through the bags to the surrounding jar solution during the course of the 2 week

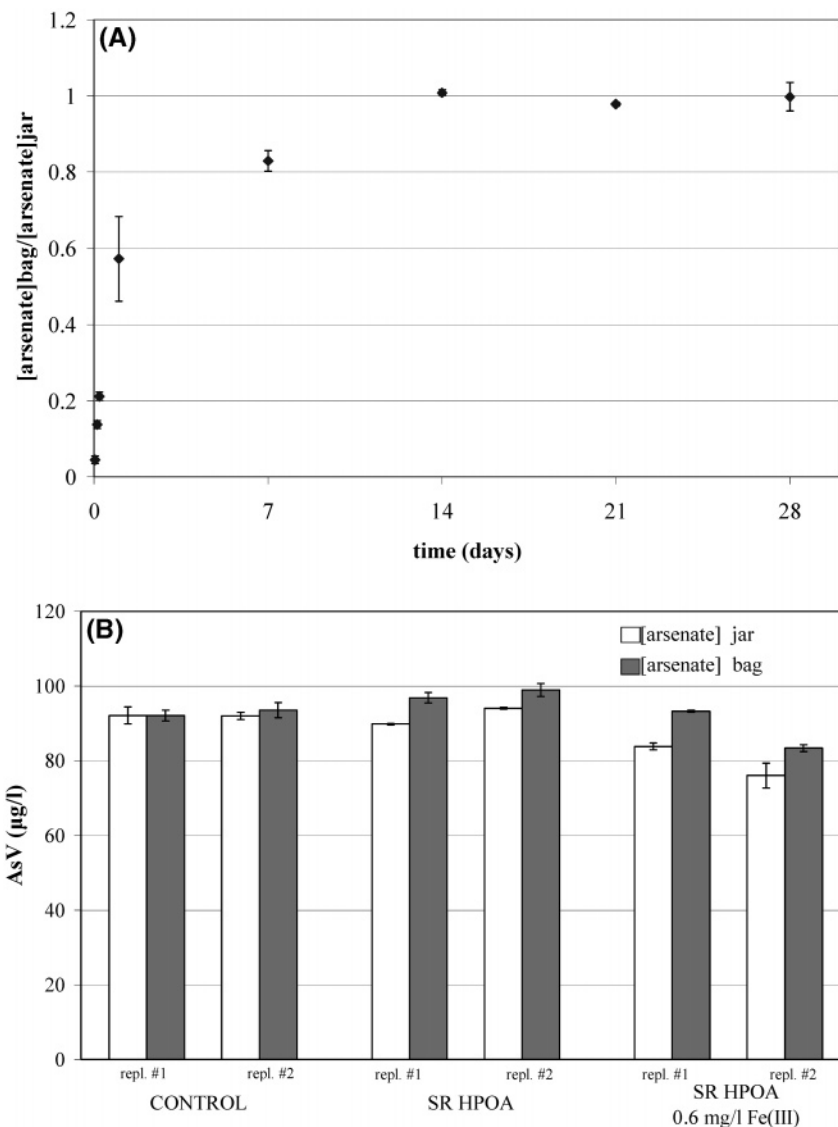


FIGURE 1. (A) Diffusion kinetics of arsenate for the 1000 MWCO Spectra-Por CE dialysis membrane. Fourteen days were required to reach $[\text{arsenate}]_{\text{bag}} = [\text{arsenate}]_{\text{jar}}$. The error bars show the range of data. (B) The results of dialysis experiments conducted with SR-HPOA, 90 $\mu\text{g/L}$ arsenate, and 0.6 mg/L Fe.

equilibration period (Figure 4A). Hence, the prerinsing effectively minimized the amount of leaching that occurred during the 2 week equilibration period, and the leaching that did occur was not significant enough to inhibit the experiments. Final NOM concentrations in the dialysis bags were approximately 20 mg C/L (1.7 mM C), and 0.3 mg C/L (0.03 mM C) in the jars (Figure 4A). The Fe(III) mass balances show that there were low levels of iron measured in the jars at the completion of the 2 week equilibration period (SR-HPOA = 24 ± 10 , EG-FA = 13 ± 8 , and SR-WW = 42 ± 16 ppb). However, these values are within experimental uncertainty of the iron level in the jar blank of 19 ± 9 ppb (no iron, no As(V), no NOM added) and, hence, are comprised mainly iron from the background electrolyte, only a small fraction resulting from leakage from the dialysis bags during the course of the experiments (Figure 4B). While the presence of low levels of both iron and NOM in the jars may have resulted in the binding of a small fraction of the arsenate outside of the dialysis bags (rather than inside as intended), this would have had only a minimal effect on the experiments. The average Fe(III) content of the jars was $0.05 \mu\text{mol}$ of Fe(III), assuming the iron was complexed to NOM, and on the basis of the relationship between iron concentration and

complexed arsenate given below, this would result in a maximum of $0.009 \mu\text{mol}$ of arsenate bound by Fe(III)-NOM, or 1% of the average arsenate content of the jars of $0.84 \mu\text{mol}$ of As. The worst case scenario, with SR-WW, assuming a jar Fe(III) level 1 standard deviation above the mean would involve less than 3% error.

Complexation of Arsenate by HPOA Amended with Incremental Levels of Fe(III). The importance of Fe(III) in the aquatic association of arsenate with NOM was further delineated when experiments were conducted with SR-HPOA to which was added incremental amounts of Fe(III). Figure 5 shows that within the wide range of iron concentrations used here, there was a strong linear relationship ($r^2 = 0.97$) between the total Fe(III) content of the NOM and the amount of complexed arsenate. Figure 5 includes data from the Fe-amended EG-FA and SR-WW NOM experiments. These combined results strongly indicate that it is the iron content of the NOM that is critical to its ability to bind arsenate, with little evidence to support aquatic interactions of arsenate with NOM that do not involve iron. Instead, the lack of aquatic interactions between arsenate and EG-FA (iron below detection), and the fact that the linear relationship shown in Figure 4 passes near the origin, both suggest that

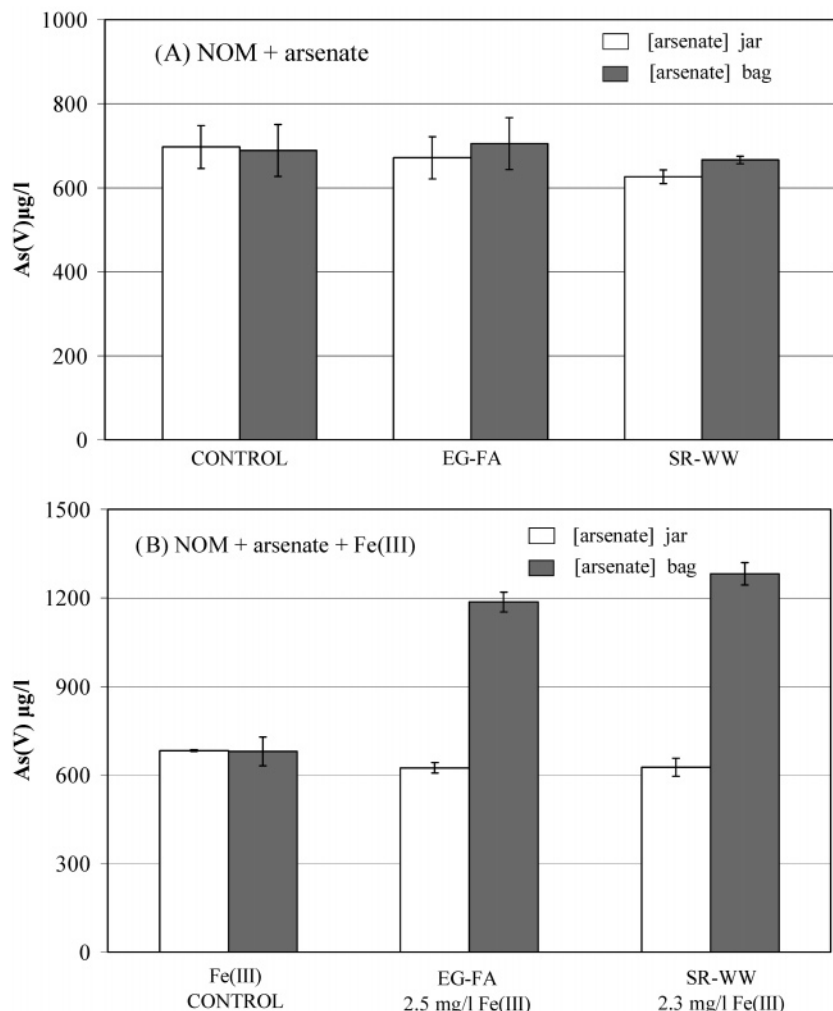


FIGURE 2. (A) Results of dialysis experiments with EG-FA and SR-WW, showing an increase in arsenate in the bag relative to that of the solution in the jar when NOM was in the bag. Control = no NOM. (B) Effect of amending the NOMs with Fe(III). Fe(III) control = Fe(III) in the dialysis bag but no NOM (the initial solution was 5 mg/L Fe(III), but the final concentration in the bag was much lower, see Figure 5).

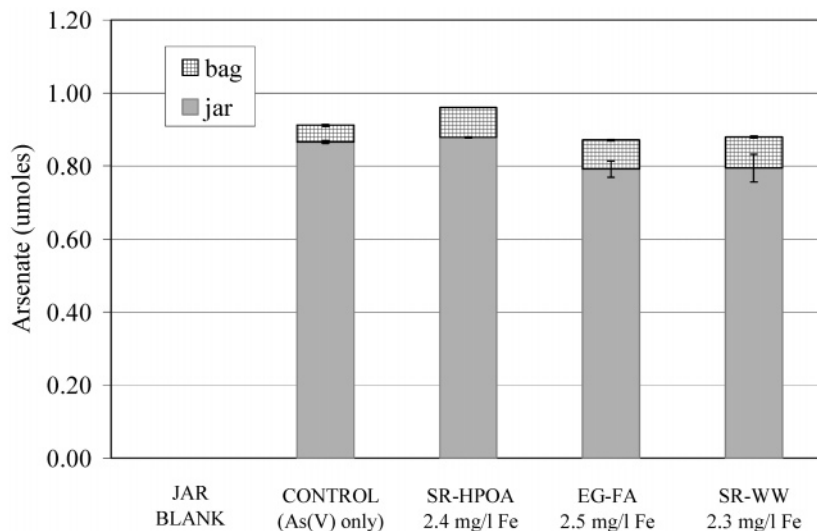


FIGURE 3. Arsenate mass balance for the dialysis experiments conducted with the three NOMs and ~ 2 mg/L Fe(III). The total arsenate added was $0.96 \mu\text{mol}$. Control = no NOM. The jar blank = no added arsenate, Fe(III), or NOM and no dialysis bag.

aquatic interactions of arsenate and NOM are not significant in the absence of iron.

The possibility that the increased concentration of arsenate measured in the dialysis bags was due to the formation

of inorganic Fe(III)–arsenate associations is largely discounted by the results obtained in the control experiments. In the Fe(III) controls (no NOM), no increase in arsenic in the dialysis bags occurred relative to that of the surrounding

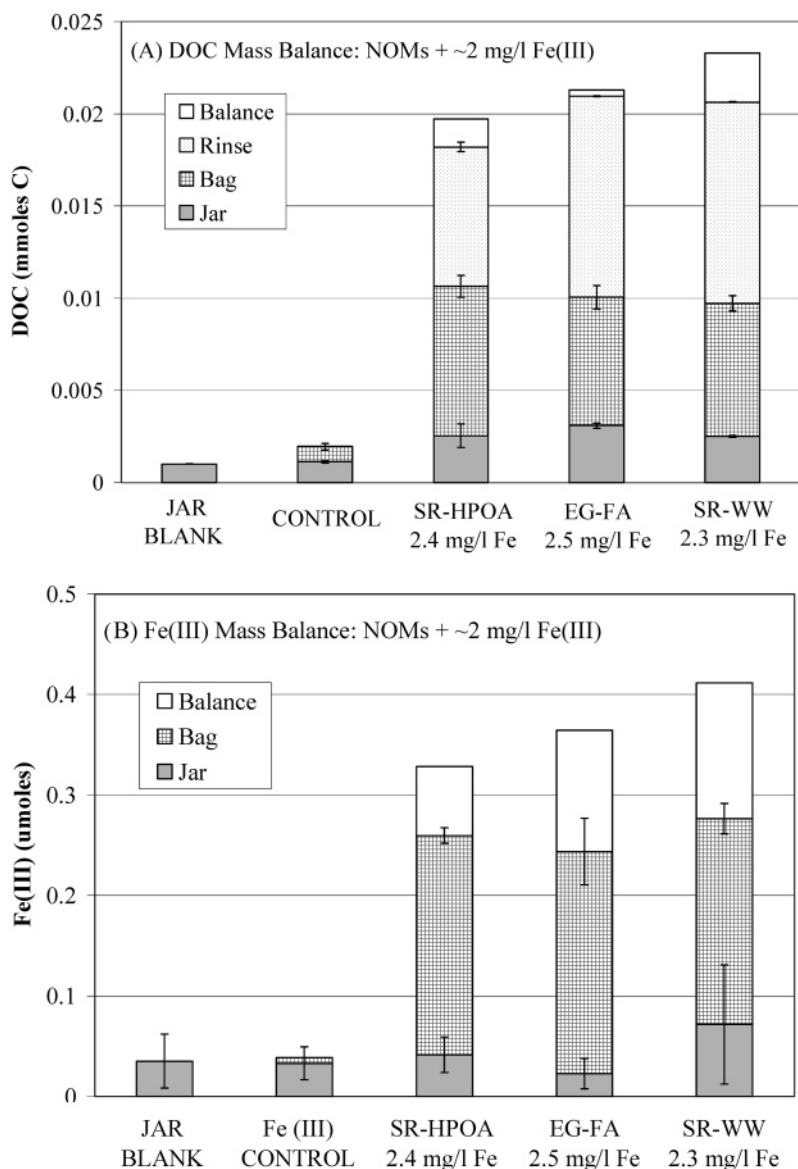


FIGURE 4. (A) DOC mass balance for the dialysis experiments conducted with the three NOMs and ~2 mg/L Fe(III). Control = no NOM. (B) Fe(III) mass balance for the same experiments. Fe(III) control = no NOM and an initial solution of 5 mg/L Fe(III). The balance of the Fe(III) is assumed to have leached from the bags during the 1 week prerinse, presumably associated with the smaller NOM molecules that were also flushed from the bags during the prerinse. For both graphs, the jar blank = no added arsenate, Fe(III), or NOM and no dialysis bag.

solution (Figure 2). When the control solutions were made, there was visible iron precipitation upon adjusting the pH to 6, consistent with the low solubility of ferric iron above pH 3.5 (36 and refs therein). Subsequent filtration at 0.45 μm then removed most of the Fe(III) from solution, as indicated by the total Fe measured in solution (Figure 4B). Hence, at the pH of these experiments, and in the absence of NOM, dissolved Fe(III) is largely absent from the solution phase, and as such, inorganic Fe(III)–arsenate cannot account for the observed aquatic complexation of arsenate. Instead, the data are interpreted as follows: the NOM served to suspend the added Fe(III) in solution, through the formation of noncolloidal NOM–Fe complexes and/or through colloidal Fe(III)–NOM interactions. The NOM-suspended iron then served as binding sites for the arsenate, resulting in the formation of dissolved, noncolloidal As(V)–Fe(III) cation–NOM complexes and/or NOM-suspended Fe(III)–arsenate colloidal associations. Hence, both the NOM and the Fe(III) have a critical role to play, and both are necessary compo-

nents for the aquatic binding of arsenic observed in our system.

Nature of the Arsenate–Fe(III)–NOM Association. Sequential filtration experiments revealed that even at the lowest molar ratio of Fe/C of 0.001, 23% of the dissolved iron (i.e., iron in solution after filtration at 0.45 μm) was present as colloids between the size range of 0.1 and 0.45 μm (Table 3). Note that the total fraction of colloidal iron may have been even larger, due to the possible presence of colloids smaller than 0.1 μm in diameter. At the upper Fe/C molar ratio of 0.12, upward of 84% of the dissolved iron was present within the 0.1 and 0.45 μm size fraction. Hence, while the possible presence of noncolloidal ferric cations chelated to NOM molecules cannot be discounted in our system, a significant proportion of the iron is colloidal at all Fe/C ratios. The suspension of colloidal iron by NOM has been demonstrated by numerous authors, including Pullin and Cabaniss (21), who showed that at an Fe/C ratio of 0.024, roughly 35% of the Fe(III) suspended by a Suwannee

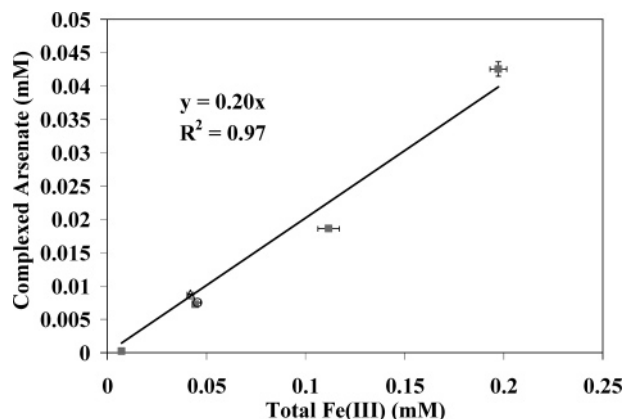


FIGURE 5. Complexed arsenate concentration in the dialysis bags as a function of the Fe(III) content of SR-HPOA (squares). For comparison, the EG-FA + 2.5 mg/L Fe (open circle) and the SR-WW + 2.3 mg/L Fe (open triangle) are also plotted.

TABLE 3. Results of the Sequential Filtration Experiment with SR-WW at Two Different Dilutions (10 and 40 mg C/L) and Two Different Concentrations of Amended Ferric Iron (0.1 and 0.005 mM Fe(III))^a

organic matter content	Initial Amount of Iron Added: 100 μ M Fe(III) Fe(III) measured in solution (μ M)				% of Fe(III) filtered between 0.45 and 0.1 μ m
	unfiltered	0.45 μ m	0.1 μ m	Fe/C mol ratio	
0 mg C/L	66.1	0.18	0		
10 mg C/L	82.9	61.0	9.75	0.12	84
40 mg C/L	82.9	73.4	36.4	0.03	50

organic matter content	Initial Amount of Iron Added: 5 μ M Fe(III) Fe(III) measured in solution (μ M)				% of Fe(III) filtered between 0.45 and 0.1 μ m
	unfiltered	0.45 μ m	0.1 μ m	Fe/C mol ratio	
0 mg C/L	1.86	0.32	0.11		
10 mg C/L	3.79	3.43	2.39	0.006	30
40 mg C/L	4.89	4.00	3.07	0.001	23

^a n = 1.

River fulvic acid NOM sample was present in the colloidal size range.

Dzombak and Morel (37) summarize data showing that ferrihydrite colloids at pH's near 6 have densities of type 2 surface sites capable of complexing cations, oxyanions such as arsenate, and neutral species such as arsenite, in the range of 0.1–0.2 mol of sorption sites/total mol of Fe. The slope of the graph shown in Figure 5 is 0.2. Hence, our data are consistent with arsenate binding through adsorption to NOM-suspended iron oxide colloids, if it is assumed that all of the iron in the system is present as ferrihydrite colloids and that all available iron surface sites are occupied by arsenic. While this is possible, it is not likely, as a fraction of the sites would be by necessity occupied by NOM moieties suspending the colloids, and it is likely that at least a small percentage of the iron in our system is not colloidal. Alternate forms of As–Fe–NOM interactions are also consistent with our results. Clearly, a significant fraction of the iron is colloidal. However, the issue of whether these colloids are dominantly NOM-stabilized (oxy)hydroxides or formed by Fe(III)-induced coagulation of NOM is unresolved, and the constancy of the ratio of complexed arsenate to iron through a wide range of

iron concentrations (Figure 5) suggests that the latter may be more important in our system. If this is the case, then arsenate chelation by ferric cations entrained within the coagulated NOM may be the dominant arsenate binding mechanism.

While the exact nature of arsenic binding by NOM-suspended Fe(III) is not yet fully characterized, and is worthy of further study, the results of this work are nonetheless striking, as they have clearly established the formation of aquatic complexes between arsenate and natural organic matter. The work has further shown the critical role that ferric iron plays in the aquatic association and the importance of stable colloidal moieties in these systems. The dominant effect of iron, independent of the NOM sample employed, suggests a broader role of Fe (and perhaps Al (38)) in other studies of binding of species such as arsenite (13) and Sb (39) to solution-phase NOM.

Acknowledgments

The assistance of Jarrod Gasper of the USGS with the dialysis experiments is gratefully acknowledged. Funding was provided by a Sussman Summer Internship, the American Water Resources Association (AWRA) Herbert Memorial Scholarship held by K. Ritter, and U.S. EPA Grant R82951501. Funding for Markus Bauer was provided by the German academic exchange service (DAAD). We also thank Robert W. Gillham for his support. Helpful comments from B. Voelker and the three anonymous reviewers are also appreciated.

Literature Cited

- (1) Comprehensive Environmental Response, Compensation, and Liability Act (CERCLA) Priority List of Hazardous Substances. <http://www.atsdr.cdc.gov/clist.html> (accessed 2003).
- (2) Smedley, P. L.; Kinniburgh, D. G. A review of the source, behaviour and distribution of arsenic in natural waters. *Appl. Geochem.* **2002**, *17*, 517–568.
- (3) Mandal, B. K.; Chowdhury, T. R.; Samanta, G.; Mukherjee, D. P.; Chanda, C. R.; Saha, K. C.; Chakraborti, D. Impact of safe water for drinking and cooking on five arsenic-affected families for 2 years in West Bengal, India. *Sci. Total Environ.* **1998**, *70*, 976–986.
- (4) Dixit, S.; Hering, J. G. Comparison of arsenic(V) and arsenic(III) sorption onto iron oxide minerals: Implications for arsenic mobility. *Environ. Sci. Technol.* **2003**, *37*, 4182–4189.
- (5) Appelo, C. A. J.; van der Weiden, M. J. J.; Tournassat, C.; Charlet, L. Surface complexation of ferrous iron and carbonate on ferrihydrite and the mobilization of arsenic. *Environ. Sci. Technol.* **2002**, *36*, 3096–3103.
- (6) Jain, A.; Loeppert, R. H. Effect of competing anions on the adsorption of arsenate and arsenite on ferrihydrite. *J. Environ. Qual.* **2000**, *29*, 1422–1430.
- (7) Goldberg, S.; Johnston, C. T. Mechanisms of arsenic adsorption on amorphous oxides evaluated using macroscopic measurements, vibrational spectroscopy, and surface complexation modeling. *J. Colloid Interface Sci.* **2001**, *234*, 204–216.
- (8) Manning, B. A.; Fendorf, S. E.; Goldberg, S. Surface structures and stability of arsenic(III) on goethite: Spectroscopic evidence for inner-sphere complexes. *Environ. Sci. Technol.* **1998**, *32*, 2383–2388.
- (9) Macalady, D. L.; Ranville, J. F. The chemistry and geochemistry of natural organic matter (NOM). In *Perspectives in Environmental Chemistry*; Macalady, D. L., Ed.; Oxford Press: New York, 1998.
- (10) Leenheer, J. A.; Wershaw, R. L.; Reddy, M. M. Strong-acid, carboxyl-group structures in fulvic acid from the Suwannee River, Georgia. 2. Major structures. *Environ. Sci. Technol.* **1995**, *29*, 399–405.
- (11) Aiken, G. R., McKnight, D. M., Wershaw, R. L., MacCarthy, P., Eds. *Humic Substances in Soil, Sediment, and Water*; Wiley-Interscience: New York, 1985.
- (12) Redman, A. D.; Macalady, D. L.; Ahmann, D. Natural organic matter affects arsenic speciation and sorption onto hematite. *Environ. Sci. Technol.* **2002**, *36*, 2889–2896.

- (13) Grafe, M.; Eick, M. J.; Grossl, P. R. Adsorption of arsenate (V) and Arsenite (III) on goethite in the presence and absence of dissolved organic carbon. *Soil. Sci. Soc. Am. J.* **2001**, *65*, 1680–1687.
- (14) Cullen, W. R.; Reimer, K. J. Arsenic speciation in the environment. *Chem. Rev.* **1989**, *89*, 713–764.
- (15) Weng, L.; Temminghoff, E. J. M.; Lofts, S.; Tipping, E.; Van Riemsdijk, W. H. Complexation with dissolved organic matter and solubility control of heavy metals in a sandy aquifer. *Environ. Sci. Technol.* **2002**, *36*, 4804–4810.
- (16) Donat, J. R.; Bruland, K. W. *Trace Elements in Natural Waters*; Salbu, B., Steinnes, E., Eds.; CRC Press: Boca Raton, FL, 1995.
- (17) Aiken, G. R.; Brown, P. A.; Noyes, T. I.; Pinckney, D. J. *Humic Substances in the Suwannee River, Georgia: Interactions, Properties, and Proposed Structures*; U.S. Geological Survey Open File Report 87-557; Averett, R. C., Leenheer, J. A., McKnight, D. M., Thorn, K. A., Eds.; U. S. Geological Survey: Denver, CO, 1989.
- (18) Thanabalasingam, P.; Pickering, W. F. Arsenic sorption by humic acids. *Environ. Pollut. Ser., B* **1986**, *12*, 233–246.
- (19) Warwick, P.; Inam, I.; Evancs, N. Arsenic's interaction with humic acid. *Environ. Chem.* **2005**, *2*, 119–124.
- (20) Lin, H.-T.; Wang, M. C.; Gwo-Chen, Li. Complexation of arsenate with humic substance in water extract of compost. *Chemosphere* **2004**, *56*, 1105–1112.
- (21) Pullin, M. J.; Cabaniss, S. E. The effects of pH, ionic strength, and iron–fulvic acid interactions on the kinetics of nonphotochemical iron transformations. I. Iron(II) oxidation and iron(III) colloid formation. *Geochim. Cosmochim. Acta* **2003**, *67*, 4067–4077.
- (22) Taillefert, M.; Lienemann, C.-P.; Gaillard, J.-F.; Perret, D. Speciation, reactivity, and cycling of Fe and Pb in a meromictic lake. *Geochim. Cosmochim. Acta* **2000**, *64*, 169–183.
- (23) Benedetti, M.; Ranville, J. F.; Ponthieu, M.; Pinheiro, J. P. Field-flow fractionation characterization and binding properties of particulate and colloidal organic matter from the Rio Amazon and Rio Negro. *Org. Geochem.* **2002**, *33*, 269–279.
- (24) Tipping, E.; Ohnstad, M. Colloid stability of iron oxide particles from a freshwater lake. *Nature* **1984**, *308*, 266–268.
- (25) Zhou, J. L.; Rowland, S.; Fauzi, R.; Mantoura, C.; Braven, J. The formation of humic coatings on mineral particles under simulated estuarine conditions—a mechanistic study. *Water Res.* **1994**, *28*, 571–579.
- (26) Perret, D.; Newman, M. E.; Negre, J.-C.; Buffle, J. Submicron particles in the Rhine River—I. Physicochemical characterization. *Water Res.* **1994**, *28*, 91–106.
- (27) Tessier, A.; Fortin, D.; Belzile, N.; De Vitre, R.; Leppard, G. G. Metal sorption to diagenetic iron and manganese oxyhydroxides and associated organic matter. Narrowing the gap between field and laboratory experiments. *Geochim. Cosmochim. Acta* **1996**, *60*, 387–404.
- (28) Shaw, P. J.; Jones, R. I.; De Haan, H. The influence of humic substances on the molecular weight distributions of phosphate and iron in epilimnetic lake waters. *Freshwater Biol.* **2000**, *45*, 383–393.
- (29) Anawar, H. M.; Akai, J.; Komaki, K.; Terao, H.; Yoshioka, T.; Ishizuka, T.; Safiullah, S.; Kato, K. Geochemical occurrence of arsenic in groundwater of Bangladesh: sources and mobilization processes. *J. Geochem. Explor.* **2003**, *77*, 109–131.
- (30) Aiken, G. R.; McKnight, D. M.; Thorn, K. A.; Thurman, E. M. Isolation of hydrophilic organic acids from water using nonionic macroporous resins. *Org. Geochem.* **1992**, *18*, 567–573.
- (31) Weishaar, J. L.; Aiken, G. R.; Bergamaschi, B. A.; Fram, M. S.; Fujii, R. Evaluation of specific ultraviolet absorbance as an indicator of the chemical composition and reactivity of dissolved organic carbon. *Environ. Sci. Technol.* **2003**, *37*, 4702–4708.
- (32) Jackson, B. P.; Ranville, R. F.; Bertsch, P. M.; Sowder, A. G. Characterization of colloidal and humic-bound Ni and U in the “dissolved” fraction of contaminated sediment extracts. *Environ. Sci. Technol.* **2005**, *39*, 2478–2485.
- (33) Van Loon, L. R.; Granacher, S.; Harduf, H. Equilibrium dialysis–ligand exchange: A novel method for determining conditional constants of radionuclide–humic acid complexes. *Anal. Chim. Acta* **1992**, *303*, 235–246.
- (34) Rose, A. L.; Waite, T. D. Reduction of organically complexed ferric iron by superoxide in a simulated natural water. *Environ. Sci. Technol.* **2005**, *39*, 2645–2650.
- (35) Haitzer, M.; Aiken, G. R.; Ryan, J. N. Binding of mercury(II) to dissolved organic matter: The role of the mercury-to-DOM concentration ratio. *Environ. Sci. Technol.* **2002**, *36*, 3564–3570.
- (36) Langmuir, D. *Aqueous Environmental Geochemistry*; Prentice Hall: Upper Saddle River, NJ, 1998.
- (37) Dzombak, D. A.; Morel, F. M. M. *Surface Complexation Modeling: Hydrous Ferric Oxide*; John Wiley and Sons: New York, 1990.
- (38) Pokrovsky, O.; Dupre, B.; Schott, J. Fe–Al–organic colloids control of trace elements in peat soil solutions: Results of ultrafiltration and dialysis. *Aquat. Geochem.* **2005**, *11*, 241–278.
- (39) Buschmann, J.; Sigg, L. Antimony(III) binding to humic substances: Influence of pH and type of humic acid. *Environ. Sci. Technol.* **2004**, *38*, 4535–4541.

Received for review September 29, 2005. Revised manuscript received April 25, 2006. Accepted May 4, 2006.

ES0519334

Study 6

Reproduced with permission from

**Mobilization of arsenic by dissolved organic matter from iron oxides, soils
and sediments**

Markus Bauer, Christian Blodau

Science of the total Environment, 2006, 345, pp 179-190

Copyright 2006 Elsevier B.V.



Mobilization of arsenic by dissolved organic matter from iron oxides, soils and sediments

Markus Bauer*, Christian Blodau

Limnological Research Station and Department of Hydrology, University of Bayreuth, D-95444 Bayreuth, Germany

Received 30 September 2004; accepted 26 January 2005
Available online 16 March 2005

Abstract

The arsenic contamination of aquifers has been linked to the input of dissolved organic matter (DOM). In light of this suggestion, the aim of this study was to quantify chemical effects of DOM on desorption and redox transformations of arsenic bound to synthetic iron oxide and natural samples from different geochemical environments (soils, shallow aquifer, lake sediment). In batch experiments, solutions containing 25–50 mg/L of two different types of DOM (purified peat humic acid and DOM from a peat drainage) were used as extractants in comparison to inorganic solutions. DOM solution was able to mobilize arsenic from all solid phases. Mobilization from iron oxides (maximum: 53.3%) was larger than from natural samples (maximum: 2.9%). The mobilization effect of extractants decreased in the order $\text{HCl} > \text{NaH}_2\text{PO}_4 > \text{DOM} > \text{NaNO}_3$. DOM solutions, therefore, mainly targeted weakly sorbed arsenic. Mobilization was complete within 24–36 h and DOM was sorbed during incubation indicating competition for sorption sites. The same patterns were observed for different DOM types and concentrations. Addition of DOM lead to (a) enhanced reduction (maximum 7.8%) and oxidation (6.4%) of arsenic in aqueous solution and (b) the appearance of arsenite in aqueous phase of soil samples (5.5%). As the primary mechanism for the arsenic release from solid phases we identified the competition between arsenic and organic anions for sorption sites, whereas redox reactions were probably of minor importance. The results of this study demonstrate that sorption of DOM has a strong potential to mobilize arsenic from soils and sediments.

© 2005 Elsevier B.V. All rights reserved.

Keywords: Arsenic; Dissolved organic matter; Iron oxide; Groundwater

1. Introduction

Arsenic is widely recognized as a dangerous contaminant and as a threat to some of the world's

water resources (Smedley and Kinniburgh, 2002). Problems with arsenic arise on a local scale related to mining or abandoned hazardous sites (Stueben et al., 2001) and on a regional scale, as in the aquifers of Bangladesh (Anawar et al., 2003). In natural waters, the oxyacids arsenite (H_3AsO_3 ; $\text{pK}_1=9.2$; uncharged at neutral pH) and arsenate (H_3AsO_4 ; $\text{pK}_1=2.2$; anionic at neutral pH) are the most important arsenic

* Corresponding author. Tel.: +49 921 552170; fax: +49 921 552366.

E-mail address: markus.bauer1@uni-bayreuth.de (M. Bauer).

species (Cullen and Reimer, 1989). Changes in speciation may be caused by abiotic reactions, for instance with MnO_2 (Chui and Hering, 2000) or H_2S (Rochette et al., 2000). Microorganisms can oxidize arsenite for detoxification (Cullen and Reimer, 1989) or reduce arsenate to arsenite during respiration (Newman et al., 1998). More reduced and organic species represent only a minor fraction of the total arsenic.

The mobility of arsenic is primarily determined by processes at mineral surfaces, particularly precipitation, dissolution, ad- and desorption. These processes are controlled by geochemical parameters such as pH, Eh, ionic composition, and mineral type (Bissen and Frimmel, 2003; Masscheleyn et al., 1991). At neutral pH and oxic conditions, arsenic is effectively immobilized by sorption or co-precipitated with metal oxides (Bissen and Frimmel, 2003; Smedley and Kinniburgh, 2002) involving surface complexation reactions and formation of specific inner sphere complexes (Sun and Doner, 1996). Low pH and reduced redox potential increase the mobility by dissolution of metal oxides. Under strongly reducing conditions the formation of sulfide minerals controls arsenic concentrations (Harvey and Swartz, 2002; Masscheleyn et al., 1991). Dissolved calcium enhances the sorption of arsenic, while in the presence of anions like phosphate and bicarbonate, arsenic sorption is reduced by competition for sorption sites (Appelo et al., 2002; Smith et al., 2002).

Dissolved organic matter, whose concentrations range from 1–20 mg/L in most fresh waters and reach higher values in wetlands (Abbt-Braun, 2002), may also influence arsenic mobility by several mechanisms. Fulvic or humic acids form stable complexes with mineral surfaces (Kaiser et al., 1997), effectively blocking arsenic from adsorption on iron oxides, alumina, quartz or kaolinite (Grafe et al., 2001; Grafe et al., 2002; Xu et al., 1991). Organic anions have consequently been found to enhance arsenic leaching from soil material (Lin et al., 2002), in which arsenic is mainly associated with the metal oxide fraction (Lombi et al., 2000), and also from fly ashes (Janos et al., 2002). A small but substantial increase of arsenic mobility was also found in wetland soils in the presence of high DOC concentrations (Kalbitz and Wennrich, 1998). The formation of aqueous arsenic/DOM complexes either by positively charged amino

groups in DOM (Saada et al., 2003) or by metal cation bridges (Redman et al., 2002) can additionally contribute to a higher mobility of arsenic. In some sediment layers of Bangladesh 10–30% of the arsenic present is associated with the solid organic phase (Anawar et al., 2003). Microbial degradation of organic matter in these sediments therefore contributes to reductive dissolution of metal oxides and release of arsenic bound in the oxides and in the organic phases as well (Harvey and Swartz, 2002). Moreover, DOM contains redox active functional groups and can thus act as an electron shuttle between microorganisms or H_2S and iron or organic pollutants (Lovley et al., 1996; Schwarzenbach et al., 1990). Accordingly, it has recently been demonstrated that the addition of arsenic to DOM solutions results in arsenate reduction as well as arsenite oxidation (Redman et al., 2002). Complexed metals are proposed to take part in these reactions. This observation is important because changes in speciation would influence the arsenic mobility.

Previous studies about chemical factors influencing arsenic mobility primarily focussed on competition of DOM and arsenic for sorption sites on synthetic minerals and often did not account for redox transformations. The objective of our study was thus to determine the abiotic effects of DOM on arsenic mobility by investigating both desorption and redox transformation in synthetic and natural soil samples. Specifically we were interested in (I) what fraction of arsenic desorbs from natural samples compared to synthetic iron oxides, such as goethite, and how DOM solutions compare to other extractants, (II) whether kinetics obtained with synthetic samples can be extrapolated to natural samples, and (III) whether DOM chemically oxidizes or reduces arsenic.

2. Materials and methods

2.1. Materials

Goethite was synthesized according to the method of Schwertmann and Cornell (1991) and examined with X-ray diffraction. The BET surface area of goethite (Goe) was $51 \text{ m}^2/\text{g}$.

Natural samples were collected from four arsenic contaminated sites in Germany. They covered a wide

range of geochemical characteristics and arsenic concentrations (Tables 2 and 3). The sandy Podsol horizons (labelled H 1; Neumarkt/Bavaria) received arsenic from infiltrating wood preservation solutions (e.g. copper–chromium–arsenic salts). In H 1/2 most arsenic was associated with metal oxides (Peiffer et al., 2003). The loamy soil columns (labelled W 1 and W 2; Wiesloch/Baden-Wuerttemberg) were contaminated by an adjacent mining dump. Therefore primary sulfidic and secondary oxidic arsenic phases can be expected there (Ruede, 1996). Material from below the groundwater table (95 cm below surface at time of sampling) was obtained from an aquifer in the riparian zone of the Leimbach stream (labelled A 1 and A 2; Wiesloch/Baden-Wuerttemberg). The arsenic stemmed from accumulation of eroded mining material or percolating solutes. A sediment core was collected from a depth of about 3 m in Lake Trebgast (labelled S 1; Bavaria). The lake is influenced by inflow of groundwater containing arsenic.

All samples were homogenized and freeze dried. Arsenic pools were quantified with the extractants proposed by Keon et al. (2001). Individual extractions with 0.1 M NaH_2PO_4 (pH 5; 24 h; strongly sorbed fraction), 1 M HCl (1 h; carbonate and amorph metal oxide fraction) and Aqua Regia (10 bar; 0.5 h; Microwave; total arsenic) were made (Tables 2 and 3). Before the DOM mobilization experiments all natural samples were autoclaved at 121 °C in wet heat for 30 min. Autoclavation can reduce the sorption of anions on soil material (Xie and Mackenzie, 1991) but was necessary to reduce microbial influences.

Two DOM solutions were used in mobilization experiments. The first solution was prepared by dissolving dry Pahokee Peat reference humic acid (labelled PA-HA; Florida; purchased from the International Humic Substances Society) at pH 8–9. PA-HA represents a well purified material (ash content ~1,7%) and has been thoroughly characterized by the IHSS. The peat humic acid has a carboxylic group content of 8.8 mmol/g C ($\text{p}K_{\text{A}}=4.26$) and a phenolic group content of 2.05 mmol/g C ($\text{p}K_{\text{A}}=9.85$). The high specific UV absorbance at 280 nm (SUVA_{280}) of 1180 L (mol organic carbon) $^{-1}\text{cm}^{-1}$ and the low Absorption $_{465\text{nm}}$ /Absorption $_{665\text{nm}}$ ratio (Abs $_{465}$ /Abs $_{665}$) of 5.5 point out a high degree of condensation and aromaticity of this DOM (Chen et al., 2002). The second DOM was collected as a solute from a

drainage tube of the mesotrophic Lehstenbach wetland (labelled FI-DOM; Bavaria). It was degassed and filtered (0.45 μm). The DOM solution also contained nitrate (51 $\mu\text{mol/L}$), sulphate (140 $\mu\text{mol/L}$) and ammonium (280 $\mu\text{mol/L}$). By acid-base titration of FI-DOM no specific $\text{p}K_{\text{A}}$ value could be determined, but a proton uptake capacity between 8.5 and 22 mmol/g C was calculated. The SUVA_{280} value (864 L (mol organic carbon) $^{-1}\text{cm}^{-1}$) indicates a lower condensation and aromaticity in FI-DOM than in PP-HA and the Abs $_{465}$ /Abs $_{665}$ ratio of 8.7 is within the fulvic acid range. Before use both solutions were brought to pH 6–6.5 and 10 mM ionic strength (NaCl or NaNO_3) and stored for up to 3 months in darkness at 5 °C.

2.2. Batch experiments

All batch experiments were carried out in acid conditioned PE-vessels and as triplicate assays except for the arsenic sorption in protocol B (duplicate assays). After the addition of any solid phase (iron oxide or natural sample) the PE-vessels were individually kept in nitrogen filled 300 mL glass containers during the whole experiment. Addition of solute and sampling was done through a mounted septum and a syringe. The pH was adjusted with 100 mM solutions of NaOH or HNO_3 . The samples were deaerated by purging them with N_2 through a cannula for 15 min. During incubation the assays were shaken (horizontal shaker, 100 rotations/min) at 20 ± 1 °C in the dark. Suspended particles in the sample aliquots were removed by centrifugation (20 min, 18,000 u/min) for iron oxide experiments and by filtration (0.45 μm , Nylon) for natural samples. The clear samples were stabilized with 1% HNO_3 in 1.5 mL Eppendorf caps and stored in darkness at 5 °C. Arsenic speciation was always determined within 48 h after sampling. Microbial activity was inhibited as far as possible by using only purified substances, conditioned reaction vessels and short reaction times.

2.2.1. Aqueous batch experiments

For the aqueous experiments 20 mL of a DOM solution was added to 20 mL of either arsenate or arsenite solution. The final conditions were 80 $\mu\text{g/L}$ arsenite or 60 $\mu\text{g/L}$ arsenate and 50 $\mu\text{g C/L}$ in 10 mM

NaNO₃ at pH 6.2±0.2. These assays were sampled after 24 h.

2.2.2. Batch experiments with synthetic iron oxide

Two experimental protocols were used for the iron oxide assays. In protocol A, experiments were carried out in a NaCl matrix and the mobilization step was done with dried oxides. 10 mg goethite were suspended in 40 mL of NaCl solution (10 mM) and equilibrated for 24 h. Either arsenate or arsenite was added (2.5 mg/L), pH was adjusted to 6.2±0.2 and the assays were incubated. After the sorption the supernatant was decanted and the remainder was dried at 50 °C and used for the mobilization experiments. To these ends 10 mg goethite with sorbed arsenic was resuspended in 40 mL of DOM solution (concentration 0 or 25 mg C/L; pH 6.2±0.2) using sonication. The suspension was degassed and incubated under nitrogen atmosphere. Sorption and desorption assays were sampled after 2, 15 and 100 or 144 h for arsenate/goethite and after 2, 24, 72 and 240 h for arsenite/goethite.

In protocol B, the mobilization was carried out without a drying step and in a NaNO₃ solution. Goethite was suspended in NaNO₃ solution (10 mM) and equilibrated for 24 h before either arsenate or arsenite was added and pH was adjusted to 6.2±0.2. The final concentrations were 500 mg/L goethite with 1.9 mg/L arsenate or 1.8 mg/L arsenite at pH 6.2±0.2. Samples were taken after 24 and 160 h. Suspension aliquots of 10 mL were then removed from these goethite/arsenic stock solutions under strong mixing and transferred to 50 mL PE-vessels. 20 mL of DOM solution at pH 6.2±0.2 were added (final concentration 0 or 25 mg C/L). The mixture was degassed and incubated under nitrogen atmosphere. Samples were taken after 36 h and 160 h.

2.2.3. Batch experiments with natural solid phases

A series of different extraction experiments was carried out. One gram of soil or sediment material was suspended in 25 mL of DOM solution (concentration 0 or 50 mg C/L) solution. The suspensions were degassed, incubated under nitrogen atmosphere and sampled after 24 h. To investigate the mobilization kinetics, aliquots were removed from the H 1/2 soil assays additionally after 0.5, 2, and 100 h. The effect of DOM concentration was tested with 1 g H 1/2 material

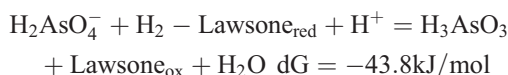
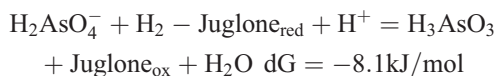
in 25 mL DOM solution of 0, 10, 50 or 100 mg C/L and sampling after 24 h. Arsenic speciation was analyzed for one set of H 1/2 samples as described above with 1 g soil suspended in 25 mL DOM (concentration 0 or 50 mg C/L) after 24 h of incubation.

2.3. Analytical techniques

Total arsenic (As_{tot}) was determined by graphite furnace atomic absorption spectroscopy (GF-AAS) (Analytik Jena AAS Zeenit 60; Limit of detection (LOD)=4.7 µg/L). Arsenic speciation was measured in a continuous HPLC-ICP-MS system, consisting of a Kontron pump 525, two guard columns (Dionex; AG7; 50×4 mm), an analytical column (Dionex; AS7/NG1; 250×4 mm) and an ICP-MS (Agilent 7500 c). The separation method of (Kohlmeyer et al., 2002) was used. Iron and manganese was measured by flame atomic absorption spectroscopy (FI-AAS; Varian Spectr AA 20; LOD=0.8 mg/L) and dissolved organic carbon by TOC Analyzer (Shimadzu 5050; LOD=1.3 mg C/L). Solid phase organic carbon was determined by CHN analysis. Total reduced inorganic sulphur (TRIS) was measured photometrically as methylene blue at 665 nm (Varian Cary 1E) after digestion (Fossing and Jorgensen, 1989).

2.4. Thermodynamic calculations

Quinone moieties present in humic substances take part in redox reactions (Scott et al., 1998). We calculated Gibb's free energies for the redox reactions between arsenic and model quinones using data of Cherry et al. (1979) for arsenic and Schwarzenbach et al. (1990) for the two organic model quinones Juglone and Lawsone, assuming equimolar concentrations of oxidized and reduced species, and a pH of 6:



Arsenate reduction combined with DOM oxidation is thus the thermodynamically favoured process under the chosen experimental conditions.

3. Results

3.1. Arsenic speciation in the aqueous DOM solution

Both arsenite and arsenate could be detected after incubation with DOM (Fig. 1). Other As species could not be detected. Arsenite oxidation was strongest with FI-DOM (7 $\mu\text{g/L}$ or 8% of total arsenic present), whereas strongest arsenate reduction occurred with PA-DOM (4 $\mu\text{g/L}$ or 8%). The results were reproducible with small deviations in a similar experiment with 72 h instead of 24 h reaction time. A small change in speciation was also observed in the reference samples without DOM.

3.2. Arsenic sorption on goethite

Sorption of arsenic was rapid in the beginning and slowed down with experimental duration (Fig. 2). Only for the arsenite in protocol B an equilibrium concentration in solution was reached within 24 h. The sorption capacity of goethite was larger for arsenate than for arsenite in both protocols used. Roughly twice the amount of arsenate was sorbed compared to arsenite. Arsenic immobilization was smaller using protocol B than protocol A (Fig. 2).

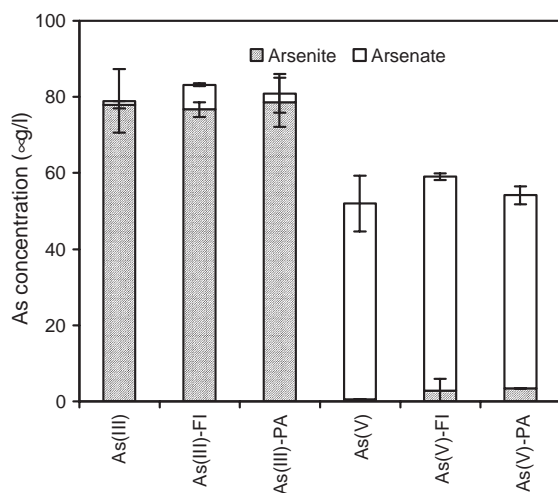


Fig. 1. Arsenic speciation measured by HPLC-ICP-MS after incubation of 80 $\mu\text{g/L}$ arsenite and 60 $\mu\text{g/L}$ arsenate, respectively, in solutions containing no DOM, 50 mg C/L FI-DOM or 50 mg C/L PA-HA ($I=10$ mM NaNO_3). Averages of triplicate assays are shown.

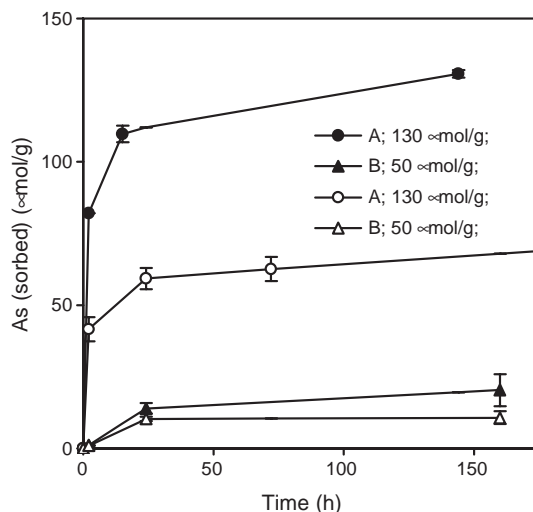


Fig. 2. Sorption of arsenic species in goethite suspensions. Closed symbols represent arsenate experiments and open symbols represent arsenite experiments. The experimental protocol applied and the initial As/Fe relation are shown in the legend. As described in the text in protocol A NaCl was used to adjust ionic strength while protocol B used NaNO_3 .

3.3. Arsenic mobilization from goethite in DOM solution

The addition of arsenic-free solution to dried (protocol A) or suspended (protocol B) arsenated iron oxides resulted in an initial increase of the total amount of dissolved arsenic in all assays (Fig. 3). In the protocol A experiment with arsenate, arsenic desorption continues until the end of the incubation after 100 h. In the other assays, arsenic was mobilised only at the beginning (2 h in protocol A experiments with arsenite, 36 h in protocol B experiments). Subsequently arsenic concentration in the solution decreased again. A maximum net mobilization of arsenic by DOM was calculated as the maximum release with DOM minus the maximum release without DOM at the same time step (Table 1). Net mobilization was higher adding PA-HA than for FI-DOM. Pre-sorbed arsenite was released more easily than pre-sorbed arsenate (Table 1).

Larger initial DOM concentrations mobilized more arsenic and immobilized more DOM. A linear relationship between arsenic release and DOM concentrations was not observed, though. DOM concentrations in solution decreased by about 5–10 mg C/L

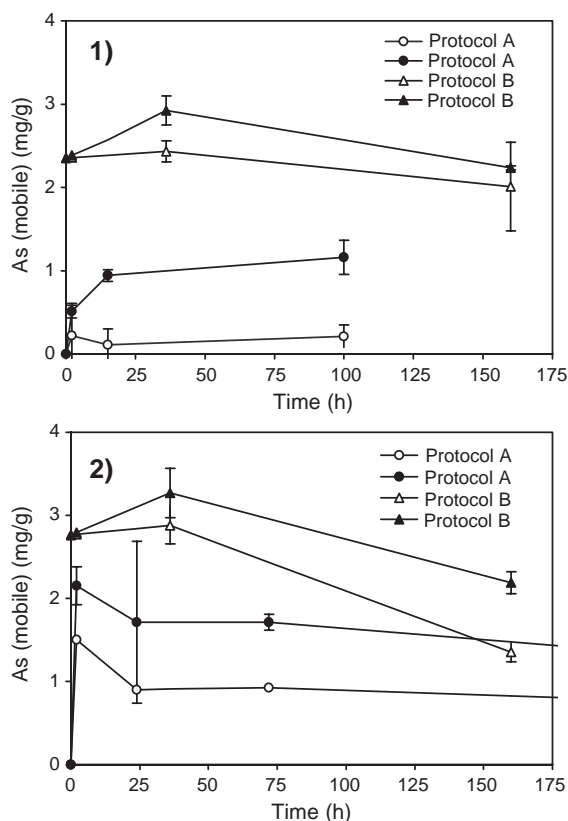


Fig. 3. Mobile As_{tot} during incubation of goethite with pre-sorbed (1) arsenate or (2) arsenite ($I=10$ mM); open symbols: solutions without DOM; closed symbols: solutions with 25 mg/L PA-HA. The legend shows the experimental protocol applied. As described in the text protocol A represents the use of NaCl as ionic strength while protocol B uses $NaNO_3$. Protocol A also includes drying the goethite after the arsenic sorption.

during incubation. Assuming a sorption of 5 mg C/L for PP-HA (8.8 mmol carboxylic groups/g C), 176 $\mu\text{mol/g}$ Goe of carboxylic group were immobilized, which exceeds the maximum molar arsenic release by a factor of 10 (maximum of 13.3 $\mu\text{mol/g}$ Goe for arsenate with protocol A; Table 1). In the protocol B mobilization experiments only arsenate was found in solution after incubation, no matter the arsenic species previously sorbed and the DOM used.

3.4. Arsenic mobilization from natural samples in DOM solution

For all samples except the lake sediments arsenic extractability increased in the order “no DOM” < PA-

HA < NaH_2PO_4 < HCl (Table 3). Extraction with PA-HA revealed a higher relative mobility of arsenic in the H 1 and A 1+2 samples (0.43–4.3% of As_{tot}) than in the W 1+2 and S (<0.4%). The total amount of arsenic released ranged from 0 (S 1) to 3.8 mg/kg (H 1/1). The biggest differences between “no DOM” and PA-HA extractable arsenic was found in the H 1 horizons. Release of arsenic with FI-DOM (applied to some samples only, results not shown) was between “no DOM” and PA-HA extracts. Initial DOM concentrations were positively correlated to dissolved arsenic concentrations for H 1/2 material (Fig. 4). An almost linear relationship was found for PA-HA ($R^2=0.999$) and also for FI-DOM ($R^2=0.968$). On a molar basis the amount of sorbed carboxylic groups in PA-HA (2.2–6.2 mmol/kg) exceeded the amount of arsenic molecules released (maximum: 0.05 mmol/kg) by more than one order of magnitude.

In the kinetic experiments with H 1/2 material two phases were observed (Fig. 5). The first phase ended within 24 h and was characterized by arsenic release to the solution. In the second phase arsenic was immobilised. DOM sorption continued throughout the experiment. Mostly arsenate and only small amounts of arsenite were found in the speciation analysis (Fig. 5). The addition of DOM, however, resulted in an increase of arsenite concentrations compared to the control.

3.5. Characterization of the natural solid phases

The analytical results of this section are summarized in Tables 2 and 3. The pH in the H 1 Podsol soil samples was significantly lower than in the other materials. The W 1+2 and A 1+2 samples from Wiesloch contained between 0.23% and 2.59% inorganic carbon. Calcite signature (1428 and 878 cm^{-1}) was visible in the FTIR spectra. Large amounts of organic carbon were particularly present in the sediment samples, whereas in the H 1 soils and A 2/2 aquifer amounts were low. Except for the H 1 horizons and the A 2 sediment all samples contained substantial amounts of iron (up to 6.3%) and manganese (up to 1.2%). The amorphous metal oxides, comprised about 1/10th of the total metal content in these samples, but was larger in the H 1 and A 2 material. Total reduced inorganic sulphur (TRIS) was increased in the aquifer material (A 2) and high in

Table 1
Sorption and desorption of arsenic from goethite or hematite (*) in this study and estimated from literature

Protocol/author	Solute	Sorption			Desorption		
		Init. As/Fe-ratio ($\mu\text{mol/g}$)	As sorbed ($\mu\text{mol/g}$) (%)		c(DOM) (mg C/L)	Net mobilization (As) ($\mu\text{mol/g}$) (%)	
<i>Arsenate experiments</i>							
A	NaCl	130	130	100	25	13.3	10.3
B	NaNO ₃	50	20	40	25	6.5	32.7
Dixit and Hering (2003)	NaClO ₄	100	90	90			
Dixit and Hering (2003)	NaClO ₄	50	50	100			
Grafe et al. (2002)	NaNO ₃	200	160	80	12	46.7	23.3
Redman et al. (2002) (*)	NaNO ₃	100	90	90	10	0.7	22.2
<i>Arsenite experiments</i>							
A	NaCl	130	70	55	25	9.3	13.3
B	NaNO ₃	50	10	22	25	5.3	53.3
Dixit and Hering (2003)	NaClO ₄	100	75	75			
Dixit and Hering (2003)	NaClO ₄	50	40	80			
Grafe et al. (2002)	NaNO ₃	200	240	>100	12	26.7	13.3
Redman et al. (2002) (*)	NaNO ₃	100	90	90	10	0.4	13.3

The first columns display the applied salt solution, As/Fe ratio at the beginning of the sorption experiment and the amount of As sorbed. The last columns show the reaction condition and results of the arsenic desorption with DOM.

the lake sediment (S 1/2) compared to the soils. Total arsenic content was highest in the W 1+2 materials (Table 3). Arsenic in these samples was present to a large extent in forms not extracted by phosphate or HCl. Using these extractants the largest relative quantities were extracted from the H 1/2 soil and from the S 1/2 and A 2 sediments.

4. Discussion

Due to pressing concerns about arsenic contamination of water resources (Smedley and Kinniburgh, 2002), efforts have been undertaken to identify mechanisms that can increase arsenic mobility in soils, aquifers and sediments. The mobilization in Bangladesh/West Bengal type aquifers has primarily been linked to an indirect mobilization by DOM, particularly to increased substrate availability for iron reduction, causing enhanced release of iron oxide bound arsenic (Harvey and Swartz, 2002). Recent studies have also focussed on the redox activity and on electron shuttling capacity of organic matter with some organic pollutants and inorganic substances (Chen et al., 2003; Gu and Chen, 2003; Lovley et al., 1996). Chemical redox reactions and electron

shuttling between DOM and arsenic have, however, not received much attention yet.

The results of this study suggest a strong potential for DOM to mobilize arsenic from goethite and natural soil and aquifer materials within short periods of time by purely chemical interactions. Net release from goethite was up to 46 mg/kg and 53% of the total sorbed arsenic. These results are in agreement with previous studies reporting arsenic desorption from different iron oxides (goethite, ferrihydrite, hematite) in the presence of bulk DOM (Redman et al., 2002) and fulvic or humic acids (Grafe et al., 2001; Grafe et al., 2002; Simeoni et al., 2003). Adsorption capacities for arsenate and arsenite on goethite were in agreement with previously reported findings (Dixit and Hering, 2003, Table 1) increasing our confidence that the results are valid.

Also in natural samples, DOM released up to 2.48 mg/kg or 2.88% of total arsenic. This was up to three times the amount released by our weakest extractant 0.01 M NaNO₃. Lombi et al. (2000), Kalbitz and Wennrich (1998) and Keon et al. (2001) were able to desorb 0.07–5 mg/kg of arsenic from soil and sediment samples with 1 M NH₄NO₃ or 1 M MgCl₂. Despite the much lower extractant concentrations used in our study, the arsenic release was in a similar range.

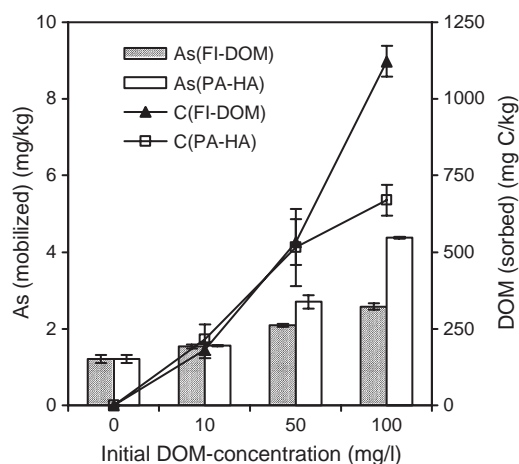


Fig. 4. Release of As_{tot} and sorption of DOM in experiments with soil material and the effect of different initial DOM concentrations. Bars represent the amount of arsenic released from H 1/2 samples during incubation with different concentrations of PA-HA and FI-DOM. Lines reflect the amount of DOM removed from solution in the same experiments.

In general the mobility of arsenic (as % of the total content) in natural samples treated with DOM was smaller than the mobility in the goethite assays. This can be explained by the reduced chemical availability of the arsenic. Arsenic bound to goethite is mainly sorbed in surface complexes. Instead in natural materials often only a small fraction of arsenic is in an exchangeable state (Lombi et al., 2000) and more

is incorporated in minerals. So differences occur between synthetic minerals and natural samples as well as among natural samples. A high percentage of arsenic release with DOM (H 1 soil, A 2 sediment) concurred with high arsenic mobilities using phosphate and HCl as extractants. The iron content in these samples is rather low but mostly in an amorphous state and soluble with HCl. We therefore believe that arsenic in these samples was primarily sorbed to metal oxides, iron in the sediment and possibly aluminium in the H 1 horizon. In contrast only little arsenic was mobilized from the W 1 + 2 soils is mobile by DOM and phosphate solutions. Roughly 70–90% of arsenic were not accessible with HCl and therefore incorporated (not sorbed) in the structure of more stable minerals, most likely crystalline oxides as TRIS content was low.

The arsenic mobilization patterns for synthetic and the H 1/2 natural samples were similar. This finding suggests that, within limits, results obtained with synthetic samples can be extrapolated also to natural conditions. Arsenic release was always fast and completed within the first 24–36 h of the experiments. The kinetic was in agreement with competition of DOM and arsenate for goethite sorption sites, which has been shown to be fairly rapid (Hongshao and Stanforth, 2001).

The experimental conditions had a substantial influence on the sorption efficiency (Table 1) and on

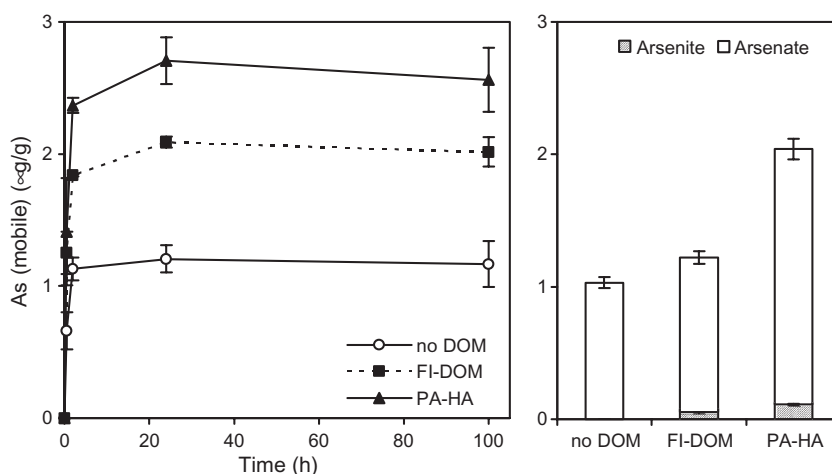


Fig. 5. Mobilization of As_{tot} from soil material and results of redox species measurement with HPLC-ICP-MS. Lines represent the As mobilization kinetic from H 1/2 samples in the first 100 h of incubation with different DOM types and concentrations. Bars represent the amount of arsenite and arsenate found in the assays.

Table 2
Characteristics of the natural samples

Sample	Type	Depth (cm)	pH	C _{inorg} (%)	C _{org} (%)	Fe _{tot} (g/kg)	Fe _{HCl} (g/kg)	Mn _{tot} (g/kg)	TRIS (mg/kg)
H 1/1	Soil	6–30	5.5	n/a	0.24	2±0.1	0.8±0.1	0.3±0.1	8.3
H 1/2	Soil	31–65	5.2	n/a	0.39	2±0.1	0.3±0.1	0.4±0.1	3.5
W 1/1	Soil	20–55	6.9	2.59	1.50	57±2.3	1.6±0.1	1.2±0.2	10.5
W 1/2	Soil	55–70	6.8	0.78	1.01	15±1.4	1.3±0.1	1.1±0.1	2.2
W 2/1	Soil	10–70	6.7	0.87	2.23	43±1.1	1.7±0.1	12.1±0.1	n/a
W 2/2	Soil	71–90	7.1	0.34	0.75	32±0.9	1.5±0.1	4.1±0.1	n/a
A 1/1	Aquifer	255–295	6.8	0.98	2.19	22±0.4	2.3±0.1	2.5±0.1	3.5
A 1/2	Aquifer	320+	6.4	0.38	2.02	63±0.7	4.3±0.1	11.1±0.1	n/a
A 2/1	Aquifer	130–220	6.9	0.23	2.23	4±0.7	3.3±0.1	0.4±0.1	66.9
A 2/2	Aquifer	250+	6.9	2.34	0.28	4±0.6	2.1±0.1	0.6±0.1	62.4
S 1/1	Sediment	0–2	n/a	n/a	9.79	34±1.5	11.3±0.1	7.2±0.3	n/a
S 1/2	Sediment	2–16	n/a	n/a	11.21	73±0.5	3.4±0.2	2.5±0.2	1008

the desorption process. Protocol A experiments showed a higher arsenic sorption than protocol B. These may be effects of the different anions Cl⁻ and NO₃⁻, even though they are reported to have an equally small effect on arsenic sorption in soils (Livesey and Huang, 1981). Also in protocol A assays, including a drying step at 50 °C before DOM addition, a smaller fraction of arsenic was accessible to DOM in the mobilization step (Fig. 3). Intense hydrothermal treatment (150 °C; autoclave) reduces sorption capacity of goethite for oxyanions like phosphate as goethite crystallinity increases (Strauss et al., 1997). But a mild treatment, like air drying, is known to increase the sorption of oxyanions on soil material (Haynes and Swift, 1985). That effect is attributed to the formation of an increased number

and stronger bonds between arsenic and minerals surfaces as water is removed. This could explain the observed reduced mobilization of arsenic after drying in our experiments. Another effect was a re-immobilization of arsenic when the goethite was treated according to protocol B without the drying step. This effect was particularly strong in samples amended with arsenite (Fig. 3). Diffusive transport to inner surfaces leading to higher sorption capacities and stronger binding of oxyanions (Matthess, 1994) may explain the re-immobilization during desorption experiments. Also it has been reported previously that DOM can raise the solid/solute partitioning coefficient of arsenic in solutions containing kaolinite (Saada et al., 2003), but such an effect was not yet observed for iron oxides or soils. The stronger re-

Table 3
Arsenic extraction from the natural samples

Sample	Type	As _{tot} (mg/kg)	As(HCl) (%)	As(H ₂ PO ₄ ⁻) (%)	As(NaNO ₃) (%)	As(PA-HA) (%)	Net mobilization (mg/kg)	(%)
H 1/1	Soil	197±17	26.1	3	0.67	1.93	2.48±0.09	1.26
H 1/2	Soil	85±10	109.5	29	1.48	4.36	2.46±0.04	2.88
W 1/1	Soil	2122±716	31.4	5	0.07	0.13	1.18±0.07	0.06
W 1/2	Soil	842±90	25.4	8	0.04	0.19	1.32±0.04	0.16
W 2/1	Soil	1394±210	8.9	n/a	0.01	0.04	0.51±0.01	0.04
W 2/2	Soil	326±58	15.2	n/a	0.02	0.14	0.41±0.02	0.12
A 1/1	Aquifer	229±19	10.3	n/a	0.31	0.43	0.29±0.04	0.13
A 1/2	Aquifer	40±2	34.5	n/a	1.54	2.17	0.25±0.1	0.63
A 2/1	Aquifer	67±14	43.3	20	2.18	2.47	0.19±0.12	0.29
A 2/2	Aquifer	22±1	52.7	18	2.07	3.52	0.32±0.02	1.45
S 1/1	Sediment	44±4	1.3	n/a	0.64	0.38	n/a	n/a
S 1/2	Sediment	6±4	100.1	n/a	0.00	0.00	0.00±0.0	0.00

immobilization of added arsenite (Fig. 3) is potentially explained by oxidation to arsenate (observed in goethite suspensions) leading to the subsequent sorption of formed arsenate. The effects of the experimental protocols on the exchange behaviour suggest that the exact laboratory setup is crucial for sorption experiments of arsenic, especially when extrapolations on processes in the environment are attempted.

The results of this study suggest a potential for DOM to chemically oxidize and reduce arsenic within short periods of time. In aqueous solution, DOM both oxidized arsenite and reduced arsenate, albeit only a small fraction of the total. In contrast to abiotic chromium reduction with DOM (Gu and Chen, 2003) the reaction was essentially completed within the first day. Redman et al. (2002) reported comparable quantities of arsenite oxidation with a variety of DOM solutions but observed reduction of arsenate only for one type of DOM. The observation of both reduction and oxidation is in contradiction to the results of our thermodynamic estimates using model compounds. The thermodynamic calculations suggested arsenate reduction with DOM to be the energetically favoured process. The redox properties of the natural DOM are therefore not accurately described by the model compounds suggesting that DOM covers a wider spectrum of redox potentials. The relative amounts of reduction of arsenate to arsenite were larger using PA-HA than using FI-DOM, which could be an effect of its higher aromaticity as indicated by SUVA₂₈₀ and Abs₄₆₅/Abs₆₆₅. A further observation was that in goethite suspensions, arsenite was completely oxidized, while arsenate speciation did not change. This reaction was independent of DOM presence and may have been caused by nitrate or dissolved Fe(III) as oxidants (McCleskey et al., 2004).

The hypothesis that reduction of solid phase arsenate by DOM may significantly contribute to the mobilization of arsenic could not be substantiated by our experiments. In the H 1/2 samples which contained only arsenate (Marx, 1993), only small amounts of dissolved arsenite were found after incubation. Reduction of solid phase arsenate was not a relevant process in the goethite experiments and was only of minor importance in the experiments with natural samples.

In conclusion, the results demonstrate that DOM has the potential to chemically mobilize arsenic from iron oxides, soils, aquifers and sediments. In goethite suspensions with pre-sorbed arsenic, dissolved concentrations increased up to 6 times in the presence of 25 mg/L DOM compared to samples without DOM. In a variety of natural samples, concentrations increased by a factor of 1.5–3. It also has to be considered that we used wide solute/solid ratios of 1 g/25 mL solution. Using narrow solute/solid ratios, as they are found in soils, the mobile arsenic fraction decreases, but absolute concentrations in solution increase (Peiffer et al., 2003).

Arsenic release to ground water is a major concern worldwide. Direct interactions of arsenic and DOM have not yet received attention to a large extent. Taking into account only sorption competition reactions, pore waters rich in DOM may release more than 3 times the amount of arsenic from some soils than waters poor in DOM. At the narrow solute/solid ratios of natural environments, this process has the potential to raise arsenic concentrations to levels exceeding drinking water standards.

Acknowledgments

This work was in part supported by BMBF (Projektfördernummer 0339476 D). The authors thank Dr. G. Illgen at BITOEK for measuring As speciation by ICP-MS. We would also like to thank Ludwig Hildebrandt for information about the sampling area in Wiesloch and support in the field.

References

- Abbt-Braun G. Huminstoffe-Vorkommen, Charakterisierung und Reaktionen. *Wasser-und Geotechnologie* 2002;1:41–9.
- Anawar HM, Akai J, Komaki K, Terao H. Geochemical occurrence of arsenic in groundwater of Bangladesh: sources and mobilization processes. *J Geochem Explor* 2003;77:109–31.
- Appelo CAJ, Van der Weiden MJJ, Tournassat C, Charlet L. Surface complexation of ferrous iron and carbonate on ferrihydrite and the mobilization of arsenic. *Environ Sci Technol* 2002;36:3096–103.
- Bissen M, Frimmel FH. Arsenic—a review: Part I. Occurrences, toxicity, speciation, mobility. *Acta Hydrochim Hydrobiol* 2003;31:9–18.

- Chen J, Gu B, LeBoeuf EJ, Pan H, Dai S. Spectroscopic characterization of the structural and functional properties of natural organic matter fractions. *Chemosphere* 2002;48:59–68.
- Chen J, Gu B, Royer RA, Burgos WD. The roles of natural organic matter in chemical and microbial reduction of ferric iron. *Sci Total Environ* 2003;307:167–78.
- Cherry JA, Shaikh AU, Tallman DE, Nicholson RV. Arsenic species as an indicator of redox conditions in groundwater. *J Hydrol* 1979;43:373–92.
- Chui VQ, Hering JG. Arsenic adsorption and oxidation at manganite surfaces: 1. Method for simultaneous determination of adsorbed and dissolved arsenic species. *Environ Sci Technol* 2000;34:2029–34.
- Cullen WR, Reimer KJ. Arsenic speciation in the environment. *Chem Rev* 1989;89:713–64.
- Dixit S, Hering JG. Comparison of arsenic(V) and arsenic(III) sorption onto iron oxide minerals: implications for arsenic mobility. *Environ Sci Technol* 2003;37:4182–9.
- Fossing H, Jorgensen BB. Measurement of bacterial sulfate reduction in sediments: evaluation of single step chromium reduction method. *Biogeochemistry* 1989;8:205–22.
- Grafe M, Eick MJ, Grossl PR. Adsorption of arsenate(V) and arsenite(III) on goethite in the presence and absence of dissolved organic carbon. *Soil Sci Soc Am J* 2001;65:1680–7.
- Grafe M, Eick MJ, Grossl PR, Saunders AM. Adsorption of arsenate and arsenite on ferrihydrite in the presence and absence of dissolved organic carbon. *J Environ Qual* 2002;31:1115–23.
- Gu B, Chen J. Enhanced microbial reduction of Cr(VI) and U(VI) by different natural organic matter fractions. *Geochim Cosmochim Acta* 2003;67:3575–82.
- Harvey CF, Swartz CH. Arsenic mobility and groundwater extraction in Bangladesh. *Science* 2002;298:1602–6.
- Haynes RJ, Swift RS. Effects of air-drying on the adsorption and desorption of phosphate and levels of extractable phosphate in a group of acid soils. *Geoderma* 1985;35:145–57.
- Hongshao Z, Stanforth R. Competitive adsorption of phosphate and arsenate on goethite. *Environ Sci Technol* 2001;35:4753–7.
- Janos P, Wildernova M, Loucka T. Leaching of metals from fly ashes in the presence of complexing agents. *Waste Manage* 2002;22:783–9.
- Kaiser K, Guggenberger G, Zech W. Dissolved organic matter sorption on subsoils and minerals studied by ¹³C-NMR and DRIFT spectroscopy. *Eur J Soil Sci* 1997;48:301–10.
- Kalbitz K, Wennrich R. Mobilization of heavy metals and arsenic in polluted wetland soils and its dependence on dissolved organic matter. *Sci Total Environ* 1998;209:27–39.
- Keon NE, Swartz CH, Brabander DJ, Harvey C, Hemond HF. Validation of an arsenic sequential extraction method for evaluating mobility in sediments. *Environ Sci Technol* 2001;35:2778–84.
- Kohlmeyer U, Kuballa J, Jantzen E. Simultaneous separation of 17 inorganic and organic arsenic compounds in marine biota by means of high-performance liquid chromatography/inductively coupled plasma mass spectrometry. *Rapid Commun Mass Spectrom* 2002;16:965–74.
- Lin H-T, Wand MC, Li G-C. Effects of water extract of compost on the adsorption of arsenate by two calcareous soils. *Water Air Soil Pollut* 2002;138:359–74.
- Livesey NT, Huang PM. Adsorption of arsenate by soil and its relation to selected chemical properties and anions. *Soil Sci* 1981;131:88–94.
- Lombi E, Sletten RS, Wenzel WW. Sequentially extracted arsenic from different size fractions of contaminated soils. *Water Air Soil Pollut* 2000;124:319–32.
- Lovley DR, Blunt-Harris EL, Phillips EJP, Woodward JC. Humic substances as electron acceptors for microbial respiration. *Nature* 1996;382:445–8.
- Matthess G. Die Beschaffenheit des Grundwassers. Gebrüder Bornträger; 1994.
- Marx HN. Untersuchungsbericht Mastenlager-Ableitung notwendiger Sicherungs- und Sanierungsmaßnahmen. Gutachterliche Stellungnahme im Auftrag von Pfeiderer Verkehrstechnik; 1993.
- Masscheleyn PH, Delaune RD, Patrick WH. Effect of redox potential and pH on arsenic speciation and solubility in a contaminated soil. *Environ Sci Technol* 1991;25:1414–9.
- McCleskey BR, Nordstrom KD, Maest AS. Preservation of water samples for arsenic (III/V) determination: an evaluation of the literature and new analytical results. *Appl Geochem* 2004;19:995–1009.
- Newman DK, Ahmann D, Morel FM. A brief review of microbial arsenate respiration. *Geomicrobiol J* 1998;15:255–68.
- Peiffer S, Hopp L, Buczko U, Dürner W. Vergleich verschiedener Elutionsverfahren im Hinblick auf die Verfahrensoptimierung zur Sickerwasserprognose von Chrom und Arsen. Sickerwasserprognose-Forschung und Praxis. Landesamt für Wasserwirtschaft 2003:89–110.
- Redman AD, Macalady DL, Ahmann D. Natural organic matter affects arsenic speciation and sorption onto hematite. *Environ Sci Technol* 2002;36:2889–96.
- Rochette EA, Bostick BC, Li G, Fendorf SE. Kinetics of arsenate reduction by dissolved sulfide. *Environ Sci Technol* 2000;34:4714–20.
- Ruede T. Beiträge zur Geochemie des Arsens. Karlsruher Geochemische Hefte; 1996.
- Saada A, Breeze D, Cruzet C, Cornu S, Baranger P. Adsorption of arsenic (V) on kaolinite and on kaolinite–humic acid complexes. Role of humic acid nitrogen groups. *Chemosphere* 2003;51:757–63.
- Schwarzenbach RP, Stierli R, Lanz K, Zeyer J. Quinone and iron porphyrin mediated reduction of nitroaromatic compounds in homogenous aqueous solution. *Environ Sci Technol* 1990;24:1566–74.
- Schwertmann U, Cornell RM. Iron oxides in the laboratory. VCH Verlagsgesellschaft; 1991.
- Scott DT, McKnight DM, Blunt-Harris EL, Kolesar SE, Lovley DR. Quinone moieties act as electron acceptors in the reduction of humic substances by humic-reducing microorganisms. *Environ Sci Technol* 1998;32:2984–9.
- Simeoni MA, Batts BD, McRae C. Effect of groundwater fulvic acid on the adsorption of arsenate by ferrihydrite and gibbsite. *Appl Geochem* 2003;18:1507–15.

- Smedley PL, Kinniburgh DG. A review of the source, behaviour and distribution of arsenic in natural waters. *Appl Geochem* 2002;17:517–68.
- Smith E, Naidu R, Alston AM. Chemistry of inorganic arsenic in soils: II. Effect of phosphorus, sodium, and calcium on arsenic sorption. *J Environ Qual* 2002;31:557–63.
- Strauss R, Brümmer GW, Barrow NJ. Effects of crystallinity of goethite: II. Rates of sorption and desorption of phosphate. *Eur J Soil Sci* 1997;48:101–14.
- Stueben D, Berner Z, Kappes B, Puchelt H. Environmental monitoring of heavy metals and arsenic from Ag–Pb–Zn mining. *Environ Monit Assess* 2001;70:181–200.
- Sun X, Doner HE. An investigation of arsenate and arsenite bonding structures on goethite by FTIR. *Soil Sci* 1996;161:865–72.
- Xie RJ, Mackenzie AF. Effects of autoclaving on the surface properties and sorption of phosphate and zinc in phosphate-treated soils. *Soil Sci* 1991;152:250–8.
- Xu H, Allard B, Grimvall A. Effects of acidification and natural organic materials on the mobility of arsenic in the environment. *Water Air Soil Pollut* 1991;57–58:269–70.

Study 7

unpublished

Mobilization of iron and arsenic from iron hydroxide coated sand columns by percolation with dissolved organic matter

Markus Bauer¹, Michaela Raber¹, Christian Blodau¹

¹Limnological Research Station and Department of Hydrology, University of Bayreuth, D-95440
Bayreuth, Germany,

Abstract

Organic matter influences arsenic (As) mobility by abiotic reactions, i.e. desorption and redox transformation, but also through the stimulation of microbial activity, leading to reductive dissolution of As binding solid phases. The relative importance of physicochemical As mobilization and the dependence of microbial processes on concentrations of dissolved organic matter (DOM) was analyzed in column experiments with As containing, Fe hydroxide coated and microbially inoculated sand. Variation of DOC concentrations did not change the sequence of redox transformations and mobilization processes in the column, but only their velocity. Arsenic mobilization increased in the presence of high organic matter solution and was coupled to the onset of reducing conditions within the column. This is supported by the almost concurrent appearance of Fe(II) in the mobile phase and suggests reductive dissolution of Fe phases to be the mechanism of As release. Reducing conditions and Fe(II) production also induced ferrihydrite transformation, possibly magnetite. When the DOC inflow concentration was high, Fe hydroxides were rapidly depleted in the column and sulphate reduction initiated. Arsenic mobility was little affected by the production of H₂S, as it was to a large extent already released from the columns when sulphate reduction began. This prevented an immobilization of As with precipitation of sulphides. Before the beginning of Fe reduction As mobility was low, indicating that physicochemical mechanisms, such DOM induced desorption or colloid formation, were unable to substantially release As into the solute phase. The results suggest that availability of DOC will lead primarily to microbial Fe reduction and As mobilization in pH-circumneutral aquifer materials rich in freshly precipitated and poorly crystalline Fe hydroxides. Only after depletion of the Fe hydroxides is a sequestration of As in sulphides likely.

Introduction

Arsenic has a high acute toxicity but is also known to be mutagenic and cancerogenic, which is why the WHO drinking water limit for As is only $10 \mu\text{g L}^{-1}$ (Mandal and Suzuki, 2002; Smedley and Kinniburgh, 2002). Numerous groundwater resources worldwide must be classified as contaminated with As and therefore a lot of research effort has been put into elucidating the processes and mechanisms leading concentrations of the toxic element. Besides anthropogenic causes for As pollution, i.e. areas with mining or smelting activities, natural geogenic processes are often responsible for high As concentrations in groundwater (Mandal and Suzuki, 2002; Smedley and Kinniburgh, 2002). Especially the reductive dissolution of As containing Fe hydroxides is seen as an important mechanism of As release into the water phase.

Fe minerals, such as goethite or ferrihydrite, are efficient sorbents for As due to their large positively charged surface area at neutral and acidic pH (Dixit and Hering, 2003). Binding of As to Fe phases has been observed in terrestrial and wetland soils, and sediments (Bauer and Blodau, 2006; Gonzalez et al., 2006). The stability of Fe hydroxides, however, is affected by changes in pH or redox conditions and dissolution of Fe hydroxides takes place under reducing conditions. The occurrence of this process has been documented for highly As contaminated aquifers of South Asia and was recently linked to the presence of sedimented peat (McArthur et al., 2004; Meharg et al., 2006). Degradable organic material in these peat layers is oxidized to CO_2 by microorganisms and this leads to decreasing redox potentials, reduction and dissolution of Fe hydroxides and the release of As.

The overall process of As release into the aqueous phase may involve different reactions, including As(V) reduction and As desorption. In microbially active batch and column experiments aqueous As was predominantly in the As(III) form (Herbel and Fendorf, 2006; Kocar et al., 2006; Sierra-Alvarez et al., 2005). The redox state affects the sorption equilibrium on Fe surfaces. As(III) was more easily released from Fe phases than As(V) in abiotic column experiments, and the presence of As reducing bacteria increased the total As mobilization (Herbel and Fendorf, 2006; Kocar et al., 2006). Even though similar sorption capacities for As(III) and As(V) were observed (Dixit and Hering, 2003), the affinity of uncharged H_3AsO_3 molecules ($\text{pK}_{\text{s}1} = 9.2$) for ferrihydrite at neutral pH was apparently lower than that of negatively charged HAsO_4^{2-} ($\text{pK}_{\text{s}1} = 2.2$). In addition to changes in redox speciation, also competition for sorption sites between As and aquatic anions, such as phosphate or organic substances, induces As release from Fe hydroxides (Geelhoed et al., 1998; Grafe et al., 2002). The As mobility in the presence of Fe reducing bacteria depends mainly on the fate of the present Fe phases. Arsenic was released from synthetic Fe hydroxide in batch experiments only after Fe(II) had been released (Islam et al., 2004), which may be due to initial As readsorption on remaining Fe hydroxide surfaces. Other studies found even stronger binding of As under Fe reducing conditions. High concentrations of Fe(II) in the water phase induce transformation of ferrihydrite to magnetite or goethite and concurrent incorporation of As in these phases (Pedersen et al., 2006). Arsenic mobility in these Fe reducing systems was only observed at the onset of reducing conditions when Fe(II)

concentrations were still low and after long periods of Fe reduction when the hydroxide phases are almost completely dissolved (Herbel and Fendorf, 2006; Kocar et al., 2006; Pedersen et al., 2006). The reductive breakup of Fe phases into smaller mineral entities and their release into the mobile phase as colloids additionally contribute to the mobility of sorbed As (Ghosh et al., 2006; Tadanier et al., 2005).

Under reducing conditions As can be immobilized by formation of sulphide minerals and the adsorption and incorporation of As into these minerals. Precipitation of As sulphides was observed in experimental column systems, requiring high aqueous H₂S concentration (Koeber et al., 2005; O'Day et al., 2004). Sulphate reduction, however, is an energetically favourable process only when other electron acceptors, such as nitrate and poorly crystalline manganese and Fe hydroxides, are mostly depleted. Under such conditions, sulphate reduction can account for a large portion of total anaerobic respiration. Alternatively, a similar situation may arise when the availability of degradable organic substrates is high, i.e. when respiration is not limited by the availability of electron donors. Under such conditions, Fe reducing bacteria may not be able to outcompete sulphate reducers for substrates, for example by lowering hydrogen concentrations to critical levels (Lovley and Goodwin, 1988).

The fate of Fe hydroxide bound As is important in aquifers and surface waters potentially used as drinking water supply (Smedley and Kinniburgh, 2002), but also in anoxic environments such as landfills or contaminated sites (Ghosh et al., 2006; Koeber et al., 2005). It is currently unclear how DOC loads influence the release and sequestration of As by competing terminal electron accepting processes and the formation and dissolution of Fe minerals. We hypothesize that increasing DOM concentrations (1) lead to higher rates of anaerobic microbial respiration, (2) increase the release of Fe and As and (3) lead to conditions under which As immobilization with sulphide minerals occurs. To this end we carried out column experiments with ferrihydrite coated sand and sorbed As, which continually received percolate containing different concentrations of dissolved organic matter.

Materials and Methods

Column experiments: Setup solid phase, and percolate

Four column experiments (C1 to 4) were run with different input concentrations of dissolved organic matter (DOM). The column filling consisted of Fe hydroxide coated quartz sand (grain size = 0.6-1.2 mm), which was prepared according to the method of (Grafe et al., 2002). Coated and uncoated sand was mixed in a ratio of 1 to 5.6 (weight/weight) and 3 kg of the mixture were suspended in 1 L of a solution containing 0.5 mmol L⁻¹ Na₂HAsO₄. Arsenic concentration of the sorption solution was only 0.005 mmol L⁻¹ in experiment 3. After 24 h of As sorption the sand was rinsed with VE water and resuspended in 1 L of a suspension containing 2 g L⁻¹ peat material. The peat was derived from the minerotrophic Schloepnerbrunnen peatland in the Fichtelgebirge/Germany and had previously been shown to contain Fe and sulphate reducing organisms (Paul et al., 2006). Between 1.7 and 1.8 kg of the wet sand was subsequently filled into

airtight plexiglass tube (l=25 cm, dia=8 cm) under constant stirring to achieve maximum packing. Seven sampling ports were installed in intervals of 3 cm along the flow path.

The percolates contained 11 mmol L⁻¹ NaCl, 1 mmol L⁻¹ Na₂SO₄, and 2 mmol L⁻¹ of MES buffer (2-(N-Morpholino)-ethanesulfonic acid; Fluka; pK_a=6.21). Dissolved natural organic matter was added to the eluent in different concentrations. The DOC stock solution was prepared from leaf litter (3.3 kg oak leafes, 40 L deionized water; (Blodau and Knorr, 2006)). After four weeks of incubation at room temperature the suspension was filtered (0.45 µm, Nylon, Roth) and the extract diluted to reach final inflow concentrations of 0, 5, 20, and 100 mg L⁻¹ DOC, which were characteristic for the experiments C1 to C4. The percolate solutions were transferred into a glass bottle, manually adjusted to pH 6.5 and purged with nitrogen for 1 h. A constant solution flux was provided by an peristaltic pump (Ismatec) through opaque and oxygen proof polyurethane tubing (Legris). For the duration of the experiment a low nitrogen overpressure was maintained in the storage bottles. Both columns and storage bottles were kept at room temperature (~21 °C) and covered in aluminium foil. All parts of the column setup and devices used for samples or storage were preconditioned in 1 % HNO₃ solution for 24 h and rinsed twice with deionized water.

Sampling intervals of 1.5 h were used at the beginning of the experiment to capture the breakthrough of the tracer Cl⁻ in the outflow with an autosampler. Later the inflow and outflow solutions were sampled manually by syringe from the percolate flux and the sampling ports. The sampling intervals were 1 d for the column outflow, 5-7 d for the inflow, and 7-10 d for the ports. The sampling solution was immediately acidified with 1 % HNO₃, and analyzed for total As, Fe(II), Fe(III), S(-II), DOC and dissolved inorganic carbon (DIC)CO₂ concentration. A stirred flow through cell was used for pH measurements. The experiments were terminated after between 12-40 pore volumes.

After the experiments, the column material was removed under argon gas in segments of 2.7-2.9 cm length, which were immediately frozen in liquid nitrogen and freeze dried. Dried subsamples of 1g mass were sequentially extracted with 1 mol L⁻¹ MgCl₂, 1 mol L⁻¹ NaH₂PO₄ (pH 5) and 1 mol L⁻¹ HCl to analyze the exchangeable, specifically sorbed and amorph Fe hydroxide bound As (Keon et al., 2001). Between the extraction steps the samples were rinsed with deionized water. Separate 1 g subsample were subjected to treatment with 6 mol L⁻¹ HCl (30 min at 60°C, (Regenspurg and Peiffer, 2005)) and the TRIS method (Fossing and Jorgensen, 1989) to extract crystalline Fe hydroxides and reduced sulfide phases (FeS₂, FeS, S⁰). All extractions were performed in duplicates and extract solutions were analyzed for concentrations of total As, Fe and S. Column porosity was determined gravimetrically.

Analytical procedures

The pH measurements were carried out with a WTW SenTix21 pH-electrode. Photometric measurements were made immediately after sampling. Fe(II) was measured photometrically at 512 nm

with the phenanthroline method (Tamura et al., 1974). Total Fe was determined with the same method after reduction of present Fe(III) to Fe(II) with ascorbate and Fe(III) was calculated by difference. H₂S was measured photometrically at 660 nm with the methylenblue method (Cline, 1969). To analyze solutions by ion chromatography, samples were filtered immediately after sampling (0.2 µm Nylon, Roth), and diluted 1 to 10. Nitrate, sulfate and chloride were determined with a Metrohm IC system (Metrosep Anion Dual 3 column, 0.8 mL flow rate, chemical suppression). Dissolved organic carbon concentrations were determined as non-purgable organic carbon (NPOC) after filtration (0.45 µm Nylon, Roth) on a Shimadzu TOC Analyzer V CPN. Solute inorganic carbon was measured by headspace technique in 1.4 ml GC vial on an Agilent 6890 GC with TCD detection (Blodau and Knorr, 2006) after acidification of 0.5 mL sample to pH<2. Arsenic was measured by graphite furnace atom absorption spectroscopy (Zeenit 60, Analytik Jena).

Calculations

The breakthrough of the Cl⁻ was approximated by inverse modelling with the CXTFIT software (Toride et al., 1999). The model is based on convection dispersion equation (Eq. 1) and uses concentration over time data, column geometry and porosity values to determine mean porewater velocity and dispersion coefficient. Peclet numbers derived by Eq. 2 characterize the column flow regime.

$$\frac{\partial}{\partial t} (\theta * c) = \frac{\partial}{\partial x} \left(\theta * D * \frac{\partial c}{\partial x} - J_w * c \right) \quad \text{Equation 1}$$

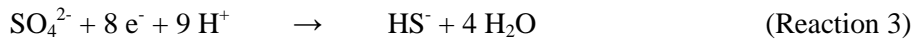
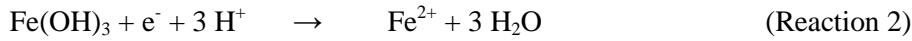
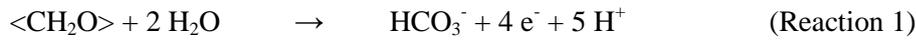
$$v_p = \frac{J_w}{\theta} \quad \text{Equation 2}$$

$$Pe = \frac{v_p * x}{D} \quad \text{Equation 3}$$

c: concentration [M L⁻³]; D: Dispersion coefficient [L² T⁻¹]; J_w:water flux density [L T⁻¹]; θ: water content [L³ L⁻³]; t: time [T]; x: length [L]; v_p: mean porewater velocity [L T⁻¹]; Pe: Peclet number;

Cumulative amounts of As, Fe, S, DOC and CO₂ export were derived from measured concentrations for a time interval multiplied by the water flux. Lacking concentration data was substituted by average values from of the previous and the subsequent time step. The mass balance calculations consider the initial input of Fe and As with the quartz sand, the aqueous inflow and outflow of Fe, As, H₂S and DIC, and the amount of Fe, As and S recovered from the solid phase material at the end of the experiment. The electron balance was calculated for every column

considering the redox reactions 1 to 4 and using the cumulative amounts of Fe, S and CO₂ in the outflow. Aquatic Fe was interpreted as Fe²⁺.



Results

Hydraulic and hydrochemical boundary condition

Chloride breakthrough occurred after one pore volume and was similar in all four columns. The Cl⁻ concentration over time could be adequately reproduced by inverse CXTFIT modelling. Table 1 shows the flow rates, dispersion coefficients and Peclet number for the different columns resulting from model calculations. High Peclet numbers above 10 and low dispersion indicate an advection dominated system. The residence times in the column were in the range of 1-2 days, such representing sufficient time for chemical reaction.

In the input solution, the pH was between 6.5 and 6.6 and all column effluents reached this value during the first pore volumes. For the duration of the experiments 1-3 the pH remained constant. Only in column 4 a further increase was observed after 25 pore volumes with maximum values of pH 7.3. Apparently MES concentration was insufficient to buffer the amount of proton consumption by other processes in the final stage of C4 and stabilize pH.

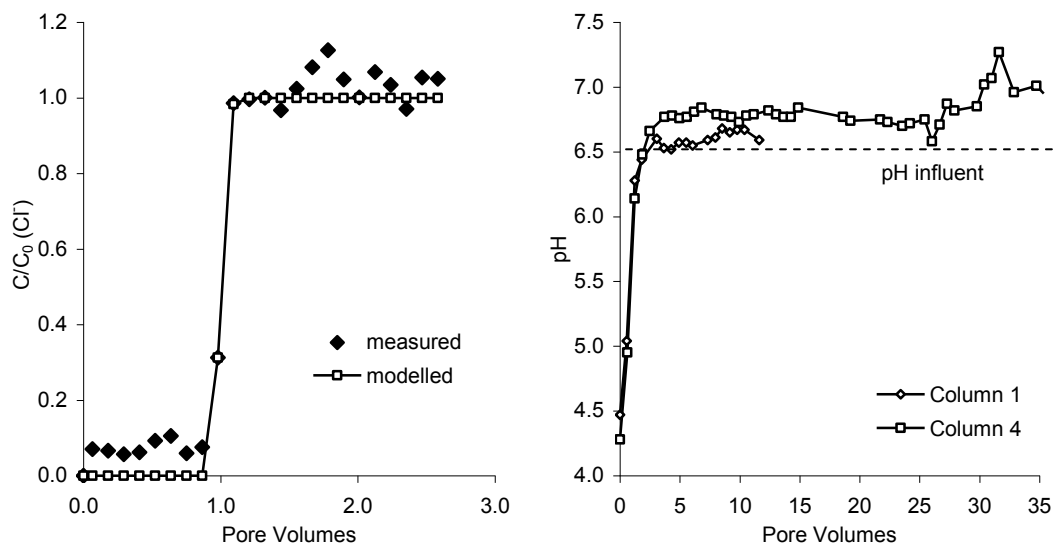


Figure 47 Time series of chloride breakthrough (S1), CXT fit (S1), and pH in the effluent of S1 and S4.

Table 18 Column hydraulic characteristics, Peclet number and residence time

Column	Pore water velocity	Dispersivity	Peclet number	Residence Time
	cm d ⁻¹	cm		D
C1	15.3	0.022	1128	1.64
C2	13.8	0.136	184	1.80
C3	14.4	0.054	460	1.74
C4	15.4	0.035	713	1.62

Fe, S, As and C dynamics in the outflow

Concentrations of Fe, S and As in the column outflow over time are shown in figure 2. The pore volumes needed to induce Fe export increased in the order C4 (3 PV) < C3 (9 PV) < C2 (20 PV) and no Fe was found in C1 after 12 PV. Maximum outflow Fe concentrations occurred within 5 pore volumes after first Fe appearance and decreased in the order C4 (597 $\mu\text{mol L}^{-1}$) > C3 (447 $\mu\text{mol L}^{-1}$) > C2 (37 $\mu\text{mol L}^{-1}$). The following decline of aqueous Fe in the outflow was faster in C4 than in C3 and C2. The strong fluctuation in C4 between PV 15 and 20 was due to a 24 h stop in the flow. This unintended event apparently caused a strong decrease in Fe concentrations at the first subsequent sampling date and subsequently an increase. Fe export continued until the experiments were stopped except for C4, where no Fe was determined in the outflow after 30 pore volumes.

No aqueous sulfide was found in the outflow of C1 and C2 and only low concentrations were found in the two samples taken after 22 and 24 PV from C3 (25 $\mu\text{mol L}^{-1}$). Much higher concentrations of up to 700 $\mu\text{mol L}^{-1}$ occurred in C4 subsequent to PV 24, but after a H₂S maximum (PV 30) concentrations continued to decrease until the end of the experiment. In the same period sulphate concentrations in the outflow were substantially lower than in the inflow.

Aqueous As concentration in the effluent was low and constant at 1 $\mu\text{mol L}^{-1}$ throughout the duration of experiment C1. The experiments C2 and C4 instead showed low initial values, but a strong increase of As concentrations in the outflow after 4 to 25 pore volumes with peak values of 14 to 25 $\mu\text{mol L}^{-1}$, which slowly decreased over time and dropped to zero in C4 after 35 pV. C3 initially contained lower amounts of As and therefore maximum concentrations were only 0.5 $\mu\text{mol L}^{-1}$ after 6 PV and dropped to zero quickly.

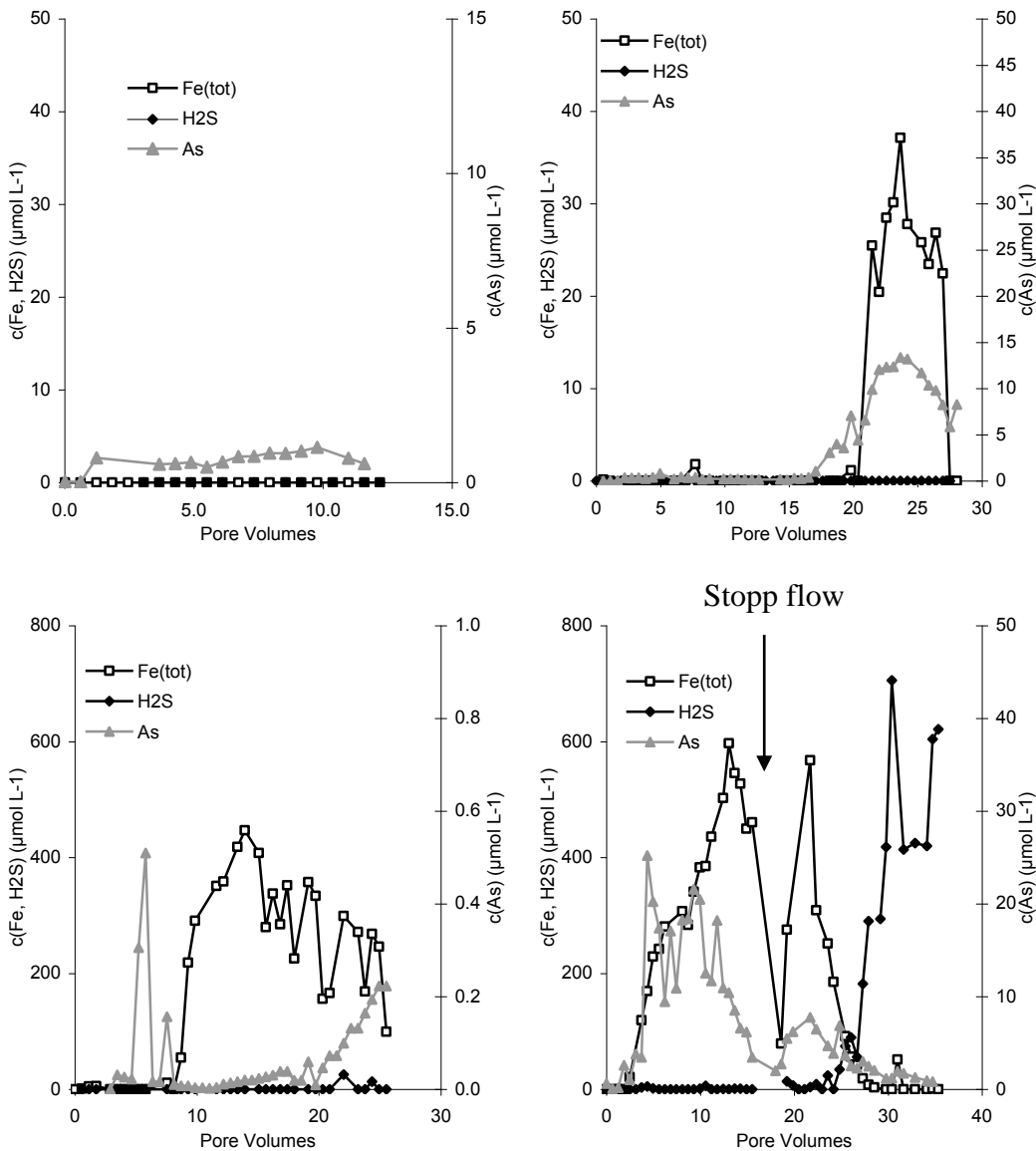


Figure 48 Effluent concentrations of column 1-4 of Fe, S and As

Fe, S and As dynamics in the sampling ports

Substantial changes in port sample concentrations were only observed for C3 and C4 experiments (Figure 3). In C4 aqueous Fe increased uniformly in all ports during the first 20 to 22 days (10-12 PV) and reached concentrations up to $360 \mu\text{mol L}^{-1}$. Subsequently concentrations decreased, reaching low values after day 35 d on the inflow side and after 45 d on the outflow side of the column. Sulfide concentration in C4 also increased uniformly in all ports after day 25 and had peak values of $150 \mu\text{mol L}^{-1}$ around day 50 (30 PV). The As distribution had two maximum values (day 11 and 35) of which the second one occurred only at the column effluent. The Fe and S distribution in C3 was similar to C4 but, similar to the outflow data concentrations were lower and peak values were reached later.

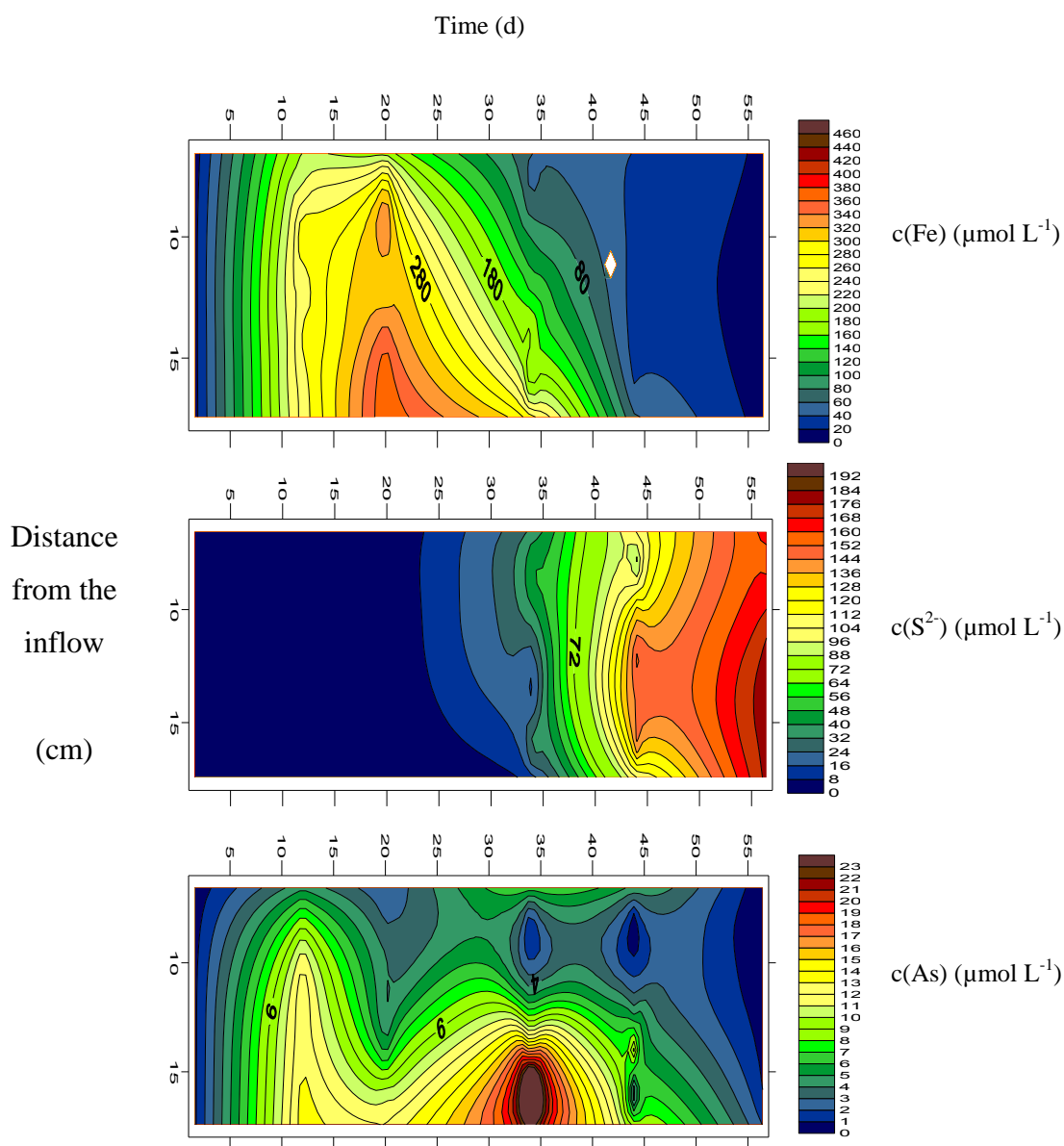


Figure 49 Time series of the concentration of Fe, S²⁻ and As in the sampling ports

Solid phase content of Fe, S and As

Fe extractable with 1 mol L⁻¹ HCl was equally distributed along the flowpath in C1 and 2, representing ~95 % of initial Fe (Figure 4). In the other experiments Fe content increased towards the column effluent and only 61 % in C3 respectively 37 % in C4 of initially added Fe were recovered. An amount of 0.07 and 0.41 mmol S were present in C3, respectively, C4 at the end of the experiment and TRIS was the main form of S present. The maximum content in C3 was in the first column half, while in C4 highest concentrations were in the central part of the column.

The amount of exchangeable As was about 7 μmol in the column material of C1 and C2, and 2.5 μmol in C4. Specifically sorbed As was only found in C1 with 23 μmol. Most As was released together with Fe in the 1 mol L⁻¹ HCl extract. The As content of this fraction at the end of the

experiments was 68 μmol C1, 107 μmol in C2, and 8 μmol in C4. While As contents in C1 and C2 were similar and uniformly distributed, the sand in C4 was almost depleted of As.

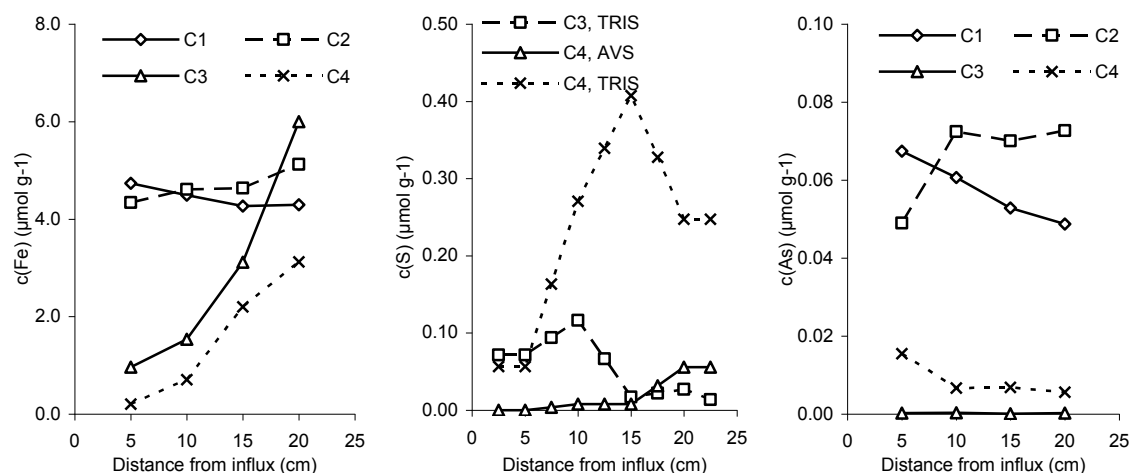


Figure 50 Solid phase distribution along the flowpath of Fe extracted with HCl, S extracted with TRIS and AVS, and total As contained in the fractions extracted with MgCl_2 , phosphate and HCl.

Mass and electron balances

The input and output of Fe, S, As and C in the solid and the aqueous phase is summarized for all columns in Table 2. The mass balances for all species strongly depended on the inflow DOC concentration. Higher DOC input resulted in an increased aqueous phase export of Fe, As, H_2S and CO_2 from the column. For the species Fe and As initially added with the quartz sand this lead to lower content in the solid phase at the end of the experiments. The increase in H_2S and CO_2 outflow instead must be due to production from SO_4^{2-} and DOC within the column.

Table 19 Mass balance of Fe, As H_2S and CO_2 and electron balance in the columns C1 to C4.

	Fe	As	H_2S	CO_2												
	mmol	μmol	mmol	mmol												
Column	C1				C2				C3				C4			
Solid (initial)	8.21	96.07	0.00	nd	8.75	115.31	0.00	0.00	8.85	1.84	0.00	0.00	6.86	92.71	0.00	0.00
Solute inflow	0.00	0.00	0.00	nd	0.00	0.00	0.00	1.61	0.00	0.00	0.00	1.93	0.00	0.00	0.00	12.16
Solute outflow	0.00	4.97	0.00	nd	0.08	43.91	0.00	2.21	2.30	0.06	0.01	2.80	3.09	92.76	1.68	15.38
Solid (final)	7.89	102.00	0.00	nd	8.28	114.00	0.00	nd	5.46	0.39	0.07	nd	2.55	14.90	0.41	nd
Mass balance	0.32	-10.90	0.00		0.39	-42.61	0.00	-0.60	1.10	1.39	-0.08	-0.88	1.22	-14.95	-2.09	-3.22
Electron balance	0.00		0.00	0.00	0.08		0.00	-2.41	2.30		0.63	-3.50	3.09		16.73	-12.88

Discussion

Dissolved organic matter (DOM) input can increase Fe and As mobility in aquifers by inducing anaerobic conditions required for microbial Fe reduction (McArthur et al., 2004). We expected that the rate of Fe and As release would depend on the DOM concentration provided with the inflow, i.e. the DOM load. Furthermore we hypothesized that a high DOM load, i.e. a limitation of bacterial Fe reduction by the availability of ferric Fe rather than electron donors would initiate sulphate reduction and immobilize As in the column by precipitation of sulphide minerals and incorporation or sorption of As. Physicochemical effects of DOM, i.e. As desorption or reduction, have been documented in chemical laboratory batch systems but their importance in presence of microorganisms is yet unclear. As the hydrodynamic conditions and the pH were similar in all four columns, differences in As concentrations and efflux can be attributed to the concentration of DOC in the inflow solution.

Influence of DOC concentration on C turnover and microbial activity

The production of ferrous Fe and sulfide requires reducing conditions in column 2-4, which were induced by microbial activity. The inoculated, peat derived bacteria oxidized degradable organic molecules in the leaf litter extract to CO₂ within the column as can be seen from the carbon mass balance between inflow and outflow (-0.6 to -3.2 mmol) in Table 2. The CO₂ surplus increased with rising DOC inflow concentration, indicating longer experimental duration but also higher microbial CO₂ production for higher substrate availability. The exact chemical composition of the leaf litter extract was not determined, but a high concentration of easily degradable fatty acids, i.e. acetate, propionate and butyrate, can be inferred from preliminary experiments (D. Burkhardt, personal communication). Various species of microorganisms are capable to respire these compounds to produce energy while inducing the reduction of As, Fe and S (Heimann et al., 2007).

High DOC input apparently increased the microbial activity and the rate of reduction processes. The results of the carbon budget should be treated qualitatively. It is unclear which carbon components were preferentially used and there was a large discrepancy between DOC loss and CO₂ production on a carbon basis. The processes not covered by the applied analytical methods include organic matter sorption in the column (Grafe et al., 2002) or formation of C containing minerals such as siderite (Lovley et al., 1998).

Influence of DOC concentration on Fe(II) and S(-II) formation

An increase in DOC inflow concentration also increased the maximum concentrations of Fe(II) and S(-II) in the outflow and the total quantities exported. The Fe(III) and S(IV) reduction during bacterial organic matter oxidation to CO₂ increased with the availability of organic substrates. Reduction of the amorphous Fe hydroxides under these conditions provided a higher energy yield than sulphate reduction, explaining the earlier increase in aqueous Fe(II) compared to H₂S. Providing higher DOC substrate concentrations also reduced the time until Fe(II) and S(-II) first appeared in outflow and sampling ports, indicating a adjustment of reducing conditions. The concentration

increase took place at the same time in all sampling ports along the flow path and no distinct redox zonation was visible in the column port concentration. The decrease of Fe concentrations, however, clearly occurred first at the inflow side of the columns, which were also depleted of iron hydroxides at the end of the experiment. A uniform increase of Fe(II) and S(-II) concentrations in all ports possibly was due to the high advection rates, concealing the occurrence of zones with strong Fe or S reduction for instance at the inflow side of the column.

In batch and column experiments with purified bacterial strains and low molecular fatty acids as substrate the increase of aqueous Fe(II) reached maximum within 5-10 d (Herbel and Fendorf, 2006; Islam et al., 2004; Kocar et al., 2006; Tadanier et al., 2005). Only at high DOC concentration in column C4 Fe was more quickly released, possibly due to longer adaption times for microbial communities and the higher complexity of the organic substrate in our experiments. The weakly crystalline ferrihydrite used in our experiments represents an easily reducible Fe phase (Koatka and Neelson, 1995; Roden and Zachara, 1996).

Influence of DOC concentrations on As mobilization

At the beginning all As was sorbed to the Fe hydroxide coated quartz sand as As(V) and As mobility was low in the first phase of all column experiments, which is characterized by absence of aqueous Fe, S and As in the outflow. Redox conditions in this phase were still too high for substantial Fe or sulphate reduction. A transfer of As from the solid to the liquid phase, i.e. due to desorption or reduction by DOM, was not observed and apparently of little importance in these microbial systems (Bauer and Blodau, 2006; Grafe et al., 2002; Tongesayi and Smart, 2006). C1 within the time of operation did not proceed beyond phase 1 and As was always mobile in low concentrations. Our results regarding this column also contrast findings of (Herbel and Fendorf, 2006), who found a much stronger As release in absence of microorganisms. We attribute this observation to the much more complex and high ionic strength solution, they used as carrier solution.

Chemical conditions in the second phase of the column experiments were characterized by Fe reducing conditions. The increase in aqueous Fe(II) concentrations in outflow and ports must be caused by reduction and dissolution of the ferrihydrite solid phases within the column. Export of Fe(II) from the column was supported by a decreased solid phase Fe content, particularly in C3 and C4. Concurrently with the beginning of Fe(II) export the colour of Fe mineral in the column changed from red-brown to grey-black. Transformation of ferrihydrite ($\text{Fe}(\text{OH})_3$) to magnetite (Fe_3O_4) occurs under high Fe(II) concentrations and might explain this colour change (Pedersen et al., 2006). One of three Fe atoms in magnetite is in the reduced Fe(II) form, so the substantial Fe(II) content (25 % of total Fe) in the 1 mol L^{-1} HCl solid phase extracts of C3 and C4 supports magnetite formation within the column. We can unfortunately not exclude the formation of other Fe(II) containing minerals, i.e. siderite.

Dissolved As concentrations increased directly before Fe(II) in the outflow after 20 PV in C2, 7 PV in C3 and 4 PV in C4. This pattern was also observed in previous studies (Herbel and Fendorf, 2006; Kocar et al., 2006) and suggests that the onset of reductive processes and the dissolution of the sorbing Fe phase was responsible for As mobilization. Even though As speciation was not determined, the predominance of As(III) in the aqueous phase can be inferred from previous studies (Herbel and Fendorf, 2006; Kocar et al., 2006; Sierra-Alvarez et al., 2005). Therefore As mobilization may have resulted from easier desorption after reduction and from release because of dissolution of the sorbent Fe hydroxides. In C2 As and Fe(II) were released in low concentrations compared to C3 and C4 and at an almost constant rate. No mineral colour change was observed there. In contrast, aqueous As in C3 and C4 declined after an initial high concentration pulse. This might suggest that after initially high As release, immobilization or incorporation of mobile As occurred during transformation of ferrihydrite to magnetite in C3 and C4 and that this process did not take place in C2 (Herbel and Fendorf, 2006; Kocar et al., 2006).

A second colour change from grey-black to the white of the quartz sand started in C3 and C4 towards the end of the experiments concurrently with appearance of high aqueous H₂S concentration. Fe(II) and As concentration in the outflow instead decreased and eventually dropped to zero. We attribute this to the low availability of reducible Fe solid phases within the column, leading microorganisms to use sulphate as electron acceptor during organic matter oxidation.

Our data set does not provide information on the mineral phases present and the dissolution, precipitation or transformation reactions occurring in C4 in the final stage of the experiment. In the ports of C4 Fe(II) and S(-II) was present at the same time and even though H₂S was exported, solid phase Fe was still present near the outflow of the column. Both microbial reduction (Koatka and Nealson, 1995) or chemical Fe reduction by produced H₂S (Poulton et al., 2004) may therefore have been involved in the depletion of solid phase Fe. Fe was more and more depleted from the column, but most of the remaining Fe was in the ferric form. This suggests the presence of ferrihydrite residues or magnetite and excludes a high importance of reduced Fe phase, i.e. siderite or sulphide. Nonetheless substantial amounts of sulphide were immobilized mainly in the central part of the column.

The export of As from C4 dropped to zero some pore volumes after Fe(II), when more than 90 % of As was already removed from the column under the Fe reducing conditions. The small remaining solid phase fraction was equally distributed in the column and apparently not associated with Fe or S phases. This does not exclude As incorporation in sulphide minerals (O'Day et al., 2004).

Conclusions

Our experiments corroborate earlier studies about the reductive mobilization of As from Fe phases in column experiments. Raising DOM input concentration did not change the sequence of redox processes, but increased the release of DIC, As, Fe(II), and S(-II). Arsenic export was coupled to reductive Fe hydroxide dissolution and Fe hydroxide transformation processes. Sulphate reduction was

observed only when Fe hydroxides were almost depleted in the column and most Fe and As had already been exported. Our hypothesis that raising the DOM load would lead to concurrent reduction of Fe hydroxides and sulphate, and in turn to a partial immobilization of released As with sulphides could not be confirmed. We cannot say to what extent such results can be extrapolated to aquifer materials, but possibly the high reactivity of the freshly precipitated Fe hydroxides played a role for the predominance of Fe reduction. Low amounts of As remained in the column in unidentified form and a preferential association with remaining Fe phases or formed sulphide minerals could not be observed. This is most likely due to the temporal decoupling of As mobilization and sulphate reduction, preventing As(III) and S(-II) concentrations to increase concurrently. Physicochemical As mobilization by sorption competition between DOM and As or chemical reduction with organic matter was not observed. Given the low initial As concentrations in the outflow, a release of substantial quantities of DOM stabilized Fe colloids also seems unlikely. We do not exclude the occurrence of these processes in the studied column experiments, but their importance for overall As mobilization was low compared to the effects of microbial Fe reduction.

Acknowledgments

We thank German Research foundation (DFG) for their support through grant BL563/7-2 to Christian Blodau.

References

- Bauer M. and Blodau C. (2006) Mobilization of arsenic by dissolved organic matter from iron oxides, soils and sediments. *Sci. Tot. Environ.* **354**, 179-190.
- Blodau C. and Knorr K.-H. (2006) Experimental inflow of groundwater induces a "biogeochemical regime shift" in iron-rich and acidic sediments. *J. Geophys. Res.* **111**(G2), G02026.
- Cline J. D. (1969) Spectrofluorometric determination of hydrogen sulfide in natural waters. *Limnol. Oceanogr.* **14**, 454-458.
- Dixit S. and Hering J. G. (2003) Comparison of arsenic(V) and arsenic(III) sorption onto iron oxide minerals: Implications for arsenic mobility. *Environ. Sci. Technol.* **37**(18), 4182-4189.
- Fossing H. and Jorgensen B. B. (1989) Measurement of bacterial sulfate reduction in sediments: Evaluation of single step chromium reduction method. *Biogeochemistry* **8**, 205-222.
- Geelhoed J. S., Hiemstra T., and Van Riemsdijk W. H. (1998) Competitive interaction between phosphate and citrate on goethite. *Environ. Sci. Technol.* **32**, 2119-2123.
- Ghosh A., Mukiibi M., Saez A. E., and Ela W. P. (2006) Leaching of arsenic from granular ferric hydroxide residuals under mature landfill conditions. *Environ. Sci. Technol.* **40**(19), 6070-6075.
- Gonzalez Z. I., Krachler M., Cheburkin A. K., and Shotyk W. (2006) Spatial distribution of natural enrichments of arsenic, selenium, and uranium in a minerotrophic peatland, Gola di Lago, Canton Ticino, Switzerland. *Environ. Sci. Technol.* **40**(21), 6568-6574.
- Grafe M., Eick M. J., Grossl P. R., and Saunders A. M. (2002) Adsorption of arsenate and arsenite on ferrihydrite in the presence and absence of dissolved organic carbon. *J. Environ. Qual.* **31**(4), 1115-1123.
- Heimann A. C., Blodau C., Postma D., Larsen F., Viet P. H., Nhan P. Q., Jessen S., Duc M. T., Hue N. T. M., and Jakobsen R. (2007) Hydrogen Thresholds and Steady-State Concentrations Associated with Microbial Arsenate Respiration. *Environ. Sci. Technol.* **41**(7), 2311-2317.
- Herbel M. and Fendorf S. (2006) Biogeochemical processes controlling the speciation and transport of arsenic within iron coated sand. *Chem. Geol.* **228**, 16-32.
- Islam F. S., Gault A. G., Boothman C., Polya D. A., Charnock J. M., Chatterjee D., and Lloyd J. R. (2004) Role of metal-reducing bacteria in arsenic release from Bengal delta sediments. *Nature* **430**(6995), 68-71.
- Keon N. E., Swartz C. H., Brabander D. J., Harvey C., and Hemond H. F. (2001) Validation of an arsenic sequential extraction method for evaluating mobility in sediments. *Environ. Sci. Technol.* **35**(13), 2778-2784.
- Koatka J. E. and Nealson K. H. (1995) Dissolution and reduction of magnetite by bacteria. *Environ. Sci. Technol.* **29**, 2535-2540.
- Kocar B., Herbel M., Tufano K., J., and Fendorf S. (2006) Contrasting effects of dissimilatory iron(III) and arsenic (V) reduction on the arsenic retention and transport. *Environ. Sci. Technol.* **40**, 6715-6721.
- Koeber R., Daus B., Ebert M., Mattusch J., Welter E., and Dahmke A. (2005) Compost-Based Permeable Reactive Barriers for the Source Treatment of Arsenic Contaminations in Aquifers: Column Studies and Solid-Phase Investigations. *Environ. Sci. Technol.* **39**(19), 7650-7655.
- Lovley D. R., Fraga J. L., Blunt-Harris E. L., Hayes L. A., Phillips E. J. P., and Coates J. D. (1998) Humic Substances as a Mediator for Microbially Catalyzed Metal Reduction. *Acta hydrochim. hydrobiol.* **26**(3), 152-157.

- Lovley D. R. and Goodwin S. (1988) Hydrogen concentrations as an indicator of the predominant terminal electron-accepting reactions in aquatic sediments. *Geochim. Cosmochim. Acta* **52**(12), 2993-3003.
- Mandal B. K. and Suzuki K. T. (2002) Arsenic round the world: A review. *Talanta* **58**, 201-235.
- McArthur J. M., Banerjee D. M., Hudson-Edwards K. A., Mishra R., Purohit R., Ravenscroft P., Cronin A., Howarth R. J., Chatterjee A., Talukder T., Lowry D., Houghton S., and Chadha D. K. (2004) Natural organic matter in sedimentary basins and its relation to arsenic in anoxic groundwater: the example of West Bengal and its worldwide implications. *Appl. Geochem.* **19**, 1255-1293.
- Meharg A. A., Scrimgeour C., Hossain S. A., Fuller K., Cruickshank K., Williams P. N., and Kinniburgh D. G. (2006) Codeposition of organic carbon and arsenic in Bengal Delta aquifers. *Environ. Sci. Technol.* **40**(16), 4928-4935.
- O'Day P. A., Vlassopoulos D., Root R., and Rivera N. (2004) The influence of sulfur and iron on dissolved arsenic concentrations in the shallow subsurface under changing redox conditions. *Proceedings of the National Academy of Sciences of the United States of America* **101**(38), 13703-13708.
- Paul S., Kusel K., and Alewell C. (2006) Reduction processes in forest wetlands: Tracking down heterogeneity of source/sink functions with a combination of methods. *Soil Biology & Biochemistry* **38**(5), 1028-1039.
- Pedersen H. D., Postma D., and Jakobsen R. (2006) Release of arsenic associated with the reduction and transformation of iron oxides. *Geochim. Cosmochim. Acta* **70**(16), 4116-4129.
- Poulton S. W., Krom M. D., and Raiswell R. (2004) A revised scheme for the reactivity of iron (oxyhydr) oxide minerals towards dissolved sulfide. *Geochim. Cosmochim. Acta* **68**(18), 3703-3715.
- Regenspurg S. and Peiffer S. (2005) Arsenate and chromate incorporation in Schwertmannite. *Appl. Geochem.* **20**, 1226-1239.
- Roden E. E. and Zachara J. M. (1996) Microbial reduction of crystalline iron(III) oxides: Influence of oxide surface area and potential for cell growth. *Environ. Sci. Technol.* **30**(5), 1618-1628.
- Sierra-Alvarez R., Field J. A., Cortinas I., Feijoo G., Moreira M. T., Kopplin M., and Gandolfi A. J. (2005) Anaerobic microbial mobilization and biotransformation of arsenate adsorbed onto activated alumina. *Water Res.* **39**(1), 199-209.
- Smedley P. L. and Kinniburgh D. G. (2002) A review of the source, behaviour and distribution of arsenic in natural waters. *Appl. Geochem.* **17**(5), 517-568.
- Tadanier C. J., Schreiber M. E., and Roller J. W. (2005) Arsenic mobilization through microbially mediated deflocculation of ferrihydrite. *Environ. Sci. Technol.* **39**(9), 3061-3068.
- Tamura H., Goto K., Yotsuyan.T, and Nagayama M. (1974) Spectrophotometric Determination of Iron(Ii) with 1,10-Phenanthroline in Presence of Large Amounts of Iron(Iii). *Talanta* **21**(4), 314-318.
- Tongesayi T. and Smart R. B. (2006) Arsenic speciation: Reduction of arsenic(v) to arsenic(III) by fulvic acid. *Environm. Chem.* **3**(2), 137-141.
- Toride N., Leij F. J., and Van Genuchten M. T. (1999) The CXTFIT code for estimating transport parameters from laboratory or field tracer experiments.

Study 8

Reproduced with permission from

**Arsenic speciation and turnover in intact organic soil mesocosms during
experimental drought and rewetting**

Christian Blodau, Beate Fulda, Markus Bauer, Klaus-Holger Knorr

Geochimica et Cosmochimica Acta, 2008, 72, pp 3991-4007

Copyright 2008 Elsevier B.V.



Arsenic speciation and turnover in intact organic soil mesocosms during experimental drought and rewetting

Christian Blodau^{*}, Beate Fulda, Markus Bauer, Klaus-Holger Knorr

Limnological Research Station, Department of Hydrology, University of Bayreuth, D-95440 Bayreuth, Germany

Received 28 August 2007; accepted in revised form 22 April 2008; available online 27 May 2008

Abstract

Wetlands are significant sources and sinks for arsenic (As), yet the geochemical conditions and processes causing a release of dissolved arsenic and its association with the solid phase of wetland soils are poorly known. Here we present experiments in which arsenic speciation was determined in peatland mesocosms in high spatiotemporal resolution over 10 months. The experiment included a drought/rewetting treatment, a permanently wet, and a defoliated treatment. Soil water content was determined by the TDR technique, and arsenic, iron and sulfate turnover from mass balancing stocks and fluxes in the peat, and solid phase contents by sequential extractions. Arsenic content ranged from 5 to 25 mg kg⁻¹ and dissolved concentrations from 10 to 300 µg L⁻¹, mainly in form of As(III), and secondarily of As(V) and dimethylated arsenic (DMA). Total arsenic was mainly associated with amorphous iron hydroxides ($R^2 > 0.95$, $\alpha < 0.01$) and deeper into the peat with an unidentified residual fraction. Arsenic release was linked to ferrous iron release and primarily occurred in the intensely rooted uppermost soil. Volumetric air contents of 2–13 % during drought eliminated DMA from the porewater and suppressed its release after rewetting for >30 d. Dissolved As(III) was oxidized and immobilized as As(V) at rates of up to 0.015 mmol m⁻³ d⁻¹. Rewetting mobilized As(III) at rates of up to 0.018 mmol m⁻³ d⁻¹ within days. Concurrently, Fe(II) was released at depth integrated rates of up to 20 mmol m⁻³ d⁻¹. The redox half systems of arsenic, iron, and sulfur were in persistent disequilibrium, with H₂S being a thermodynamically viable reductant for As(V) to As(III). The study suggests that rewetting can lead to a rapid release of arsenic in iron-rich peatlands and that methylation is of lesser importance than co-release with iron reduction, which was largely driven by root activity.

© 2008 Published by Elsevier Ltd.

1. INTRODUCTION

Arsenic (As) is a ubiquitous trace metalloid in sedimentary formations and ground waters and concentrations often exceed recommended drinking water standards (Smedley and Kinniburgh, 2002). The best known example in this respect are elevated arsenic concentration levels in aquifers of Bangladesh, where a population of about 57 million is threatened by consumption of high arsenic ground waters (BGS and DPHE, 2001). The mechanisms and geochemical conditions by which arsenic is mobilized in the subsurface are thus of great interest and have become

increasingly a focus of geochemical research over the past years. Previous work documented that redox conditions, physicochemical surface processes, and microbial mediation are important regulators of arsenic dynamics (Marschleyn et al., 1991; Bissen and Frimmel, 2003). Arsenic occurs mainly as inorganic arsenate, here referred to as As(V), under oxic conditions. It can be chemically and microbially reduced to arsenite, here referred to as As(III), when oxygen is depleted (Smedley and Kinniburgh, 2002). Most recently, thio-derivatives of arsenic oxyanions have been identified as a further, important group of arsenic species in sulfidic waters (Wallschäger and London, 2008). Methylation of inorganic species is also carried out by aerobic and anaerobic microorganisms, which produce monomethylarsonic acid (MMA), dimethylarsinic acid (DMA) and trimethylarsine oxide (TMAO); and further

^{*} Corresponding author. Fax: +49 921 55 2049.

E-mail address: christian.blodau@uni-bayreuth.de (C. Blodau).

organic species of biogenic origin have been found (Cullen and Reimer, 1989). Both the toxicity and mobility of arsenic depends on its speciation. Generally inorganic species are more toxic and less mobile than the organic forms (Mandal and Suzuki, 2002). Among the inorganic species, As(III) and As(V) differ in their toxicity and adsorption characteristics depending on pH and competitors for sorption sites (Dixit and Hering, 2003).

Peat soils have often been used to trace atmospheric arsenic pollution (Shotyky, 1996) but relatively rarely been investigated with respect to arsenic biogeochemistry, although it has become evident that organic-rich soils are often highly enriched with arsenic and that pore water concentrations in these systems can be very high (Gonzalez et al., 2006). In particular, little is yet known about the mechanisms causing a phase transfer of arsenic from dissolved to solid state in organic-rich soils and the geochemical conditions and time scales involved. In less organic-rich aquifers, arsenic dynamics have been linked primarily to the redox processes of iron and sulfur. Arsenic may for example be mobilized in oxidized form through oxidation of arsenic-bearing pyrites (Zheng et al., 2004) and immobilized through formation of arsenic-sulfide minerals and adsorption to pyrite surfaces (Bostick and Fendorf, 2003). In absence of oxygen, arsenic was generally found to be released when ferric iron hydroxides are reduced, and this has been also speculated to be the case at minerotrophic wetland sites (Huang and Matzner, 2006). The mobility of arsenic is also influenced by sorption on iron, aluminum, and manganese hydroxides (Anderson et al., 1976; Dixit and Hering, 2003) and clay minerals (Manning and Goldberg, 1996). Of importance for the distribution of arsenic between dissolved and solid phase associated state are further the competition of arsenic with phosphate and dissolved organic matter (DOM) for sorption sites (Bauer and Blodau, 2006) and the binding of arsenic to organic matter, which may proceed through both covalent binding and metal bridges (Redman et al., 2002; Buschmann et al., 2006).

Most aquifer systems and wetlands differ in their biogeochemistry in important aspects, which makes extrapolation of arsenic dynamics from one to the other geochemical environment problematic. The high content of organic matter of organic soils can result in more abundant organic binding of arsenic, which may also be the direct or indirect cause for the observed accumulation of arsenic in wetlands (Gonzalez et al., 2006). Little is, however, known about the strength and stability of organic arsenic binding under changing geochemical conditions. The soils are also often intensely rooted, which leads to the development of structured microenvironments of greatly differing redox conditions and distribution of potential adsorption surfaces (Blute et al., 2004), and entails the release of easily decomposable substrates for respiration, e.g. by bacterial iron and sulfate reduction. Furthermore, most wetlands frequently undergo strong changes in redox conditions due to water table fluctuations, which typically occur during summer droughts. Such dynamics may in the future become more pronounced, as temperate and northern regions have been predicted to undergo wetter winters, and drier periods

and stronger rainstorms in summer (IPCC, 2001). A number of studies have already addressed the effects of drying and rewetting on arsenic mobility in soil samples and laboratory systems (McGeehan, 1994; Reynolds et al., 1999), or in the solid phase of agricultural and mine drainage contaminated field sites (La Force et al., 2000; Fox and Doner, 2003). In contrast, the *in situ* dynamics of geogenic or air-borne arsenic in intact peat soils during drought and rewetting, and the way arsenic dynamics is linked to anaerobic respiration and other redox processes is not well documented.

To improve our insight into the dynamics of arsenic in natural wetlands we conducted a mesocosm study with undisturbed soils of a northern fen, in which all boundary conditions could be controlled. Arsenic, iron, and sulfate turnover in the peat were quantified in high temporal and spatial resolution by mass balance. The impact of the vegetation was analyzed by comparing a defoliated to an intact mesocosm, and the effect of drying and rewetting by comparison to a mesocosm kept with high water level. Our specific objectives were (I) to identify the spatial distribution, speciation, and binding of arsenic in the peat, (II) to elucidate the short-term temporal dynamics of pore water arsenic concentrations and its coupling to other redox processes, and (III) to identify the potential importance of the vegetation for arsenic dynamics.

2. MATERIAL AND METHODS

2.1. Experimental setup and instrumentation

The minerotrophic Schläppnerbrunnen II peatland is part of the Lehstenbach watershed (4.2 km²), situated at an elevation of 700–880 m (50°08'38"N, 11°51'41"E, Fichtelgebirge, Germany). The average annual air temperature is 5 °C, and mean annual precipitation varies between 900 and 1160 mm with a maximum both in summer and winter (Huang and Matzner, 2006). The organic soils reach a depth of 40–70 cm, were classified as Fibric Histosol, and are spatially quite heterogeneous in elemental contents and vegetation patterns on the scale of meters. The vegetation is dominated by graminoid species with only few mosses. The mean *in situ* water level at the site is 13 ± 19 cm below surface, but may drop down to below 70 cm depth during summer. Especially close to the peatland surface, iron and sulfur contents in the peat may reach as much as >16 and >4 mg kg⁻¹, respectively (Paul et al., 2006). Three intact peat monoliths (60 cm diameter, 60 cm depth, 'mesocosms') were collected in September 2005 and incubated in a 15 °C climate chamber for 10 months (~60% RH, 12 h light/dark cycles, 660 μmol s⁻¹ photosynthetic photon flux). To this end a waste water tube with a wall strength of 2 cm and PVC lining was manually driven into the soil and dug out on all sides. The mesocosm was then tilted, which disconnected the mineral material beneath from the peat core, and a PVC bottom mounted and fixed with screws. A cap was also mounted on top to protect the vegetation. The mesocosm were rolled out of the pit on a wooden plank and transported to the laboratory. The water table position at time of sampling was at

about 30 cm below surface. Two mesocosms contained *Agrostis* sp. (bentgrass), *Nardus stricta* (mat-grass), *Molinia caerulea* (purple moor grass), *Sphagnum fallax* (flat topped bog moss), *Brachythecium rivulare* (river feather moss), *Atrichum undulatum* (common smoothcap) and *Galium hercynicum* (bedstraw). One of these, which was the only containing *Carex rostrata* (beaked sedge), was kept permanently wet ('Wet-Vegetation' or 'W-V'), and the other ('Drying/Wetting-vegetation' or 'DW-V') and a defoliated ('Drying/Rewetting-defoliated' or 'DW-D') were dried and rewetted. The vegetation had been eliminated by inhibiting vegetation growth after the winter of 2005 by covering the plot with a plastic sheet. The von Post index of peat decomposition (Staneck and Silc, 1977) increased from 3 on a scale of 1–10 at depths of 0–10 cm to 7–9 at a depth of 25–60 cm.

After 40 days (first 'dry period' or 'equilibration period') the water table was raised from about 30 to 10 cm below surface by irrigation with 30 (DW-V, DW-D) and 40 mm (W-V) in two days. The water table was then kept constant at 11.9 ± 1.3 cm (DW-V) or 9.9 ± 0.9 cm (DW-D) for 70 days ('wet period'), by irrigating up to 7 mm d^{-1} . Treatments DW-V and DW-D were subsequently dried out by reducing irrigation to 0 (DW-D) and 1 mm d^{-1} (DW-V) (second 'dry period') to a water table of 55 cm within 50 days. The mesocosms were then rewetted ('rewetted period') by irrigation with 54 (DW-V) and 53 mm (DW-D) within 2 (DW-V) and 5 (DW-D) days. During the rewetted period, the mean water table was held at 12.7 ± 1.8 (DW-V) and 9.8 ± 1.8 cm (DW-D). Time series of water table levels and volumes of irrigate applied are given in the Electronic annex (Fig. 1S). The irrigate was mixed according to precipitation chemistry at the site and contained Na^+ ($5 \mu\text{mol L}^{-1}$), Ca^{2+} ($6 \mu\text{mol L}^{-1}$), SO_4^{2-} ($10 \mu\text{mol L}^{-1}$), Cl^- ($12 \mu\text{mol L}^{-1}$), NH_4^+ and NO_3^- ($40 \mu\text{mol L}^{-1}$). The solution was equilibrated with atmospheric CO_2 , yielding a DIC concentration of $\sim 15 \mu\text{mol L}^{-1}$ and adjusted to a pH of 4.82 mixing SO_4^{2-} and H_2SO_4 for the concentration adjustment.

2.2. Sampling and analytical procedures

Volumetric gas content was derived using calibrated TDR probes at 10, 20, 30, and 40 cm depth (IMKO, Germany). All sensors had a comparable slope in the signal response of 0.22 ± 0.04 units per % volumetric water content, and we used relative changes in TDR measurements and the total porosity to calculate the gas content. Water tables were monitored in two piezometers per mesocosm, which were driven into the peat after pre-drilling and either screened from 15 to 25 cm or from 40 to 50 cm. Total porosity was measured by oven drying of 100 cm^3 samples.

Soil solution was sampled from Rhizon® samplers at depths of 5, 10, 15, 20, 30, 40, and 50 cm depth (microporous polymer, $<0.2 \mu\text{m}$ pore size, fibre glass support, 10 cm sampling length). The pH and concentrations of H_2S were determined immediately on sub-samples of extracted pore water using a glass electrode, and an amperometric micro-sensor (AMT) before day 145 of the experiment, respectively. Subsequently, H_2S was measured

at 665 nm using the methylene blue method (Cline, 1969). Dissolved Fe^{2+} and Fe_{tot} were determined immediately as well using the phenanthroline method (Tamura et al., 1974). Nitrate and sulfate was measured in filtered samples ($0.2 \mu\text{M}$, nylon syringe micro filter) by ion chromatography (Metrohm IC system, Metrosep Anion Dual 3 separation column at 0.8 mL min^{-1} flow rate, conductivity detection after chemical suppression). NH_4 was measured photometrically according to the method of Searle (1984). Concentrations of arsenic species As(III), As(V), DMA, and MMA were analyzed by High Performance Liquid Chromatography/Inductively Coupled Plasma Mass Spectrometry (HPLC-ICP/MS) according to Francesconi et al. (2002). Samples were filtered to $0.2 \mu\text{M}$ and were analyzed within two days, so that further stabilization was not necessary (McCleskey et al., 2004). The limit of detection (LOD) was $0.02 \mu\text{g L}^{-1}$. Total dissolved arsenic was quantified using Graphite Furnace Atomic Absorption Spectroscopy (Gf-AAS, Zeenit 60, Analytik Jena) following filtration by $0.45 \mu\text{m}$ and acidification with 1 vol % HNO_3 . LOD was $1.4 \mu\text{g L}^{-1}$. Concentrations below LOD were set to 0 in calculations.

To analyze the solid phase peat we obtained subcores of 3 cm diameter at the beginning of the experiment. The resulting voids were filled with prepared PVC tubes of the same diameter. Total arsenic in the peat was analyzed in 0.2 g of dried and ground sample in three analytical replicates following digestion using 9 mL of HNO_3 (65%) and 0.3 mL HCl (32 %) in a microwave digester (Berghof Speedwave). The digest was filled up to 100 mL and filtered to $0.45 \mu\text{m}$. Arsenic bound to reactive and total iron hydroxides was analyzed in duplicates subsequent to a sequential extraction. For the determination of operationally defined reactive iron, we extracted 0.3 g sample with 1 N HCl (30 mL) on a shaker for 24 h. This procedure dissolves amorphous and poorly crystalline iron hydroxides, acid volatile sulfur, siderite, vivianite and partly iron bound to chlorite minerals (Wallmann et al., 1993). Subsequently we extracted the residue with 6 N HCl (30 mL) at $70 \text{ }^\circ\text{C}$ for 30 min, which dissolves goethite and other well crystalline iron hydroxides (Cornell and Schwertmann, 1996). A precipitation of orpiment As_2S_3 in presence of As(III), H_2S , and acidic conditions has been reported (Smieja and Wilkin, 2003), which may lead to an underestimate of total arsenic concentrations in such solutions. Due to the oxic conditions during extraction, which lead to rapid oxidation of H_2S , we believe that a significant precipitation of orpiment was unlikely. The samples were centrifuged following extraction at 9800 rpm for 20 min, decanted, and the solution stored at $4 \text{ }^\circ\text{C}$. Concentrations of the elements Al, Ca, Fe, K, Mn, and Al were quantified in the extracts on an ICP-AES following internal calibration accounting for matrix effects. The content of total inorganic reduced sulfur compounds (TRIS: FeS_2 , FeS , S^0) was determined using the method of (Fossing and Jorgensen, 1989). Frozen peat samples were freeze dried and 2 g of the material boiled with HCl ($c = 5 \text{ mol L}^{-1}$) and CrCl_2 ($c = 0.15 \text{ mol L}^{-1}$) under a constant nitrogen stream. The H_2S released into the nitrogen stream was trapped in 50 mL of NaOH ($c = 0.15 \text{ mol L}^{-1}$) solution. The sulfide was precipitated

by addition of zinc acetate and determined photometrically as described above.

To characterize the depth distribution of root activity, we applied a ^{13}C - CO_2 pulse label for 1 h, filling a transparent chamber, which was tightly installed on the mesocosms, with a 63% ^{13}C - CO_2 atmosphere of ~ 900 ppm total CO_2 , and traced the label in soil CO_2 . We extracted CO_2 from pore water and air using nitrogen-filled silicon tubes of a diameter of 10 mm, which were horizontally installed at the same depth as rhizon porewater samplers. Equilibration time of the samplers was approx. 6 h. A volume of 2 ml was extracted and thereafter replaced by nitrogen. The isotopic signature of the soil CO_2 was measured using a Trace GC 2000 gas chromatograph connected via Combustion III interface to a DELTA^{plus} isotope ratio mass spectrometer (Thermo Finnigan MAT, Bremen, Germany).

2.3. Calculations, statistics, and visualization of data

The mesocosms represent a system that is closed at the bottom and, with the exception of the unsaturated zone, transport thus proceeded by diffusion. Net turnover of ferrous iron and arsenic in the peat could thus be calculated by mass balance from Eq. (1) for individual depth layers:

$$R_{t(i)} = \underbrace{\frac{d}{dz} \left(-D^w \cdot (\bar{\varphi})^2 \cdot \frac{dc_{t(i)}}{dx} \right)}_{\text{mean diffusive flux } \Delta J} + \underbrace{\left(\frac{dc_{t(i\pm 1)} \cdot \varphi}{dt_{t(i\pm 1)}} \right)}_{\text{mean change in storage } \Delta S} \quad (1)$$

D^w	diffusion coefficient in water ($\text{cm}^2 \text{d}^{-1}$)
φ	porosity (–)
c	concentration (nmol cm^{-3})
$c_{t(i)}$	mean of $c_{t(i-1)}$ and $c_{t(i+1)}$ in a depth increment
z	boundary between depth layers (cm)
x	sampling depth (cm)
t	time (d)
$t(i)$	time between sampling $t(i-1)$ and $t(i+1)$

$R_{t(i)}$ represents the sum of changes in dissolved storage ΔS within a depth layer in a time period $t(i \pm 1)$, and the mean diffusive flux ΔJ at time $t(i)$, which is calculated from the mean concentration gradients in period $t(i \pm 1)$. The diffusion coefficient of arsenic (HASO_2^{2-}) ($7.18 \times 10^{-6} \text{ cm}^2 \text{d}^{-1}$) and of Fe(II) ($5.42 \times 10^{-6} \text{ cm}^2 \text{d}^{-1}$) were calculated for water and 15 °C using a linear temperature correction according to (Lerman, 1979) and corrected for porosity φ using $D = D_0\varphi^2$. The diffusive flux at the upper and lower boundary of upper- and lowermost depth layers 1 and 7 was set to 0. To reduce noise, ΔS was calculated using the floating mean of concentrations of the two preceding and following sampling dates. For the calculation of total turnover in the peat, the turnover in individual depth layers were integrated over depth. $R > 0$ was defined as release into the dissolved phase.

The thermodynamics of potential elemental transformations in the peat was analyzed by calculating redox potentials for the individual half redox couples $\text{Fe}(\text{OH})_3/\text{Fe}^{2+}$, $\text{SO}_4^{2-}/\text{HS}^-$, and $\text{As}(\text{V})/\text{As}(\text{III})$, standardized to the standard hydrogen electrode, and using the Nernst equation (Eq. (2)) (Stumm and Morgan, 1996). Standard redox potentials were calculated from standard Gibbs free energy

of formation according to Eq. (3), with thermodynamic data taken from Pankow (1991) for iron and sulfur and Sergeyeva and Khodakovskiy (1969) for arsenic. For the estimate we used concentrations, as the ionic strength of solution was low ($\sim 10^{-3}$).

$$E_h = E_h^\circ + \frac{R \cdot T}{n \cdot F} \cdot \ln \frac{\prod_i \{\text{Ox}\}^{n_i}}{\prod_j \{\text{Red}\}^{n_j}} \quad (2)$$

$$E_h^\circ = \frac{-\Delta G^\circ}{n \cdot F} \quad (3)$$

Statistical correlations between parameters, such as between solid phase contents of arsenic and metals, were calculated using the non-parametric Spearman method using SPSS (release 10) because not all data were normally distributed even after log-transformation, and tested for their significance. Time series of dissolved concentrations were visualized using SURFER (release 8) using natural neighbor interpolation, which is particular suited for anisotropic data (Sibson, 1981). This was the case as data varied more strongly with depth than with time. An anisotropy factor of 1.5 was implemented, which causes a stronger interpolation along the time axis. Arsenic concentrations are reported in units of $\mu\text{g L}^{-1}$, as this notation is more commonly used than the chemically more meaningful unit of $\mu\text{mol L}^{-1}$.

3. RESULTS

3.1. Solid phase contents of arsenic, metals, and sulfur

Contents of total arsenic were similar in the mesocosms, peaked at 18 to 25 mg kg^{-1} , and remained $>5 \text{ mg kg}^{-1}$ down to a depth of 60 cm. Standardized to dry mass, contents were highest near the soil surface, at a depth of 7.5 cm in all mesocosms. In the uppermost peat of the W-V and DW-V treatment, most of the arsenic could be extracted by application of 1N HCl (Fig. 1). In treatment W-V this fraction decreased from 25 mg kg^{-1} (90 %) to $<5 \text{ mg kg}^{-1}$ (30%) with depth, whereas the residual fraction, consisting of the difference between total arsenic and HCl extractable arsenic, gained in relative importance up to $>60\%$ of the total arsenic. Arsenic contained in the 6N HCl extract amounted to 5–20% and peaked at a depth of 7.5 cm. A very similar depth pattern was found in the DW-V treatment. Most of the iron, whose concentrations ranged from 4 to 10 g kg^{-1} and also peaked near the surface on a per mass basis, could be extracted by 1 N HCl (Fig. 1). Contents of 6 N HCl extractable iron were similar to the residual iron in the peat of the permanently wet treatment W-V (0.5–2 mg kg^{-1}) and became relatively less important only in the deeper peat of the DW-V treatment. Acid extractable aluminum contents were in a similar concentration range as iron contents in treatment W-V and DW-V (Table 1). Mn could only be detected in the uppermost peat of the DW-V treatment with contents of $<0.2 \text{ mg kg}^{-1}$. Contents of analyzed metals are summarized in the Electronic annex.

Total reduced inorganic sulfur (TRIS) was present at all depths in substantial contents of 50–135 mg kg^{-1} , even in the near surface peat, which had not been water saturated at the time of sampling in fall 2005 (Table 1). TRIS had thus been formed, or not fully been reoxidized during the

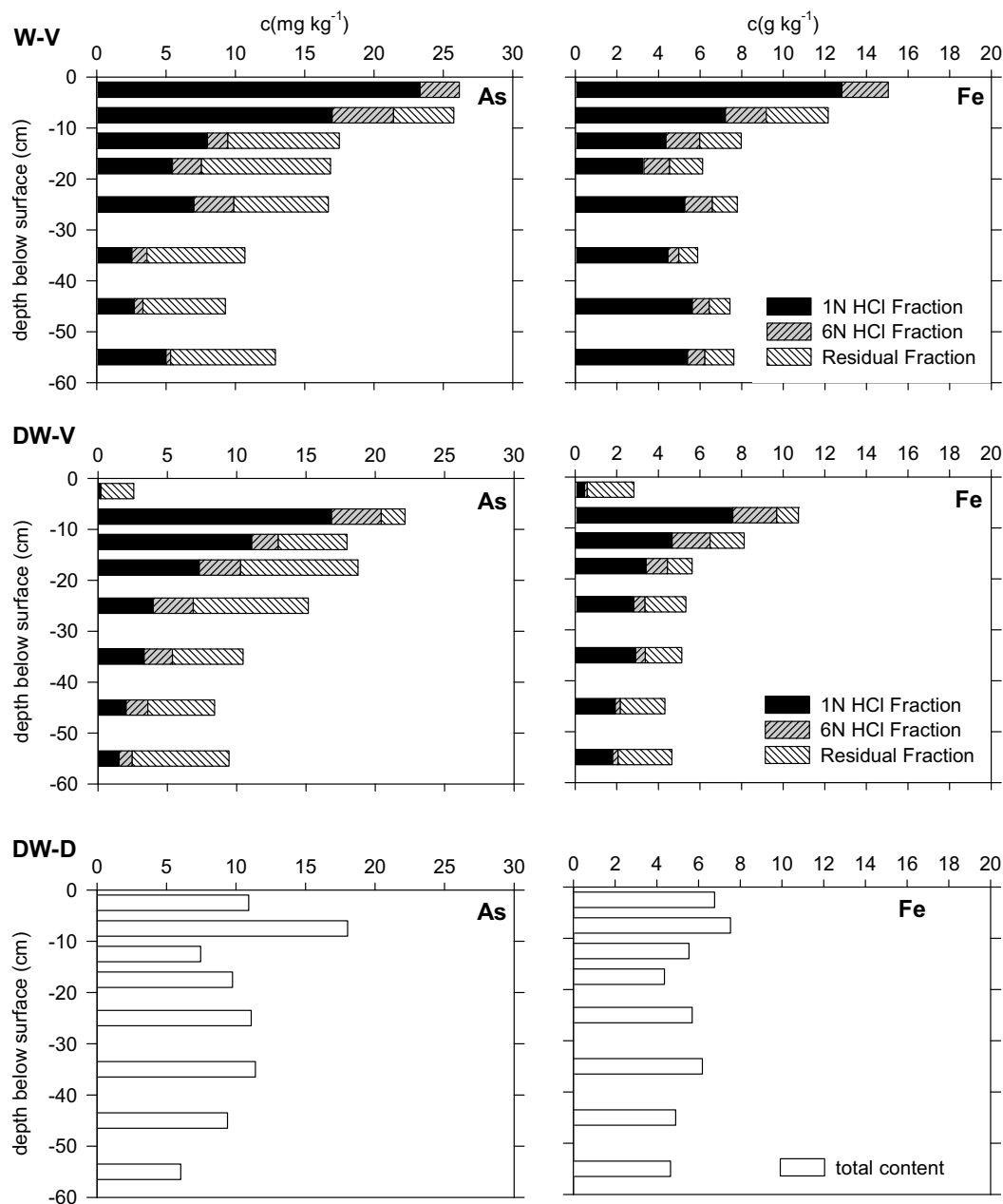


Fig. 1. Depth profiles of arsenic and iron contents in the acid dissolvable fractions and the residual fraction (residual = total content–acid dissolvable fractions) in the permanently wet treatment (W-V), the dried and wetted vegetation treatment (DW-V) and the dried and wetted defoliated treatment (DW-D).

summer of 2005. Contents were largest at intermediate depths in W-V and DW-V, and near the surface in DW-D.

3.2. Correlation between solid phase contents

Statistical relationships between arsenic and contents of other metals than iron were not fully consistent, but iron and arsenic contents significantly correlated in the 6N HCl extracts in the W-V and DW-V treatment and in the 1N HCl extracts in the DW-V treatment (Table 2). Dissolution of reactive and crystalline ferric iron hydroxides by

HCl thus resulted in a similar release of arsenic into solution, confirming the association of arsenic with ferric iron hydroxides in the peat. In the remaining residual fraction, arsenic and Fe were not significantly correlated. Total arsenic also significantly correlated with total iron and the iron in HCl extracts ($R^2 > 0.93$, $\alpha < 0.01$) of the DW-V, but not the W-V treatment. In the DW-D treatment we did not carry out the sequential extraction due to time constraints but total arsenic and iron were also significantly correlated ($R^2 > 0.76$, $\alpha < 0.05$). In the W-V treatment, ferric iron hydroxides were thus likely overall less important as

Table 1

Total contents of iron in the peat of aluminum in the acid extractions (g kg⁻¹) and in total reduced inorganic sulfur (TRIS) (mg kg⁻¹)

Depth (cm)	Fe	Control (C)			With vegetation (V)			Without vegetation (NV)	
		Al ^a	TRIS	Fe	Al ^a	TRIS	Fe	Al ^b	TRIS
0–5	15.05	5.36	88.88	2.83	0.36	35.69	6.77	—	121.29
5–10	12.16	7.86	54.09	10.74	9.57	95.17	7.54	—	116.83
10–15	7.98	7.68	49.28	8.13	8.61	59.12	5.54	—	64.51
15–20	6.12	9.25	130.99	5.63	10.94	104.69	4.36	—	71.26
20–30	7.79	9.94	135.09	5.33	9.65	102.83	5.69	—	92.80
30–40	5.88	8.53	71.01	5.13	9.01	84.26	6.18	—	100.60
40–50	7.44	9.61	97.51	4.32	7.12	40.52	4.90	—	68.13
50–60	7.62	9.30	79.55	4.65	8.52	27.88	4.66	—	76.27

^a Sum of 1 and 6 N HCl extractable aluminum; total contents were not determined.^b No extraction data available.

Table 2

Spearman-correlation ($N = 8$) of arsenic with major elements in extracts of treatments C and V

	1 N HCl fraction		6 N HCl fraction		Residual	
	Control	Vegetation	Control	Vegetation	Control	Vegetation
Al	—	—	—	0.762*	‡	‡
Fe	—	0.976**	0.738*	0.833*	—	—
Mn	†	†	†	†	†	†
Ca	—	—	†	†	‡	‡
Mg	0.881**	—	—	—	‡	‡
K	0.881**	—	—	—	‡	‡

* Correlation significant at $\alpha = 0.05$ level (two-sided), ** correlation significant at $\alpha = 0.01$ level (two-sided), ‡ not determined, † could not be calculated as value set to = 0.

binding partners for arsenic than in the DW-V and DW-D treatment. A correlation between TRIS and total arsenic was found in the DW-V and DW-D treatment ($R^2 > 0.7$, $\alpha < 0.05$).

3.3. Water table, volumetric water content, and root activity

Initially, in phase I, and during the period of drought, in phase III, volumetric gas contents (VGCs) increased from about 2% near the water table to 9–12% at a depth of 10 cm in both dried and rewetted treatments (Fig. 2). Deeper into the unsaturated zone, VGCs remained low, particularly in the DW-V treatment. In this treatment, VGCs decreased rapidly to 2–3% following rewetting. In DW-D the complete filling of VGC to <4% was delayed by 30 days. The treatments DW-V and DW-D thus primarily differed with respect to the time needed for filling of VGC and the stronger desiccation of DW-D during drought (phase III). The analysis of ¹³C–CO₂ in pore water after application of the ¹³C–CO₂ tracer to the surface indicated a rapid transfer of the label into the soil by root respiration in the permanently wet treatment W-V and the vegetated treatment DW-V (Fig. 3). After 49 h, $\delta^{13}\text{C}$ of CO₂ had risen by 3 ‰ (DW-V) and 10 ‰ (W-V) in the uppermost layer and smaller amounts deeper into the peat. The respiratory activity of the roots was thus highest in the near-surface peat, particularly of the W-V treatment. In the DW-D treatment no change in $\delta^{13}\text{C}$ was detected.

3.4. Dissolved concentrations and thermodynamic data

We selected four time points for the visualization of dissolved ferrous iron, and sulfate concentrations and pH in the pore waters of the peat, representing the beginning of the first wet period (day 38), the end of this period (day 101), the end of the dry period (day 143), and the rewetting period (day 206) (Fig. 4). Ferrous iron concentrations rapidly increased after the initial irrigation during the first wet period and peaked at and above the water table at concentrations of up to 5000 $\mu\text{mol L}^{-1}$ (treatment W-V), and 170 and 300 $\mu\text{mol L}^{-1}$ in the other treatments. Ferrous iron concentrations stayed high in treatment W-V, particularly near the water table, throughout the duration of the experiment. In contrast, ferrous iron was effectively eliminated from the pore water in the upper 20 cm of peat in the treatments DW-V and DW-D during the dry period, as can be seen from a comparison between day 101 and day 143 in Fig. 4. This was followed by resumed release after rewetting, resulting in concentrations of 100–200 $\mu\text{mol L}^{-1}$ (Fig. 4). Unsaturated conditions in the deeper peat of treatments DW-V and DW-D apparently resulted in a much slower loss of ferrous iron from the pore water than near the surface. Sulfate concentrations ranged from below LOD to 300 $\mu\text{mol L}^{-1}$, strongly varied with time as well, and followed an inversed pattern compared to ferrous iron, i.e. decreased during saturated condition and increased in the upper peat layers during experimental drought (Fig. 4). In treatment W-V sulfate was depleted after about 100 days

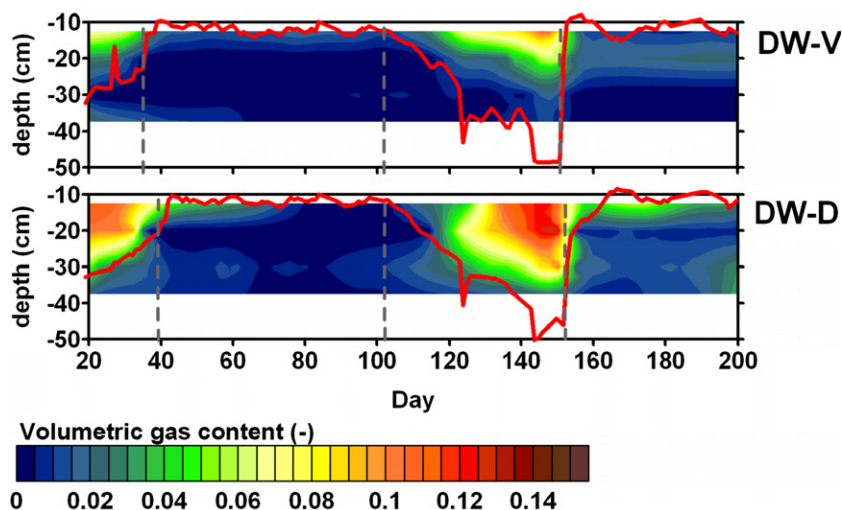


Fig. 2. Volumetric gas content in $\text{m}^3 \text{m}^{-3}$ and water table depth (red solid line) in DW-V (top) and DW-D (bottom). Gas content was calculated from total porosity and changes in TDR soil volumetric water content. Note that the time scale in Fig. 1 ends at 200 days. (For interpretation of the references to color in this figure legend, the reader is referred to the web version of the article.)

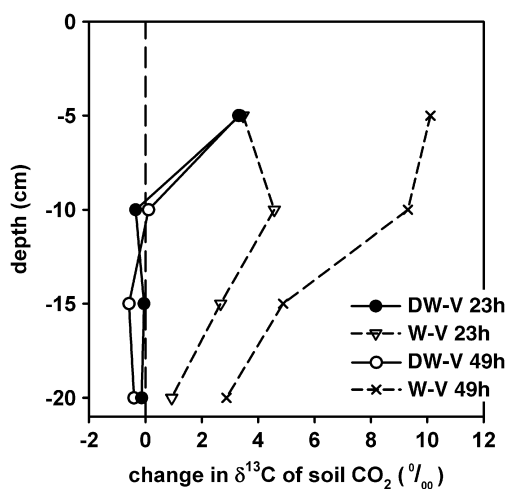


Fig. 3. Root activity as determined from $\delta^{13}\text{C}$ of the soil CO_2 , 23 and 49 h after the ^{13}C - CO_2 pulse label in treatments W-V and DW-V. A transparent chamber containing a ~ 900 ppm CO_2 atmosphere with $\sim 63\%$ ^{13}C - CO_2 was placed on top of the mesocosms for 1 h and changes of $\delta^{13}\text{C}$ of soil CO_2 were monitored for the following 100 h. Positive $\delta^{13}\text{C}$ shifts indicate transfer of the labeled CO_2 into the soil atmosphere by root respiration or heterotrophic respiration of root exudates.

throughout the profile. H_2S concentrations generally ranged from 3 to $12 \mu\text{mol L}^{-1}$ in all treatments during the first wet period and decreased with sulfate depletion in treatment W-V and drying in treatments DW-V and DW-D to concentrations of LOD to $5 \mu\text{mol L}^{-1}$.

Rewetting of the peat was followed by increasing H_2S concentration. Only in the DW-D treatment, however, did H_2S concentrations increase to levels determined before the drought. H_2S remained mostly detectable also in the unsaturated peat (data not shown). Nitrate was detected in all treatments during the first dry and wet periods for

about 50 days before concentrations dropped to $<5 \mu\text{mol L}^{-1}$. Unsaturated conditions resulted in the accumulation of nitrate and ammonium to concentrations >150 and $>200 \mu\text{mol L}^{-1}$, respectively, in the DW-D and a smaller accumulation of ~ 40 and $\sim 30 \mu\text{mol L}^{-1}$, respectively, in the DW-V treatment. DOC concentrations were highest in the W-V treatment at levels of 50 to $>400 \text{mg L}^{-1}$, and peaked in 5–15 cm and 50 cm depth (data not shown). In the other treatments concentrations were highest in the surface layer as well, but concentrations remained below 100mg L^{-1} . Drying resulted in lowered DOC concentrations. The pore water pH ranged from 4 to 6 and often co-varied with ferrous iron concentrations (Fig. 4).

Total dissolved arsenic concentrations were strongly affected by the treatments as well (Fig. 5). In treatment W-V, arsenic accumulated to levels of up to $300 \mu\text{g L}^{-1}$ in the unsaturated zone just above the water table. Also ferrous iron concentrations peaked at this depth. A second maximum of concentrations developed in deeper layers. After about 100 days, concentrations began to decrease in these zones, whereas in intermediate depths concentration did not change. Concentrations also increased in the other treatments during the first wet period, albeit to lower levels of 20 and $70 \mu\text{g L}^{-1}$. The development of air-filled pore space during drying resulted in a concentration decrease to LOD within a few days to two weeks, with a larger time lag and smaller response at greater depths (Fig. 5). At depths of 40–50 cm the impact of drying was small, and at depths of 20 to 40 cm arsenic release following rewetting faster and more intensive than in the near surface peat, especially in DW-V. Rewetting resulted in almost immediate release of arsenic, and previous concentration levels were reattained after about 20–40 days, with the exception of the uppermost peat layer.

During the first wet period, the depth distribution of As(III), As(V), and DMA was highly correlated (Fig. 6).

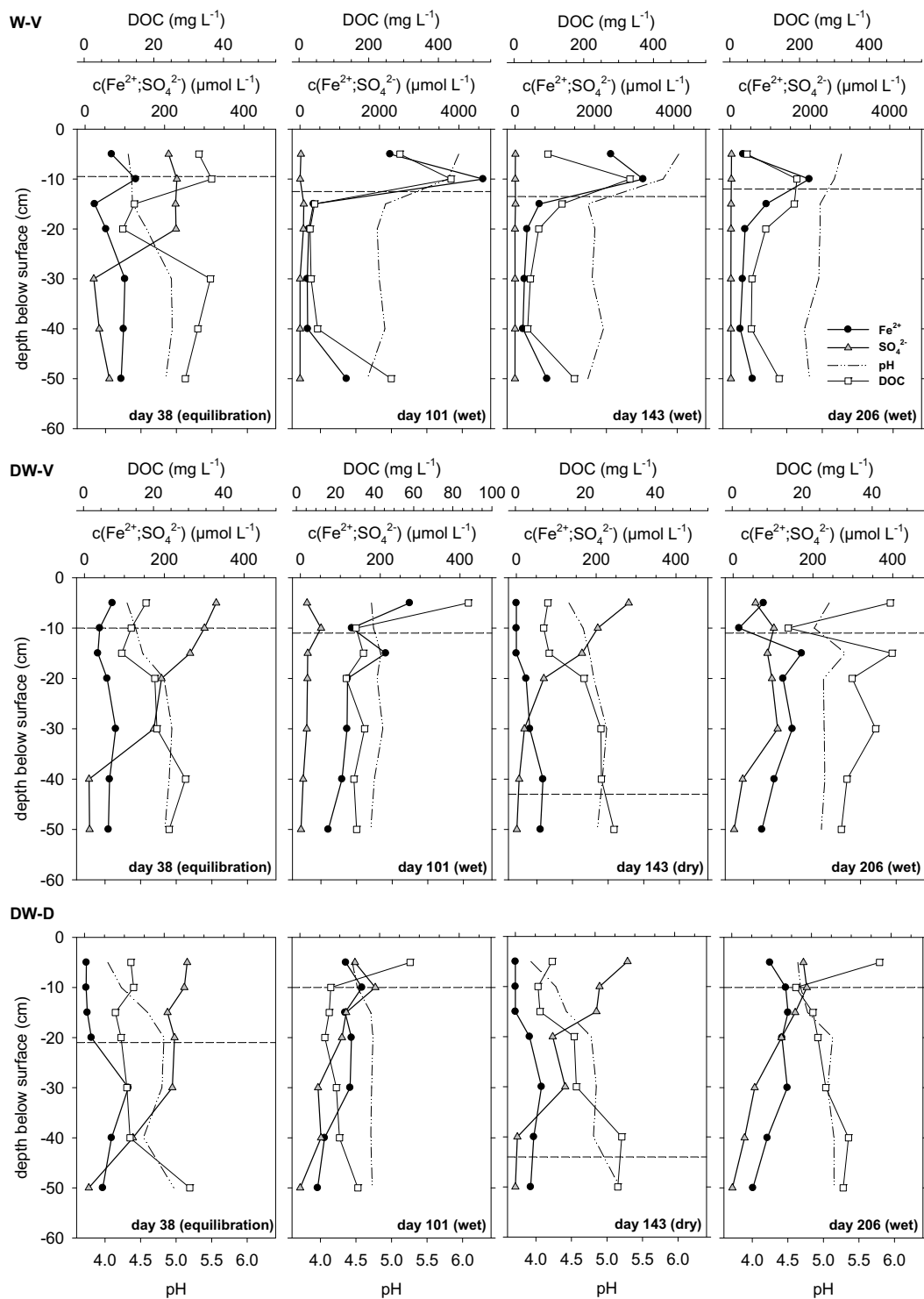


Fig. 4. Concentrations of dissolved ferrous iron, sulfate and dissolved organic carbon (DOC), and pH towards the end of the initial dry equilibration period (day 38), the first wet (day 101), the second dry (day 143) and the middle of the rewetted period (day 206) in the permanently wet treatment (W-V), the dried and wetted vegetation treatment (DW-V) and the dried and wetted defoliated treatment (DW-D). Note the change in scale of ferrous iron and the dotted lines which represent the water table. The DOC concentrations during the wet period were determined at day 66 due to missing data.

As(III) dominated (> 85%) and smaller concentrations of As(V) (<10%) and DMA (<5%) were present. MMA was only detected in treatment W-V down to a depth of 20 cm

where concentrations ranged from 0.1 to 4 μg L⁻¹. Drying and rewetting had a large impact on arsenic speciation (Fig. 7). The development of air filled pore space during the dry

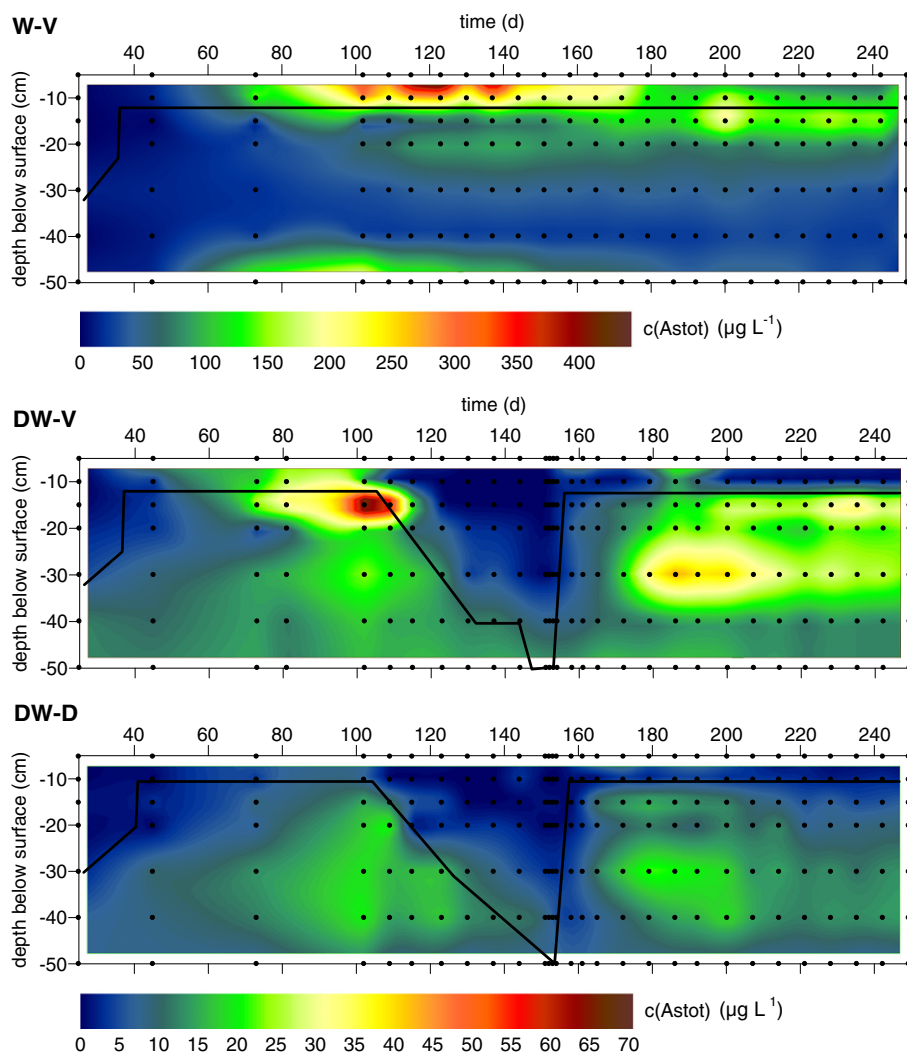


Fig. 5. Temporal dynamics of dissolved arsenic ($\mu\text{g L}^{-1}$) in the permanently wet treatment (W-V), the dried and wetted vegetation treatment (DW-V) and the dried and wetted defoliated treatment (DW-D). Black dots indicate sampling points in time and space. The line represents the average water table. Note the scale differences.

period resulted in a strong decrease of As(III)/As(V) ratios from 4–12 to <0.25 in the uppermost 5–15 cm. Below, impacts were small and in one sample even reversed. After rewetting, As(III) began to dominate and As(V) contributed more to the total dissolved arsenic only near the water table. DMA concentrations ranged from <0.4 to $2.8 \mu\text{g L}^{-1}$ and reacted similarly as As_{tot} to the development of unsaturated conditions (Fig. 8). DMA was eliminated more effectively deeper into the peat, though, and production did not resume within 30 days after rewetting. Presence of oxygen thus inhibited DMA release strongly and in a sustained way, even after the reestablishment of anaerobic conditions.

The calculated *in situ* E_h values of the half redox couples $\text{Fe}(\text{OH})_3/\text{Fe}^{2+}$, $\text{SO}_4^{2-}/\text{HS}^-$, and As(V)/As(III) varied both with depth and time and ranged from 0 to 270 mV for As(V)/As(III), -150 to 90 mV for $\text{SO}_4^{2-}/\text{HS}^-$, and -210 to 290 mV for $\text{Fe}(\text{OH})_3/\text{Fe}^{2+}$ (Fig. 9). The redox couples were generally in strong thermodynamic disequilibrium. The ΔE_h was always positive for a reaction of HS^- with

As(V), confirming that HS^- could be utilized to reduce As(V) under release of free energy. This was not always the case for potential reactions between iron and arsenic, whose E_h strongly overlapped. Averaged over the whole period, conditions in the W-V treatment were on average more reducing than in the other treatments, particularly in the uppermost peat layers where lowest E_h values were recorded for all redox couples.

3.5. Turnover rates of arsenic and ferrous iron

Arsenic was mobilized in treatment W-V for about 100 days (Fig. 10) at rates of up to $0.01 \text{ mmol m}^{-3} \text{ d}^{-1}$ and later on mostly immobilized at rates of 0 to $0.15 \text{ mmol m}^{-3} \text{ d}^{-1}$. During the initial dry and wet period, the same pattern also occurred in the DW-V and DW-D treatment at lower rates, but arsenic was not yet immobilized. Drying resulted in immediate net arsenic loss from solution, when integrated over depth, in DW-V and DW-D mesocosms

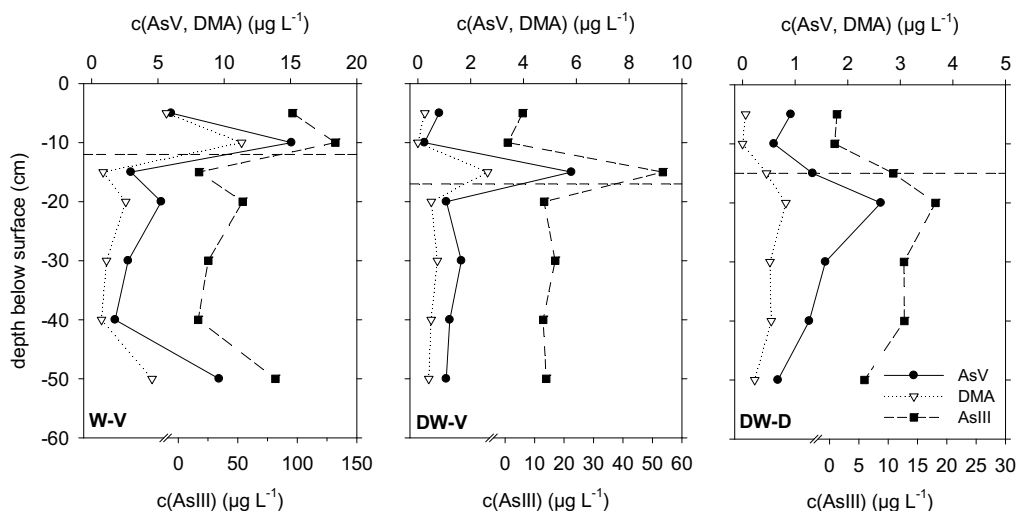


Fig. 6. Speciation of dissolved arsenic at the beginning of the drying period (day 109) in the permanently wet treatment (W-V), the dried and wetted vegetation treatment (DW-V) and the dried and wetted defoliated treatment (DW-D). The interrupted line indicates the position of the water table.

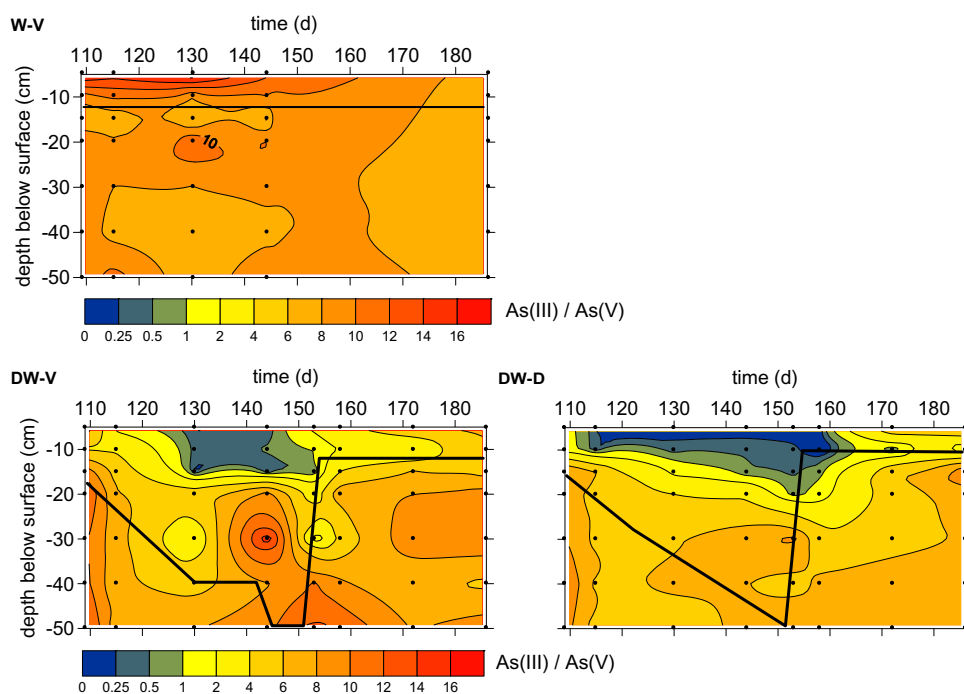


Fig. 7. As(III)/As(V) quotient in vegetation treatment DW-V and defoliated treatment DW-D during drying and rewetting periods. Black dots indicate sampling points in time and space. The line represents the position of the water table.

at rates of up to $-0.01 \text{ mmol m}^{-3} \text{ d}^{-1}$ (DW-V) and $-0.004 \text{ mmol m}^{-3} \text{ d}^{-1}$ (DW-D). Rewetting resulted in a short-term pulse of dissolved arsenic release of $0.05 \text{ mmol m}^{-3} \text{ d}^{-1}$ (DW-V) and $0.02 \text{ mmol m}^{-3} \text{ d}^{-1}$ (DW-D) before arsenic was lost from the pore water at low rates about 40 days after rewetting. The temporal dynamics of dissolved arsenic release and loss was coupled to ferrous iron dynamics, although at times a decoupling occurred (Fig. 10). This was for example the case during the first wet period in W-V and at the beginning of the dry period in DW-V and

DW-D, when ferrous iron loss from the pore water preceded the loss of arsenic. Rates of ferrous iron loss and release ranged from -20 to $18 \text{ mmol m}^{-3} \text{ d}^{-1}$ and were thus about 3 orders of magnitude larger than net turnover rates of arsenic. Ferrous iron and arsenic release were lower in the DW-D treatment by 24% (Fe) and 55% (As) compared to the DW-V treatment and integrated over the wet periods. These differences were mainly caused by the strong release of arsenic and ferrous iron in the intensely rooted near-surface peat of the DW-V treatment.

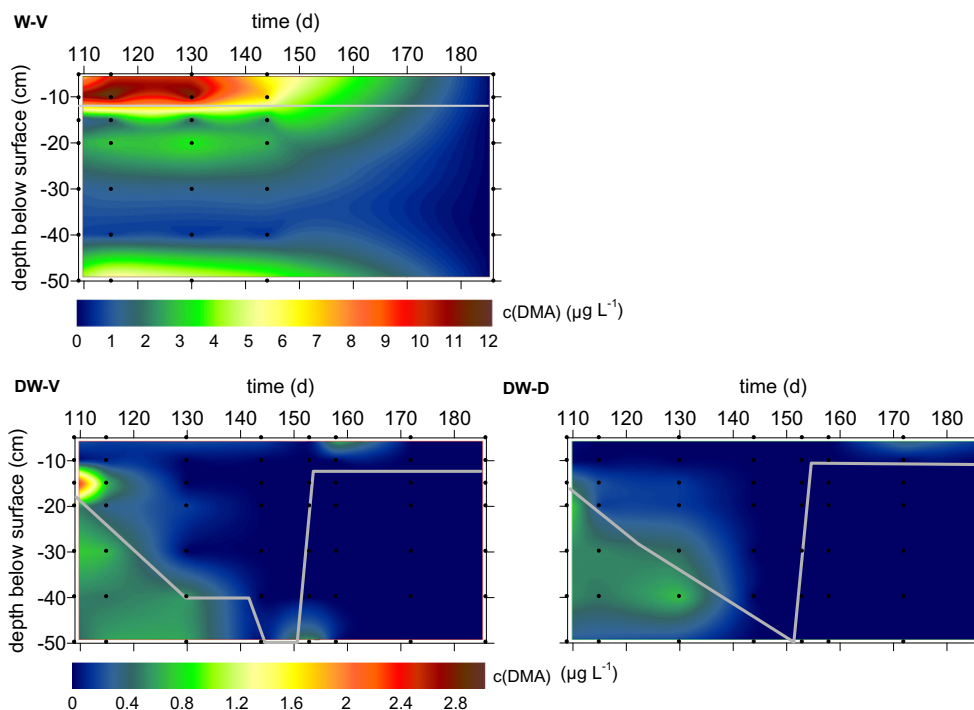


Fig. 8. Temporal dynamics of DMA concentrations ($\mu\text{g L}^{-1}$) in the permanently wet treatment (W-V), the dried and wetted vegetation treatment (DW-V) and the dried and wetted defoliated treatment (DW-D). Black dots indicate sampling points in time and space. The line represents the position of the water table. Note the scale differences.

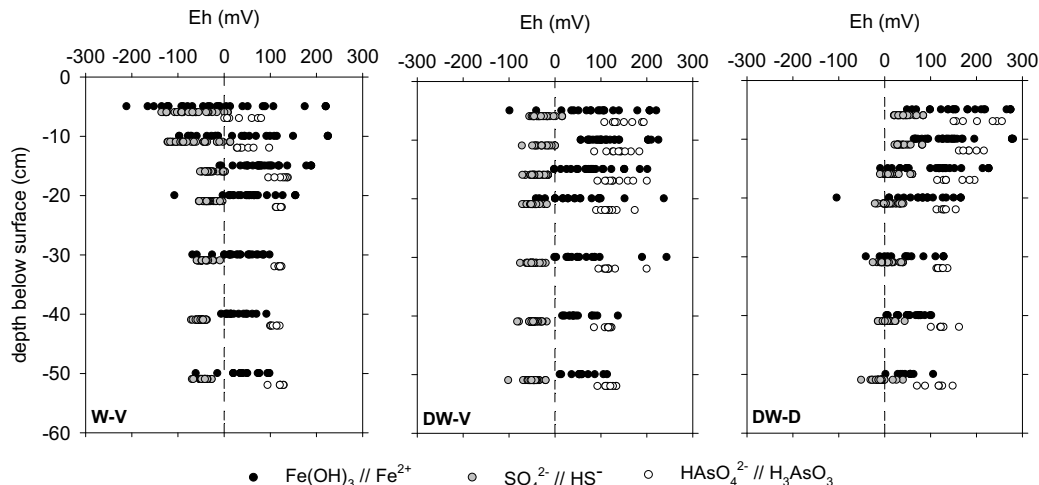


Fig. 9. Variation of redox potentials E_h for iron, sulfur and arsenic redox couples, recalculated for *in situ* geochemical conditions in the permanently wet treatment (W-V), the dried and wetted vegetation treatment (DW-V) and the dried and wetted defoliated treatment (DW-D). Data for redox couples are slightly displaced for better legibility.

4. DISCUSSION

4.1. Distribution, binding, and speciation of Arsenic

Arsenic can be sequestered in soils under different redox regimes. Arsenic is generally removed from pore water by adsorption to iron, manganese, and aluminum hydroxides (Pierce and Moore, 1980; Bowell, 1994; Dixit and Hering,

2003) and clay minerals (Manning and Goldberg, 1997) under oxic conditions. Under anoxia, association with the solid phase may primarily occur by binding to sulfides or the formation of arsenic containing sulfide minerals (Rochette et al., 2000; Meng et al., 2003; O'Day et al., 2004). A binding to organic matter may also occur. Binding of arsenic to dissolved organic matter (DOM), in particular humic substances, has been documented. The binding of arsenate

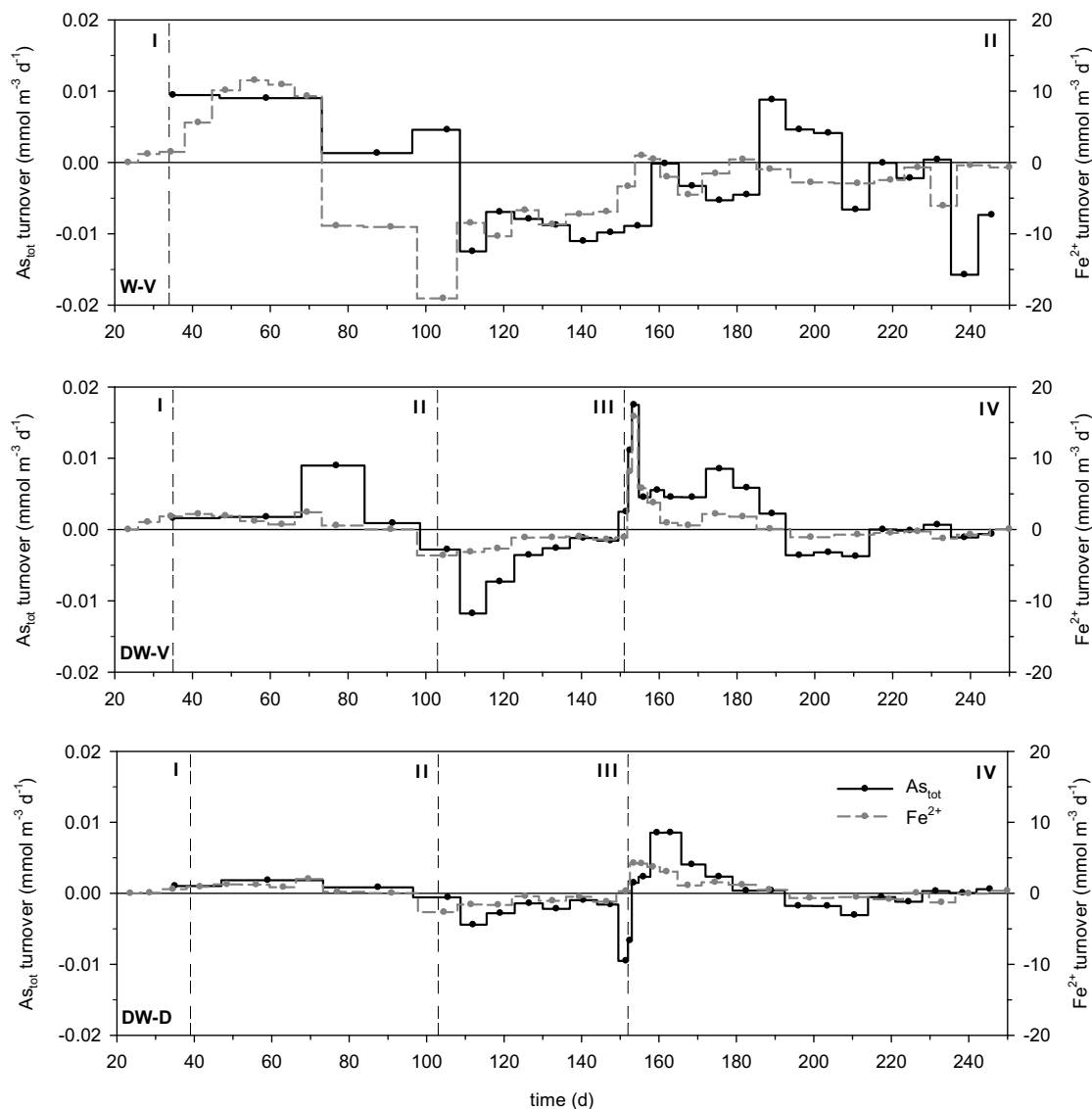


Fig. 10. Depth integrated turnover of arsenic and ferrous iron during the experiments in the permanently wet treatment (W-V), the dried and wetted vegetation treatment (DW-V) and the dried and wetted defoliated treatment (DW-D). In treatment W-V depth integration was only carried out for depth at and below the water table. Values >0 indicate release into the pore water.

and arsenite to negatively charged DOM has been linked to complexation and metal bridges (Redman et al., 2002; Lin et al., 2004) and binding by covalent mechanism and moieties such as phenolic, carboxylic, sulfhydryl and amino groups may also occur (Thanabalasingam and Pickering, 1986; Buschmann et al., 2006).

In the peats investigated, arsenic was obviously mostly bound to the solid phase over the full range of redox conditions that occur with depth and seasonally. The binding mechanisms were apparently altered depending on average redox conditions. Arsenic contents contained in the solid phase decreased with depth but varied only moderately between 5 and 25 mg kg⁻¹ and were within the range of arsenic contents found in the soils of the Lehstenbach watershed, albeit higher than previously documented for an adjacent peatland by Huang and Matzner, 2006). In

the unsaturated uppermost peat, arsenic was primarily found in acid extracts, which dissolve metal hydroxides, acid volatile sulfides, and carbonates (Wallmann et al., 1993). The correlation analysis further suggested that among the hydroxides, iron hydroxides were most important as binding sites (Table 2). Sorption moreover primarily occurred on the reactive hydroxide fraction, which was also most abundant in the peat and typically provides a larger sorption capacity than the crystalline fraction due to its hydrated structure and larger surface area (Pierce and Moore, 1982; Dixit and Hering, 2003). The residual fraction, which may contain organically bound and stable sulfidic arsenic, gained only in relative importance in the deeper, mostly anoxic, and strongly reduced peat.

The exact nature of the binding mechanism in the residual fraction cannot be clarified by the acquired data. We as-

sume that both sorption by iron hydroxides and association with organic matter and sulfides occurred. Rochette et al., (2000) showed experimentally that at low pH and with S/As ratios <20, arsenous sulfide precipitates can form under anoxia. Such conditions were present in the peats. Total reduced inorganic sulfur, primarily in form of iron sulfides had formed prior to the experiments in substantial quantities throughout, albeit at contents that were about two orders of magnitude lower than total ferric iron contents (Table 1). Some insight regarding the significance of arsenic association with iron sulfides can further be gained from the concentration dynamics of arsenic, ferrous iron, and sulfate during the experiments. Although sulfate was actively reduced and iron sulfides formed during the wet periods, at least initially less arsenic associated with the solid phase than was released coupled to iron reduction, and dissolved arsenic concentrations in the pore water consequently increased. Similar findings were reported by Huang and Matzner (2006) under field conditions in an adjacent peatland. Paul et al. (2006) further showed that the formation of iron sulfides at the site occurs only on a temporary basis due to reoxidation during dry periods. A release of arsenic bound to sulfides during reoxidation and subsequent association with iron hydroxides thus likely occurs on a seasonal basis. Binding to organic matter was not explicitly investigated in this study. A substantial binding to organic matter seems likely in view of the large residual arsenic fraction and previous work on binding of arsenic to organic moieties (Thanabalasingam and Pickering, 1986; Buschmann et al., 2006).

Arsenic concentrations in the solid phase were far lower than in naturally more enriched minerotrophic peatlands (Gonzalez et al., 2006), and relatively evenly distributed within the peats and between the three mesocosms. In spite of this fact, dissolved arsenic concentrations reached locally very high values of $300 \mu\text{g L}^{-1}$, and always exceeded common drinking water standards of $10 \mu\text{g L}^{-1}$ when the peat was saturated. Arsenic concentrations exceeded previously reported values from a field investigation conducted by Huang and Matzner (2006) by an order of magnitude. These results confirm that moderately arsenic bearing organic soil have a large potential to remobilize bound arsenic under reducing conditions. As(III) was the predominant species in soil solution, with the exception of highly unsaturated, near-surface peat during the dry period (Fig. 7). In the DW-V and DW-D treatment, As(III) further gained in importance with depth (Fig. 7), which is in agreement with more reducing conditions as indicated by the E_h values of the $\text{SO}_4^{2-}/\text{HS}^-$ and the $\text{Fe}(\text{OH})_3/\text{Fe}^{2+}$ redox couples. The difference in E_h values $\text{SO}_4^{2-}/\text{HS}^-$ and As(V)/As(III) further implied a considerable free energy available for electron transfer from HS^- to As(V) that could potentially also be utilized by microorganisms mediating this process (Oremland and Stolz, 2003), thus contributing to the predominance of dissolved As(III) deeper into the peat.

The occurrence of hot spots of arsenic release near the water table in the W-V and DW-V treatments was likely related to the activity of roots. The application of the ^{13}C - CO_2 tracer showed that the arsenic hot spots were located in layers of highest root density and respiratory activity,

particularly in the W-V treatment (Fig. 3). The comparison between the DW-V and DW-D treatment moreover indicated lower rates of arsenic and Fe release in absence of vegetation and smaller As(III)/As(V) ratios, which may—giving the pH of <5—enhance re-adsorption of released arsenic (Dixit and Hering, 2003). Furthermore, the presence of vegetation slowed the elimination of arsenic from the porewater and As(III)/As(V) quotients decreased in the drained peat during drought (Fig. 7). A statistical confirmation of these findings is not possible due to the lack of replication of the treatments but the results qualitatively indicate that the activity of vascular plants can contribute to the release of dissolved arsenic in wetlands during wet periods and to slow association with the solid phase during dry periods. The likely reason for this phenomenon is the exudation of easily decomposable substrates by roots, which lowers the oxygen concentrations in poorly aerated peat and enhances rates of bacterial iron reduction.

Previously, a sequestration of arsenic in the rhizosphere of plants has also been reported due to the formation of iron hydroxide coatings along roots and subsequent arsenic sequestration (Otte et al., 1995; Doyle and Otte, 1997). In the W-V treatment, the grass *C. rostrata* dominated, which is capable of aerenchymatic oxygen transport into the rhizosphere. A visual examination also revealed iron coatings in the peats of the W-V treatment, which may also explain the high iron enrichment in this treatment. The comparison of total arsenic contents between mesocosms accordingly illustrates that the presence of *C. rostrata* in the W-V treatment coincided with increased arsenic accumulation in the uppermost peat (Fig. 1). Integrated over depth and in the short-term the net effect of root activity was an enhanced release of dissolved arsenic following rewetting, however. This effect was particularly pronounced in the uppermost horizon of the W-V treatment, which was characterized by the highest root activity (Fig. 3) and the largest content in reactive iron and arsenic associated with reactive iron (Fig. 1). Given the large differences in dissolved arsenic concentration between this and the other treatments, a combination of these factors obviously is of great importance regarding arsenic release.

The previous observation by Huang and Matzner (2006) that dissolved arsenic primarily occurs in organic form in adjacent peatland Schlöppnerbrunnen I, mainly as MMA, could not be substantiated in this study. The methylation of arsenic is believed to be microbially mediated and to proceed under anaerobic conditions (Bentley and Chasteen, 2002; Bolan et al., 2006). The contrasting findings may be related to more persistent anaerobic conditions in the soils of Schlöppnerbrunnen I compared to Schlöppnerbrunnen II (Paul et al., 2006). Continuous anoxia may facilitate methylation of arsenic by methanogenic and sulfidogenic populations (Bolan et al., 2006). An inhibition of MMA and DMA formation by temporarily oxic conditions would also be in agreement with the lack of DMA formation in the DW-V and DW-D treatment after rewetting (Fig. 8). Regardless of the exact causes for the smaller importance of methylation in the investigated Schlöppnerbrunnen II peat, the process was of little relevance and may hence not be an important mechanism for the release of arsenic

into the soil water in all peatlands, if the results of this mesocosms study can be extrapolated to the field. In this respect it has to be considered that the temperature in the mesocosms reflected mid-summer conditions instead of yearly averages and that vertical and lateral flow in the mesocosms were eliminated. Both factors may have altered relative concentration levels of individual arsenic species and lead to a build up of total dissolved arsenic in the soil.

4.2. Impact of drying and rewetting on arsenic speciation and phase transfer

The temporal and spatial patterns of dissolved arsenic concentrations and the associated turnover was connected to ferric iron release during the wet periods and removal of ferrous iron from the pore water during drought (Fig. 10). This finding supports the hypothesis that dissolved arsenic release is mainly driven by bacterial iron reduction in iron rich peat soils, in analogy to less organic-rich anoxic aquifers. Likewise, oxic conditions resulted in co-precipitation of arsenic with ferric iron hydroxides. This pattern is plausible giving the intense association of arsenic with reactive ferric iron hydroxides, which are generally also more readily used than crystalline iron hydroxides by ferric iron reducing bacteria under neutral and weakly acidic conditions (Lovley and Phillips, 1988). A similar coupling of arsenic and iron dynamics has already been demonstrated or inferred from several field studies and laboratory experiments, but not been verified for natural peatlands with natural arsenic background (Masscheleyn et al., 1991; La Force et al., 2000; Fox and Doner, 2003). The dissolved arsenic dynamics furthermore suggests that adsorption on sulfides or precipitation of arsenic with sulfides was of little importance for the total arsenic turnover. A similar finding was recently reported based on analyses of solid phase materials in a near-neutral, iron-rich and mine drainage impacted wetland (Beauchemin and Kwong, 2006).

During the dry period, gas filled porosity in the peat increased from <2% to 2–13%. Oxygen penetrated deeper into the peat resulting in release of sulfate, likely by reoxidation of reduced inorganic and organic sulfur, and elimination of ferrous iron by oxidation and subsequent precipitation as reactive iron hydroxide phase (Reynolds et al., 1999). Arsenic was not only co-precipitated in its reduced form with the forming iron hydroxide precipitates, as can be expected due to its affinity for iron hydroxides (Dixit and Hering, 2003), but apparently also effectively and rapidly reoxidized: As(III)/As(V) ratios dropped below 1 within days in the uppermost peat layers of the DW-D treatment and more slowly in the DW-V treatment. The transformation of As(III) to As(V) and the decreasing pH (Fig. 4) contributed to the subsequent association of dissolved arsenic with solid phase soil material, since sorption of As(V) to ferric iron hydroxides increases with acidification (Dixit and Hering, 2003). Arsenite oxidation was probably in some way mediated by microorganisms because the chemical oxidation of As(III) by oxygen is slow, with a reported half-life of 4–9 days in natural waters (Kim and Nriagu, 2000). Arsenate oxidation as a detoxification mechanism and dissimilatory microbial respiration coupled to oxygen and nitrate reduc-

tion are both known to occur (Oremland and Stolz, 2003) and are in agreement with elevated concentrations of nitrate and oxygen during this period. The rapid oxidation of arsenic in the DW-D treatment, which contained less As(III) relative to As(V) even before the dry period, was likely caused by a lower respiratory oxygen demand and thus higher oxygen availability in the peat (Knorr et al., 2008).

Initial wetting and rewetting resulted in iron reduction in all treatments, either by iron reducing bacteria or by reaction of H₂S with ferric iron hydroxides, and entailed the release of arsenic associated with the solid phase, as previously described by McGeehan and Naylor (1994) and Reynolds et al. (1999). Changes in concentration were particularly strong in the uppermost, reactive iron and arsenic-rich, and intensively rooted horizon of the W-V treatment, which was at or above the water table. Smaller changes in soil moisture in this horizon, as they occurred on a regular basis due to the irrigation regime (Electronic annex, Fig. 1S) apparently also lead to local release and removal of arsenic from the pore water (Fig. 5, treatment W-V, e.g. day 180–200), which strongly influenced the depth integrated arsenic turnover in the mesocosm (Fig. 10, treatment W-V, e.g. day 180–200). We did not analyze the speciation of arsenic in the solid phase and the nature of As(V) reduction in the peats and a discussion about the mechanism of the phase transfer of arsenic following rewetting can only be speculative. It is possible that in the near surface peat arsenic was primarily remobilized as arsenate from exchange sites and subsequently slowly reduced in the pore water as described for example by Cummings et al. (1999); an *in situ* reduction of sorbed arsenate has previously also been inferred based on sediment depth profiles and XANES and EXAFS spectroscopic characterization of arsenic adsorbed to iron hydroxides (Kneebone et al., 2002; Beauchemin and Kwong, 2006). Arsenate may have been reduced in solution by dissimilatory respiration, as described for example by Campbell et al., (2006), although concentrations were low compared to environments where this process has been documented to be important, such as at contaminated sites and hypersaline lakes. A microbial detoxification process leading to excretion of As(III) from heterotrophic bacteria (Oremland and Stolz, 2003) may have occurred as well. A chemical reduction of As(V) by hydrogen sulfide, which is rapid under acidic conditions (Rochette et al., 2000) and was thermodynamically possible (Fig. 9), cannot be ruled out either.

The rapid release of dissolved arsenic coupled to iron reduction was possibly assisted by the production and accumulation of DOM. Concentrations of up to 400 mg L⁻¹ DOC were attained in treatment W-V (Fig. 4) where the maximum of dissolved arsenic concentrations occurred. With the exception of these hot spots, concentrations were in the range of 10–100 mg L⁻¹ DOC that is typical for peat soils and organic-rich soil horizons (Blodau, 2002; Michalzik and Matzner, 1999). Negatively charged DOM is a competitor for exchange sites on iron hydroxides, and concentrations of 10–50 mg L⁻¹ have been demonstrated to mobilize arsenic in batch experiments with synthetic iron hydroxides and materials from soils and sediments (Bauer and Blodau, 2006). An effective re-adsorption of desorbed arsenic to newly available iron hydroxide surfaces may have been impeded

to some extent. Re-adsorption of As(V) following chemical iron reduction of ferrihydrite by ascorbic acid has been previously described (Pedersen et al., 2006). Both re-adsorption and competition of arsenic with DOM for adsorption sites potentially contributed to the observed temporal decoupling of iron and arsenic turnover in the peat.

5. CONCLUSIONS

The study demonstrates the strong impact of drying and rewetting events on arsenic concentrations in wetland soils and the potential of uncontaminated and moderately arsenic bearing peat to mobilize arsenic in form of arsenite after rewetting. Methylated arsenic species were, in contrast, of subordinate importance for arsenic release, and their formation was inhibited by temporary intrusion of oxygen even after rewetting and development of anoxia. The dynamics of arsenic and iron were essentially coupled. Arsenic and iron were immobilized following oxidation during dry periods and rapidly mobilized by iron reduction and the associated release of arsenic after rewetting, leading to arsenic concentrations of up to $300 \mu\text{g L}^{-1}$ and release of up to $0.02 \text{ mmol m}^{-3} \text{ d}^{-1}$. A combination of factors apparently contributed to this dynamics. In the near-surface peat, arsenic was primarily adsorbed on ferric iron hydroxides, which were also most rapidly reduced in the uppermost intensely rooted and iron-rich soil horizons, where electron donors were abundant. Microbial activity also lead to very high DOC concentrations, which may have promoted arsenic release by impeding a re-adsorption. Aerenchymatic transport of oxygen by *C. rostrata* roots was apparently of little significance for the arsenic dynamics in the short-term, as were interactions between arsenic, organic matter, and iron sulfides. On the time scale of years to millennia, minerotrophic wetlands such as the Schlöppnerbrunnen II site seem to serve as effective sinks for arsenic due to the abundance of reactive iron hydroxides in the peat. Temporarily, however, arsenic can be mobilized at high concentration levels when water saturated and anoxic conditions are established in the uppermost biologically active peat layer.

ACKNOWLEDGMENTS

The investigation was funded by DFG Grants BL563/7-2 and BL563/2-1 to C. Blodau. The assistance of Martina Heider, Karin Söllner, Marieke Osterwoud, Jan Pfister, Björn Thomas, Tobias Biermann, Severin Irl, Niklas Gassen, and Benjamin Kopp is greatly appreciated.

APPENDIX A. SUPPLEMENTARY DATA

Supplementary data associated with this article can be found, in the online version, at [doi:10.1016/j.gca.2008.04.040](https://doi.org/10.1016/j.gca.2008.04.040).

REFERENCES

Anderson M. A., Ferguson J. F. and Gavis J. (1976) Arsenate adsorption on amorphous aluminum hydroxide. *J. Colloid Interf. Sci.* **54**(3), 391–399.

- Bauer M. and Blodau C. (2006) Mobilization of arsenic by dissolved organic matter from iron oxides, soils and sediments. *Sci. Total Environ.* **354**(2–3), 179–190.
- Beauchemin S. and Kwong Y. T. J. (2006) Impact of redox conditions on arsenic mobilization from tailings in a wetland with neutral drainage. *Environ. Sci. Technol.* **40**, 6297–6303.
- Bentley R. and Chasteen T. G. (2002) Microbial methylation of metalloids: arsenic, antimony, and bismuth. *Microbiol. Mol. Biol. Rev.* **66**(2), 250–271.
- BGS and DPHE. (2001) Arsenic contamination of groundwater in Bangladesh. In Volume 1: Summary. British Geological Survey Report WC/00/19 (ed. D.G. Kinniburgh and P.L. Smedley). British Geological Survey.
- Bissen M. and Frimmel F. H. (2003) Arsenic—a review. Part I: Occurrence, toxicity, speciation, mobility. *Acta Hydrochim. Hydrobiol.* **31**(1), 9–18.
- Blodau C. (2002) Carbon cycling in peatlands: a review of processes and controls. *Environ. Rev.* **10**, 111–134.
- Blute N. K., Brabander D., Hemond H. F., Sutton S., Newville M. G. and Rivers M. L. (2004) Arsenic sequestration by ferric iron plaque on cattail roots. *Environ. Sci. Technol.* **38**, 6074–6077.
- Bolan N. S., Mahimairaja S., Megharaj M., Naidu R. and Adriano D. C. (2006) Biotransformation of arsenic in soil and aquatic environments. In *Managing Arsenic in the Environment* (eds R. Naidu, E. Smith, G. Owens, P. Bhattacharya and P. Nadebaum). CSIRO, pp. 433–453.
- Bostick B. C. and Fendorf S. (2003) Arsenite sorption on troilite (FeS) and pyrite (FeS₂). *Geochim. Cosmochim. Acta* **67**(5), 909–921.
- Bowell R. J. (1994) Sorption of arsenic by iron-oxides and oxyhydroxides in soils. *Appl. Geochem.* **9**(3), 279–286.
- Buschmann J., Kappeler A., Lindauer U., Kistler D., Berg M. and Sigg L. (2006) Arsenite and arsenate binding to dissolved humic acids: influence of pH, type of humic acid, and aluminum. *Environ. Sci. Technol.* **40**(19), 6015–6020.
- Campbell K. M., Malasarn D., Saltikov C. W., Newman D. K. and Hering J. G. (2006) Simultaneous microbial reduction of iron(III) and arsenic(V) in suspensions of hydrous ferric oxide. *Environ. Sci. Technol.* **40**(19), 5950–5955.
- Cline J. D. (1969) Spectrophotometric determination of hydrogen sulfide in natural waters. *Limnol. Oceanogr.* **14**(3), 454.
- Cornell R. M. and Schwertmann U. (1996) *The iron oxides—structure, properties, reactions, occurrence and uses*. VCH Weinheim.
- Cullen W. R. and Reimer K. J. (1989) Arsenic speciation in the environment. *Chem. Rev.* **89**(4), 713–764.
- Cummings D. E., Caccavo J. R., Fendorf S. and Rosenzweig R. F. (1999) Arsenic mobilization by the dissimilatory Fe(III)-reducing bacterium *Shewanella* alga BrY. *Environ. Sci. Technol.* **33**, 723–729.
- Dixit S. and Hering J. G. (2003) Comparison of arsenic(V) and arsenic(III) sorption onto iron oxide minerals: implications for arsenic mobility. *Environ. Sci. Technol.* **37**(18), 4182–4189.
- Doyle M. O. and Otte M. L. (1997) Organism-induced accumulation of iron, zinc and arsenic in wetland soils. *Environ. Pollut.* **96**(1), 1–11.
- Fossing H. and Jorgensen B. B. (1989) Measurement of bacterial sulfate reduction in sediments—evaluation of a single-step chromium reduction method. *Biogeochemistry* **8**(3), 205–222.
- Fox P. M. and Doner H. E. (2003) Accumulation, release, and solubility of arsenic, molybdenum, and vanadium in wetland sediments. *J. Environ. Quality* **32**(6), 2428–2435.
- Francesconi K., Visoottiviset P., Sridokchan W. and Goessler W. (2002) Arsenic species in an arsenic hyperaccumulating fern, *Pityrogramma calomelanos*: a potential phytoremediator of arsenic-contaminated soils. *Sci. Total Environ.* **284**(1–3), 27–35.

- Gonzalez Z. I., Krachler M., Cheburkin A. K. and Shoty W. (2006) Spatial distribution of natural enrichments of arsenic, selenium, and uranium in a minerotrophic peatland, Gola di Lago, Canton Ticino, Switzerland. *Environ. Sci. Technol.* **40**(21), 6568–6574.
- Huang J. H. and Matzner E. (2006) Dynamics of organic and inorganic arsenic in the solution phase of an acidic fen in Germany. *Geochim. Cosmochim. Acta* **70**(8), 2023–2033.
- IPCC. (2001) Climate Change 2001, Third Assessment Report. In *Third Assessment Report*. Intergovernmental Panel on Climate Change.
- Kim M.-J. and Nriagu J. (2000) Oxidation of arsenite in groundwater using ozone and oxygen. *Sci. Total Environ.* **247**(1), 71–79.
- Kneebone P. E., O'Day P. A., Jones N. and Hering J. G. (2002) Deposition and fate of arsenic in iron- and arsenic enriched reservoir sediments. *Environ. Sci. Technol.* **36**, 381–386.
- Knorr K.-H., Osterwoud M. and Blodau C. (2008) Experimental drought alters rates of soil respiration and methanogenesis but not carbon exchange in soil of a temperate fen. *Soil Biol. Biochem.* **40**, 1781–1791.
- La Force M. J., Hansel C. M. and Fendorf S. (2000) Arsenic speciation, seasonal transformations, and co-distribution with iron in a mine waste-influenced palustrine emergent wetland. *Environ. Sci. Technol.* **34**(18), 3937–3943.
- Lerman A. (1979) *Geochemical Processes: water and sediment environments*. John Wiley & Sons, New York.
- Lin H. T., Wang M. C. and Li G. C. (2004) Complexation of arsenate with humic substance in water extract of compost. *Chemosphere* **56**(11), 1105–1112.
- Lovley D. R. and Phillips E. J. P. (1988) Novel mode of microbial energy metabolism: organic carbon oxidation coupled to dissimilatory reduction of iron or manganese. *Appl. Environ. Microbiol.* **45**, 187–192.
- Mandal B. K. and Suzuki K. T. (2002) Arsenic round the world: a review. *Talanta* **58**(1), 201–235.
- Manning B. A. and Goldberg S. (1996) Modeling arsenate competitive adsorption on kaolinite, montmorillonite and illite. *Clay Clay Miner.* **44**(5), 609–623.
- Manning B. A. and Goldberg S. (1997) Adsorption and stability of arsenic(III) at the clay mineral–water interface. *Environ. Sci. Technol.* **31**(7), 2005–2011.
- Masscheleyn P. H., Delaune R. D. and Patrick W. H. (1991) Effect of redox potential and pH on arsenic speciation and solubility in a contaminated soil. *Environ. Sci. Technol.* **25**(8), 1414–1419.
- McCleskey R. B., Nordstrom D. K. and Maest A. S. (2004) Preservation of water samples for arsenic(III/V) determinations: an evaluation of the literature and new analytical results. *Appl. Geochem.* **19**(7), 995–1009.
- McGeehan N. D. V. (1994) Sorption and redox transformation of arsenite and arsenate in two flooded soils. *Soil Sci. Soc. Am. J.* **58**, 337–342.
- McGeehan S. L. and Naylor D. V. (1994) Sorption and redox transformation of arsenite and arsenate in 2 flooded soils. *Soil Sci. Soc. Am. J.* **58**(2), 337–342.
- Meng X. G., Jing C. Y. and Korfiatis G. P. (2003) A review of redox transformation of arsenic in aquatic environments. In *Biogeochemistry of Environmentally Important Trace Elements*, vol. 835 (eds. Y. Cai and O. C. Braid). American Chemical Society, pp. 70–83.
- Michalzik B. and Matzner E. (1999) Dynamics of dissolved organic nitrogen and carbon in a Central European Norway spruce ecosystem. *Eur. J. Soil Sci.* **50**, 579–590.
- O'Day P. A., Vlassopoulos D., Root R. and Rivera N. (2004) The influence of sulfur and iron on dissolved arsenic concentrations in the shallow subsurface under changing redox conditions. *Proc. Natl. Acad. Sci. USA* **101**(38), 13703–13708.
- Oremland R. S. and Stolz J. F. (2003) The ecology of arsenic. *Science* **300**, 939–944.
- Otte M. L., Kearns C. C. and Doyle M. O. (1995) Accumulation of arsenic and zinc in the rhizosphere of wetland plants. *Bull. Environ. Contam. Toxicol.* **55**(1), 154–161.
- Pankow J. F. (1991) *Aquatic chemistry concepts*. Lewis Publishers, Boca Raton.
- Paul S., Kusel K. and Alewell C. (2006) Reduction processes in forest wetlands: tracking down heterogeneity of source/sink functions with a combination of methods. *Soil Biol. Biochem.* **38**(5), 1028–1039.
- Pedersen H. D., Postma D. and Jakobsen R. (2006) Release of arsenic associated with the reduction and transformation of iron oxides. *Geochim. Cosmochim. Acta* **70**(16), 4116–4129.
- Pierce M. L. and Moore C. B. (1980) Adsorption of arsenite on amorphous iron hydroxide from dilute aqueous-solution. *Environ. Sci. Technol.* **14**(2), 214–216.
- Pierce M. L. and Moore C. B. (1982) Adsorption of arsenite and arsenate on amorphous iron hydroxide. *Water Res.* **16**(7), 1247–1253.
- Redman A. D., Macalady D. L. and Ahmann D. (2002) Natural organic matter affects arsenic speciation and sorption onto hematite. *Environ. Sci. Technol.* **36**(13), 2889–2896.
- Reynolds J. G., Naylor D. V. and Fendorf S. E. (1999) Arsenic sorption in phosphate-amended soils during flooding and subsequent aeration. *Soil Sci. Soc. Am. J.* **63**(5), 1149–1156.
- Rochette E. A., Bostick B. C., Li G. C. and Fendorf S. (2000) Kinetics of arsenate reduction by dissolved sulfide. *Environ. Sci. Technol.* **34**(22), 4714–4720.
- Searle P. S. (1984) The berthelot or indophenol reaction and its use in the analytical chemistry of nitrogen. *Analyst* **109**, 549–568.
- Sergeyeva E. and Khodakovskiy I. (1969) Physicochemical conditions of formation of native arsenic in hydrothermal deposits. *Geochem. Int. USSR* **6**(4), 681.
- Shoty W. (1996) Natural and anthropogenic enrichments of As, Cu, Pb, Sb, and Zn in ombrotrophic versus minerotrophic peat bog profiles, Jura Mountains, Switzerland. *Water Air Soil Pollut.* **90**(3–4), 375–405.
- Sibson R. (1981) A brief description of natural neighbor interpolation. In *Interpreting Multivariate Data* (ed. V. Barnett). John Wiley and Sons, New York, pp. 21–36.
- Smedley P. L. and Kinniburgh D. G. (2002) A review of the source, behaviour and distribution of arsenic in natural waters. *Appl. Geochem.* **17**(5), 517–568.
- Smieja J. A. and Wilkin R. T. (2003) Preservation of sulfidic waters containing dissolved As(III). *J. Environ. Monitor.* **5**, 913–916.
- Stanek W. and Silc T. (1977) Comparisons of 4 methods for determination of degree of peat humification (decomposition) with emphasis on von Post method. *Can. J. Soil Sci.* **57**, 109–117.
- Stumm W. and Morgan J. J. (1996) *Aquatic chemistry*. Wiley, New York.
- Tamura H., Goto K., Yotsuyan T. and Nagayama M. (1974) Spectrophotometric determination of iron(II) with 1,10-phenanthroline in presence of large amounts of iron(III). *Talanta* **21**(4), 314–318.
- Thanabalasingam P. and Pickering W. F. (1986) Arsenic sorption by humic acids. *Environ. Pollut. B, Chem. Phys.* **12**(3), 233–246.

Wallmann K., Hennies K., König I., Petersen W. and Knauth H. D. (1993) New procedure for determining reactive Fe(III) and Fe(II) minerals in sediments. *Limnol. Oceanogr.* **38**(8), 1803–1812.

Wallschäger D. and London J. (2008) Determination of methylated arsenic-sulfur compounds in groundwater. *Environ. Sci. Technol.* **42**(1), 228–234.

Zheng Y., Stute M., van Geen A., Gavrieli I., Dhar R., Simpson H. J., Schlosser P. and Ahmed K. M. (2004) Redox control of arsenic mobilization in Bangladesh groundwater. *Appl. Geochem.* **19**(2), 201–214.

Associate editor: Martin Novak

Supporting Information

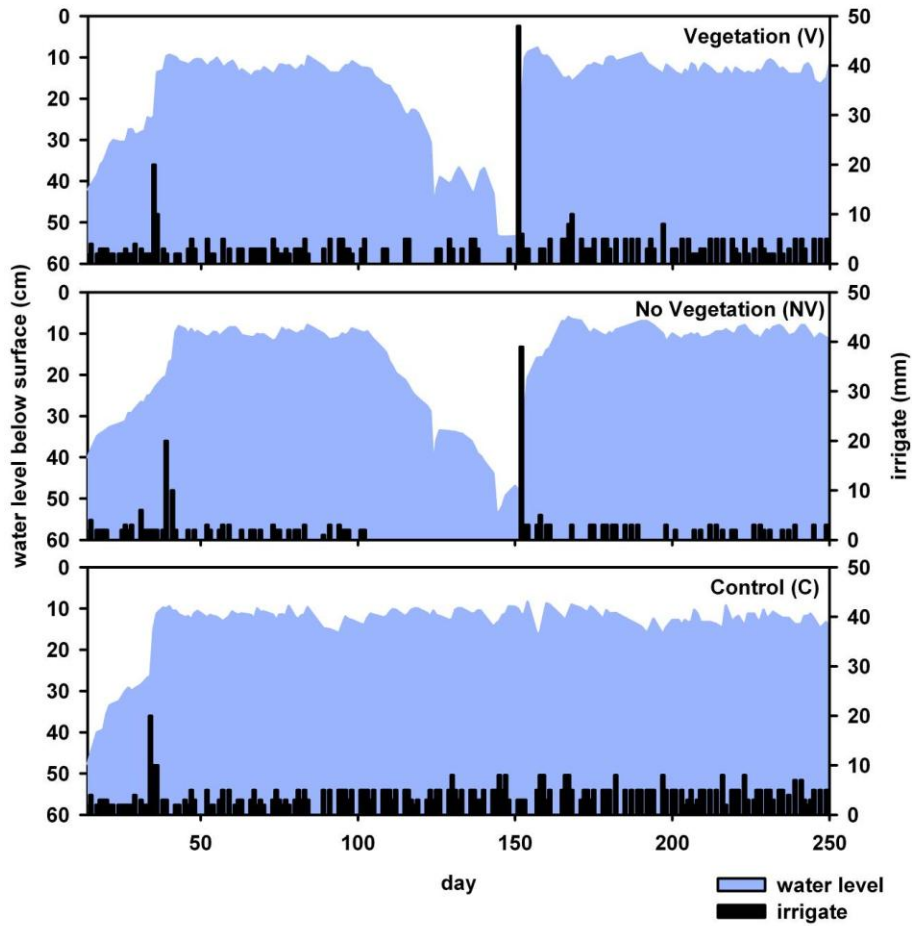


Figure 61 Time series of water levels (light blue area) and irrigate applied (bars) for each mesocosm. Abrupt drops in water levels of V and NV at days ~120 and ~145 were due to sampling of water from piezometers.

Table 22 Elemental contents in acid extracts of peat from control treatment and vegetated treatment V

depth (cm)	Al [*]	Al ^{**}	Fe [*]	Fe ^{**}	Ca [*]	Ca ^{**}	Mg [*]	Mg ^{**}	K [*]	K ^{**}
	(g kg ⁻¹)		(g kg ⁻¹)		(g kg ⁻¹)		(g kg ⁻¹)		(g kg ⁻¹)	
Control treatment (C)										
0-5	4.70	0.66	12.82	2.23	0.66	<	0.20	<	0.47	<
5-10	5.92	1.95	7.22	1.96	0.19	<	0.18	0.27	0.16	0.17
10-15	6.15	1.53	4.36	1.63	0.29	<	0.21	0.19	0.29	0.16
15-20	7.66	1.59	3.30	1.24	0.36	<	0.14	0.12	0.16	0.06
20-30	8.35	1.59	5.27	1.33	0.61	<	0.12	0.01	0.10	<
30-40	7.50	1.03	4.46	0.51	0.71	<	0.07	<	0.04	<
40-50	8.52	1.09	5.63	0.81	1.03	0.02	0.11	<	<	<
50-60	8.32	0.98	5.40	0.83	0.93	<	0.10	<	0.03	<
Treatment with vegetation (V)										
0-5	0.36	<	0.46	0.13	0.79	0.02	0.49	<	1.52	0.08
05-10	7.46	2.10	7.58	2.11	0.53	<	0.31	0.25	0.51	0.11
10-15	6.64	1.97	4.67	1.83	0.41	<	0.32	0.30	0.46	0.22
15-20	9.32	1.61	3.42	1.02	0.45	<	0.14	0.04	0.15	<
20-30	8.21	1.44	2.83	0.54	0.46	<	0.07	<	0.10	<
30-40	7.73	1.28	2.91	0.46	0.48	<	0.04	<	0.08	<
40-50	5.91	1.22	1.93	0.25	0.33	<	0.02	<	0.08	<
50-60	7.20	1.32	1.81	0.26	0.55	<	0.03	<	0.03	<

Study 9

Reproduced with permission from

**Groundwater derived arsenic in high carbonate wetland soils: Sources,
sinks, and mobility**

Markus Bauer, Beate Fulda, Christian Blodau

Science of the total Environment, 2008, 401, pp 109-120

Copyright 2008 Elsevier B.V.

available at www.sciencedirect.comwww.elsevier.com/locate/scitotenv

Groundwater derived arsenic in high carbonate wetland soils: Sources, sinks, and mobility

Markus Bauer, Beate Fulda, Christian Blodau*

Limnological Research Station and Department of Hydrology, University of Bayreuth, D-95440 Bayreuth, Germany

ARTICLE INFO

Article history:

Received 22 January 2008

Received in revised form

20 March 2008

Accepted 20 March 2008

Available online 21 May 2008

Keywords:

Arsenic

Iron

Organic matter

Carbonate

Peatland

Wetland

Groundwater

ABSTRACT

Wetlands and organic soils have been recognized as important sinks for arsenic in the environment, yet sources and immobilization mechanisms of As are often unclear. To begin rectifying this deficiency, we investigated As retention and binding mechanisms at a degraded, minerotrophic wetland site in contact with groundwater rich in As and Fe. Arsenic occurred in high dissolved concentrations of up to $467 \mu\text{g L}^{-1}$ in the groundwater, but dropped to values below $10 \mu\text{g L}^{-1}$ towards the surface. The solid phase As content instead was high in the topsoil with up to 3400 mg kg^{-1} and decreased with depth to 15 mg kg^{-1} . A similar pattern was observed with respect to Fe. Amorphous and crystalline iron precipitates were the main sorbents for arsenic in the soil horizons according to results from wet chemical sequential extractions. Arsenic was apparently not associated with inorganic carbon phases, but a substantial portion of up to 31% of As_{tot} could be mobilized by dispersion of soil organic matter. Ratios of dissolved As(III)/As(V) decreased from the deeper As(III) dominated groundwater to the As(V) dominated soil porewaters, where As was apparently immobilized in its oxidized form. Concentrations of the organic species DMA and MMA were negligible. According to the results of simple one-dimensional estimates the vertical arsenic transport from the source in the groundwater to the topsoil was slow given an extrapolation of current conditions. These results suggest that As accumulation started before the beginning of drainage in the now degraded peatland soils and the degradation and mass loss of organic matter under oxic conditions caused the very high As concentrations found in the topsoil horizon today.

© 2008 Elsevier B.V. All rights reserved.

1. Introduction

Arsenic is one of the most widespread and dangerous toxic substances in the environment, and the contamination of drinking water is especially problematic in developing countries (Mandal and Suzuki, 2002; Naidu et al., 2006; Smedley and Kinniburgh, 2002). Arsenic pollution of groundwaters can occur through natural and anthropogenic processes. In South Asia, for instance, the geogenic release of arsenic from sedimented iron phases under reducing conditions is seen as the main cause for groundwater contamination (Stuben et al., 2003). Co-deposition of organic matter with arsenic enriched

iron phases in these sediments probably favours this subsequent reductive arsenic mobilization (McArthur et al., 2004; Meharg et al., 2006).

Oxidizing conditions often lead to lower As mobility because of the formation of As(V) and its subsequent adsorption to metal oxides. Arsenic binding by carbonates (Magalhães, 2002) and silicates (Goldberg, 2002) has been demonstrated but Al, Mn and especially Fe oxides are the most important As sorbents under oxic conditions due to their large surface area (Smedley and Kinniburgh, 2002). The oxygenation of Fe(II) containing water to induce iron precipitation is used to sorb and remove As during water treatment (Jessen

* Corresponding author. Tel.: +49 921 552223; fax: +49 921 552366.

E-mail address: christian.blodau@uni-bayreuth.de (C. Blodau).

et al., 2005). At circumneutral pH As(V) ($pK_{s1}=2.2$) occurs mainly in the charged $H_2AsO_4^-$ or $HAsO_4^{2-}$ forms, whereas As(III) ($pK_{s1}=9.2$) is predominantly uncharged H_3AsO_3 (Cherry et al., 1979). Nonetheless the sorption capacity of As(V) and As(III) on positively charged ferrihydrite or goethite at neutral pH were found to be similar (Dixit and Hering, 2003). Sorption competition is known for anions, such as phosphate (Geelhoed et al., 1998), but also for dissolved organic carbon (Bauer and Blodau, 2006; Redman et al., 2002). Natural organic matter (NOM) influences arsenic mobility in several ways (Wang and Mulligan, 2006). Dissolved humics induce As redox transformation (Buschmann et al., 2005; Palmer et al., 2006; Tongesayi and Smart, 2006), form chemical bonds with aqueous As (Buschmann et al., 2006; Thanabalasingam and Pickering, 1986; Warwick et al., 2005) and influence the stability of As bearing colloids (Ritter et al., 2006). Finally organic matter promotes microbial activity, which changes the redox conditions and may induce methylation of arsenic (Huang and Matzner, 2006; Huang et al., 2007).

The relative immobility of As in organic matter rich peat bogs was used for instance to trace the history of atmospheric immission (Shotyk et al., 1996; Ukonmaanaho et al., 2004), but retention mechanisms of As have not been sufficiently investigated yet. Arsenic was also found to accumulate in minerotrophic peatlands and fens, which are in contact with more mineralized groundwaters (Shotyk, 1996; Steinmann and Shotyk, 1997; Szramek et al., 2004). The strong correlation of aqueous As(III) and Fe(II) concentrations during times of low redox potential, for example, suggested a binding of As and Fe in the same solid phase pool of a minerotrophic and iron rich fen (Blodau et al., in press; Huang and Matzner, 2006). Iron oxides typically precipitate in oxic surface layers or at the surfaces of oxygen conducting plant roots and may function as arsenic adsorbers. Pfeifer et al. (2004) hypothesized that Fe oxides formed in such organic rich layers are especially amorphous and have a large surface area available for sorption. Also in wetland soils influenced by geothermal waters, iron precipitates provided the main arsenic adsorption sites, even in presence of high contents of calcite, which is also a potential adsorber for As (Cornu et al., 2001). The storage of As in wetland soils may not be permanent though. Burial with ongoing decomposition and inundation of organic soils can entail decreasing redox potentials. Such changes are expected to lead to release of arsenic by iron oxides dissolution and peat degradation, which may to some extent be balanced by As binding in sulphide minerals under sulphate reducing conditions (Gonzalez et al., 2006; Meharg et al., 2006).

Wetland soils often cover large areas in valleys and lowlands, where groundwater occurs close to the land surface and promotes the transfer of arsenic rich water into the soil (Gonzalez et al., 2006; Pfeifer et al., 2004; Szramek et al., 2004). Many wetland systems are also subject to changes in the water regime such as drainage and rewetting, which may be the consequence of land use and climate change (Gorham, 1991). Little is yet known about the impact on the mobility of stored arsenic in the short- and long-term. In this study we thus focussed on arsenic dynamics in a groundwater influenced former wetland that has been subject to drainage and peat degradation for more than two centuries. The soils of this site are rich in organic and inorganic carbon, iron, and arsenic.

Our specific goals were (I) to analyse the current As distribution and the main soil arsenic pools, (II) to identify current processes of As mobilisation and immobilisation, and (III) to infer potential mechanisms and time periods leading to the extraordinary high As contents found in these soils. To achieve these goals, the soil solid phase and the porewater were sampled in the most important soil horizons and in the upper aquifer of two sites differing in iron oxide content in the top soils. The samples were analyzed with chemical and spectroscopic methods to determine the distribution of As between aqueous and solid phase and As speciation. These data were related to hydrological and geochemical controls at the site. We hypothesized that the As enrichment in the topsoil was primarily a result of a flux of ferrous Fe and As(III) from the deeper ground water, leading to Fe and As oxidation and enrichment in Fe oxides and As associated with the oxides. Other possible controls, such as association of dissolved As with the organic matter and carbonates, and enrichment in the solid phase due to degradation of the peat soils were considered as well.

2. Materials and methods

2.1. Site description

The study was carried out at a field site on the quaternary gravel plain north of Munich (Germany). The quaternary aquifer consists of dolomitic, fluviglacial material and is underlain by semipermeable marly silts of tertiary origin (Zahn and Seiler, 1992). The groundwater on the field site today is within 0.5–1 m of the land surface. Until the beginning of drainage in the 18th century minerotrophic peatlands dominated the study area, which have since then been degraded and converted into calcic or mollic gleysols (FAO). Arsenic enrichment was found with varying concentrations ($10\text{--}50\ \mu\text{g kg}^{-1}$, peaks $>500\ \mu\text{g kg}^{-1}$) in the topsoil on a regional scale (personal communication, Bayrisches Landesamt für Umwelt). Arsenic and iron content in quaternary aquifer material is low, and both elements are believed to be transported into the quaternary groundwater with water infiltrating from the subjacent tertiary aquifer at zones of high permeability (Rauert et al., 1993).

2.2. Field instrumentation and sampling

We selected two locations (site A and B), about 50 m apart, on an extensively used grassland for the investigation. The horizons 1 and 2 had a dark brown colour on site A, whereas ochre to red colours were prevalent at site B. The two sites differed strongly with respect to the solid phase iron content in the topsoil, and were chosen to elucidate the effect of different iron oxide content on As enrichment in the degraded wetland soil. Soil profiles were divided into 4 soil horizons (site A and B, horizon 1 to 4) above the coarse grained, dense aquifer material. The water table, averaged from measurements at all 4 sampling dates, was at 68 cm (site A) and 50 cm (site B) below the surface.

Soil samples were taken in triplicates from the four soil horizons in December 2005. To account for spatial heterogeneity three separate soil profiles about 1 m apart from one

another were sampled per site. The samples were frozen and freeze dried in the lab. Gravimetric water content was determined as the difference of field fresh and freeze dried samples. After sieving (<2 mm grain size) and removal of large roots, samples were ground for pH measurements, extractions, and spectral measurements.

The two sites were instrumented for porewater and groundwater sampling up to a depth of 130 cm below the surface. Suction cups consisting of a polyamide membrane on polyethylene frame (10 cm long; 0.45 μm pore size; preconditioned with 0.1 mol L⁻¹ HCl; Ecotech) were used above the water table. Below the groundwater table polyvinylchloride tubes (diameter 4.5 cm, perforated length of 10 cm, covered by nylon mesh) were installed as piezometers. To account for spatial heterogeneity in the aquifer, piezometers were set up in triplicate in 110 cm depth and in duplicate in 130 cm depth. The hand-drilled piezometer bore holes were refilled with layers of coarse and fine quartz, followed by bentonite up to the surface to prevent preferential flow along the tube. Every piezometer was fitted with a floating diffusion barrier on the water table, thus minimizing gas exchange with the atmosphere. A permanently installed groundwater well located nearby was used to sample groundwater from a depth of 2.5 m. Long-term recordings of the groundwater table were also available for this well. Soil solution and groundwater was sampled on 4 dates between November 2005 and June 2006. Samples from the piezometers and the groundwater well were taken after pumping and exchange of at least 2 piezometer or well volumes. Aqueous samples were immediately prepared and stabilized for analysis in the field as described in Section 2.3. Redox speciation of As and Fe was measured within 24 h after sampling.

2.3. Laboratory and analytical procedures

The wet chemical sequential extraction procedure consisted of four steps. As extractants we used 0.1 mol L⁻¹ NaNO₃, 1 mol L⁻¹ HCl, 6 mol L⁻¹ HCl, and 65% HNO₃. Soil samples of 0.3 g were shaken overhead in duplicates and darkness with the extraction solution and centrifuged before sampling. Samples contained no visible particles or colloids. Between extraction steps the soil was rinsed with Millipore water. Separate assays were made, in which 0.6 g soil was extracted in duplicates with Na₂P₄O₇, NaH₂PO₄ and Na-Acetate. The aqua regia digestion encompassed a reaction of 0.2 g sample with 1 ml HNO₃ (65%)

and 0.3 ml HCl (32%) for 24 h at room temperature and in triplicate. This step was followed by a microwave extraction with an additional volume of 8 ml HNO₃ and 0.2 ml HCl for a period of 1 h. Reaction conditions, target fractions, and references are listed for all extracts in Table 1. Extractions with NaNO₃ and Na₂P₄O₇ were carried out in an oxygen free glovebox to avoid changes in arsenic speciation.

The elemental composition of the soil extracts was analysed after filtration (0.45 μm Nylon, Roth) and acid stabilisation (1% HNO₃) by ICP-OES (Varian Vista-Pro) and Graphite Furnace AAS (Analytik Jena, Zeenith 60).

X-ray powder diffraction data were collected at room temperature using a Philips X Pert Pro X-ray diffraction system operating in reflection mode, with Co-Ka₁ ($\lambda=1.78897$ Å) radiation selected with a focusing monochromator, a symmetrically cut curved Johansson Ge₍₁₁₁₎ crystal, and a Philips X celerator detector. The Ka₂ line was reduced by the monochromator to <2% of the intensity of the Ka₁ line. The samples were X-rayed with diffractometer settings step size 0.03°, scan width 0.004 °/s, spinning platform rotation 1/s, and collection range 2 theta=7°–90°. XRD bands were identified by comparison to single mineral spectra of the mincryst database (Chichagov, 1997). FTIR spectra were measured with a Bruker Vector FTIR device (KBr pellets; transmission mode; wavelength 2–25 μm) and analyzed using the Salisbury spectral library (Salisbury, 1991). Apart from silicates, i.e. quartz, feldspar, mica, and clay minerals, various Ca, Fe and Al oxides, i.e. calcite, dolomite, goethite, siderite, gibbsite, and sulfides, i.e. pyrite and arsenopyrite, were considered. The soil pH was determined in 1 mol L⁻¹ KCl with a Sentix 21 electrode (WTW). Inorganic and organic carbon was determined by C/N analysis (Thermo Quest, Flash EA, 1112) before and after a 1 mol L⁻¹ HCl extraction.

Field measurements in the aqueous samples included pH (Sentix 21 electrode, WTW) and dissolved oxygen (Optical O₂ measurement system LDOM; Hach). Elemental composition and total As analysis was carried out as described above. Additionally, total and reduced iron was measured photometrically (Varian Cary 2e) using phenanthroline as spectral reagent at 512 nm (Tamura et al., 1974). Ion chromatography of 0.2 μm filtered samples was carried out for anions (Cl⁻, NO₃⁻, SO₄²⁻) using a Metrohm IC system (Metrosep Anion Dual 3 column, 0.8 mL min⁻¹, with chemical suppression) and dissolved organic carbon (DOC) was measured as non-purgable organic carbon (NPOC) on a Shimadzu TOC analyzer

Table 1 – Extraction procedures applied on the soil samples

Extractant	Conditions	Target As phase	Mechanism	Step no.	References
NaNO ₃	0.1 mol L ⁻¹ 24 h	Exchangeable	Exchange	1	Cai et al. (2002)
HCl	1 mol L ⁻¹ , 1 h	Amorph metal oxide, Carbonate, Acid volatile sulfide	Dissolution	2	Keon et al. (2001)
HCl	6 mol L ⁻¹ 30 min, 70 °C	Crystalline metal oxides	Dissolution	3	Regenspurg and Peiffer (2005)
HNO ₃	16 mol L ⁻¹ 1 h, microwave	Alumosilicates, sulfides	Dissolution, oxidation	4	Keon et al. (2001)
NaH ₂ PO ₄	0.1 mol L ⁻¹ , pH 5, 24 h	Specifically sorbed	Desorption	Separate	Cai et al. (2002)
Na-Acetate	1 mol L ⁻¹ , pH 5 24 h	Carbonate	Dissolution	Separate	Tessier et al. (1979)
Na ₂ P ₄ O ₇	0.1 mol L ⁻¹ 16 h	Organic matter bound	Dispersion	Separate	Bhattacharya et al. (2001)
HNO ₃ /HCl	Conc.HNO ₃ /HCl 1 h, microwave	All except silicates	Dissolution	Separate	

(TOC V CPN). Dissolved inorganic carbon (DIC) and CH_4 in the water samples were analyzed by headspace technique after sample acidification to $\text{pH} < 2$ (GC-FID/TCD; HP 6890; Beer and Blodau, 2007).

The arsenic speciation was measured by HPLC-ICP-MS (PRP X100 column, Hamilton; Agilent 7500ce). The separation method of Francesconi et al. (2002) allows for the quantification of arsenite, arsenate, dimethylarsinic acid (DMA) and monomethylarsonic acid (MMA). Sample preparation required a $0.2 \mu\text{m}$ filtration step ($0.2 \mu\text{m}$, Nylon, Roth), which was carried out in the field. To address As recovery problems, i.e. discrepancies between total As determined by AAS and the sum of As species detected by HPLC-ICP-MS, different other stabilization protocols were executed. Testing included the additional measurements of unfiltered samples and the chemical stabilization of samples filtered in the field with 2 mmol L^{-1} EDTA or 20 mmol L^{-1} HCl.

2.4. Calculations and modeling

The contribution of aqueous transport processes to the depth distribution of As was considered separately for the saturated and the vadose zones.

The As concentration versus depth profile for the aqueous phase below the groundwater table was simulated using a simple hydraulic box-model (Figure S1 of the supporting information) implemented in a STELLA system dynamics software (Beer and Blodau, 2007). The STELLA model consisted of five boxes representing the As or Cl pool in the four aqueous sampling depths in the saturated zone of site A and the nearby groundwater well (Figure S1 of the supporting information). The pools were linked to adjacent pools above and below through bidirectional diffusion and a vertical downward advection term as shown in Eqs. (1) and (2), which results also in some vertical numerical dispersion when a simulation is run.

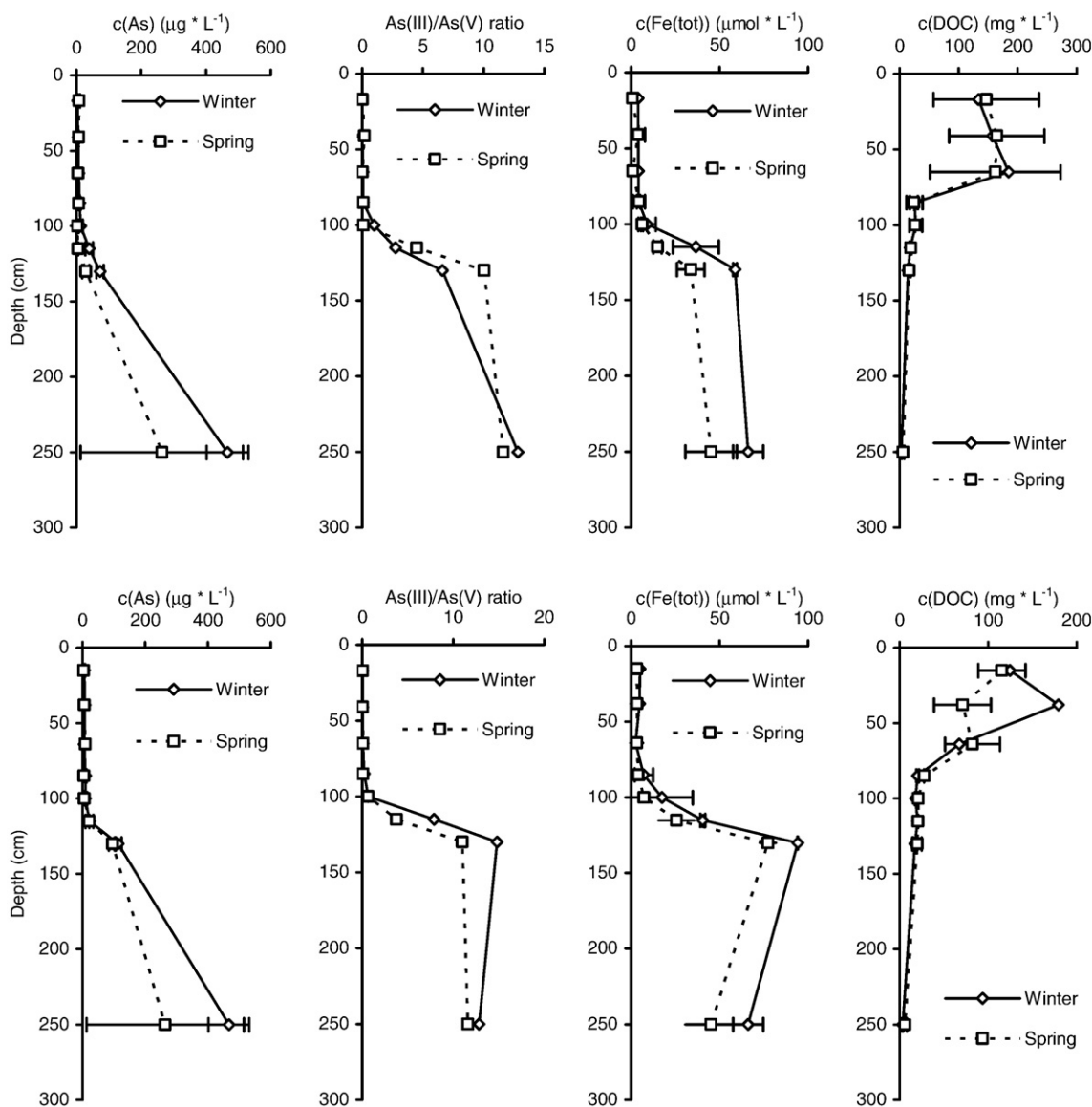


Fig. 1–Aqueous concentrations of total As, the As(III)/As(V) ratio, total Fe and DOC in soil porewater and in the quaternary groundwater (left to right). Values are depicted for site A (top) and B (bottom) in winter 2005/2006 (diamonds) and spring 2006 (squares). The lowest depth represents data from a groundwater well at the site.

An aquifer porosity of 0.26 (Zahn and Seiler, 1992) and a groundwater recharge of 100 mm a⁻¹ was estimated by difference between rainfall (700–800 mm a⁻¹) and evapotranspiration (500–600 mm a⁻¹; Winnegge and Maurer, 2002). Due to the lateral groundwater velocity (1–3 m d⁻¹, Rauert et al., 1993) and resulting Peclet numbers of >100, dispersion in vertical direction can be assumed to outweigh diffusion in this direction (Appelo and Postma, 2006). A transversal, i.e. vertically oriented, dispersion coefficient of 0.002 m² d used in the model was approximated according to Appelo and Postma (2006) by $D_{\text{transversal}} = 0.1 * D_{\text{longitudinal}}$. Concentration in segment 5 was kept constant to account for the source in the deep groundwater. Model calculations were performed until pool concentrations in the 4 upper segments were constant. Chloride served as a conservative tracer for comparison.

$$F_x = -D_T * \frac{\partial c}{\partial x} + v_x * c \quad (1)$$

$$v_x = \frac{q_x}{n} \quad (2)$$

F_x =flux [M L⁻² T⁻¹]; D_T =transversal diffusion–dispersion coefficient [L² T⁻¹]; c =concentration [M L⁻³]; x = length [L]; v =velocity [L T⁻¹]; q_x =flux density [L T⁻¹]; n =porosity [%].

Transport in the unsaturated zone above the groundwater table was estimated through water balance considerations. In the vadose zone of the upper soil horizons rainwater seepage, capillary rise and evapotranspiration take place. We used an evaporation rate of 500–600 mm a⁻¹ (Winnegge and Maurer, 2002) as the maximum estimate for upward water transport and calculated annual rates of mass transport with measured groundwater iron and arsenic concentrations data (Eq. (3)).

$$q(\text{element}) = c(\text{element}) * q(\text{water}) \quad (3)$$

q_x =flux density [M T⁻¹]; c =concentration [M L⁻³]; q =flux density [L³ T⁻¹].

Chemical saturation indices (SI) were calculated as the quotient of ion activity product (IAP) and saturation product (K_{sp}) with Phreeqc (Parkhurst and Appelo, 1999). Aqueous data from profile A was used and calcite, ferrihydrite, and goethite were considered.

Half cell redox potentials E_h were calculated according to the Nernst equation (Eq. (4)) for the redox pairs Fe(OH)₃/Fe²⁺ and HAsO₄²⁻/H₃AsO₃. Standard potentials E_h^0 were determined from standard energy of formation values by Eq. (5) (Pankow, 1991; Sergejeva and Khodakovskiy, 1969).

$$E_h = E_h^0 + \frac{R^*T}{n^*F} * \ln \left(\frac{\prod_i \{Ox\}^{n_i}}{\prod_j \{Red\}^{n_j}} \right) \quad (4)$$

$$E_h^0 = \frac{-\Delta G^0}{n^*F} \quad (5)$$

3. Results

3.1. Water chemistry

The water samples had circumneutral pH between 8.1 in the soil porewater and 7.0 in the groundwater. Dissolved oxygen in the piezometers decreased with depth from >6 mg L⁻¹ at the

surface to 1.5 mg L⁻¹ in the groundwater. Dissolved NO₃⁻ followed a similar trend from 34 mg L⁻¹ in the topsoil to <1 mg L⁻¹ in the aquifer. In contrast SO₄²⁻ concentrations were between 12 and 50 mg L⁻¹ and increased slightly with depth. CH₄ was found in low concentration of less than 3 μmol L⁻¹ in the groundwater below 100 cm depth. The redox potential on the field site therefore must be expected to decrease with depth, but conditions were not strongly reducing even in the groundwater, as the CH₄ concentration was low and both oxygen and nitrate were not fully depleted.

The concentrations of DIC (2–8 mmol L⁻¹), Ca (150–300 mg L⁻¹), Mg (12.5–30 mg L⁻¹), Mn (0.1–0.8 mg L⁻¹) and Al (0–0.2 mg L⁻¹) did not vary systematically along the depth profile. Because of different pH the SI of calcite was ~0 in the groundwater but increased to 1.2 in the topsoil, indicating calcite supersaturation in the topsoil horizons.

In contrast, concentrations of As, Fe, and DOC strongly varied with depth (Fig. 1). DOC concentrations were above 100 mg L⁻¹ in the upper part of the profiles and peaked in the third horizon at site A, and the first and second horizon at site B. Iron concentrations were 2–10 μmol L⁻¹ down to a depth of 100 cm, and increased strongly below, particularly in the form of Fe(II) contributing between 82% and 99% of total Fe. With SI well above 1, ferrihydrite formation was thermodynamically favourable at all depths, even in the groundwater. Arsenic was similarly distributed with depth. Concentrations were below 10 μg L⁻¹ in the upper 100 cm but reached 50–100 μg L⁻¹ in the lowest piezometer, and 250–500 μg L⁻¹ in the groundwater well, mostly in form of As(III). The As(III)/As(V) ratio changed from <1 to >10. DMA was detected at both sites at levels of 0.4–3.3 μg L⁻¹ only during winter. Organic species were previously shown to contribute significantly to the aqueous and mobile arsenic pool (Huang and Matzner, 2006; Huang and Matzner, 2007a; Huang and Matzner, 2007b). With DMA concentrations of 0.4–3.3 μg L⁻¹ and no detectable MMA, organic species accounted for less than 5% of As(tot) including the organic

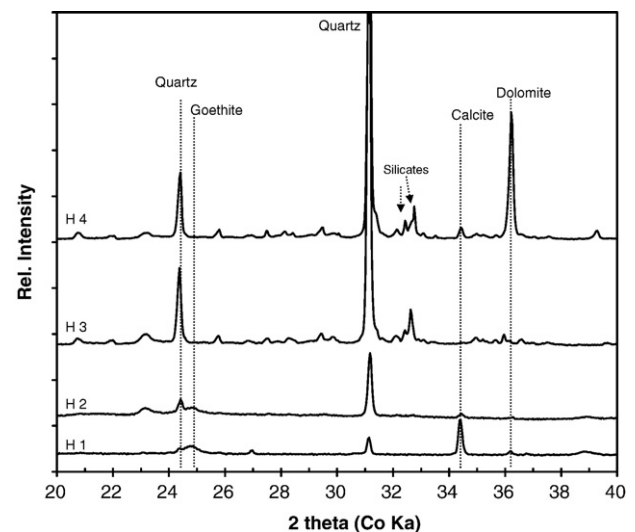


Fig. 2–Detail of the X-ray diffractograms recorded in material of horizons 1 to 4 of site B. Labels indicate the identified mineral phases quartz, goethite, calcite and dolomite. Clay/feldspar/mica peaks in the center of the diagram could not be attributed to specific minerals.

Table 2 – Physical and chemical properties of the soil horizons at sites A and B

Horizon	Depth cm	Water content %	pH _{KCl}	C _{org} %	C _{inorg} %	Ca	Mg	Fe	Al	As
						g kg ⁻¹	g kg ⁻¹	g kg ⁻¹	g kg ⁻¹	mg kg ⁻¹
Site A										
A 1	0–23	38	6.97	6.9	4.0	112.8	28.8	45.5	26.8	605.3
A 2	23–48	58	6.75	21.6	1.5	107.1	7.0	24.6	28.7	207.4
A 3	48–75	38	7.00	3.9	0.1	12.0	9.6	28.4	45.3	67.0
A 4	75+	22	7.22	0.7	4.7	80.0	46.8	18.0	19.4	27.9
Site B										
B 1	0–18	48	6.90	12.4	3.3	106.4	6.0	206.8	12.1	3239.2
B 2	18–43	66	6.86	24.8	3.6	58.7	3.8	45.1	20.7	509.1
B 3	43–70	31	6.83	1.7	0.5	11.1	9.5	27.3	37.2	22.3
B 4	70+	22	7.24	0.9	4.4	80.6	43.7	15.2	19.8	7.9

Total metal and arsenic content refers to the soil dry weight.

matter rich horizon, and were of minor importance on the investigated field site.

The total aqueous concentrations of As, Fe and DOC varied more strongly with depth than with sampling season or sampling site. Site B samples showed slightly higher concentrations of aqueous Fe and As in the groundwater and differences in concentrations occurred between sampling dates but clear temporal trends could not be identified. The general depth distribution pattern did not change with sampling time or site.

The sum of the concentrations of arsenic species, i.e. arsenite, arsenate, DMA and MMA, determined by HPLC-ICP-MS was up to 100 µg L⁻¹, or 70% lower than the total As concentration measured by AAS in acidified samples. Deviations were similar in unfiltered samples and samples filtered in the field, and largest deviations occurred at site B and in samples from greater depth. Addition of either EDTA or HCl to the filtered samples in the field increased As recovery in species measurements to about 90% of total As, but only EDTA preserved the As species distribution. Total iron concentration increased with depth, and the formation of iron precipitates was therefore most likely responsible for arsenic loss. In accordance with McCleskey et al. (2004), the As(III)/As(V) ratio was preserved using EDTA to stabilize the samples.

The calculated in situ Eh of the redox couples Fe(OH)₃/Fe²⁺ and As(V)/As(III) decreased with depth from -85 to -300 mV for Fe and 0 to -25 mV for As. Lowest values were reached

below the groundwater table at both sites. Similarly to the As_{tot} concentrations, Cl⁻ concentrations increased with depth below the groundwater table and reached 30 mg L⁻¹ in the groundwater. The concentration profiles of both As and Cl⁻ in the saturated zone could be adequately modelled with diffusion/longitudinal dispersion and advection as the only vertical transport processes (Figure S2 of the supporting information).

3.2. Solid phase

High pH values between 6.9 and 7.2 predominated in the soil and carbonates were important crystalline mineral phases at the site (Fig. 2). X-ray diffractograms showed bands for calcite (i.e. 34.4°, 2 theta, Co Ka) and dolomite (i.e. 36.2°, 2 theta, Co Ka) in the horizons B1, B2 and B4. This is in accordance with chemical extraction data, indicating largest contents of inorganic carbon, Ca and Mg in horizons 1 and 4 on sites A and B (Table 2) and high Ca and Mg extraction with 1 mol L⁻¹ HCl (Table 3). Calcite dominated in the topsoil. The prominence of the dolomite bands and the high Mg content in B4 indicates that this horizon represents the uppermost layer of the dolomite dominated aquifer (Zahn and Seiler, 1992).

Silicate minerals became more important in the two lower horizons. The X-ray diffractograms contained characteristic quartz bands (24.4°; 31.2°; 2 theta, Co Ka) throughout the profile, but highest intensities were found for B3 and B4

Table 3 – Calcium, iron, and arsenic content as fraction of soil dry weight in different extracts of the soil horizons on sites A and B

Horizon	Depth cm	0.1 mol L ⁻¹ NaNO ₃				1 mol L ⁻¹ HCl				6 mol L ⁻¹ HCl				0.1 mol L ⁻¹ Na ₂ P ₄ O ₇			
		%				%				%				%			
		Ca	Mg	Fe	As	Ca	Mg	Fe	As	Ca	Mg	Fe	As	Ca	Mg	Fe	As
Site A																	
A 1	0–23	0.0	0.0	0.0	0.1	92	85	30	43	2	5	45	51	4	0.0	0.0	23
A 2	23–48	0.1	0.0	0.0	0.2	84	32	29	46	2	13	48	50	6	0.0	0.0	24
A 3	48–75	0.3	0.0	0.0	0.3	52	11	17	52	1	35	44	37	29	0.0	0.0	27
A 4	75+	0.0	0.0	0.0	0.9	90	93	27	46	1	5	46	43	3	0.0	0.0	20
Site B																	
B 1	0–18	0.0	0.0	0.0	0.0	92	70	7	5	2	0	67	75	5	0.0	0.0	9
B 2	18–43	0.1	0.0	0.0	0.1	75	16	31	32	3	8	54	55	14	0.0	0.0	31
B 3	43–70	0.2	0.0	0.0	0.3	44	19	21	55	0	33	43	34	25	0.0	0.0	13
B 4	70+	0.0	0.0	0.0	1.7	90	94	25	36	1	5	43	41	3	0.0	0.0	16

material. Diffractograms from these two horizons also displayed bands in a range characteristic for feldspars, mica, and clay minerals ($32.23\text{--}32.75^\circ$, 2θ , Co Ka), which could not be allocated to specific mineral phase. Most Al in the soil was released only in the aqua regia extract and was associated with silicate minerals.

Iron content was highest in the topsoil. Site B contained more than 4 times greater quantities of Fe in horizon 1 than site A. Due to a strong decline with depth the Fe content was similar at both sites in horizons 3 and 4. Between 7 and 30% of Fe_{tot} was extracted by 1 mol L^{-1} HCl and therefore in the operationally defined amorphous iron oxide fraction (Table 3, Fig. 3). But despite high Fe content at all depths, the low and broad goethite band (24.9° , 2θ , Co Ka) was the only observed XRD signal representing an iron phase. Most iron was apparently found in non-crystalline phases, which were not detected by X-ray diffraction and predominantly extracted by 6 mol L^{-1} HCl (48–55% of Fe_{tot}).

The abundance of mineral solid phases was lowest in the organic carbon rich horizon B2, with up to 24.8% C_{org} . The high soil organic matter content apparently also lead to a high gravimetric water content of 50–60%. With the exception of total Fe and C_{org} content, the chemical composition of the different horizons at site A was very similar to site B. The FTIR spectra confirmed a similar mineral composition at both sites, with common FTIR spectral bands of calcite ($7\text{ }\mu\text{m}$; $11.4\text{ }\mu\text{m}$), quartz ($9.2\text{ }\mu\text{m}$), and clay minerals ($6\text{ }\mu\text{m}$; $9.6\text{ }\mu\text{m}$).

The soil arsenic content was between 7.9 mg kg^{-1} and more than 3 g kg^{-1} , decreased strongly with depth and was about 5 times higher in horizon 1 at site B than at site A. Despite the high total content, the exchangeable arsenic fraction in the soils was low, ranging from 0.13 to 0.82 mg kg^{-1} and thus accounting for $<2\%$ of the total arsenic present. Most arsenic could be extracted using 1 mol L^{-1} and 6 mol L^{-1} HCl together accounting for 77 to 96% of As in all horizons. The higher total As content at the iron rich site B suggests association of Fe and

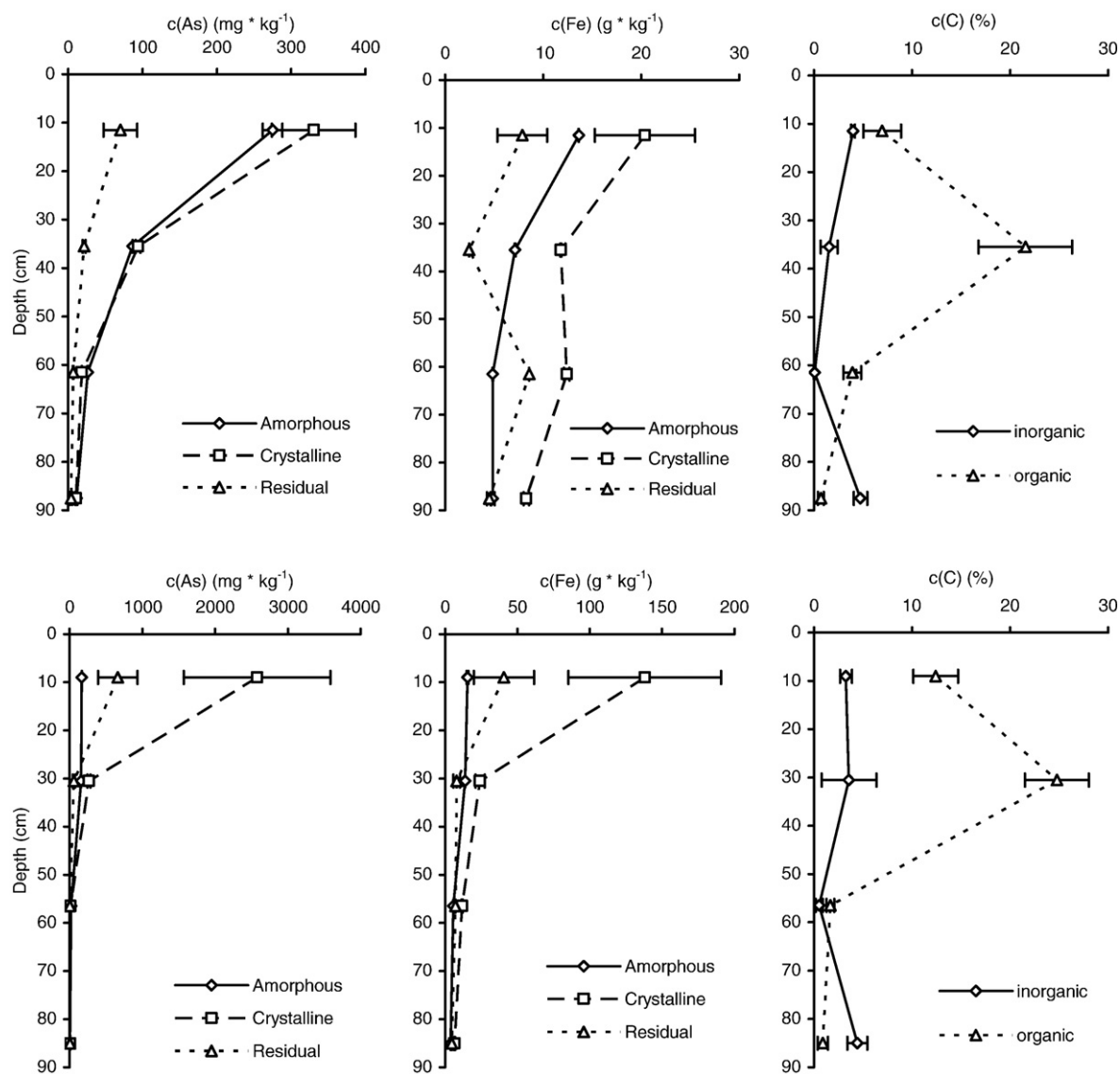


Fig. 3 – Solid phase content of As and Fe in extracts representative of amorphous metal oxides and carbonates (diamonds; 1 mol L^{-1} HCl), crystalline metal oxides (squares; 6 mol L^{-1} HCl) and a residual fraction (triangles; conc. HNO_3). Also shown is the content of organic (diamonds) and inorganic (triangles) carbon based on soil dry weight in the horizons of sites A (top) and B (bottom).

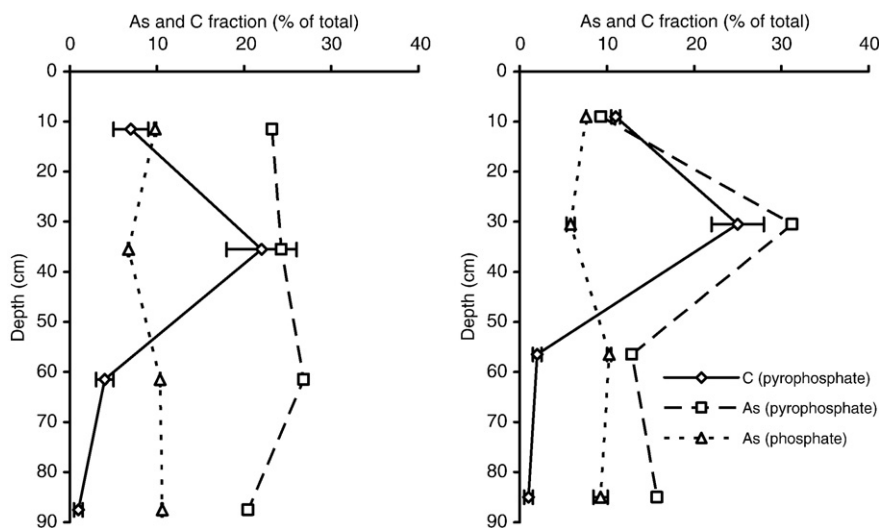


Fig. 4—Solid phase content of organic carbon (diamonds) and As (squares) as mobilized by $0.1 \text{ mol L}^{-1} \text{ Na}_2\text{P}_4\text{O}_7$ and of specifically sorbed As (triangles; $0.1 \text{ mol L}^{-1} \text{ NaH}_2\text{PO}_4$). Results refer to soil dry weight in the horizons of site A (left) and the iron enriched site B (right).

As. This is supported by the statistical correlation found for soil As_{tot} and Fe_{tot} content ($R=0.885$) using the ranking method by Spearman and a significance level of $p=0.01$.

The content of C_{org} in the soil was also correlated to As_{tot} ($R=0.776$) and in fact a substantial As fraction, representing 10–30% of As_{tot} , was released by dispersion of organic matter with pyrophosphate (Table 3). The largest fraction was extracted from the horizons at site A and in the second horizon of site B (Fig. 4). Between 5 and 25% of the soil organic carbon was released, particularly from the organic matter dominated horizons A2 and B2, but the mobilization of Ca, Mg, Fe or Al was negligible. More arsenic was extracted by pyrophosphate than with phosphate (5 to 10%) at all depths. Phosphate has a similar molecular structure as arsenate and can therefore be used to account for possible desorption reactions.

4. Discussion

Wetlands represent retention and enrichment zones for trace metals and metalloids including As (Gonzalez et al., 2006; Meharg et al., 2006; Pfeifer et al., 2004; Steinmann and Shoty, 1997). In spite of this well known fact, the importance of different As binding forms and As sorbents in these soils, i.e. oxides, sulfides and organic matter, has not yet been fully understood. Moreover, information about As sources and transport to wetland soils and the conditions and processes leading to As enrichment is often lacking. Our field site is characterized by a flat topography, a groundwater table close to the land surface, and a groundwater rich in As and thus provided ideal conditions to study As transport and retention processes in an organic matter rich soil.

4.1. Distribution and binding mechanisms of As in the solid phase

Iron oxides typically have a positive surface charge at circumneutral and slightly acidic pH, as the pH of zero charge

(pH_{pzc}) of ferrihydrite ranges from 7.8 to 7.9 and of goethite from 7.5–9.4 (Cornell and Schwertmann, 1996), which promotes an electrostatic association with negatively charged As (V). The minerals furthermore efficiently adsorb arsenic in specific surface complexes (Dixit and Hering, 2003; Fendorf et al., 1997). The soils at the studied field site were rich in amorphous and crystalline iron oxides. Contents decreased with depth and were greater at site B than at site A, which allows for comparisons regarding the role of iron hydroxides for As retention. The As content in the solid phase at all depths and both sites followed a similar trend and the total content of As and Fe in the amorphous and crystalline metal oxide fractions were correlated. Iron oxides were the most important As scavengers at our site at all depths, including the shallow aquifer. Previous studies already indicated that As was associated with iron in organic matter rich soils (Gonzalez et al., 2006; Pfeifer et al., 2004). Our new findings show that iron oxides are the predominant As sorbing phase in the degraded peatland studied. The As content in the soils amounted to between 10 and $200 \mu\text{mol (g Fe)}^{-1}$. The reported sorption capacities for iron oxides depend on surface area and are higher with respect to ferrihydrite ($1500 \mu\text{mol (g Fe)}^{-1}$) than to goethite ($120 \mu\text{mol (g Fe)}^{-1}$; Dixit and Hering, 2003). Especially owing to the substantial fraction of amorphous iron oxides, the sorption capacity of iron phases was sufficient to explain As binding at all depths.

Apart from an association of As with Fe, we also found As and organic carbon content to be correlated in the different soil samples. A considerable fraction of As could further be mobilized by dispersion of organic matter especially in the second soil horizon. Arsenic was thus apparently also associated with the organic soil phase. The importance of this As fraction increased with decreasing iron content and was larger in horizon 2 compared to horizon 1 and also larger at site A than site B. Bhattacharya et al. (2001) reported As association with organic phases in lake sediments as well, but information about binding mechanisms and capacities are lacking.

Covalent binding mechanisms and cation bridging complexes have been proposed to facilitate As binding reactions to dissolved organic matter molecules (Buschmann et al., 2006; Ritter et al., 2006; Thanabalasingam and Pickering, 1986) and it has been suggested that binding capacities reach up to $1000 \mu\text{mol As (g C)}^{-1}$ (Warwick et al., 2005). Such a number well exceeds the measured As content of 8–180 $\mu\text{mol As (g C)}^{-1}$ in the organic matter rich two topsoil horizons. Moreover, the presence of organic matter was hypothesized to cause a more amorphous structure of iron precipitates (Pfeifer et al., 2004). In similarity to the formation of iron colloids in organic matter rich solutions (Bauer and Blodau, submitted for publication), this might lead to smaller mineral particles and a higher surface area, increasing the overall quantity of sites available for As binding.

Alternative sorbents at the studied field site, such as calcite, dolomite, and silicates, were not found to considerably contribute to As binding in the solid phase. Despite the high contents of calcite in the topsoil and dolomite in the fourth soil horizon, the results from Na-Acetate extractions and correlation analysis did not indicate any association of arsenic with these carbonate minerals. This is in accordance with findings of Cornu et al. (2001), who documented that in the presence of iron phases As binding to calcite precipitates was negligible. A substantial contribution of silicate minerals to As binding was unlikely due to their low pH_{pzc} of 3–4.5 and a low As sorption capacity of 0.2 to 0.5 $\mu\text{mol g}^{-1}$ on clay (Goldberg, 2002) and 2 to 5 $\mu\text{mol g}^{-1}$ on mica (Chakraborty et al., 2007). No correlation between As and Al was found in the extraction solutions, suggesting that As association with Al containing minerals was negligible (Dousova et al., 2003). Our dataset provided no indication for arsenic binding to reduced iron sulphide minerals. XRD spectra showed no pyrite or arsenopyrite bands, redox conditions were only mildly reducing, and As content in the residual fraction was mostly low.

4.2. As source and aqueous transport in the saturated zone

Arsenic accumulation in soils and minerotrophic peatlands has previously been attributed to high As input stemming from streams or groundwater (Gonzalez et al., 2006; Steinmann and Shoty, 1997; Szramek et al., 2004). Often, however, the source of As and its transport to the enrichment zones were not investigated and documented. The highest aqueous As concentrations at our site were found in the deepest groundwater samples and, therefore, groundwater presumably represented the source of As present in the top soil. High dissolved As concentrations are known to occur in tertiary sediment layers of southern Germany (Heinrichs and Udluft, 1996; Heinrichs, 1998). The occurrence of locally high concentrations of As in the quarternary aquifer water close to the surface was attributed to zones of a locally high permeability of the aquitard and water exchange between quarternary and tertiary sediment layers.

Along the concentration gradient towards the groundwater table, the strongest decrease in aqueous As concentration occurred in the saturated zone at a depth of 100 to 250 cm. The applied hydraulic transport model was able to adequately explain the measured As depth profile in the saturated zone

with vertical advection and diffusion/dispersion processes. Alternatively, also the presence of an As sink in the solid phase might have been responsible for declining As concentrations at these depths. In spite of this current apparent sink for arsenic, soil material from the deepest soil horizons A4 and B4 had the lowest measured total As content of all solid phases. This is in agreement with the mineralogy of these horizons, which was similar as in the aquifer material below and dominated by dolomite (Zahn and Seiler, 1992). These horizons thus had a low capacity to bind As in the solid phase (Thornburg and Sahai, 2004). A substantial sequestration of As in the lowest soil horizons, where the apparent sink occurred, thus seems unlikely also from a mechanistic point of view.

The discrepancy between current apparent As sinks and contents of As in the solid phase cannot be resolved conclusively. Models of the type used were previously applied at field sites with less lateral water flux (Beer and Blodau, 2007), but due to the flat regional topography and low inclination of the groundwater table we expected effects of lateral flow on the vertical distribution of arsenic to be low at this site as well. We cannot exclude a solid phase sink as the reason for the decrease of aqueous As in the groundwater, because of an inadequate representation of reality in the model. It may also be that dilution of groundwater rich in As by infiltrating precipitation did cause the observed aqueous As profile in the saturated zone.

4.3. Transport and enrichment in the vadose zone

The dissolved concentrations of As and Fe above a depth of 100 cm were low and more or less uniform. Ferric iron was the predominant iron species in contrast to ferrous iron which predominated in the deeper groundwater. The supersaturation of the solution with respect to dissolved Fe and the precipitation of ferrihydrite likely caused the low total dissolved iron concentration. Dissolved As concentrations are strongly affected by sorption and coprecipitation with ferrihydrite phases, explaining the low fraction of As being in a dissolved state (Dixit and Hering, 2003; Jessen et al., 2005). The coupling of Fe and As dynamics was exemplified by the similar concentration profiles of both elements and the correlation of As and Fe content in the solid phase. The sorption capacities of ferrihydrite for As(III) and As(V) were found to be similar at neutral pH, even though As(V) species are negatively charged due to acidity constants of $\text{pK}_{\text{s}1}=2.2$ and $\text{pK}_{\text{s}2}=6.8$ and thus should have a higher affinity for positively charged iron phases than the uncharged As(III) species, which has a $\text{pK}_{\text{s}1}$ of 9.2 (Cherry et al., 1979; Dixit and Hering, 2003). If this finding holds true also for the field site investigated, the change in redox speciation, from As(III) predominant in the groundwater to mainly As(V) in the topsoil, supposedly had only a minor effect on As binding by the solid phase. The sorption or incorporation of As in the water-unsaturated soil horizons was apparently not decisively impeded by high concentration of dissolved organic matter, which may lead to desorption of As from soil materials (Bauer and Blodau, 2006; Grafe et al., 2002). This finding may be a consequence of the high total iron content at the site. The total surface area available in the soils obviously provided a sufficient capacity of sorption sites for both organic and As anions.

The highest As accumulation was found in the topsoil horizons and measured As contents were high compared to literature values for soils (Mandal and Suzuki, 2002; Smedley and Kinniburgh, 2002). Under current conditions, capillary water movement was the only possibility for transport of As and Fe through the vadose zone to the highly enriched surface horizon. The small grain size and high organic matter content in horizons A2 and B2 most likely caused the high capillary water content in these horizons and allowed water transport into the topsoil horizon (Hoeltig, 1996). Using the local evaporation rate of 500–600 mm a⁻¹ as maximum estimate for upward water flux and water concentrations at the groundwater table, transport rates of 2 mg m⁻² a⁻¹ As and 60–80 mg m⁻² a⁻¹ Fe can be reached. To accumulate the amount of Fe and As found in the A1 and B1 horizons under current conditions by this process alone, time periods of more than 10,000 years would be required. We know that water regime at the site changed substantially with the beginning of drainage for agricultural purposes two centuries ago, and this supposedly led to a substantial change in the water fluxes and geochemical conditions. Our assessment of the As accumulation time scale is therefore restricted to the conclusion that As enrichment must have started more than 200 years ago and probably considerably before this time.

Assessing the reasons for arsenic accumulation in the originally undrained, minerotrophic peatland is speculative. We assume that the process proceeded analogously to other peatland sites where As accumulated in soils with high organic matter content, high water table and under partly reducing conditions (Blodau et al., in press; Gonzalez et al., 2006; Meharg et al., 2006; Pfeifer et al., 2004). Arsenic binding to metal oxides phases in these systems primarily occurred in surface layers with at least temporarily oxic conditions or in the partly oxic rhizosphere of plants capable of oxygen transport into the soil (Blodau et al., in press; Keon-Blute et al., 2004). At another site pyrite minerals or organic phases have been conjectured to be more important as As sorbents but the authors did not provide data about As associated with different solid phases (Gonzalez et al., 2006). We thus assume that a higher groundwater table improved As transport from the groundwater into the soil at our site (Szramek et al., 2004). With the beginning of drainage As released by oxidation of iron sulphide minerals and organic matter probably was efficiently reabsorbed on present or freshly forming iron oxide phases (Thornburg and Sahai, 2004). The soil mass loss due to the decomposition of the organic peat material under oxic conditions likely intensified the enrichment and accumulation of inorganic soil constituents in the topsoil layer. Even though this is speculative, this scenario outlines another explanation for the very high As enrichment found in the topsoil at the studied field site, which is more difficult to explain alone by an extrapolation of current conditions backward in time.

The solid phase content of As and Fe was substantially different at sites A and B (Table 2), confirming our original hypothesis. Site B contained up to four times more As and Fe in the topsoil horizons than site A. Given that crystalline Fe oxides were the primary sorbent for As according to the results of the sequential extraction (Table 3) the additional enrichment of As at the more iron rich site B is not surprising and again highlights the importance of iron oxide content for arsenic retention in these wetland soils. The exact reasons why Fe and

As contents were so much higher at site B cannot be clarified conclusively. It may be that the As enrichment reflects an effect of more sorption sites being available during degradation of the wetland soils and the resulting potential As release from sulfides and organic matter. In this case only the historic flux of dissolved ferrous Fe and associated formation of iron oxides into the topsoil of site B was higher. Alternatively both the As and Fe flux were elevated and As co-precipitated with ferric iron oxides, which were subsequently diagenetically transformed in well crystalline iron oxides and incorporated the As. Differences in the flux of both elements into the soils could be attributed to local differences in water flux from subjacent, more As and Fe rich, tertiary aquifer (Rauert et al., 1993).

5. Conclusions

Dissolved As concentrations were in the low range of reported groundwater data up to 1 m depth and below the WHO guideline value of 10 µg L⁻¹ (Mandal and Suzuki, 2002; Smedley and Kinniburgh, 2002). The very large solid phase arsenic pool in the oxic topsoil was not exchangeable and strongly sorbed mainly to crystalline iron oxide phases (Mandal and Suzuki, 2002; Smedley and Kinniburgh, 2002). This indicates a high stability of the present As pool in the soil under current conditions. A change of the redox regime to more reducing conditions, however, would probably initiate a slow release of As due to As reduction, As desorption and reductive dissolution of the iron oxides, which might be balanced by reabsorption on remaining iron phases and binding in reduced solid phases like sulfides (Blodau et al., in press; Kocar et al., 2006; O'Day et al., 2004; Tadanier et al., 2005). Arsenic was primarily associated with iron oxide phases and no binding to calcite precipitates was found. Instead a considerable association was found between As and humics in the most organic matter rich horizons.

The primary As source at the field site was in the groundwater but current vertical transport towards the surface was low in the vadose zone. This implies that As accumulation at the site started already in the peatland soil before the beginning of drainage. Even though we can only speculate about conditions in the peat prior to drainage, the occurrence of As binding to metal oxide phases at the surface or reduced mineral and organic matter in greater depth can be inferred from previous studies (Blodau et al., in press; Gonzalez et al., 2006; Keon-Blute et al., 2004). Arsenic enrichment in the surface layer was possibly amplified by soil mass loss due to peat degradation under the oxic conditions after drainage. Secondly low As transport to the surface also shows that under current conditions only a small fraction of groundwater derived As is retained in the soil surface layer. The fate of the large As pool remaining in the solute phase of the groundwater is unknown and As monitoring downstream of the sampling site and on the regional scale should be the concern of future studies.

Acknowledgments

We thank the Bayrisches Landesamt für Umwelt for introducing us to the field site and Tiziana Boffa-Balaran (Bavarian Research Institute of Experimental Geochemistry and

Geophysics) for XRD measurements and help during interpretation. Thanks also to Karin Soellner, Martina Rohr and a number of students for contributing significantly to field and laboratory work. Finally we want to thank the German Research foundation (DFG) for their support through grants BL563/7-1 and BL563/7-2 to Christian Blodau.

Appendix A. Supplementary data

Supplementary data associated with this article can be found, in the online version, at [doi:10.1016/j.scitotenv.2008.03.030](https://doi.org/10.1016/j.scitotenv.2008.03.030).

REFERENCES

- Appelo CAJ, Postma D. *Geochemistry, groundwater and pollution*. Leiden: A.A. Balkema Publishers; 2006.
- Bauer M, Blodau C. Mobilization of arsenic by dissolved organic matter from iron oxides, soils and sediments. *Sci Total Environ* 2006;354:179–90.
- Bauer M, Blodau C. Experimental colloid formation in aqueous solutions rich in dissolved organic matter, ferric iron, and As. *Geochim Cosmochim Acta* submitted for publication.
- Beer J, Blodau C. Transport and thermodynamics constrain belowground carbon turnover in a northern peatland. *Geochim Cosmochim Acta* 2007;71:2989–3002.
- Bhattacharya P, Jacks G, Jana J, Sracek O, Gustafsson JP, Chatterjee C. KTH Special Publication, TRITA-AMI-Report 3084. 2001.
- Blodau C, Fulda B, Bauer M, Knorr KH. Arsenic speciation and turnover in intact organic soils during experimental drought and rewetting. *Geochim Cosmochim Acta* in press.
- Buschmann J, Canonica S, Lindauer U, Hug SJ, Sigg L. Photoirradiation of dissolved humic acid induces arsenic(III) oxidation. *Environ Sci Technol* 2005;39:9541–6.
- Buschmann J, Kappeler A, Lindauer U, Kistler D, Berg M, Sigg L. Arsenite and arsenate binding to dissolved humic acids: influence of pH, type of humic acid, and aluminum. *Environ Sci Technol* 2006;40:6015–20.
- Chakraborty S, Wolthers M, Chatterjee D, Charlet L. Adsorption of arsenite and arsenate onto muscovite and biotite mica. *J Colloid Interface Sci* 2007;309:392–401.
- Cai Y, Cabrera JC, Georgiadis M, Jayachandran K. Assessment of arsenic mobility in the soils of some golf courses in South Florida. *Sci Tot Environ* 2002;291:123–34.
- Cherry JA, Shaikh AU, Tallman DE, Nicholson RV. Arsenic species as an indicator of redox conditions in groundwater. *J Hydrol* 1979;43:373–92.
- Chichagov AV. 1997. WWW-MINCRYST: Crystallographic and Crystallochemical Database for Mineral and their Structural Analogues. <http://database.iem.ac.ru/mincryst/index.php>. 2007, August.
- Cornell RM, Schwertmann U. *The iron oxides. Structures, properties, reactions, occurrences and uses*. Weinheim: VCH Verlagsgesellschaft; 1996.
- Comu S, Negrel P, Brach M. Impact of carbo-gaseous saline waters registered by soils. *Catena* 2001;45:209–28.
- Dixit S, Hering JG. Comparison of arsenic(V) and arsenic(III) sorption onto iron oxide minerals: implications for arsenic mobility. *Environ Sci Technol* 2003;37:4182–9.
- Dousova B, Machovic V, Kolousek D, Kovanda F, Dornicak V. Sorption of As(V) species from aqueous systems. *Water Air Soil Pollut* 2003;149:251–67.
- Fendorf S, Eick MJ, Grossl PR, Sparks DL. Arsenate and chromate retention mechanism on goethite. 1. surface structure. *Environ Sci Technol* 1997;31:315–20.
- Francesconi K, Visoottiviset P, Sridokchan W, Goessler W. Arsenic species in an arsenic hyperaccumulating fern, *Pityrogramma calomelanos*: a potential phytoremediator of arsenic-contaminated soils. *Sci Total Environ* 2002;284:27–35.
- Geelhoed JS, Hiemstra T, Van Riemsdijk WH. Competitive interaction between phosphate and citrate on goethite. *Environ Sci Technol* 1998;32:2119–23.
- Goldberg S. Competitive adsorption of arsenate and arsenite on oxides and clay minerals. *Soil Sci Soc Am J* 2002;66:413–21.
- Gonzalez ZI, Krachler M, Cheburkin AK, Shotykh W. Spatial distribution of natural enrichments of arsenic, selenium, and uranium in a minerotrophic peatland, Gola di Lago, Canton Ticino, Switzerland. *Environ Sci Technol* 2006;40:6568–74.
- Gorham E. Northern Peatland—role in the carbon cycle and probable responses to climate warming. *Ecol. Appl* 1991;1:182–95.
- Grafe M, Eick MJ, Grossl PR, Saunders AM. Adsorption of arsenate and arsenite on ferrihydrite in the presence and absence of dissolved organic carbon. *J Environ Qual* 2002;31:1115–23.
- Heinrichs G. Arsen im Grund- und Trinkwasser Bayerns; 1998.
- Heinrichs G, Udluft P. *Geogenes Arsen in den Grundwaessern Deutschlands unter Berücksichtigung der Aquifergeologie*. Zeitung der deutschen geologischen Gesellschaft 1996;147:519–30.
- Hoelting B. *Hydrogeologie*. Ferdinand Enke Verlag. Stuttgart; 1996.
- Huang JH, Matzner E. Dynamics of organic and inorganic arsenic in the solution phase of an acidic fen in Germany. *Geochim Cosmochim Acta* 2006;70:2023–33.
- Huang JH, Matzner E. Mobile arsenic in unpolluted and polluted soils. *Sci Total Environ* 2007a;377:308–18.
- Huang JH, Matzner E. Biogeochemistry of organic and inorganic arsenic species in a forested catchment in Germany. *Environ Sci Technol* 2007b;41:1564–9.
- Huang JH, Scherr F, Matzner E. Demethylation of dimethylarsinic acid and arsenobetaine in different organic soils. *Water Air Soil Pollut* 2007;182:31–41.
- Jessen S, Larsen F, Koch CB, Arvin E. Sorption and desorption of arsenic to ferrihydrite in a sand filter. *Environ Sci Technol* 2005;39:8045–51.
- Keon-Blute N, Brabander DJ, Hemond HF, Sutton SR, Newville MG, Rivers ML. Arsenic sequestration by ferric iron plaque on cattail roots. *Environ Sci Technol* 2004;38:6074–7.
- Keon NE, Swartz CH, Brabander DJ, Harvey C, Hemond HF. Validation of an arsenic sequential extraction method for evaluating mobility in sediments. *Environ Sci Technol* 2001;35:2778–84.
- Kocar B, Herbel M, Tufano KJ, Fendorf S. Contrasting effects of dissimilatory iron(III) and arsenic (V) reduction on the arsenic retention and transport. *Environ Sci Technol* 2006;40:6715–21.
- Magalhães CMF. Arsenic. An environmental problem limited by solubility. *Pure Appl Chem* 2002;74:1843–50.
- Mandal BK, Suzuki KT. Arsenic round the world: a review. *Talanta* 2002;58:201–35.
- McArthur JM, Banerjee DM, Hudson-Edwards KA, Mishra R, Purohit R, Ravenscroft P, et al. Natural organic matter in sedimentary basins and its relation to arsenic in anoxic groundwater: the example of West Bengal and its worldwide implications. *Appl Geochem* 2004;19:1255–93.
- McCleskey RB, Nordstrom DK, Maest AS. Preservation of water samples for arsenic(III/V) determinations: an evaluation of the literature and new analytical results. *Appl Geochem* 2004;19:995–1009.
- Meharg AA, Scrimgeour C, Hossain SA, Fuller K, Cruickshank K, Williams PN, et al. Codeposition of organic carbon and arsenic in Bengal Delta aquifers. *Environ Sci Technol* 2006;40:4928–35.
- Naidu R, Smith E, Owens G, Bhattacharya P, Nadebaum P. *Managing arsenic in the environment*. Collingwood: CSIRO Publishing; 2006.
- O'Day PA, Vlassopoulos D, Root R, Rivera N. The influence of sulfur and iron on dissolved arsenic concentrations in the shallow

- subsurface under changing redox conditions. *Proc Natl Acad Sci U S A* 2004;101:13703–8.
- Palmer NE, Freudenthal JH, von Wandruszka R. Reduction of arsenates by humic materials. *Environ Chem* 2006;3:131–6.
- Pankow JF. *Aquatic chemistry concepts*. Chelsea: Lewis Publications; 1991.
- Parkhurst DL, Appelo CAJ. 1999. User's guide to PHREEQC — A computer program for speciation, batch-reaction, one dimensional transport, and inverse geochemical calculations. US department of the interior.
- Pfeifer HR, Gueye-Girardet A, Reymond D, Schlegel C, Temgoua E, Hesterberg DL, et al. Dispersion of natural arsenic in the Malcantone watershed, Southern Switzerland: field evidence for repeated sorption–desorption and oxidation–reduction processes. *Geoderma* 2004;122:205–34.
- Rauert W, Wolf M, Weise SM, Andres G, Egger R. Isotope-hydrogeological case study on the penetration of pollution into deep Tertiary aquifer in the area of Munich, Germany. *J Contam Hydrol* 1993;14:15–38.
- Redman AD, Macalady DL, Ahmann D. Natural organic matter affects arsenic speciation and sorption onto hematite. *Environ Sci Technol* 2002;36:2889–96.
- Regenspurg S, Peiffer S. Arsenate and chromate incorporation in Schwertmannite. *Appl Geochem* 2005;20:1226–39.
- Ritter K, Aiken GR, Ranville J, Bauer M, Macalady DL. Evidence for the aquatic binding of arsenate by natural organic matter (NOM)-suspended Fe(III). *Environ Sci Technol* 2006;40:5380–7.
- Salisbury JW. *Infrared (2.1–25 μm) spectra of minerals*. Baltimore: Johns Hopkins Univ. Press; 1991.
- Sergeyeva E, Khodakovskiy I. Physicochemical conditions of formation of native arsenic in hydrothermal deposits. *Geochem Int USSR* 1969;6:681–94.
- Shotyk W. Natural and anthropogenic enrichments of As, Cu, Pb, Sb, and Zn in ombrotrophic versus minerotrophic peat bog profiles, Jura mountains, Switzerland. *Water Air Soil Pollut* 1996;90:375–405.
- Shotyk W, Cheburkin AK, Appleby PG, Fankhauser A, Kramers JD. Two thousand years of atmospheric arsenic, antimony, and lead deposition recorded in an ombrotrophic peat bog profile, Jura mountains, Switzerland. *Earth Planet Sci Lett* 1996;145: E1–7.
- Smedley PL, Kinniburgh DG. A review of the source, behaviour and distribution of arsenic in natural waters. *Appl Geochem* 2002;17:517–68.
- Steinmann P, Shotyk W. Geochemistry, mineralogy, and geochemical mass balance on major elements in two peat bog profiles (Jura mountains, Switzerland). *Chem Geol* 1997;138:25–53.
- Stuben D, Berner Z, Chandrasekharam D, Karmakar J. Arsenic enrichment in groundwater of West Bengal, India: geochemical evidence for mobilization of As under reducing conditions. *Appl Geochem* 2003;18:1417–34.
- Szramek K, Walter LM, McCall P. Arsenic mobility in groundwater/surface water systems in carbonate-rich Pleistocene glacial drift aquifers (Michigan). *Appl Geochem* 2004;19:1137–55.
- Tadanier CJ, Schreiber ME, Roller JW. Arsenic mobilization through microbially mediated deflocculation of ferrihydrite. *Environ Sci Technol* 2005;39:3061–8.
- Tamura H, Goto K, Yotsuyan T, Nagayama M. Spectrophotometric determination of iron(II) with 1,10-phenanthroline in presence of large amounts of iron(III). *Talanta* 1974;21:314–8.
- Tessier A, Campbell PGC, Bisson M. Sequential extraction procedure for speciation of particulate trace metals. *Analyt Chem* 1979;51:844–51.
- Thanabalasingam P, Pickering WF. Arsenic sorption by humic acids. *Environ Pollut* 1986;12:233–46.
- Thornburg K, Sahai N. Arsenic occurrence, mobility, and retardation in sandstone and dolomite formations of the Fox River Valley, Eastern Wisconsin. *Environ Sci Technol* 2004;38:5087–94.
- Tongesayi T, Smart RB. Arsenic speciation: reduction of arsenic(V) to arsenic(III) by fulvic acid. *Environ Chem* 2006;3:137–41.
- Ukonmaanaho L, Nieminen TM, Rausch N, Shotyk W. Heavy metal and arsenic profiles in ombrogenous peat cores from four differently loaded areas in Finland. *Water Air Soil Pollut* 2004;158:277–94.
- Wang SL, Mulligan CN. Effect of natural organic matter on arsenic release from soils and sediments into groundwater. *Environ Geochem Health* 2006;28:197–214.
- Warwick P, Inam E, Evans N. Arsenic's interaction with humic acid. *Environ Chem* 2005;2:119–24.
- Winnegge R, Maurer T. *Water resources management country profile Germany*. Federal Institute of Hydrology. Koblenz; 2002.
- Zahn MT, Seiler KP. Field studies on the migration of arsenic and cadmium in a carbonate gravel aquifer near Munich (Germany). *J Hydrol* 1992;133:201–14.

Supporting Information

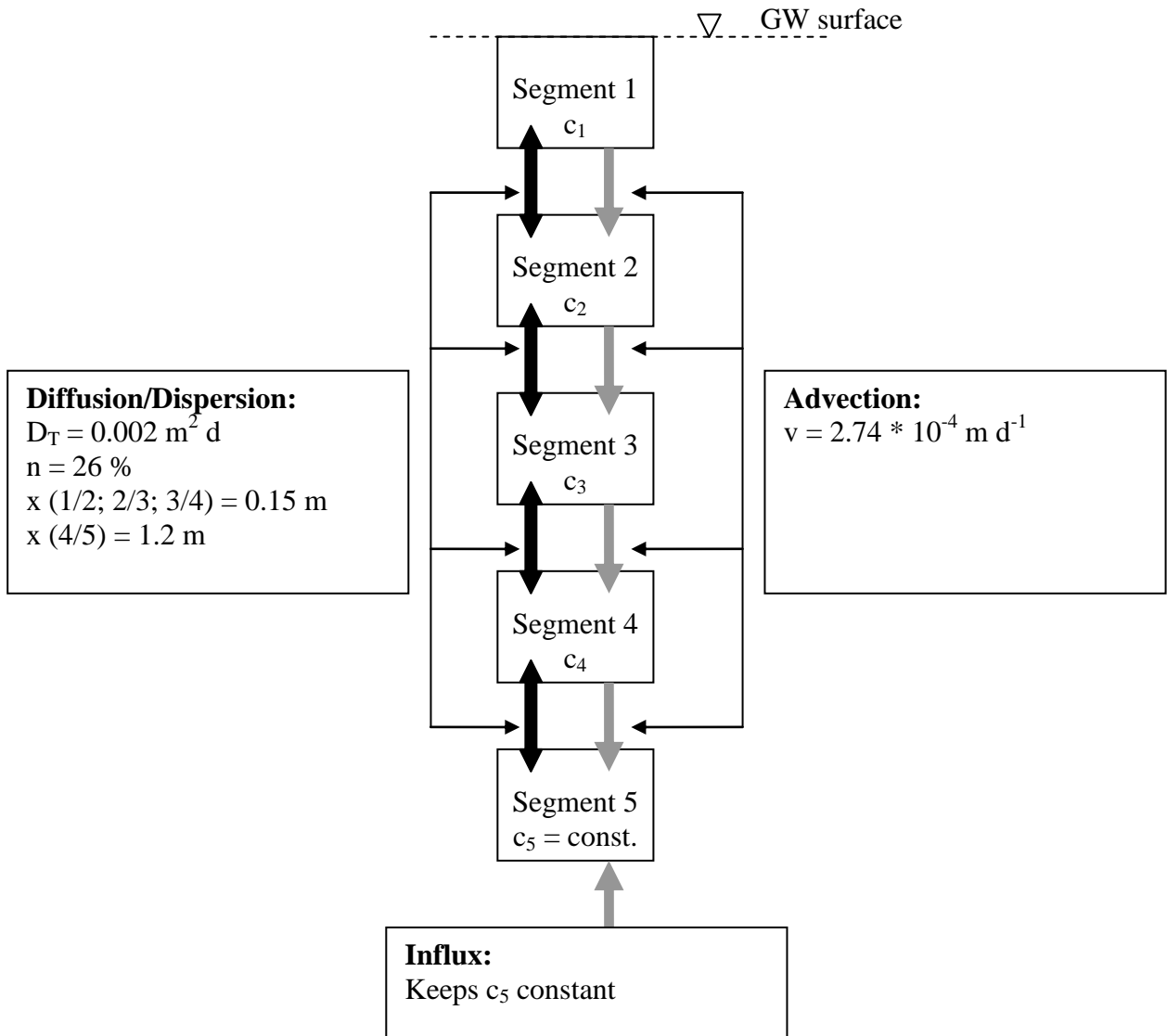


Figure 67 Structure of the used STELLA model

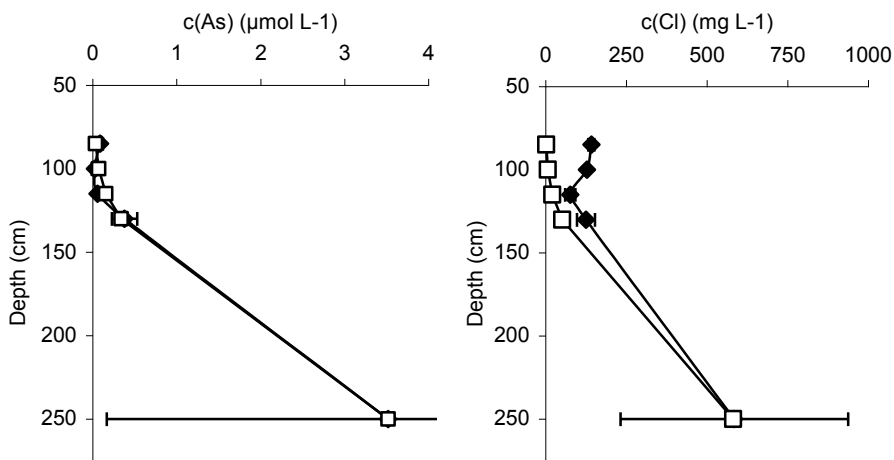


Figure 67 Measured and modelled depth profile of As and Cl

Redox reactions and redox potentials

The redox potential E_h for a reduction or oxidation half reaction is calculated by the Nernst equation (Eq. 1) and is related to the Gibbs free energy of reaction (Eq. 2). Standard redox potential values E_h^0 are derived for a half reaction by comparison to the standard hydrogen electrode (SHE). Redox potentials E_h (W) for neutral pH were calculated with the Nernst equations for each redox half reaction as shown in Table 26. Where necessary redox potentials were additionally corrected for other experimental pH conditions and species, yielding the values documented in Table 4 of supporting information to study 1. The determination of the direction of electron flow for two half reaction requires the calculation of the electromotive force (EMF, Eq. 3) and positive EMF values indicate energy yield.

$$E_h = E_h^0 + \frac{R * T}{n * F} * \ln \frac{\prod_i \{Ox\}^{n_i}}{\prod_j \{Red\}^{n_j}} \quad (\text{Eq. 1})$$

$$E_h^0 = \frac{-\Delta G^0}{n * F} \quad (\text{Eq. 2})$$

$$EMF = E_{h,Reduction} - E_{h,Oxidation} \quad (\text{Eq. 3})$$

Table 27 Reactions and their respective half cell Nernst equation

Reaction	Nernst Equation
(1) $H_2AsO_4^- + 2 e^- + 3 H^+ = H_3AsO_3 + H_2O$	$E_{h,As} = E_h^0 - 0.088 \bullet pH + \frac{0.059}{2} \bullet \lg \frac{a(H_3AsO_3)}{a(H_2AsO_4^-)}$
(2) $HAsO_4^{2-} + 2 e^- + 4 H^+ = H_3AsO_3 + H_2O$	$E_{h,As} = E_h^0 - 0.118 \bullet pH + \frac{0.059}{2} \bullet \lg \frac{a(H_3AsO_3)}{a(HAsO_4^{2-})}$
(3) $Q + 2 e^- + 2 H^+ = H_2Q$	$E_{h,Quinone} = E_h^0 - 0.059 \bullet pH + \frac{0.059}{2} \bullet \lg \frac{a(H_2Q)}{a(Q)}$
(4) $Jug + 2 e^- + 2 H^+ = H_2Jug$	$E_{h,Juglone} = E_h^0 - 0.059 \bullet pH + \frac{0.059}{2} \bullet \lg \frac{a(H_2Jug)}{a(Jug)}$
(5) $Law + 2 e^- + 2 H^+ = H_2Law$	$E_{h,Lawson} = E_h^0 - 0.059 \bullet pH + \frac{0.059}{2} \bullet \lg \frac{a(H_2Law)}{a(Law)}$
(6) $AQDS + 2 e^- + 2 H^+ = AH_2QDS$	$E_{h,AQDS} = E_h^0 - 0.059 \bullet pH + \frac{0.059}{2} \bullet \lg \frac{a(AH_2QDS)}{a(AQDS)}$
(7) $DOM_{(ox)} + 2e^- + 2H^+ = DOM_{(red)}$	$E_{h,DOM} = E_h^0 - 0.059 \bullet pH + \frac{0.059}{2} \bullet \lg \frac{a(DOM_{red})}{a(DOM_{ox})}$
(8) $[Fe(bipy)_3]^{3+} + e^- = [Fe(bipy)_3]^{2+}$	$E_{h,Fe} = E_h^0 + 0.059 \bullet \lg \frac{a([Fe(bipy)_3]^{3+})}{a([Fe(bipy)_3]^{2+})}$
(9) $[Fe(CN)_6]^{3-} + e^- = [Fe(CN)_6]^{4-}$	$E_{h,Fe} = E_h^0 + 0.059 \bullet \lg \frac{a([Fe(CN)_6]^{3-})}{a([Fe(CN)_6]^{4-})}$
(10) $[Fe(C_6O_7H_8)]^0 + e^- = [Fe(C_6O_7H_8)]^{1-}$	$E_{h,Fe} = E_h^0 + 0.059 \bullet \lg \frac{a([Fe(C_6O_7H_8)]^0)}{a([Fe(C_6O_7H_8)]^{1-})}$
(11) $Fe(OH)_3 + e^- + 3 H^+ = Fe^{2+} + 3 H_2O$	$E_{h,Fe} = E_h^0 - 0.177 \bullet pH + 0.059 \bullet \lg \frac{1}{a(Fe^{2+})}$
(12) $S_2O_3^{2-} + 8 e^- + 10 H^+ = 2 H_2S + 3 H_2O$	$E_{h,S} = E_h^0 - 0.073 \bullet pH + \frac{0.059}{8} \bullet \lg \frac{a(S_2O_3^{2-})}{a(H_2S)^2}$
(13) $Zn^{2+} + 2 e^- = Zn^0$	$E_{h,Zn} = E_h^0 + \frac{0.059}{2} \bullet \lg a(Zn^{2+})$

Table 28 E_h^0 values and the calculated half cell redox potential values at pH 7 E_h (W)

	E_h^0 (mV)	E_h (W) (mV)	Source
(1)	+ 640	+ 70	(Stumm and Morgan, 1996)
(2)	+ 860	+ 90	(Stumm and Morgan, 1996)
(3)	+ 699	+320	(Helburn and Maccarthy, 1994)
(4)	+ 430	+40	(Schwarzenbach et al., 1990)
(5)	+ 350	-30	(Schwarzenbach et al., 1990)
(6)	+ 250	-130	(Rosso et al., 2004)
(7)	+ 228 to +528	+ 250 to - 180	(Oesterberg and Shirshova, 1997; Palmer et al., 2006)
(8)	+1110	+1110	(Bard et al., 1985)
(9)	+360	+360	(Matthiessen, 1994)
(10)	+372	+372	(Straub et al., 2001)
(11)	+840	-400	(Majzlan et al., 2004)
(12)	+340	-190	(Stumm and Morgan, 1996)
(13)	-760	-1060	(Stumm and Morgan, 1996)

References

- Bard A. J., Parsons R., and Jordan J. (1985) *Standard potentials in aqueous solutions*. International Union of pure and applied chemistry.
- Helburn R. S. and Maccarthy P. (1994) Determination of Some Redox Properties of Humic-Acid by Alkaline Ferricyanide Titration. *Analyt. Chim. Acta* **295**(3), 263-272.
- Majzlan J., Navrotsky A., and Schwertmann U. (2004) Thermodynamics of iron oxides: Part III. Enthalpies of formation and stability of ferrihydrite (Fe(OH)₃), schwertmannite (FeO(OH)_{3/4}(SO₄)_{1/8}), and -Fe₂O₃. *Geochim. Cosmochim. Acta* **68**(5), 1049-1059.
- Matthiessen A. (1994) Evaluating the redox capacity and the redox potential of humic acids by redox titrations. In *Humic substances in the global environment and implications on human health* (ed. N. Senesi and T. M. Miano), pp. 187-192. Elsevier Science.
- Oesterberg R. and Shirshova L. (1997) Oscillating, nonequilibrium redox properties of humic acids. *Geochim. Cosmochim. Acta* **61**(21), 4599-4604.
- Palmer N. E., Freudenthal J. H., and von Wandruszka R. (2006) Reduction of arsenates by humic materials. *Environm. Chem.* **3**(2), 131-136.
- Rosso K. M., Smith D. M. A., Wang Z. M., Ainsworth C. C., and Fredrickson J. K. (2004) Self-exchange electron transfer kinetics and reduction potentials for anthraquinone disulfonate. *J. Phys. Chem. A* **108**(16), 3292-3303.
- Schwarzenbach R. P., Stierli R., Lanz K., and Zeyer J. (1990) Quinone and Iron Porphyrin Mediated Reduction of Nitroaromatic Compounds in Homogeneous Aqueous-Solution. *Environ. Sci. Technol.* **24**(10), 1566-1574.
- Straub K. L., Benz M., and Schink B. (2001) Iron metabolism in anoxic environments at near neutral pH. *FEMS Microbiol. Ecol.* **34**(3), 181-186.
- Stumm W. and Morgan J. J. (1996) *Aquatic chemistry*. Wiley Interscience.

Danksagung

Allen die mich während meiner Doktorandenzeit unterstützt haben möchte ich sehr herzlich danken. Besonderer Dank gilt dabei:

Christian Blodau, für die ungezählten Ideen und fachliche Anregungen, ob sie nun verwirklicht wurden oder nicht. Für viele Diskussionen und noch viel mehr Korrekturen. Ohne dich wäre diese Arbeit sicher nicht in der jetzigen Form entstanden.

Stefan Peiffer, für die Möglichkeit meine Promotion am Lehrstuhl Hydrologie durchzuführen. Danke auch für das stets große Interesse am Thema und für kritische Fragen zum richtigen Zeitpunkt, so unangenehm sie auch sind.

Donald Macalady, für viele Ideen und viel Zeit für offene Diskussionen. Für Freude und Enthusiasmus, von dem sich jeder etwas abgucken kann. Und nicht zuletzt für eine fantastische Zeit in Golden. Thank you a lot, Don.

Beate Fulda, für deinen immensen Einsatz und deine Ausdauer bei der Erhebung und Auswertung von Daten, die einen Teil der Basis für diese Arbeit bilden. Es hat großen Spaß gemacht mit dir zu diskutieren.

Tobias Heitmann, Simona Regenspurg, Kaylene Ritter, Michaela Raber und Klaus-Holger Knorr, für viele Versuche und Messungen, gute Zusammenarbeit, hilfreiche Tipps und schöne Stunden bei Laborraddudelmainwellemusik.

Michael Radke, Martin Back, Katrin Hellige, Julia Beer, Sabine Thüns, Jan Fleckenstein und Sandrine Deglin. Für Engagement im täglichen Laboreinsatz und an der Computerfront aber auch für schöne Zeiten in Labor und Büro. Und schöne Stunden weit davon entfernt, von Oberfranken über die Pfalz bis nach Grand Junction. Schön, dass ihr da wart.

Karsten Kalbitz, Andreas Kappler, George Aiken, Jim Ranville, Gunther Ilgen, Ludwig Hildebrandt, die alle auf die eine oder andere Art am Entstehen dieser Arbeit beteiligt waren. Danke für die Unterstützung.

Allen TAs, Diplomanden, Hiwis und überhaupt der ganzen Hydro-Familie für Laborarbeit und Unterstützung und Hilfe, für Klatsch und Tratsch und alle Kaffeepausen. Martina Rohr, Jutta Eckert,

Karin Söllner, Martina Haider, Silke Hammer, Heidi Zier, Jan Schwieker, Lina Fürst, Sebastian Häfele, Jen Bilbao, Tobias Goldhammer und viele andere. Ihr wart alle wichtige Bausteine des großen Ganzen.

Meinen Eltern und meinem Bruderherz, die mich immer unterstützt, egal wobei. Und das obwohl ich euch wahrscheinlich nur einen Bruchteil von dem erklären konnte was ich denn da eigentlich gemacht habe. Danke für alles.

Deshalb in Abwandlung eines berühmtes Zitates:

If I have seen further than others it is because you helped me stand on the shoulders of giants.

Erklärung

Hiermit erkläre ich, dass ich diese Arbeit selbständig verfasst und keine anderen als die angegebenen Quellen und Hilfsmittel verwendet habe. Ich erkläre ferner, dass ich an keiner anderen Hochschule als der Universität Bayreuth ein Promotionsverfahren begonnen und diese oder eine gleichartige Doktorprüfung endgültig nicht bestanden habe.

Bayreuth, April 2008